Investigating the Effects of High Reactivity Fuel with Gasoline-Bioethanol Blends on Reactivity Controlled Compression Ignition (RCCI) Engine

Habtamu Deresso Disassa

A dissertation is submitted to the Department of Mechanical Engineering
School of Mechanical, Chemical, and Materials Engineering

Presented in fulfillment of the requirement for the Degree of Doctor of Philosophy in Automotive Engineering

Office of Graduate Studies
Adama Science and Technology University

August 2024
Adama, Ethiopia

Investigating the Effects of High Reactivity Fuel with Gasoline-Bioethanol Blends on Reactivity Controlled Compression Ignition (RCCI) Engine

Habtamu Deresso Disassa

Main Supervisor: Venkata Ramayya Ancha (Prof.)
Co-supervisor: Ramesh Babu Nallamothu (Ph.D.)
Co-supervisor: Bisrat Yoseph (Ph.D.)

A dissertation is submitted to the Department of Mechanical Engineering
School of Mechanical, Chemical, and Materials Engineering

Presented in fulfillment of the requirement for the Degree of Doctor of Philosophy in Automotive Engineering

Office of Graduate Studies
Adama Science and Technology University

August 2024
Adama, Ethiopia

DECLARATION

I hereby declare that this dissertation entitled "Investigating the effects of high reactivity fuel with gasoline-bioethanol blends on reactivity controlled compression ignition (RCCI) engine" is my original work. That is, it has not been submitted for the award of any academic degree, diploma, or certificate in any other university. All sources of materials used for the dissertation have been duly acknowledged through appropriate citations.

Habtamu Deresso Disassa	___________________	________________
Name of student	Signature	Date

RECOMMENDATION

We, the supervisors of this dissertation, hereby certify that we have read and revised the dissertation entitled *"Investigating the effects of high reactivity fuel with gasoline-bioethanol blends on reactivity controlled compression ignition (RCCI) engine"* prepared under our guidance by Mr. Habtamu Deresso Disassa submitted in fulfillment of the requirements for the degree of Doctor of Philosophy in Automotive Engineering. Therefore, we recommend the submission of the dissertation to the department for further review and defense.

Venkata Ramayya (Prof.)	____________________	____________________
Major Supervisor	Signature	Date
Ramesh Babu (Ph.D.)	____________________	____________________
Co-supervisor (1)	Signature	Date
Bisrat Yosef (Ph.D.)	____________________	____________________
Co-supervisor (2)	Signature	Date

APPROVAL SHEET

We hereby certify that the recommendations and suggestions made by the board of examiners are appropriately incorporated into the final version of the dissertation entitled "*Investigating the effects of high reactivity fuel with gasoline-bioethanol blends on reactivity controlled compression ignition (RCCI) engine*" prepared under our guidance by Habtamu Deresso.

Venkata Ramayya (Prof.) Major Supervisor	Signature	Date
Ramesh Babu (Ph.D.) Co-supervisor (1)	Signature	Date
Bisrat Yosef (Ph.D.) Co-supervisor (2)	Signature	Date

We, the undersigned, members of the board of examiners of the dissertation open defense by Habtamu Deresso Disassa have read and evaluated the dissertation entitled "*Investigating the effects of high reactivity fuel with gasoline-bioethanol blends on reactivity controlled compression ignition (RCCI) engine*" and examined the candidate during open defense. This is, therefore, to certify that the dissertation is accepted for fulfillment of the requirement of the degree of Doctor of Philosophy in Automotive Engineering.

Chairperson	Signature	Date
Internal Examiner	Signature	Date
Samson Mekbib Atnaw (PhD) External Examiner 1	Signature	Date
Dr. Anteneh Mohammed External Examiner 2	Signature	Date

Finally, approval and acceptance of the dissertation are contingent upon submission of its final copy to the Office of Postgraduate Studies (OPGS) through the candidate's Department Graduate Council (DGC) and School Graduate Committee (SGC).

Department Head	Signature	Date
School Dean	Signature	Date
Office of Postgraduate Studies, Dean	Signature	Date

ACKNOWLEDGEMENT

First, and foremost let me praise and honor the almighty God for the opportunity and capacity given to me to realize my aspiration to finish the Ph.D. research work. Next, I would like to express my deepest gratitude to **Venkata Ramayya (Prof)** for his trustful support in academic endeavors throughout the whole work of the research. His genuine and kind advice helped me to overcome several troubles and accomplish the work. Their prodigious knowledge empowers me to rise my academic endeavor and professional ethics competently bringing my work into meaning. I would like to extend my thanks a lot to him also for the opportunity that he gave me to experiment on the test rig engine found in his laboratory. I would like to express my honest gratitude to my Co-advisers **Ramesh Babu (Dr.)** and **Bisrat Yoseph (Dr.)** for their supervision, continuous encouragement, and follow-up, professional advice throughout the entire research and let I appreciate **Balkeshwar Singh (Prof)** for his much professional supports.

I would like to extend my heart full thanks to ASTU's higher officials, OPGS, SCoMCME, Department of Mechanical Engineering, SGC, DGC, doctorial committee for their repetitive cooperation and support in each progress evaluation. In addition, I would like to thank **Dr. Alemayehu Wakjira (Dean, SCoMCME)** and **Sintayehu Legesse (Head, Mechanical Engineering), Addis Alemayeuh,** and **Aby Bekele** for their usual support in every query. I would like to thank Jimma University (JiT) Centre of Excellence management, Faculty of Engineering, Balewgize Amare Zeru (Assoc Prof); Ethiopian Technical University, **Eshetu Abera,** Metehara Sugar Factory's management, and Ethiopian Petroleum Institute for their contributions and support in the fulfillment of the research.

Several other individuals from graduate students of Agricultural Mechanization, and Automotive Engineering such as **Yared Seifu, Amanuel Gebissa, Hadush T/himanot, Tatek Mamo, and Samuel Tamirat** appreciated their engaged support. Last but not least, I would like to thank and appreciate my sister **Shibre Deresso** for her financial support in every challenge both in my research and livelihood aspects, and my lovely couple **Menalush Feyissa** and our Kids for all they share whatever the rigorous and virtuous conditions that they pass through.

TABLE OF CONTENTS

DECLARATION .... **i**
RECOMMENDATION .... **ii**
APPROVAL SHEET .... **iii**
ACKNOWLEDGEMENT .... **iv**
LIST OF TABLE .... **ix**
LIST OF FIGURES .... **x**
LIST OF ACRONYMS AND ABBREVIATIONS .... **xiii**
NOMENCLATURES .... **xviii**
ABSTRACT .... **xx**
CHAPTER ONE **1**
1. INTRODUCTION **1**
1.1. Rationale 1
1.2. Background of the study 4
1.3. Problem Statements 9
1.4. Objectives 10
1.4.1. General objective 10
1.4.2. Specific objectives 10
1.5. Significances and benefits of the study 10
1.6. Scope of the study 11
1.7. Limitations of the study 11
1.8. Organization of the dissertations 12
CHAPTER TWO **14**
2. LITERATURE REVIEW **14**
2.1. Introduction 14
2.2. Conventional diesel engine combustion(CDC) 15
2.3. Advanced internal combustion engine(LTC) 16
2.3.1. Homogenous charge compression ignition (HCCI) 17
2.3.2. Premixed charge compression ignitions (PCCI) 18
2.3.3. Partially pre-mixed charge ignition (PPCI) 19
2.3.4. Reactivity control compression ignition (RCCI) 23

2.3.5. RCCI combustion based on the types of fuels used 26
2.3.5.1. Single-fuel RCCI Combustion 26
2.3.5.2. Dual-fuel RCCI Engine (Diesel-NG/CNG) 27
2.3.5.3. Dual Fuel RCCI Engine (Diesel-Gasoline) 29
2.3.5.4. Dual-fuel (Diesel-alcohol) RCCI Combustions 30
2.3.6. RCCI and its appropriate piston bowl design 36
2.3.7. Injection timing effects on RCCI engine 41
2.3.8. Ehaust gas recirculation(EGR) 42
2.4. Literature review summary 44
2.5. Research Gaps 45
CHAPTER THREE 47
3. MATERIALS AND METHODS 47
3.1. Introduction 47
3.2. Materials 47
3.2.1. Diesel engine test rig 47
3.3. Exhaust gas analyzers 49
3.3.1. Lubricating oil and fuels 51
3.3.1.1. Lubricating oil for the experiment engine 51
3.3.1.2. Fuels used for baseline and advanced engine 51
3.4. Methods 54
3.4.1. Engine experimental investigation processes 55
3.4.1.1. Baseline experiments 55
3.4.1.2. Advanced engine experiments (RCCI) 56
3.4.2. Designs of experiment 59
3.4.2.1. Taguchi method design of experiment 59
3.4.2.2. Error Analysis 60
3.4.3. Modeling of combustion simulation 61
3.4.3.1. Combustion simulation based on piston bowl shape 61
CHAPTER FOUR 67
4. RESULTS AND DISCUSSIONS 67
4.1. Speed and fuel blend ratio effect on the diesel and RCCI engine 67

4.1.1. Combustions at the same speed and various blend ratio 68
4.1.2. Combustion analysis at the same fuel and different speeds 70
4.1.3. Engine performance characteristics of the experiment 72
4.1.3.1. The brake power of the experiment result 72
4.1.3.2. The brake torque of the experiment result 74
4.1.3.3. Brake thermal efficiency 74
4.1.3.4. Brake-specific fuel consumption 77
4.1.4. Engine emission 77
4.2. Triple fuel physiognomies on light-duty RCCI engine 80
4.2.1. Cylinder pressure and heat release rate 81
4.2.1.1. Cylinder pressure results of the experiment 81
4.2.1.2. Heat release rate 82
4.2.1.3. The cylinder temperature of the simulation result 83
4.2.2. Engine tail pipe exhaust emissions 84
4.2.3. Engine performances 86
4.2.3.1. Engine brake power and torque 87
4.2.3.2. Brake thermal efficiency 88
4.2.3.3. Brake-specific fuel consumption 88
4.2.4. Result validations using other similar work 89
4.3. Statistical response analysis of the experiment results 90
4.3.1. Taguchi method approach optimizations 91
4.3.1.1. Linear model analysis: SNR Vs Speed and PMFB-ratio 91
4.3.1.2. Linear model analysis: Means vs. speed, PMF-ratios 93
4.3.1.3. Linear model analysis: Standard Deviations vs Speed, and PMF-ratio 94
4.3.1.4. Analysis of variance 95
4.3.1.5. Main effects plots of SNR, Means, and STD 95
4.3.1.6. Residual plots of SNR, Means, and STD 95
4.3.2. Interaction plot analysis 96
4.3.3. Contour plots analysis 98
4.3.4. An interval plot analysis 99
4.4. Start of diesel fuel injection timing effects 101

4.5. Combustion simulation 101
4.5.1. Cylinder combustion analysis 102
4.5.1.1. In-cylinder combustion pressure 102
4.5.1.2. In-cylinder temperature and heat release rate 103
4.5.2. Engine exhaust emissions 105
4.5.3. Simulation of fuel sprays in the swirling airflow 106
4.5.4. Ignition delay period 110
4.5.5. Present work validation 114
4.5.6. Effects of injection timing (SOI) 114
CHAPTER FIFE 118
5. CONCLUSION AND RECOMMENDATION 118
5.1. Conclusions 118
5.2. Recommendations 119
5.3. Future Direction 120
REFERENCES 121
APPENDIX A. ENGINE WHEN CONDUCTING EXPERIMENT 136
APPENDIX B. EMISSION INTERVAL PLOTS 136
APPENDIX C. BOXPLOT OF EMISSION 137
APPENDIX D. BOXPLOT OF PERFORMANCE 138
APPENDIX E. POTENTIOMETER ANGLE AND INJECTIONS VOLUME 138
PPENDEX F. FUEL PROPERIES FROM EPE 139

LIST OF TABLE

Table 2.1 Analysis comparing the CI, SI, and HCCI engines 18
Table 2.2 Fuel characteristics of LRF, DTBP, and 2-EHN cetane improver 27
Table 2.3 Single fuel and dual fuel RCCI engine 35
Table 3.1 Fuel percentage compositions 49
Table 3.2 Materials used for the study 50
Table 3.3 Diesel fuel properties 52
Table 3.4 Specification of gasoline fuel 53
Table 3.5 Ethanol fuel properties 54
Table 3.6 L9 Experiment data of emissions and performances 59
Table 3.7 Performance accuracy and its maximum uncertainty 61
Table 3.8 Measurement uncertainty and instrument accuracy 61
Table 4.1 Engine operation data from the data acquisition system 76
Table 4.2 EV and IV opening and closing point 81
Table 4.3 Single fuel and dual fuel RCCI engine, Single fuel RCCI engine 90
Table 4.4 L9 Experiment results of emissions and performances 91
Table 4.5 Estimated model coefficients for SNR. 92
Table 4.6 Analysis of variance for SNR (ANOVA) 92
Table 4.7 Estimated model coefficients for means 93
Table 4.8 Estimated model coefficients for Standard deviations 94
Table 4.9 Analysis of variance for standard deviations 94
Table 4.10 Response for SNR; means, and STD 96
Table 4.11 Pilot, main, and post injections in the piston 2 and 3. 110
Table 4.12 Emission, CP, and CT simulation and experiment results and their comparison 114
Table 4.13 Maximum performance, efficiency, and power 117

LIST OF FIGURES

Figure 1.1 Advanced engine and renewable energy....................4
Figure 1.2 Emissions contour plot....................8
Figure 2.1 Historical development of diesel engines....................16
Figure 2.2 Evolution of internal combustion engine....................17
Figure 2.3 Single-cylinder HCCI and PCI engines....................18
Figure 2.4 Engine temperature with altered λ....................21
Figure 2.5 Engine PRR and NITE are impacted by EGR.....................21
Figure 2.6 Performance and trends required to achieve DOE....................33
Figure 2.7 Dual-fuel RCCI and R-RCCI operations (PFI, DI)....................34
Figure 2.8 T-distributions and the equivalence ratio for Low-A, B at CA50.....................37
Figure 2.9 Equivalence ratio and T- distributions Mid-A and B.....................38
Figure 2.10 Temperature distributions and equivalence ratio....................38
Figure 2.11 Pistons bowl geometry....................39
Figure 2.12 Percentage energy content of the base and advanced engine....................40
Figure 2.13 Changes in MBF due to different fuel amounts and SOI....................42
Figure 2.14 Variations in MBF when fuel amounts and SOI are changed....................42
Figure 3.1 Diesel engine test rig....................48
Figure 3.2 Schematic diagram of the RCCI engine....................49
Figure 3.3 Exhaust gas analyzers used to measure emission....................50
Figure 3.4 Recommended oil types....................51
Figure 3.5 Over all conceptual framework of the research....................55
Figure 3.6 Baseline experiment schematic diagram....................56
Figure 3.7 Triple fuel RCCI engine strategies applied....................57
Figure 3.8 Schematic diagram of the RCCI engine experiment....................58
Figure 3.9 Timing and lift of the valves and Piston position and volume....................58
Figure 3.10 Fuel spray pattern....................63
Figure 3.11 Different piston bowl shape geometry configurations....................64
Figure 3.12 Diesel fuel spray zone diagram before and after impregnation....................66
Figure 4.1 Cylinder pressure and heat release rate....................69
Figure 4.2 Cylinder pressure and heat release rate....................70

Figure 4.3 Cylinder pressure and Heat Release Rate 70
Figure 4.4 Cylinder pressure and heat release rate 71
Figure 4.5 Cylinder pressure and HRR (J/CA) 72
Figure 4.6 Cylinder pressure and heat release rate 72
Figure 4.7 Brake power 73
Figure 4.8 Brake torque of the engine 74
Figure 4.9 Brake thermal efficiency 76
Figure 4.10 Brake-specific fuel consumption 77
Figure 4.11 NOx emissions 78
Figure 4.12 HC emission 79
Figure 4.13 CO emissions 79
Figure 4.14 CO_2 emission (in % Vol) 79
Figure 4.15 Cylinder pressure 82
Figure 4.16 Heat release rate 83
Figure 4.17 Cylinder Temperature 84
Figure 4.18 Oxides of nitrogen emission 84
Figure 4.19 Carbon dioxide emissions 85
Figure 4.20 Carbon monoxide emissions 86
Figure 4.21 Hydrocarbon emissions 86
Figure 4.22 Brake power 87
Figure 4.23 Brake torque 88
Figure 4.24 Brake thermal efficiency 88
Figure 4.25 Brake-specific fuel consumption 89
Figure 4.26 Main effect pilots for SN-Ratios 92
Figure 4.27 Residual pilots for Signal-N-Ratios 92
Figure 4.28 Main effect pilot for means 93
Figure 4.29 Residual pilots for means 93
Figure 4.30 Main effect plot for standard deviations 94
Figure 4.31 Residual pilots for standard deviations 94
Figure 4.32 Interaction plot for emissions and performances 97
Figure 4.33 NOx emissions of contour pb 98

Figure 4.34 CO2 emissions of the contour plot..98
Figure 4.35 Contour pilot of CO of CDC and RCCI Emission..99
Figure 4.36 Contour pilot of HC of CDC and RCCI Emission..99
Figure 4.37 Interval plot for NOx..100
Figure 4.38 Interval plot for CO..100
Figure 4.39 Interval plot for CO2..100
Figure 4.40 Interval plot for HC..101
Figure 4.41 In-cylinder pressure at various PBSDG...103
Figure 4.42 In-cylinder temperature for PBSD geometry...104
Figure 4.43 The HRR at various piston bowl geometries 104
Figure 4.44 NOx emissions concentrations...105
Figure 4.45 Particulate matter concentrations...106
Figure 4.46 The EFM motion from the injection, spray front zone, and spray tip.................108
Figure 4.47 Spray and NWF dilution and fuel fraction in the core of free spray...................109
Figure 4.48 Fuel fraction in FOFS and Core of near well flow 109
Figure 4.49 DSEVL2 BMW_M472 piston spry core, dilute, front, and NWF. 110
Figure 4.50 Shallow Heselman piston spry core, dilute, front, and NWF. 110
Figure 4.51 Lambardini 15LD350 piston spry core, dilute, front, and NWF.........................111
Figure 4.52 The DOSANP158FE piston spry core, dilute, front, and NWF effects..............111
Figure 4.53 Spray angle and tip penetration for the single fuel injection. 112
Figure 4.54 Spray angle of the triple fuel injection...113
Figure 4.55 STP for the triple (pilot, main, and Post) fuel injection......................................113
Figure 4.56 In-cylinder pressure and temperatures 115
Figure 4.57 The heat release rate...115
Figure 4.58 NOx and PM emission contour plot...116
Figure 4.59 Ringing intensity and ignition delay 117

LIST OF ACRONYMS AND ABBREVIATIONS

AASTU	Addis Ababa Science and Technology University
AHRR	Apparent heat release rate
AOHR	Apparent heat release
ANOVA	Analysis of variance
ASOI	Advancing the start of injection
AFR	Air fuel ratio
ANR	Advance neutral and retarded injection timing
AUTO	Automotive
BMEP	Brake mean effective pressure
BSFC	Brake specific fuel consumption
BTDC	Before top dead center
BTE	Brake thermal efficiency
BP	Brake power
BT	Brake torque
CA	Crank angle
CATIA	Computer aided three-dimensional interactive application
CI	Compression ignitions
CIDI	Compression ignition direct injection
CN	Cetane number
CRDI	Common rail direct injection
CDCE	Conventional diesel combustion engine
CDC	Conventional diesel combustion
CDE	Conventional diesel engine
CFD	Computational fluid dynamics
CHCCI	Controlled homogenous charge compression ignition
CNG	Compressed natural gases
CP	Cylinder pressure
DI	Direct-injection
DGC	Department graduate council
DIT	Diesel injection timing

DMDF	Dual-mode dual-fuel
DOE	Design of experiment
DPF	Diesel particulate filter
DSDoPBG	Different shape design of piston bowl geometry
DIT	Delay ignition timing
DOC	Double overhead camshaft
DOE	Design of experiment
DAQS	Data acquisitions system
DTBP	Di-tert butyl peroxide
EGA	Exhaust gas analyzer
EVC	Exhaust valve closing
ECU	Electronic control unit
EHN	Ethylhexyl nitrate
EVO	Exhaust valve open
EFM	Elementary fuel mass
EGB	Ethanol-gasoline blends
EGR	Exhaust gas recirculation
FEF	Fumigant energy fractions
FMEP	Friction means effective pressure
GDCI	Gasoline direct compression ignition
GHG	Greenhouse gas
GIE	Gross indicated thermal efficiency
GTE	Gross thermal efficiency
GBE	Gasoline bioethanol
HC	Hydrocarbon
HCCI	Homogenous charge compression ignition
HD	Heavy duty
HPRR	High-pressure rise rate
HRR	Heat release rate
HTE	High thermal efficiency
HRF	High reactivity fuel

IVC	Intake valve closing
IC	Internal combustion
ID	Ignition delay
IMEP	Indicated mean effective pressure
ISR	Integrated system reactor
ITE	Indicated thermal efficiency
IMEP	Indicated mean effective pressure
JiT	Jima University Institute of Technology
LCPT	Lower cylinder pressure and temperature
LD	Light duty
LHV	Lower heating value
LIVC	Late intake valve closing
LRF	Low reactivity fuel
LTC	Low-temperature combustion
LCPT	Lower cylinder pressure and temperature
LRF	Low reactivity fuel
LTC	Low-temperature combustion
MCPT	Maximum cylinder pressure and temperature
MCT	Maximum cylinder temperatures
MN	Methane number
MPRR	Maximum pressure rise rate
MRCCI	Maximum reactivity control compression ignition
MS	Mean square
NADI	Narrow-angle direct injection
NG	Natural gas
NI	National Instruments
NIE	Net indicated efficiency
NITE	Net indicated thermal efficiency
NWF	Near well flow
OBD	On-board diagnostic
OEM	Original equipment manufacturer

OPGS	Office of Postgraduate Studies
OCPT	Optimum cylinder pressure and temperature
PPRR	Peak pressure rise rate
PBD	Piston bowl design
PBG	Piston bowl geometry
PBSD	Piston bowl shape design
PBS	Piston bowl shape
PCCI	Premixed charge compression ignition
PIF	Port injection fuel
PFI	Port fuel injection
PM	Particulate matter
PMEP	Pumping means effective pressure
PPC	Partially premixed combustion
PPCI	Partially premixed charge ignition
PRF	Primary reference fuel
PPCI	Partially pre-mixed charge ignition
PR	Pressure rise
PRR	Pressure rise rate
RCCI	Reactivity-controlled compression ignition
RI	Ringing intensity
RSOI	Retarded start of injection
SCOTE	Single-cylinder oil- test engine
SE	Summary emission
SI	Spark ignition
SOIT	Start of injection timing
STP	Spray tip penetration
HCCI	Homogeneous charge compression ignition
HRR	Heat release rate
ID	Ignition delay
MRCCI	Maximum reactivity-control compression ignition
PM	Particulate matter

REB	Re-entrant bowl
SCR	Selective catalytic reduction
SOI	Start of injection
TRB	Toroidal bowl
FFS	Fuel fraction spray
GHG	Greenhouse gas
HC	Hydrocarbon
HD	Heavy duty
HPRR	Higher pressure rise rate
HR	Heat release
HTE	High thermal efficiency
LDRCCI	Light duty reactivity control compression ignition
LD	Light duty
LHV	Lower heating value
LIVC	Late intake valve closing
MPRR	Maximum pressure rise rate
NIE	Net indicated efficiency
NITE	Net indicated thermal efficiency
NWF	Near wall flow
NOx	Oxides of nitrogen
OCPT	Optimum cylinder pressure and temperature
OEV	Open of exhaust valve
PBD	Piston bowl design
PBS	Piston bowl shape
PFI	Port fuel injection
PR	Pressure rise
PRR	Pressure rise rate
QLHV	Lower heating value
RSA	Reduced spray angle
REGR	Redirected exhaust gas recirculation
ROHR	Rise of heat release

SCoMCME	School of mechanical chemical material Engineering
SMD	Sauter mean diameter
SOMI	Start of more injection timing
SAE	Society of automotive engineering
SAS	Spray angle system
SNR	Signal to noise ratio
SOC	Start of combustion
STD	Standard deviations
SCOTE	Single-cylinder oil- test engine
SCR	Selective catalytic reduction
SE	Summary emission
SI	Spark ignition
SGC	School graduate committee
TDC	Top dead center
THC	Total hydrocarbon
HC	Hydrocarbon
US	United States
VOL	Valve overlap
VPBSG	Various piston bowl shape design
VGT	Variable geometry turbocharging
VSA	Variable swirl actuation
SNR	Signal-to-noise ratio
SOC	Start of combustion
SOI	Start of injection
SOIT	Start of injection timing
STD	Standard deviation
STP	Spray tip penetration

NOMENCLATURES

D100G0E0	100% Diesel fuel
G25E50	25% gasoline and 75% Ethanol of port-injected fuel

G50E50	50% gasoline and 50% Ethanol of port-injected fuel
G5E15	5% gasoline and 15% Ethanol of the total
G10E10	10% gasoline and 10%Ethanol of the total
γ	Specific heat ratio
Φ	Total equivalence ratio
Φ_p	Partial equivalence fraction of the premixed fuel
Φ_d	Partial equivalence ratio of direct injected fuel
r_p	Pre-mixed ratio
T_{max}	Maximum cylinder temperature
U_t	Swirl direction
γ_j	The shape of NWF spot depends on the impingement angle
l_{wj}	Length of NWF spot in each direction
Φ	0.6 constant factor of lose due to impingent
τ_{sw}	Time of impingement
$\tau_{s\ max}$	Time of complete spray evolution
U	EFM velocity
Uo	EFM velocity in injections
L	Distance between EFM and injectors
l_m	Penetration length of EMF until the stop in front of the spray
W_t	Local tangential velocity
Rs	Swirl ratio
N	Engine speed
X	Swirl damping factors
g_j	Impingement angle
γ_a	Spray angle
Δy	Spray angle shift

ABSTRACT

The diesel engine is the main prime mover widely used for land transportation and power generation applications on account of higher thermal efficiency. Research on better combustion technologies and renewable and clean energy sources is being driven by environmental contamination as well as the current energy crisis with a special emphasis on reducing pollutant emissions from internal combustion engines. Developing advanced control strategies is a significant research gap in RCCI engines. Optimal control strategies need to be developed to achieve stable engine operation. Combustion rate control deficiency at higher engine loads is due to higher self-ignition features of the direct-injected diesel fuel. This includes addressing issues related to combustion phasing control without using EGR which has a negative impact on increasing soot emission and reducing power output. In this study, an experimental investigation on a triple-fuel reactivity control compression ignition (RCCI) engine running on port-injected gasoline-ethanol blend and direct-injected diesel fuel was conducted. The intake system was modified to use port fuel injection in RCCI operations for controlling emissions, in-cylinder charge reactivity, and combustion phasing. Taguchi method experimental design optimization was employed to assess the impact of various independent variables utilizing three set levels and two factors with the L9 orthogonal array. The combustion simulation was carried out to analyze the effect of four different piston bowl shapes (P1, P2, P3, and P4) and was successfully validated. The simulation model shows that the peak cylinder pressure (PCP) of P2 is 131 bar and the PCP of P4 is 113 bar. The combustion temperature was found to be maximum at 2048.2k for P2, and the lowest for P4 at 1680.9k while the same for P2 was 18% higher than that of P4. The peak heat release rate (HRR) for P3 was determined to be 0.082 J/CA with a great variation between maximum and minimum due to the presence of pre-and post-injection, and the HRR for P4 was 0.035 J/CA with the single injection. The HRR was the highest for P3 and P4 was lower by 39%. The NOx emissions for P1, P2, P3, and P4 were found to be 25.62, 16, 18.2, and 12.74 g/kWh respectively. The lower NOx for P2 was due to a lower fuel fraction of near-wall flow dilution on the outer portion of the sleeve, low fuel fraction in the core region of the free spray, in the front portion of the free spray, and the core of the fuel-free spray. The experimental investigation on G25E75-RCCI operation showed a PCP of 91 bars at 3000 rpm and a minimum of 58 bars at 2600 rpm with baseline as diesel (D100G0E0) alone. The peak HRR is 62 J/CA at 3000 rpm when operating with the G25E75-RCCI engine and a minimum of 12 J/CA for G50E50-RCCI operation. The engine operating with G25E75 pre-mixed fuel had a minimum NOx and CO2 emission. The brake power is maximum at 3000 rpm, and the brake torque is maximum at 2400 and 2500 rpm with the engine running on a G50E50-RCCI engine. Varying the amount of hydrous bioethanol in the port injected premixed fuel, the engine performance and emissions were observed to be greatly affected. Taguchi optimization results showed that speed (delta 10.75, rank = 1) has the largest effect on the signal-to-noise ratio (SNR), and delta 38.96, rank = 1, has the largest effect on the response of means at 3000 rpm. The fuel G25E75 (delta 87.30, rank 1) has the largest effect on the standard deviations (STD). The strongest means in engine speed and premixed fuel were NOx, CO, HC, and brake power. At 3000 rpm, the speed had the larger main effect plots of SNR. The G25BE75 operating mode had the strongest main effect plots for means and STD. ***High*** *engine speeds and higher ethanol content in the RCCI premixed fuel are preferred for reducing NOx and CO2, while hydrocarbon (HC) and CO showed a slightly increasing trend even though observed to be lower than that of diesel in the lower speed range. The brake thermal efficiency while being lower with RCCI at lower speeds, is almost on par with conventional diesel at high-speed range, with the present blends tested, higher speeds seem to be preferable from a performance perspective while the best emission performance has been observed at intermediate speed.*

Keywords: Emission, fuel blend ratio, speed, heat release rate, and RCCI.

CHAPTER ONE

1. INTRODUCTION

1.1. Rationale

The world's interest in renewable energy has increased due to several factors, including the reduction of fossil fuels, fears about energy security, and ecological concerns (Yasiria et al., 2020; Yi et al., 2023). To lessen reliance on fossil fuels and the environmental effects of emissions such as carbon monoxide (CO), carbon dioxide (CO_2), hydrocarbons (HC), particulate matter (PM), and oxides of nitrogen (NOx), the development of renewable energy has become essential (Albayrak et al., 2023). In an attempt to slow down environmental deterioration and decrease dependency on petroleum derivatives, abundant work has been done in recent years to identify alternate energy sources. Numerous alternative fuels have been intensively studied in this area, including hydrogen and oxygenated fuels like ethanol, dimethyl ether, biodiesel, and biogas (Prasad, 2023; Hoang et al., 2023). Based on their oxygenated, sulfur-free, biodegradable, and sustainable properties, recent research indicates that biofuels are the most potential substitute fuel for diesel engines (Fernandes et al., 2007; Joshi et al., 2017). Furthermore, biofuels have significant strategic implications, especially when utilized as a transportation fuel to lower vehicle emissions and advance sustainability (Giampietro et al., 1997; Takors, 2023; Zhang, 2023). Due to their growing popularity, gasoline and diesel engines are the primary global producers of greenhouse gas emissions from the transportation industry. According to projects made by the International Energy Agency (IEA), transportation account for 92% of all carbon dioxide (CO_2) emissions by 2020, or 8.6 billion metric tons of CO_2 emissions to the atmosphere was recorded between 2020 and 2035 (Biermann, 2015; Yanagisawa, 2015). The excessive use of petroleum by the transport sector harms the environment, and the deterioration of urban air quality is mostly the result of automobile emissions. Alternative fuels and advanced IC engines explore the use of alternate energies, including biofuels, natural gas, hydrogen, and synthesized fuels. These fuels suggested prospective advantages in terms of lower emissions, reduced dependence on fossil fuels, and improved sustainability (Akalin et al., 2021).

Advanced engines refer to innovative engine designs and technologies that aim to improve efficiency, reduce emissions, and enhance overall performance. These advancements can be applied to both SI and CI engines. Some key areas of advancement in innovative IC engines are downsizing and turbocharging. Downsizing and turbocharging result in improved fuel economy without sacrificing performance (Ram et al., 2023; Silva et al., 2023). Systems with variable valve timing (Xu et al., 2019) and variable valve lift (Jia et al., 2013) provide the ability to precisely change the intake air charge and exhaust gas respectively when intake and exhaust valves open and close. This technology optimizes the engine's breathing capabilities, improving efficiency, power delivery, and emissions performance across different operating conditions (Mikulski et al., 2018). Cylinder deactivation technology selectively shuts down specific cylinders when the engine works under light load conditions. By deactivating cylinders, the engine can reduce pumping losses, improve efficiency, and save fuel. Cylinder deactivation is particularly effective in engines with a large number of cylinders (Allen et al., 2021; Nageswaran et al., 2015).

Variable compression ratio engines allow for the adjustment of the compression ratio during operation. By varying the compression ratio, the engine can optimize efficiency across different load and speed conditions. This technology can improve both fuel economy and performance (Aydın, 2021; Xu et al., 2019). The integration of electrification and hybridization technologies with IC engines has gained significant attention. Hybrid powertrains, such as mild hybrids, full hybrids, and plug-in hybrids, combine IC engines with electric motors and energy storage systems. The integration enhances overall efficiency, reduces emissions, and provides additional power for improved performance (García et al., 2021; Shahbakhti, 2016). Advanced control systems, such as model-based predictive control, real-time optimization, and adaptive algorithms, are employed to optimize engine performance and efficiency. These systems utilize sensors, actuators, and advanced algorithms to continuously monitor and adjust engine parameters, improving combustion control and overall operation (Belgiorno et al., 2019; Raut et al., 2018). Advancements in materials science and manufacturing techniques contribute to lighter and more durable engine components. The use of lightweight materials, such as aluminum alloys and composites, reduces engine weight, improving efficiency and performance (Immanuel. 2021; Tung. 2016). The combination of multiple technologies and innovative approaches is crucial to achieving the desired improvements in IC engine performance. Low-temperature reactivity-controlled compression ignition engines offer several advantages that make them an attractive choice in the field of ICEs. Here are some reasons why advanced engines are pursued:

- The achievement of higher thermal efficiency compared to diesel engine combustion modes, such as SI or CI engines. By combining the benefits of CI and SI combustion, RCCI engines can operate at high compression ratios, leading to improved fuel efficiency and reduced fuel consumption (Boronat, et al., 2017; Olmeda et al., 2018). RCCI engines had the potential to decrease discharges of nitrogen oxides (NOx) and soot, which are major pollutants from IC engines.
- By controlling the reactivity of the air-fuel mixture, RCCI engines can achieve lower peak combustion temperatures, reducing the formation of NOx (Poorghasemi et al., 2017). Additionally, the use of low-reactivity fuels can lead to reduced PM emissions. RCCI engines offer fuel flexibility, allowing the use of a wide range of fuels with different reactivity characteristics. This flexibility enables the utilization of various fuel sources, including conventional gasoline, diesel, biofuels, and alternative fuels.
- By optimizing fuel selection and blending, RCCI engines can adapt to regional fuel availability and meet specific emission regulations. RCCI engines can achieve high power density due to the controlled combustion process. The use of high-reactivity fuel in the CI mode provides efficient power delivery, while the low-reactivity fuel mode enhances combustion stability.
- The controlled combustion process reduces pressure fluctuations and combustion noise, resulting in quieter engine operation. This can contribute to improved driving comfort and reduced noise pollution. RCCI engines retain some of the advantages associated with CI engines, such as the high energy density of diesel fuel, high torque output, and well-established infrastructure for diesel distribution.

By incorporating the CI mode into RCCI operation, these benefits can be harnessed while achieving improved efficiency and emissions control. Renewable energy and advanced internal combustion engines' potential advantages and disadvantages are shown in Fig.1.1.

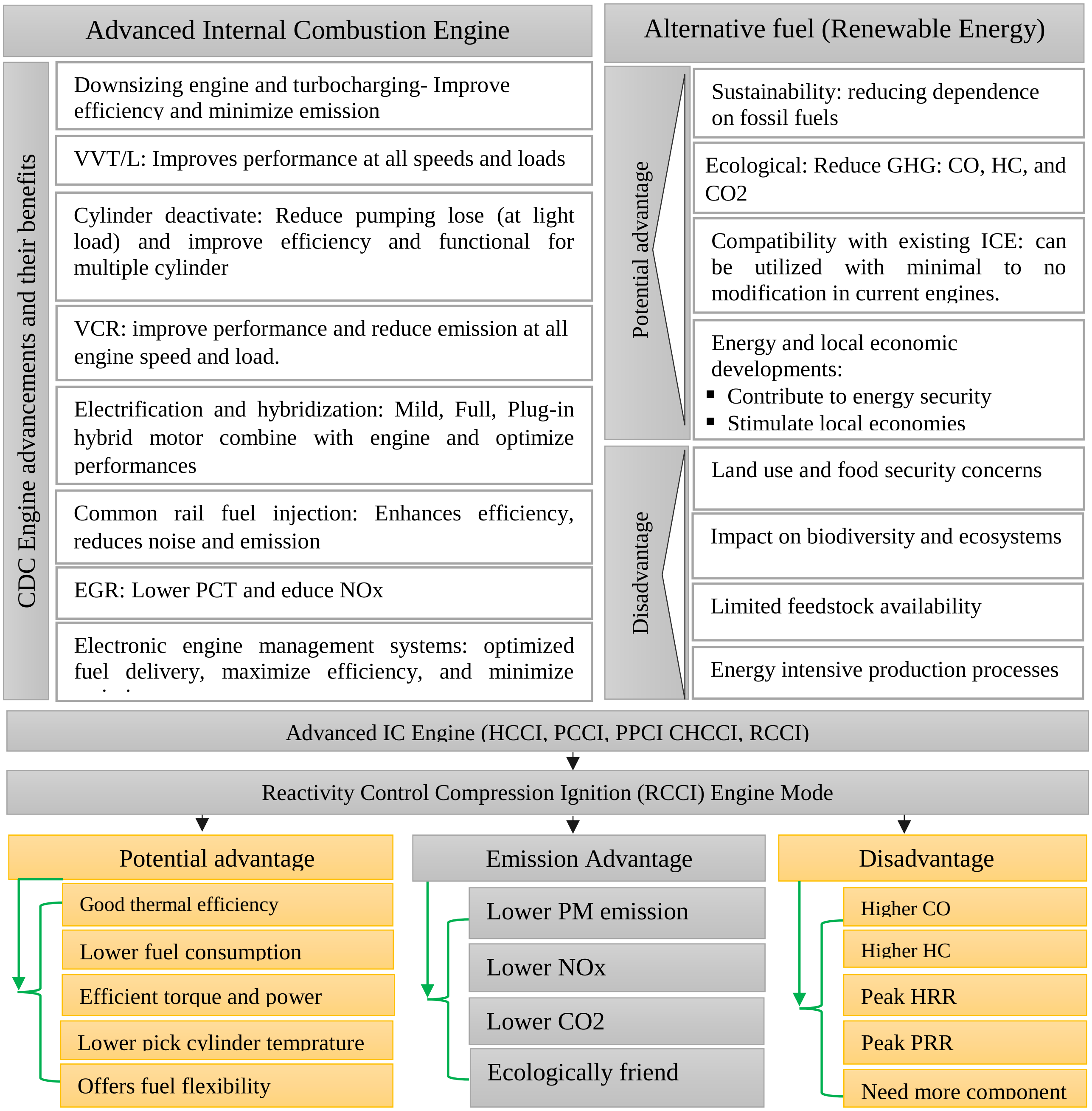

Figure 1.1 Advanced engine and renewable energy

The reason why the research is concentrated on ethanol biofuel and advanced internal combustion engines is due to the aforementioned advantages in sustainability, performance, and emission (ecological) aspects as stated in the chart above.

1.2. Background of the study

At one time, the primary sources of power for the work of peace were man's muscles; trained animals, wind, and running steam respectively had harnessed. However, the greatest steps were taken in the direction when man learned the art of energy conversion, the engine. In the current world, internal combustion engine spark and compression ignition engines have the best role in the wider range of applications due to their reliability and power density toward the advancements of human living life (Ganesan, 2006). The reciprocating internal combustion engine is arguably the most elegant invention in human history, with far-reaching effects on the environment, and economy of the nation. This wonderful discovery was found to be essential to the automotive system, which is utilized nearly entirely now, for many years. Over the past years, both kinds of IC engines have seen significant efficiency gains. Regretfully, the development of improved combustion engines that completely mitigate exhaust emissions and maximize engine efficiency is currently imperative (Firmansyah et al., 2018). Diesel engines are a type of power plant that can produce energy on their own. Their horsepower ranges from a few to a large amount, and they are used to generate mechanical power for various applications such as pumping, off-road machinery, agricultural tractors, shipping, and power generation for the transportation industry (Wategavea et al., 2021). Unwanted emissions are caused by the high temperature reached during the CDC and the oxygen available outside of the spray plume (Şener et al., 2019). It is known that compression ignition engines typically have a higher thermal efficiency but produce more NOx and soot than spark ignition engines. As a result, since the 1990s, more and more emphasis has been paid to advanced and alternative compression ignition engine designs to satisfy the criteria of additional NOx and particulate matter (PM) reductions as well as better efficiency. Low-temperature combustion (LTC) is a category that most of these tactics fall under (Deshwar et al., 2023; Soo-Young, 2019). The engine research community faces a major hurdle in the form of rigorous restrictions introduced around the globe to reduce pollutant outputs from internal combustion engines. The internal combustion of gasoline and diesel engines with two and four-stroke engines was most commonly used in the world for different purposes. An internal combustion engine uses a set of thermodynamic processes to transform the chemical energy of the fuel into mechanical work, providing power to drive a vehicle's wheel via the drive train in most transportation applications. The higher efficiency of CI engines has played an indispensable role in human life due to their higher reliability, lower running cost, and high power density (Gu¨rbu¨z and Sandalc, 2022; Thomas, 2018).

An increased focus on powertrain development to lower fuel consumption and exhaust emissions has resulted from growing concerns about climate change caused by air pollution, human health, and energy consumption that were not concerns in previous decades (Deshwar et al., 2023; Dwarshala et al., 2023). Because of the necessary limits on CO_2 and non-CO_2 emissions imposed by a set of severe emissions legislation, internal combustion engine performance, and emissions have significantly improved over the previous 20 years. In the 1960s, California (Thomas, 2018) established pollution rules to lower vehicle tailpipe emissions through a technology-focused strategy (Uherek et al., 2010). Since then, numerous governmental groups have been founded all over the world to put up emission rules that can safeguard both the environment and public health. Since the early years of its establishment, emission regulations have been amended and changed annually to reduce the maximum amount of harmful exhaust gas emissions and increase fuel efficiency (Golzari, 2018). Stricter emission laws are being driven by the ongoing degradation of urban air quality and environmental acidification, which is mostly caused by rising car emissions. For the continued development of diesel engines, it is increasingly important to reduce fuel consumption, NOx, and particle emissions.

For gasoline and diesel engines, many development lines are available to enhance torque generation while reducing fuel consumption, emissions, and noise. Their current development is characterized by decreased fuel consumption, decreased specific emissions (CO2, HC, CO, NOx, PM, dust), good driving behavior, increased specific power (downsizing, charging), decreased friction, minimized energy consumption, and decreased noise and oscillations. To attain lower emissions, more developments in common-rail direct injection, combustion processes, charging, and exhaust-gas treatment are needed (Shinde et al., 2020). Two stages to increase combustion temperature, emissions, and noise levels using common-rail direct injection are higher pressures of 2200 bar and multiple injections. Solenoid and fast piezoelectric injectors allow for various combinations of pre-, main, and post-injection pulses. Strong cooling and an increase in the exhaust-gas recirculation rate were used to produce low NOx emissions. Conversely, an overabundance of EGR rise restricts the power of the turbocharger. Consequently, a cooler can be used to apply a low-pressure EGR to the compressor inlet following the particle filter (Shen et al., 2013). Good cylinder fill-in could be achieved by combining increased EGR rates with an intercooler to create a low temperature and a balanced mixture of new air and exhaust gas had seen by (Shenawy, et al., 2022).

Additionally, by boosting the specific output, diesel engines allow for some downsizing. Particular focus is paid to exhaust treatment, which reduces CO, HC, NOx, and particles by employing particulate filters and oxidation catalytic converters. SCR (selective catalytic reduction) with dissolved urea injection provides an option, especially for heavy-duty cars. Engines are equipped with mechatronic components to accommodate rising variabilities and control functions (Isermann, 2014). According to (Li et al. 2017), the primary obstacles for compression ignition engines are the comparatively elevated levels of soot and nitrogen oxide (NOx) emissions. Right now, reducing NOx and particle emissions in particular is the most crucial factor in lowering environmental pollution. Strict regulations on vehicle fuel economy and exhaust emissions are in force both now and in the future. According to (Splitter et al., 2013) and (Kokjohn et al., 2011), this calls for the development of innovative engine technologies that can produce high efficiency, low fuel consumption, and low exhaust engine emissions all at once.

To satisfy the demands of clean, efficient, and productive engines in the future, numerous combustion techniques have been researched. Low-temperature combustion encompasses the majority of current techniques. Because low combustion temperatures cause NOx reduction, low-temperature combustion is preferred. Additionally, it makes use of injection timing, which enables greater air-fuel mixing before the commencement of combustion, reducing fuel-rich areas and preventing the development of soot (Said et al., 2022; Ryskamp., 2016). Fig 1.2 displays the operating regimes for the RCCI (Benajes et al., 2014), PCCI (Gurusamy and Subramanian, 2023), HCCI (Dec et al., 2011), PPCI (Habtamu et al., 2022), and CDC plotted on a local temperature space diagram and local equivalence ratio, which were adapted from the work of (Kim et al., 2009).

Advanced combustion strategies are used for the internal combustion engine for the decrease of NOx and soot emission to minimize the complexity and expense of exhaust after-treatment systems. Most of the recent publication efforts fall into the area of HCCI, PCCI, PPCI, and RCCI which have approximately comparable thermal efficiency with conventional diesel engines by decreasing peak combustion temperature and lower combustion emissions (Kokjohn et al., 2011). One of the LTC technologies, RCCI controls the rate of pressure rise and combustion phasing at both high and low engine loads by blending two fuels with various reactivity and one fuel with a tiny cetane improver blended into the direct-injected fuel. The majority of HCCI and PCCI studies were carried out with either neat diesel or neat gasoline fuel, both of which have drawbacks when it comes to premixed compression ignition operation. At low engine loads, combustion is difficult to achieve due to gasoline's weak auto-ignition quality. Nevertheless, diesel fuel has better auto-ignition quality, which raises questions about combustion phasing control at high enough loads. Fuel blending can be utilized to customize fuel reactivity, resulting in reactivity stratification that can adapt to changes in engine load (Dempsey, 2013; Jagankumara et al., 2020; Kuzuoka et al., 2016; Wang et al., 2016). The CDC surrounds areas with high local temperatures and local equivalence ratios, which results in high PM and NOx concentrations. It also suggests that peak local equivalence ratios shouldn't be significantly over stoichiometric to achieve clean and complete combustion. It is recommended to maintain minimum and maximum temperatures between around 1400K and 2000K, which is a very tight range. Plotting of soot, NOx, HC, and CO contours on the T diagram space derived from n-heptane–air mixtures homogeneous reactor simulations (Paykani et al., 2016).

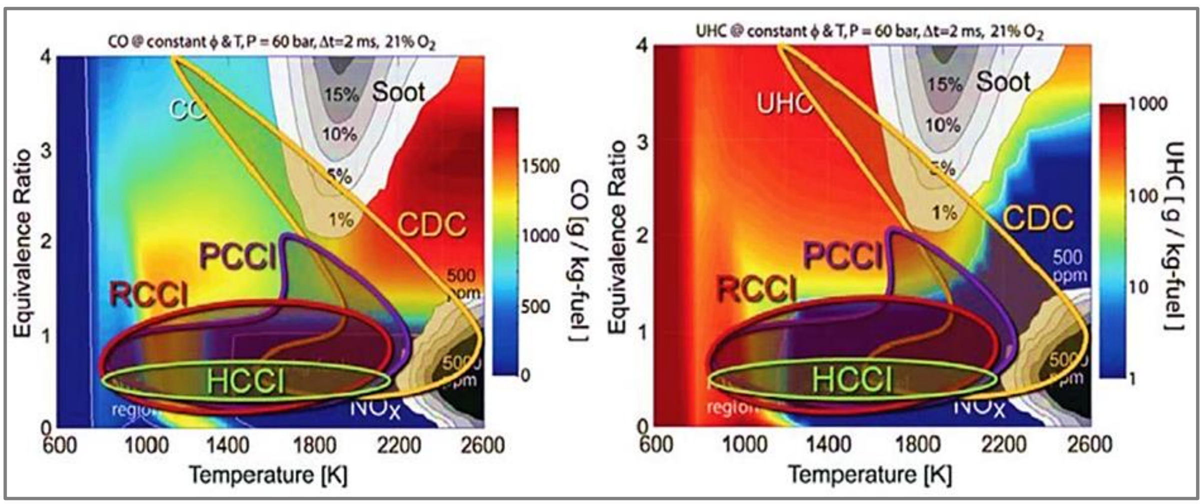

Figure 1.2 Emissions contour plot

Sources: (Martin et al., 2009; and Paykani et al., 2016a)

The literature review shown in Table 2.3 shows the research gaps on higher direct-injected diesel fuel auto-ignition quality, which raises questions about combustion phasing control at high engine loads. Therefore, lower self-ignition quality fuel blending can be utilized to customize fuel reactivity, resulting in reactivity stratification that can adapt to high engine load to achieve stable engine operation. The challenges of the dependence on the naturally limited petroleum oil that has been shrinking from time to time is also a driving force for alternative energy. The RCCI diesel engine emits low NOx and PM emissions that have uncontrolled combustion and higher HC and CO emissions. Gasoline-bioethanol blends for the port injection have a low auto-ignition property that can control combustion phasing and reduce HC and CO emissions.

1.3. Problem Statements

Even though, the conventional diesel engine had been functioning for a while because of a wide range of applications due to their high reliability, high power density, higher thermal efficiency as a result of their capability to operate at higher compression ratio, leaner fuel-air charge, and lower throttling losses; its challenges are high level of soot and oxides of nitrogen (NO_X) emissions. The other challenge is the dependence on naturally limited petroleum oil which has been shrinking from time to time.

The RCCI engine is an advanced LTC engine that was invented to reduce NOx and soot emissions has the shortcomings of higher HC and CO emissions similar to other LTC strategies. Hydrocarbon and carbon monoxide emissions from RCCI engines are greater than those from conventional diesel combustion.

Direct-injected diesel fuel has higher auto-ignition quality, which raises questions about combustion phasing control at high engine loads. Therefore, lower self-ignition quality fuel blending can be utilized to customize fuel reactivity, resulting in reactivity stratification that can adapt to high engine load to achieve stable engine operation.

A piston bowl design can optimize the interaction between diesel and premixed fuel, resulting in a more uniform mixture for better control of combustion phasing. This optimization improves combustion stability, efficiency, and emissions. The optimized design enhances fuel spray pattern, injection timing, and fuel-air mixing, allowing for precise control of combustion timing to achieve the desired balance between efficiency and emissions. By reducing peak cylinder temperatures and minimizing NOx emissions, the optimized piston bowl design improves overall performance and alleviates environmental impact.

Several researchers contributed their parts towards the advancements of the internal combustion engine and looked for alternative energies to overcome the problem stated. One of the best options on which many researchers are working is on low-temperature combustion which looks at the engine to minimize the emission and optimize thermal efficiency. Therefore, this research investigated by using engine hardware redesign of the intake manifold and fuel controlling mechanism for the port injector integration, alternative fuels, and emission at the same time and uses parameters like speeds, fuel blend ratio, piston bowl geometry, and load to have another advanced input.

1.4. Objectives

1.4.1. General objective

The primary objective of the research was to investigate the effects of high reactivity fuel with gasoline-bioethanol blends on reactivity controlled compression ignition (RCCI) engine.

1.4.2. Specific objectives

The specific research objectives to attain the goal were to:

- Investigate the combustion, performance, and emission level of a diesel engine running with conventional diesel fuel (Baseline experiment)**.**
- Carry out experimental investigation on RCCI engine under high reactivity fuel (DI) and low reactive fuel blend ratio through (PFI) into the intake manifold including validation with baseline**.**
- Study numerically the combustion, performance, and emission of diesel engines under varying piston bowl designs (piston bowl shape geometry).
- Study the effect of main fuel start of injection timing on combustion, performance, and emissions characteristics of the diesel fuel with the low reactivity fuel**.**

1.5. Significances and benefits of the study

After accomplishing this dissertation work, the investigation of HRF with the blends of low reactivity effects on the RCCI engine had the following significance and benefits:

Ecological effect: engine operation with G25E75 port injected fuel had a minimum of NOx, and CO2, which were a maximum for the engine running with the baseline experiment (neat diesel fuel). HC and CO are lower with G50E50-RCCI engine combustion mode.

Performance effect: the power of the engine is higher at maximum engine speeds of 3000, and the brake torque is the maximum during the speed range of 2400-2600 rpm with a premixed blend ratio of G25E75. RCCI engine had better thermal efficiency at a speed range of 1900-

2100rpm with a premixed blend ratio of G50E50 and for the speed ranges of 2200-2700 was maximum at baseline fuel and at the engine speeds range of 2800-3000rpm was good at premixed blend ratio of G25E75-RCCI engine respectively.

Economic aspects: foreign currency savings due to ethanol substitution to realize the performance and emissions of RCCI compared with the conventional diesel compression engines.

New knowledge generation: this study can be used for several types of research to come up with and the finding can create another new insight that can aid as a preliminary reference point for the other researchers while motivating further research on alternative fuels and RCCI engines. This can also; support poverty reduction issues by finding ways of reducing dependence on petroleum-based fuels that appear to have increased prices and demand.

1.6. Scope of the study

Engine research is a broad and interdisciplinary field that encompasses multiple aspects, including combustion physics, engine design, control systems, fuel chemistry, emissions control, and overall engine performance. However, for the current investigation, the research scope focuses on the combustion of internal combustion engines. Experimental performance metrics such as brake power, brake torque, brake thermal efficiency, and brake-specific fuel consumption; analyzing combustion characteristics (cylinder pressure, cylinder temperature, and heat release rate) and measuring emissions (nitrogen oxides, PM, carbon dioxide, hydrocarbons, and carbon monoxide) and their validations and numerical investigations based on piston bowl shape are considered.

Other factors related to combustion, performance, and emissions, such as ignition delay period, mechanical efficiency, friction power, and summer emission concentrations, were not included in the study due to various constraints.

1.7. Limitations of the study

Research limitations refer to the factors or constraints that may hinder the scope, validity, or generalizability of a research study. The limitations that arose in the present study were due to various factors. Some of the limitations are as shown below:

- Studies on the particulate matter from the emission were not measured and analyzed in the research due to the lack of a PM emission tester.

- Even though the effect of the cylinder temperature is shown indirectly by the CP and normalized volume; the cylinder temperature was not directly acquired from combustion because of the lack of a temperature sensor embedded within the engine cylinder and hence not included in the data logger from the engine test rig.
- One of the limitations faced during the research was the lack of a well-established automotive laboratory at the university. The absence of fundamental hardware, instruments, and infrastructure, such as an engine test rig and emission testers for NOx and PM, further compounded the difficulties. The limited availability of laboratory supplies had a notable impact on the research process, leading to extended timelines and delays. Despite these challenges, efforts are made to overcome the limitations and ensure the validity and reliability of the research findings within the given constraints.
- The research encountered financial limitations, which imposed constraints on the available budget. These financial constraints created troubles in conducting an extensive study. The expenses associated with obtaining fundamental materials and accessing expertise from distant sources posed significant challenges. The recent inflation in the Ethiopian market further exacerbated the situation, making it more challenging to afford the basic materials required for the research.
- Despite these challenges, we remained committed to producing meaningful results within the available resources. Every effort is made to maximize the impact of the research by ensuring the validity and reliability of the study's findings. Adapting the approaches and making the most of the available resources, it is achieved the highest possible quality and significance of the study within the financial constraints faced.

1.8. Organization of the dissertations

Chapter 1 Introduction: Included brief description of the background and motivation of the study, pin pointed justification for CDC and RCCI engine, states the problem of the research, fixed the goals, elaborates importance, and scope of the studies included, and particularize the benefits of the investigation.

Chapter 2 Literature review: reviewed the literature on conventional and advanced engine combustion concepts under development (SI, CI, HCCI, PCCI, PPCI, and RCCI); fundamentals of RCCI engine combustion mode that had done before; evolution of LTC strategies; system description of RCCI with different fuel engine, and identified research gaps are included in this section.

Chapter 3 Materials and method: Consisted of different materials, machines, and fuels that are used to experiment are listed and all methodological approaches that followed to accomplish the research are briefly incorporated in this chapter.

Chapter.4 Results and discussions: The investigation of various piston bowl geometry shapes (DSDoPBG) numerically for diesel engine combustion in a light-duty single-cylinder engine; experimental investigation of the RCCI engine speed and port-injected fuel blend ratio; the diesel engine of the LDRCCI has three fuel physiognomies. Comparatively and in detail, the baseline experiments on the RCCI engine depending on the main fuel start of injection findings

Chapter 5: Conclusions and recommendations: depending on the results of the study, conclusions for the general output shown and recommendations as well as the future research direction for the next generations are clearly defined.

References: to assure the academic property of the other that serves me as a baseline for my investigation, all concepts of the papers that are used in these dissertations are properly cited.

Appendices: Different supplementary materials used for the studies are properly placed on the last paper' page.

CHAPTER TWO

2. LITERATURE REVIEW

2.1. Introduction

The CIE is one of the most popular engines, which has the advantages of low fuel consumption, lower CO and HC emissions, lower running costs, more efficiency due to the capability of operating at a higher compression ratio, a leaner air-fuel charge, and lower throttling losses. The problems are caused by comparatively high emissions of soot and nitrogen oxides (Hanson et al., 2013; Soloiu et al., 2013). The current focus for diesel engine development is on reducing fuel consumption, NOx emissions, and PM. Research on clean, efficient, and alternative combustion principles has been going on for more than 20 years. The CDC engine progressed to higher pressures of common-rail direct injection, pre and post-main injection, exhaust-gas recirculation rate with powerful cooling, and turbocharger (Naima et al., 2013). Additionally, by boosting the specific output, diesel engines allow for some downsizing. Particular focus is paid to exhaust treatment, which uses particulate filters and oxidation catalytic converters to minimize CO, HC, NOx, and particulates (Sharma et al., 2015). Particularly for heavy-duty vehicles, selective catalytic reduction (SCR) with dissolved urea injection offers an alternative.

There are various development lines for petrol and diesel fuel engines to improve force generation while lowering fuel consumption, emissions, and noise. Their current development is characterized by reduced fuel consumption, declining emissions (CO_2, HC, CO, NOx, particulates, dust), good driving behavior, enhanced specific power, reduced friction, minimized energy consumption, reduced oscillations, and reduced noise. Engines are equipped with mechatronic components to accommodate rising variabilities and control functions (Isermann, 2014). When compared to traditional combustion strategies, low-temperature combustion is an advanced combustion strategy that can concurrently minimize soot and NOx emissions. LTC is a sophisticated combustion concept that might satisfy the strictest environmental regulations. There are other advanced strategies as well, such as homogeneous charge compression ignition (HCCI), premixed charge compression ignition (PCCI), partially premixed charge ignition (PPCI), and reactivity control compression ignition engine (RCCI), all of which have characteristics in common with LTC. The RCCI is a more modern low-temperature combustion engine technique, whereas the HCCI was the first low-temperature combustion engine. Some evolutional developments on the internal combustion engine are elaborated as it is shown below:

2.2. Conventional diesel engine combustion(CDC)

Since compression ignition is the most reliable and efficient method of combustion, it is used in conventional diesel engines. This powertrain is considered to be the most promising. In today's passenger light and heavy-duty cars, as well as commercial vehicles and industrial uses, it is widely employed. Diesel engineering is rapidly expanding as an applied engineering profession to fulfill the challenges of creating optimal diesel engines due to modern emissions rules and consumer requests. Diesel engine design engineers are becoming more and more numerous. Optimizing engine performance requires a system design approach, which makes the process run more smoothly. System design, from high-level product strategy planning to detailed production designs, is critical to the integration of concurrent engineering processes for the development of diesel engine products. Comparing engine combinations and creating system performance parameters using a variety of analytical techniques were used in the system design process. Several fundamental technical areas are covered by the system design, such as the integration of the vehicle's engine and after-treatment system, thermodynamic cycle performance, matching the engine's induction system and turbocharger, system friction, and electronic controls. For engine system design and powertrain technology assessment, it is crucial to comprehend the basic properties of diesel engines (Isermann, 2014).

Diesel engines have an advantages over gasoline engines, including reduced fuel consumption, reduced CO_2 emissions, high thermodynamic cycle efficiency, reduced pumping loss, high torque at low speeds, improved drivability, and reduced emissions of hydrocarbons (HC) and carbon monoxide (CO) because of the high air-fuel ratio used in diesel combustion. Diesel engines are widely used as medium to heavy-duty power plants because of their superior fuel economy, great power, and high low-end (low speed) torque. When compared to their gasoline counterparts, diesel engines have several design obstacles. Higher particulate matter (PM) emissions from engines as a result of heterogeneous combustion; decreased air usage as a result of heterogeneous combustion; and more challenging tailpipe outlet NOx control. Diesel engines run with a lean air-to-fuel ratio, so the three-way catalyst used for NOx control in gasoline engines cannot be employed in diesel engines. According to (Heywood, 2018), lean burn combustion results in lower exhaust temperatures, which helps manage emissions from diesel engines.

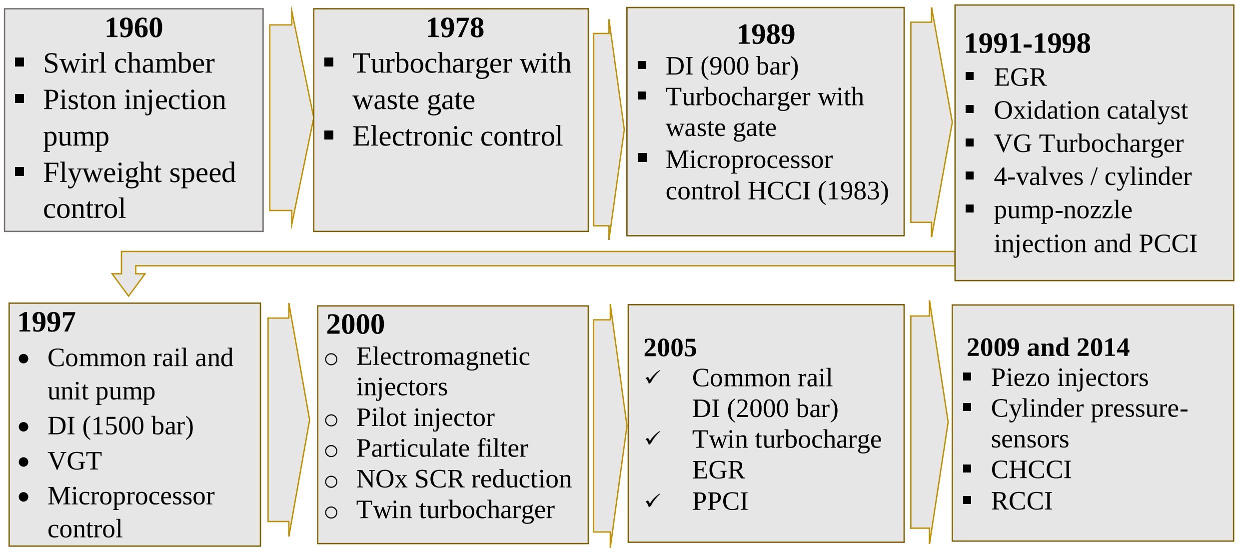

Figure 2.1 Historical development of diesel engines

Sources**:** (Paykani et al., 2015)

Due to increased noise from fuel injection, combustion, and mechanical impact, heavier engine weight, and the requirement for a robust construction to withstand the high peak cylinder pressure brought on by a high compression ratio, these factors may make diesel particulate filter (DPF) regeneration challenging. Additionally, a reduced engine-rated speed because diesel engines' heterogeneous combustion is limited to a modest combustion speed. Automotive diesel engines typically have a rated speed of 2,000-to-4,000 rpm as opposed to 6,000-to-7,000 rpm like gasoline engines, which results in a lower power density (Xin. 2011). Reduced specific power per volume of engine displacement, more challenging to start in cold conditions, is caused by the restriction of rated speed and, consequently, rated power. Due to the aforementioned issues, researchers are compelled to look into internal combustion diesel engines further in the ways listed below:

2.3. Advanced internal combustion engine(LTC)

Because low-temperature combustion reduces nitrogen oxide (NOx) and particulate matter (PM), it is a widely accepted technology in internal combustion engines. Rich districts are characterized by low-temperature combustion techniques that use injection timing to boost air-fuel emulsion before the onset of ignition, hence repressing the generation of particulate matter. Based on the self-ignition chemistry of diesel fuel, low-temperature combustion is primarily regulated knock (Manente et al., 2010). Modern internal combustion diesel engines use a variety of advances and technology to increase performance, lower emissions, and improve efficiency. As seen in Fig 2.2, these are some significant developments (evolutions) from the early to the more sophisticated current IC engines.

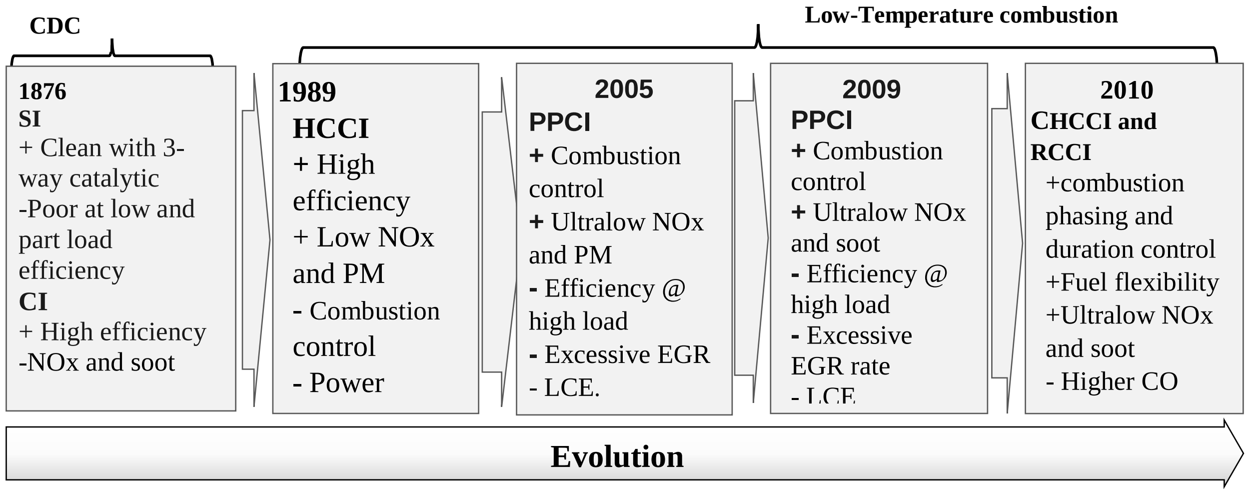

Figure 2.2 Evolution of internal combustion engine

Sources**:** (Paykani et al., 2015)

2.3.1. Homogenous charge compression ignition (HCCI)

Internal combustion engines use a sophisticated combustion mechanism called homogeneous charge compression ignition, or HCCI. It combines components of compression and spark ignition. By lowering emissions from conventional engines, HCCI seeks to match the efficiency of diesel engines. Conventional spark and compression ignition engines operate satisfactorily, but spark ignition engines have poor component quality, low load efficiency, and excessive CO emissions. High emissions of NOx and particulate matter are produced by compression ignition engines. The first HCCI combustion system and homogeneous mixture preparation which involved early fuel injection into the combustion chamber were developed in the late 1990s. The most promising concept for future internal combustion engines is the HCCI combustion engine. When it came to brake efficiency, they were on par with diesel engines and better than modern gasoline engines. The advantages of HCCI engines are reduced particulate matter, ultra-low NOx emissions, and high engine efficiency. These advantages are ascribed to volumetric auto-ignited combustion of the compressed lean air-fuel mixture. Low specific output, limited operating range, lack of control over the ignition process, lengthy start-up times, and high pollutants such as CO and HC emissions are some of the disadvantages of

HCCI engines (Liu et al., 2021). Having the combined qualities of the SI and CI engines makes it one of the first LTC concepts. Premixed air-fuel charge is used in HCCI engines, just like in spark ignition (SI) engines. The air-fuel combination is compression-ignition or self-ignited, like in diesel engines. A novel combustion technology called homogeneous charge compression ignition may eventually replace diesel engines, which have minimal emissions of NOx and particulate matter and excellent efficiency. Since the HCCI Engine runs on lean fuel by nature and typically reaches an ultimate flame temperature well below 2000K, it produces significantly less NOx and soot. It had effectively demonstrated to several investigators that, in comparison to traditional CI engines, the rate of NOx and soot formation was incredibly low. Fig 2.3 depicts the dual fuel supply system (Ryskamp et al., 2016; Splitter et al., 2010).

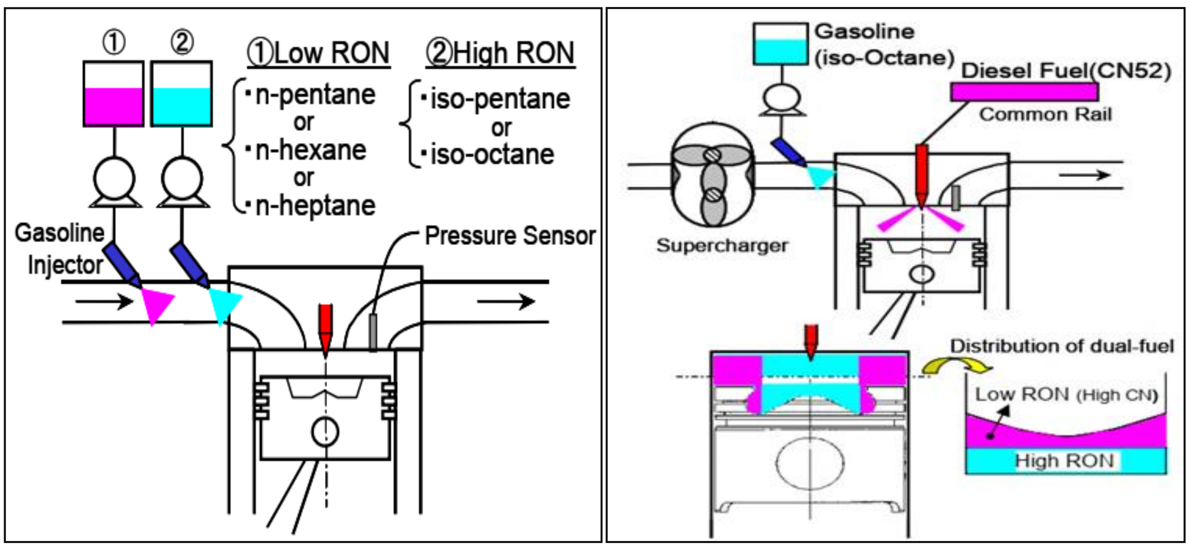

Figure 2.3 Single-cylinder HCCI and PCI engines

Source: (Inagaki et al., 2018).

Table 2.1 Analysis comparing the CI, SI, and HCCI engines

	Comparison of CDC SI engine and HCCI			Comparison b/n CDC CI engine and HCCI		
No	Basis comparison	SIE	HCCIE	Basis comparison	Diesel engine	HCCI
1	Efficiency	Less	More	Efficiency	High	Equally high
2	Throttle losses	More	No	Combustion-T°	1900–2100 K	800–1100 K
3	Compression ratios	Low	High	Cost	Higher	Lesser
4	Combustion duration	More	Low	Ignition duration	Higher	Lesser
5	NOx	greater	Low	PM and NOx	More	Less

Source: (Aceves et al., 1999)

2.3.2. Premixed charge compression ignitions (PCCI)

PCCI is a combustion concept that combines elements of both conventional gasoline SI and CI to attain enhanced fuel efficiency and reduced emissions in ICE. PCCI seeks to attain the benefits of both combustion modes by partially premixing the fuel and air before ignition. Premixed charge compression ignitions (PCCI) offer superior control over combustion rate and timing than homogenous charge compression ignitions(HCCI) because of the uncontrolled combustion mode, which dictated all injection time and the start of combustion (Selvan et al., 2018; Srihari et al., 2017). The difficulty of backfiring at lower loads; knock at maximum load and HPRR due to uncontrolled combustion was somehow better solved using a PCCI engine (Splitter et al., 2010). Research into the possibility of adjusting fuel reactivity to regulate premixed charge compression ignition combustion techniques. At both high and low engine loads, in-cylinder fuel mixing with port fuel injection of LRF and early cycle direct injection of diesel fuel was utilized to manage the rate of pressure rise and to regulate the phasing of combustion. In the first portion of the study, optimal fuel blends and EGR combinations were suggested for HCCI operation at two engine loads of 6 and 11-bar net IMEP using the KIVA-CHEMKIN code and a reduced primary reference fuel (PRF) mechanism. It was discovered that the ideal fuel reactivity needed to be reduced with increasing load and that the lowest fuel consumption could not be attained with just neat gasoline or neat diesel fuel. PRF 80 and 50%, respectively, were found to be the ideal fuel blend and EGR rate for HCCI operation at 11 bar net IMEP. Engine tests with a dual-fuel PCCI method were conducted, utilizing a wide angle and big nozzle hole conventional diesel injector for early cycle numerous injections of diesel fuel and port fuel injection of gasoline (Splitter et al., 2010). Because low temperatures minimize NOx, low-temperature combustion ignition is preferable. Additionally, LTC techniques use injection timing to promote air-fuel mixing before the ignition, reducing rich regions and suppressing PM generation. It is based on the fuels' chemistry of self-ignition and is, in theory, a controlled knock.

2.3.3. Partially pre-mixed charge ignition (PPCI)

Partially premixed charge ignition has the advantage over homogenous charge compression ignition and the diesel combustion approach. The PPCI engine operating style maximizes the benefits of the dual-fuel working strategy while reducing the drawbacks of HCCI. According to (Juneja and Sandhu 2019), the partially premixed charge ignition approach involves injecting some fuel through a typical direct injection system and mixing the remaining fuel externally before spraying it into the cylinder. The fuel is not continuously blended with air. The PPCI combustion technique was extended to high-load scenarios by the pilot injection, which had the greatest impact on combustion. The apparatus of combustions affected by cylinder pressure levels and pressure rise rates based on main and pilot burning were analyzed. To meet the future requirements of clean and efficient engines, numerous combustion techniques have been researched to reduce NOx and soot emissions while preserving acceptable thermal efficacy.

Partially premixed charge ignition (PPCI) combustion is considered an effective approach for achieving low-temperature combustion. PPCI involves different levels of fuel stratification and has been inspired by combustion research. According to a study by (Splitter et al., 2010), PPCI is identified as the most effective technique for reducing emissions. It utilizes diesel fuel and offers distinct advantages for both compression ignition and spark ignition engines.

To meet the future requirements of clean and efficient engines, numerous combustion techniques have been researched to reduce NOx and soot emissions while preserving acceptable thermal efficacy. Combustion research has supported PPCI, as stated by (Marriott and Reitz, 2002). These methods dealt with the stratification of fuels at different ranks. Improved charge indication, a minimum compression ratio, increased injection pressure, and excess emission recirculation are used to achieve ignition delay. Exhaust gas recirculation (EGR) reduction and delayed injection of a single LRF can be used to achieve PPCI. This combustion approach has been accepted in work with a different term using controlled-kinetic diesel fuel introduced by (Kimura et al. 2001) and an identical large ignition system presented by a study that looked into the effects of temperature for different emulsion induction and surplus-air amount (λ) on combustion and discharge features of a PPCI engine run on an n-butanol/petrol mixture. The rise in the cylinder (T_{in}), maximum pressure P_{max}, HRR_{max}, and crank angle (CA) position for the test fuels B100, B90, B80, and B70 exhibit a repeating growing trend and progressively move towards the crank angle of 10% heat release rate at CA10 and CA50. The length of the combustion process is decreased, and the $COVP_{max}$ (coefficient of variation for peak pressure) decreases as well. Generally speaking, the best fuel emulsion is B90G10, which is 90% biodiesel and 10% gasoline. As seen in Fig 2.4, T_{in} had the greatest effect on the two mixes' partially premixed charge ignition.

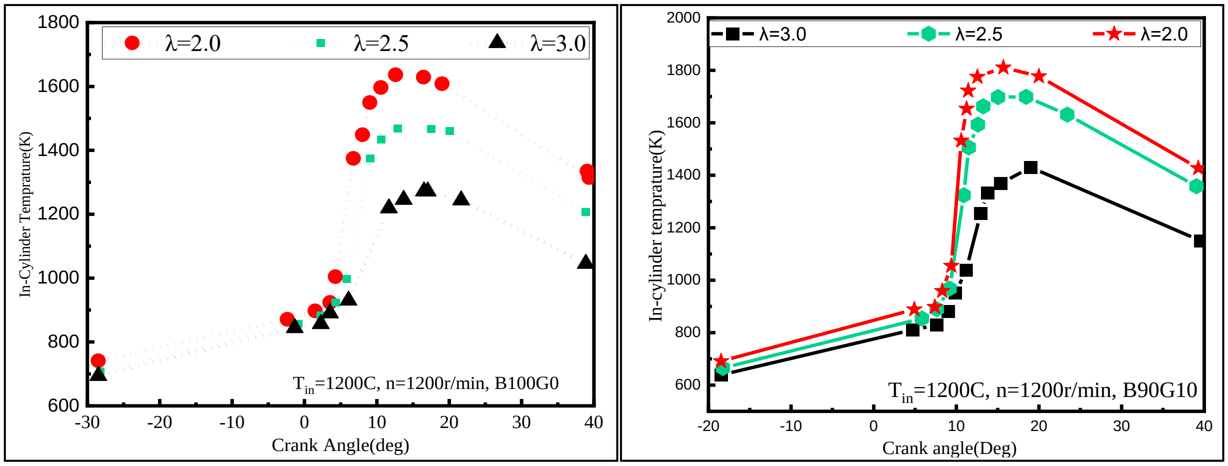

(a) CT at B100G0 and 1200 r/min (b) CT at B90G10 and 1200 r/min

Figure 2.4 Engine temperature with altered λ

The combustion and emission characteristics of PPCI were investigated by (Wang et al. 2018) using a two-stage fuel oil delivery system that combined direct injection and PFI. The advanced position was secured at 9°CA before the top dead center (bTDC) was supplied with low reactivity primary references fuel oil. The study focused on the responses between the diffusion combustion DI fuel and the PPCI fuel at both high and low temperatures. With more than 50% EGR, LTC attributes of reduced NOx and PM emissions may be successfully achieved. As illustrated in Fig 2.5, the NITE increased by using maximum EGR rates while retaining ultra-low NOx and PM emissions. More EGRs in conjunction with the proper pre-mixed proportion could potentially result in more effective low-temperature combustion. Compared with normally inducted situations, enhanced intake had the power to instantaneously reduce engine NO_x and PM emissions.

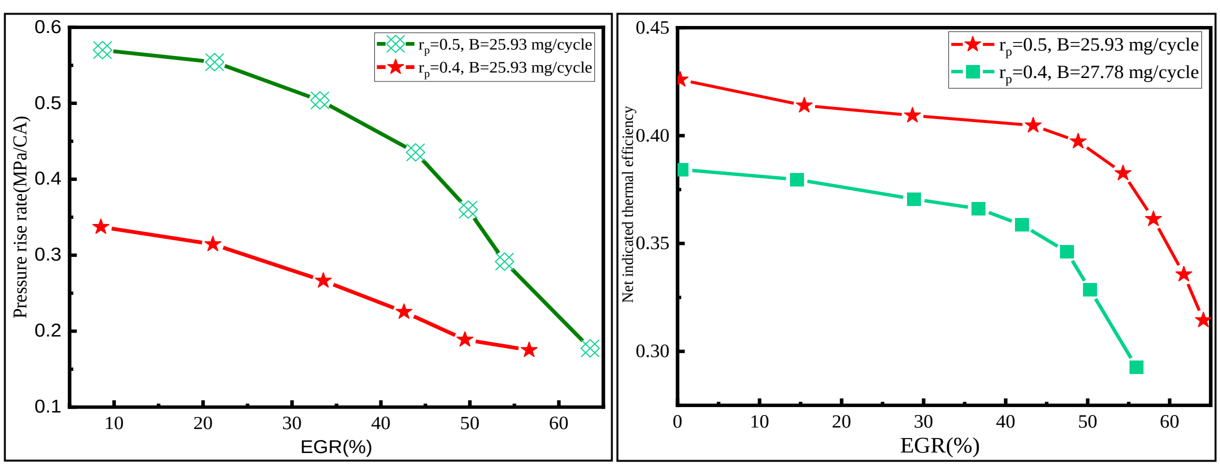

(a) EGR effect on PRR (b) EGR effect on NITE

Figure 2.5 Engine PRR and NITE are impacted by EGR.

The test fuel-air and petroleum consumption rates were measured throughout the inquiry process. Thus, it was possible to obtain the following ratios: pre-mixed ratio r_p, partial equivalence ratio of direct-injected fuel Φ_d, partial equivalence fraction of the premixed fuel Φ_p, and total equivalence ratio Φ:

$$r_p = \left(\frac{\dot{m}_p}{\dot{m}_d + \dot{m}_p}\right) \qquad \text{(Eq 2.1)}$$

$$\Phi_p = \left(\frac{\dot{m}_p + AF}{G_{air}}\right) \qquad \text{(Eq 2.2)}$$

$$\Phi_d = \left(\frac{\dot{m}_d + AF}{G_{air}}\right) \qquad \text{(Eq 2.3)}$$

The fuel depletion rate of PFI and DI PRF50 is indicated by $\dot{m}_p$ and $\dot{m}_d$, respectively; G_{air} denotes the mass flow rate of air, and AF signifies the stoichiometric air-fuel proportion of PRF50.

$$\Phi = \Phi_p + \Phi_d \qquad \text{(Eq 2.4)}$$

The stability and combustion efficiency of petrol PPCI engines presents challenges when operating at low loads. Auto-ignition issues with higher octane gasoline fuels, unburned hydrocarbon fuel, and carbon monoxide discharge at lower load and engine speed operating conditions are challenges in petrol PPCI machines. Another issue is low incineration efficiency, which increases fuel depletion. Therefore, it calls for reducing CO and unburned hydrocarbon emissions before their atmospheric release (Zhang, 2018). The removal of the HCCI mode's drawbacks, such as the engine's limited range of operation, backfiring at low loads and knocking at higher loads, and poorer combustion regulation, as well as the enhancement of the dual operation approach's benefits and reduction of the NOx and PM challenges associated with CDE, is a positive advantage of the PPCI. The PPCI combustion technique is extended to the high-load situation by the effects of the first or pilot injection on the combustion. Because gasoline PPCI increases fuel consumption, it has issues with low engine speed operating settings, auto igniting problems with higher octane fuels, low combustion efficiency, and stability and effectiveness of combustion at low load. Compared to diesel oil, gasoline fuel shows lower soot emissions under all operating conditions. It achieved incineration at a high load by using a dual infusion to lower HRR. The core injects improve combustion, and the early pilot injects of diesel oil commence per low temperature-heat discharge bTDC. Unlike most other LTC approaches, the combustion method's inspirational outcome may be directly regulated by the start of injection (SOI) timing. Diesel PPCI requires greater EGR charges but can lower the tradeoff between NOx and PM. Diesel PPCI's comparatively high boiling point and reduced volatility, which increased the fuel problem while using advanced injection, are further drawbacks. Diesel fuel is therefore not the best option for PPCI setup due to these factors.

2.3.4. Reactivity control compression ignition (RCCI)

Numerous benefits come with reactivity control compression ignition, such as reduced emissions of nitrogen oxide (NOx) and particulate matter, good thermal efficiency, and the ability to use a variety of fuels. To achieve stable combustion across a range of operating situations and optimize fuel injection parameters, RCCI necessitates advanced engine management and fuel control systems. Research and development into reactivity control compression ignition is now underway, with the goals of streamlining the combustion process, enhancing control schemes, and tackling problems related to emissions control and combustion stability.

Low reactivity fuels (LRF) such as gasoline, bioethanol, methanol, and natural gas (NG) are pre-mixed through port fuel injection in reactivity control compression ignition. On the other hand, highly reactive fuels such as diesel, biodiesel, and (LRF+ cetane improver) are directly injected during the compression stroke. Similar to the dual-fuel HCCI, DF-PCCI, and single-fuel PPCI, the RCCI offers improved control over ignition-related issues. Its increased thermal efficiency of up to 60% has been described. Reactive control compression ignition was developed based on research by (Kokjohn et al. 2010), and it demonstrated superior fuel reactivity compared to other advanced combustion approaches. Numerous advanced combustion techniques have been presented in the past few decades. As a result, the RCCI uses a range of fuel blends, such as gasoline and diesel (Kokjohn, 2012), Methanol-diesel (Karthik et al., 2021), ethanol-diesel (Willems et al., 2021a), Gasoline-biodiesel (Yang et al., 2016), diesel-NG (Mohammadnejad et al., 2019), diesel-CNG (Dahodwala et al., 2020) and gasoline-gasoline (Dempsey et al., 2015) with small cetane number improver(DTBP, 2-EHN). It is better in efficiency than other advanced combustion techniques in fuel reactivity (Pedrozo et al., 2021; Reitz, et al., 2010b). The utilization of natural gas (NG) in dual-fuel heavy-duty engines has the potential to significantly decrease pollutant and greenhouse gas emissions in the transportation sector compared to conventional diesel engines. However, the composition of NG and the occurrence of methane slip are important factors to consider as they can impact the benefits of NG as an alternative fuel, particularly concerning greenhouse gas emissions. Through their research, (Curran et al., 2014) demonstrated that combining reactivity-controlled compression ignition (RCCI) combustion with low-temperature internal exhaust gas recirculation (LIVC) can result in up to 80% lower methane and nitrogen oxide (NOx) emissions, as well as relatively higher net indicated efficiency, when compared to conventional dual-fuel systems, regardless of the NG composition. For their study, (Curran et al., 2014) utilized a modified 2007 GM 4-cylinder 1.9L turbocharged diesel engine. The original equipment manufacturer (OEM) pistons were replaced with RCCI-modified pistons, which had a specially designed bowl geometry optimized using computational fluid dynamics (CFD) modeling. The modified piston design aimed to minimize surface area and reduce heat transfer losses. Additionally, the compression ratio was lowered from 17.1 in the OEM configuration to 15.1, allowing for higher load operation while maintaining reasonable pressure rise rate limits. In-cylinder blending of gasoline and diesel fuel was employed to achieve RCCI combustion, which has been shown to reduce NOx and particulate matter (PM) emissions while maintaining or improving brake thermal efficiency compared to conventional diesel combustion (CDC). The use of a low-reactivity fuel, E30, enabled higher load operation during drive cycles. It is conceivable and being researched to increase the RCCI drive cycle coverage by altering the engine hardware and fuel selection. The car equipped with a 2009 PFI gasoline engine is compared to the results of the RCCI fuel simulation over several drive cycles, with the former demonstrating at least a 20% increase in fuel efficiency over the PFI baseline.

Fang.,(2016) conducted an experimental inquiry titled "Experimental investigation of reactivity-controlled compression ignition combustion in diesel engines using hydrous ethanol". In this investigation, a modified Isuzu 4HK1-TC medium-duty diesel test engine with direct injection and four-stroke, four-cylinder inline 1.298-liter engine displacements was used for the experiments. The engine was connected to a DC dynamometer that could operate in two modes; power absorption and engine motoring. Diesel fuel distribution and fuel injection management were handled by the standard common-rail direct-injection diesel fuel supply system. Using hydrous ethanol as the main fuel, a thorough experimental inquiry was carried out in this work to investigate the operability region, characterize the performance and emissions, and optimize the key operational parameters of RCCI operation. Hydrous ethanol has been demonstrated to function well in RCCI operation with an ethanol energy percentage of up to 75% across a broad variety of engine load conditions, even with a water concentration of up to 25% by volume. On the other hand, high load circumstances necessitate exhaust gas recirculation (EGR) and low load heating of the intake charge.

Li et al., (2017) researched a clean and highly efficient combustion approach for engines that use compression ignition. To minimize emissions, low-temperature combustion with a highly diluted and premixed charge is typically combined with low-heat rejection principles. Lean operation or high-level exhaust gas recirculation (EGR) is commonly used to achieve dilution. These methods all have the trait of having a lower flame temperature to minimize NO_X and soot emissions while preserving high thermal efficiency. LTC can be divided into three categories based on the types of LTC like HCCI, PCCI, and RCCI.

Kaddatz et al. (2018) employed a light-duty, single-cylinder research engine to conduct experiments to examine RCCI combustion utilizing a single fuel and the addition of 2-ethylhexyl nitrate (EHN), a cetane improver. The two methods of fuel delivery are direct injection of E10 blended with 3% EHN and port-fuel injection of E10, or 10% ethanol in gasoline. The outcomes of comparing an E10+diesel dual-fuel strategy against an E10+EHN strategy. It was discovered that the additional E10 blend could achieve regulated PCI operating under a variety of circumstances and operated similarly to diesel fuel. The current work demonstrates that in contrast to other low-temperature combustion studies utilizing EHN, the nitrogen in the fuel only slightly increases NOx emissions because the amount of EHN is so little (about 0.3% of the total fuel). While NOx emissions from E10-EHN RCCI are marginally greater than those from E10-diesel RCCI, overall NOx levels are less than 1 g/kW-hr. The "Mexican-hat" piston bowl design was created using a genetic algorithm in conjunction with a computational fluid dynamics (CFD) code to implement a narrow-angle direct injection (NADI) approach.

An inline 6-cylinder heavy-duty turbocharged 8.4L CR of 17.5:1 with a rated speed of 2200 rpm and a port fuel injection system fixed at 5.5 bar and 360° CA ATDC, respectively, was the subject of an experimental investigation by (Pan et al. 2020). The research team self-developed the port fuel injection system and common rail system controlled by the ECU. the operation is managed by an eddy current dynamometer with a 4000 Nm rated power and a 2800 rpm rated speed. The data acquisition and analysis system, which included a shaft encoder (Omron

E6C2-CWZ3E), charge amplifier (Kistler 5011B10), data acquisition card (NI USB6353), and cylinder pressure transducer (Kistler 6125C), was used to measure the combustion parameters. Gaseous emissions were analyzed using a HORIBA MEXA-7100DEGR gas analyzer. The PM was measured using a combustion DMS500 MKII particle spectrometer, which has a measuring range of 5–1000 nm for particle diameter. Furthermore, in this study, the upper dead center of the compression stroke is 0°CA. The iso-butanol/diesel RCCI combustion mode achieves lower CO, HC, NOx, number concentration of nucleation mode particles, number concentration of accumulation mode particles, and total particle mass when compared to the gasoline/diesel RCCI combustion mode. Additionally, compared to the gasoline/diesel RCCI combustion mode, the iso-butanol/diesel RCCI combustion mode produces less NOx and particle emissions (Pan et al., 2020a).

2.3.5. RCCI combustion based on the types of fuels used

2.3.5.1.Single-fuel RCCI Combustion

To produce effective and low-emission combustion in internal combustion engines, single fuel reactivity regulated compression ignition combustion ideas (RCCI) use a single fuel (LRF) for the port injection and direct injection (LRF+Cetane improver). Single-fuel RCCI combustion is optimized by adjusting the intake conditions, fuel properties, and injection strategy to achieve desired performance, efficiency, and emissions characteristics. Advanced engine management systems and control algorithms are employed to optimize the combustion process. Single-fuel RCCI offers benefits such as high thermal efficacy, low NOx and PM emissions, and the potential for using a single fuel instead of multiple fuels (Kakaee, and Paykani, 2020). However, it also presents challenges in terms of controlling combustion timing, managing the spatial distribution of reactivity, and achieving stable and consistent combustion across various engine-operating conditions. The cetane number is a commonly used statistic in compression ignition engines to describe reactivity. This word refers to a fuel's quality of ignition. The behavior of the fuel in comparison to two reference fuels, n-hexadecane (CN=100) and heptamethyl nonanes (HMN) (CN=15), is the basis for the determination of the cetane number. CN is defined as follows:

$$CN = (\text{n-hexadecane in \%}) + (0.15*\%\ HMN)$$

All fuels have a cetane number, although fuels that ignite easily have a higher CN value (~46 typical of U.S. diesel), whereas fuels that resist auto-ignition have a lower CN value (~15 typical of gasoline). The fuel's composition determines its CN; the more reactive the constituents, the higher the CN of the fuel. By adding or removing highly reactive fuel species, the CN of a fuel can be artificially altered using this connection. According to (Splitter., 2012), 2-HEN and DTBP are the most often utilized cetane improvers in fuels. They are often blended into low-reactivity fuel intended for use in diesel engines. For premixed port injection and in-cylinder direct fuel injection, the majority of single-fuel RCCI combustion modes use a single-fuel LRF. However, because direct injected fuel has a lower cetane number, its LRF is less reactive. To increase the reactivity, the cetane number improvers such as 2-HEN and DTBP are employed to increase the CN of the fuel that is directly injected, as indicated in Table 2.2 below.

Table 2.2 Fuel characteristics of LRF, DTBP, and 2-EHN cetane improver

	Cetane Improver		Low Reactive Fuels for DI and PFI			
Properties	2-EHN	DTBP	Gasoline	Ethanol	Methanol	NG
Chemical Formula	$C_8H_{17}NO_3$	$C_8H_{18}O_2$	C_8H_{15}	C_2H_5OH	CH_3OH	CH_4
Molecular weight(g/mol)	175.23	146.23	111	46	32	16
Heat of vaporization (KJ/kg)	-	-	307	873	1147	509
Low heating value (MJ/kg)	27.4	33.8	43	26.95	20.05	49.77
Stoichiometric A/F in mass	8.48	10.85	14.6	9	6.5	17.2
Density at 25°C	0.963	0.796	750	783	787	0.7
Cetane Number	-	-	14.5-20	6.5	7	0
Motor Octane Number	-	-	80-91	107	106	120
Research Octane Number	-	-	92-99	89	92	120

Sources: (Splitter, 2012)

Owing to iso-butanol's higher octane number, a notably large amount of direct injection fuel is required to match ignition phasing. Nearly negligible NOx and soot emissions are shown by PFI of E10 and DI of E10 doped with 3% 2-EHN by volume when compared to RCCI operation utilizing PFI gasoline and direct injection diesel fuel at a load of 5.5 and 9 bar IMEP. The different researchers use a single fuels RCCI Engine of low reactivity fuel for PFI and DI with cetane improver. The amounts of cetane improver depend on the octane value of the direct-injected fuel. The percentage of DTBP addition on ethanol and iso-butanol alcohol should be more than gasoline because of their higher value of octane number to improve the fuel reactivity of directly injected fuel fraction to get NOx and PM mandate in a cylinder.

2.3.5.2.Dual-fuel RCCI Engine (Diesel-NG/CNG)

Hockett et al., (2017) studied MD-CFD Simulation compared with injecting time curve from a diesel engine improved with the port-injected natural gas. However, the overly fast combustion speed at combustion could not be eliminated. CONVERGE 3-D computational fluid dynamics incineration model by extensive reaction mechanisms was established to simulate an LD diesel-NG reactivity control CI engine. A parametric study was done to investigate the influence of the diesel direct fuel injection approach, first diesel fuel injection pressure, and injectors spray angle of RCCI performance and released pollutant emission characteristics. Increasing PR, the NG causes a lesser combustion rate and extended ignition delay. Therefore, the PHRR, RI, and combustion temperature declined. The ringing force was used as the indicator of knocking RCCI engines that can be computed by the following equation:

$$\mathrm{RI}\left(\frac{\mathrm{MW}}{\mathrm{m}^2}\right) = \frac{1}{2\gamma}\times\frac{\left[0.5\left(\frac{\mathrm{dp}}{\mathrm{dt}}\right)_{\mathrm{max}}\right]^2}{\mathrm{P}_{\mathrm{max}}}\sqrt{\gamma \mathrm{RT}_{\mathrm{max}}} \qquad \text{(Eq 2.5)}$$

Where: R is a gas constant = 8.3144598 $J.K^{-1}.mol^{-1}$, T_{max} is the maximum in-cylinder temperature (K), P_{max} is the maximum in-cylinder pressure, γ is the ratio of specific heats, ringing intensity RI (J/kg. K) is the gas constant, and (dp/dt) max is the MPRR of in-cylinder pressure (kPa/ms). RI has a restriction of less than 5 MW/m2.

The diesel fuel injection method regulates the in-cylinder control's local responsiveness. By using a split injection technique, the local equivalence ratio of ignition temperature increases as the combustion temperature rises due to the initial SOI retarded to TDC. The amplified local reactivity blend of the second injecting pulse increases incineration temperature and consequently increases NOx creation. Wall impingement results from the increased diffusion of diesel droplets caused by the higher first injection compression. A high HC and CO release is thus caused by the narrow SAS in the vicinity of the wall and crevice volumes. Accordingly, richer materials produce a locally higher reactive zone at a higher combustion temperature, and more NOx emission at a lower spray angle (Dhahad et al., 2021; Kakoee et al., 2018).

Methane numbers (MN) of 80.9, 87.6, and 94.1 are available when using the various gas combinations designated to replicate different NG compositions at 0.6, 1.2, and 1.8 MPa IMEP load. When compared to traditional diesel engines, natural gas in dual-fuel heavy-duty engines has the potential to reduce transportation-related pollutant and greenhouse gas emissions. The traditional NG-diesel dual-fuel method was shown to be less susceptible to changes in MN than the RCCI incinerator. At 0.6 MPa IMEP, the auditory effects of MN on the NIE were more noticeable. Overall, the study showed that, regardless of the composition of the natural gas, the combination of the RCCI and LIVC may produce up to 80% reduced methane slip and NOx discharges and relatively higher NIE than the traditional dual-fuel regime (Pedrozo et al., 2021; Paykani, et al., 2020).

2.3.5.3.Dual Fuel RCCI Engine (Diesel-Gasoline)

To accomplish efficient and low-emission combustion in internal combustion engines, an advanced combustion system called a dual fuel reactivity regulated compression ignition (RCCI) engine, or more precisely the diesel-gasoline RCCI configuration, combines the use of both diesel and gasoline fuels. In this setup, gasoline is employed as a secondary fuel to adjust the mixture's reactivity, while diesel fuel serves as the primary fuel for ignition and combustion control.

In-depth research on CI engines running at minimum load and powered by port-injected gasoline and in-cylinder direct-injected diesel fuel was conducted by (Benajes et al., 2014). In response, the local equivalence ratio evaluation following the SOI and up to the SOC was calculated using 1-D spray modeling. This resulted in RCCI outcomes in a stage combustion process controlled by mixture reactivity stratification. As the amount of in-cylinder fuel emulsion varies toward a low global reactivity blend (up to 25/75% diesel-gasoline percentage), the ignition delay lengthens and the fuel reactivity of the stratification improves. Diesel has improved IT, a more stratified fuel mixture, and fewer zones of poor local reactivity throughout the cylinder. This combustion plan illustrates feasible emission limits for EURO VI. Cons; high levels of CO and HC were detected, primarily as a result of the crevice effect, such as those seen in top land crevices, where burning low-reactivity oil is more challenging (Benajes et al., 2014).

Wang et al., (2016) saw a parametric investigation for allowing RCCI operation in a CI engine at altered loads. Very minimum soot and NOx with HTE at mid-to-high engine loads. The small load process was excessively high in hydrocarbon and carbon monoxide emissions. Further raised diesel proportions to widen the low-load operational range, and raise the global/entire chemical reactivity of in-cylinder air-fuel charge. The main issues to the simplicity of great load reactivity-control combustion ignition operation are higher EGR rates, higher gasoline operation, and advanced injection timing. Though, ultra-high EGR rate or early injection timing might create instable combustion, creating the combustion phasing controller extremely tough (Wang et al., 2016). RCCI was increased as a solution control PCI strategy, that avoided PM, and NOx formation by prompting a lean A/F mixture and low-temperature combustion. Therefore, the study by (Molina et al., 2015) focuses on invasive results of multiple engine operational factors over combustion to suggest suitable techniques for extending RCCI operation in an HD single-cylinder research engine from low to full load. Using parametrical research, many strategies are applicable for low, medium, and high load, varying fuel and air reactivity. 3D-CFD modeling and engine testing are used to examine efficiency and emission outcomes. Lastly, RCCI activities' engine release and performance output are synchronized with CDC. The outcome implies that RCCI operation from low-mid load may be achieved by the twofold injection strategy. However, to minimize the excessive in-cylinder pressure gradient from high-full load operation, a single injection technique must be adopted from Molina et al., (2015). Thermal efficiency was maximized in dual fuel RCCI combustion, with 87 and 99 percent reductions in PM and NOx emissions, respectively, in comparison to CDC. When comparing the two-fuel RCCI combustion to the combustion of ordinary diesel fuel and diesel PCCI, the emissions of HC, CO, aldehyde, and ketone increased. The study found that the DOC was efficacious in eliminating formaldehyde, HC, and CO from exhaust under high speed and load conditions. Particle in contrast to diesel PCCI combustion, no size distribution for the dual-fuel RCCI emission suggested a smaller diameter or fewer concentration particles; yet, the particle mass emission was around two times higher. According to (Kokjohn et al., 2010b), this indicates that although semi-volatile organic was gathered in the dual-fuel RCCI PM filter samples, saturation ratios were insufficient for nucleation and droplet formation to elevate the particle number concentration.

2.3.5.4. Dual-fuel (Diesel-alcohol) RCCI Combustions

Dual-fuel RCCI combustion with a blend of diesel and alcohol fuels is an advanced combustion concept that aims to achieve efficient and low-emission combustion in internal combustion engines. In this configuration, diesel fuel is used as the primary fuel for ignition and combustion control, while alcohol (such as ethanol or methanol) is used as a secondary fuel to modulate the reactivity of the mixture. In the dual-fuel (Diesel-Alcohol) RCCI combustion, diesel fuel is directly injected into the combustion chamber during the compression stroke, similar to conventional diesel combustion. The diesel fuel injection is timed and controlled to achieve the desired ignition and combustion characteristics. The alcohol fuel, injected into the intake manifold, mixes with the intake air before entering the combustion chamber. The mixture formation and distribution are optimized to ensure the desired reactivity gradient within the combustion chamber. The presence of alcohol in the intake air modulates the reactivity of the overall mixture. The combustion process is carefully controlled to achieve efficient and low-emission combustion. These controls are crucial for achieving stable combustion, controlling the reactivity gradient, and optimizing performance and emissions. The diesel-alcohol RCCI combustion configuration offers advantages such as improved fuel efficiency, reduced nitrogen oxide (NOx) and particulate matter emissions, and the potential for using renewable and sustainable alcohol fuels. However, challenges related to fuel system integration, combustion control, and managing the reactivity gradient need to be addressed for practical implementation.

Hanson et al., (2013) investigated the special effects of biofuel emulsion in RCCI combustion to maximize ethanol content in a commercial fuel from 10 to 20%. Ethanol in the LTC has been shown peak load to be maximized from 8-to-11 bar and peak BTE to be maximized from 40 to 43%. MPRR and HRR were reduced at E20, which improves a load from 8-to-10 bar BMEP, while the purposes of E85 allowed further increase from 10-to-11bar and E20 was found to decrease combustion efficiency, heat transfer, and exhaust losses (Hanson et al., 2013)**.**

The influence of hydride ethanol fuel in combustion and emission in a dual fuel RCCI ignition was investigated by (Liu et al., 2018). It uses port-injected wet ethanol and direct-injected diesel fuel. Effects of intake temperature, rate of EGR, and the injected fuel pressure were also investigated. Accordingly, the higher the ratio of port-injected pure ethanol amongst the entire fuels cause's decrease in combustion effectiveness and ITE. Even though the concentration of ethanol can be reduced, CO and THC emissions still rise. In every test condition, soot emissions are almost zero. A suitable increase in intake temperature is beneficial for improving combustion and emissions, as evidenced by the fact that higher incoming temperatures increase peak HRR and MPRR and have a positive impact on combustion efficiency. Additionally, higher intake temperatures minimize the release of CO, NOx, and total hydrocarbons. Longer ID and more homogeneous charge, improved combustion productivity, and decreased release of NOx, THC, and CO without increasing soot emissions are all results of the higher EGR rate. Increasing injection pressure results in a decrease in ID and a rise in peak HRR, which further improves the ignition efficiency and reduces the THC and CO emissions, especially for ethanol impurity conditions (Liu et al., 2018).

Rosa et al., (2020) investigated the start of injection effects and wet ethanol contained in the RCCI explosion engine. This uses renewable fuel and potential to operate in an engine for RCCI combustion. Wet ethanol as an LRF is port injected and DI into the engine performance, and make possible RCCI process and the parameters are varying wet-ethanol concentration, ethanol PFI duration, and the starts of injections. The different water in ethanol concentrations in many substitution rates is tested, and the impacts of varying starts of diesel injection were studied. Increasing the ethanol fraction under all test conditions increased the ignition delay. In a whole conditions test, the combustion constancy was within the standard range. Only an advanced start of injection is a possibility to achieve RCCI combustion. The highest peak pressures were acquired with the earliest SOI that delivers extra time for mixing diesel-wet ethanol in the air (Rosa et al., 2020).

Pan et al. (2020) compared the results of an experimental investigation into the combustion and discharge characteristics of iso-butanol-diesel RCCI at low load to those of gasoline-diesel RCCI. The outcome demonstrates that iso-butanol-diesel RCCI outperforms gasoline-diesel RCCI in terms of power recovery. The IMEP of iso-butanol-diesel RCCI is 1.4 and 3.9% less than CDC mode, respectively, when a premixed ratio (Rp) is 50 and 60%. ID, combustion duration, CA50-CA10, extreme mean in-cylinder temperature, and ITE all climb in response to an increase in Rp in RCCI combustion means, combustion phase delay, an ultimate HR value, and MPRR reduction. Rp stands for the low reactivity fuel energy to ethanol ratio in this study. It can be computed using the formula that follows:

$$\mathrm{R_P} = \frac{\mathrm{M_L + Hu_L}}{\mathrm{M_L + Hu_L + M_H + Hu_H}} \qquad \text{(Eq 2.6)}$$

Where: - M and Hu represent mass, the tested fuel respectively flows, and LHV. The subscript L and H denotes low and high reactivity fuel respectively.

The late combustion phase, extended ID, combustion duration, CA50, CA10, excessive mean in-cylinder hotness, and ITE are features of the iso-butanol-diesel RCCI. Furthermore, for gasoline-diesel and iso-butanol-diesel RCCI, the increase of Rp, CO, soot, and NOx is decreased but the growth of HC is increased. When compared to gasoline-diesel RCCI exhaust pollutions, the iso-butanol-diesel RCCI achieves lower CO, HC, NOx, and PM emissions (Pan et al., 2020b). An initial experimental instance that was chosen to serve as a baseline ran under typical RCCI conditions, using the r_c = 14.9:1 piston at 1300 [r/min]. The study determined the BTE from a given gross thermal efficiency (GTE) and gross indicated mean effective pressure (IMEPg) by using the friction mean effective pressure (FMEP) and pumping mean effective pressure (PMEP). What we have at the crankshaft is the brake mean effective pressure (BMEP). The difference between the indicated mean effective pressure (IMEP) and friction mean effective pressure (FMEP) is known as the BMEP.

$$\mathrm{BMEP} = \mathrm{IMEP} - \mathrm{FMEP} \qquad \text{(Eq 2.7)}$$

The total of the pumping mean effective pressure (PMEP), mechanical rubbing mean effective pressure (RMEP), and auxiliary mean effective pressure (AMEP) is the friction mean effective pressure (FMEP).

$$\mathrm{FMEP} = \mathrm{PMEP} + \mathrm{RMEP} + \mathrm{AMEP} \qquad (2.8)$$

A certain level of gross efficiency is attained, assuming the corresponding losses and the impact on brake performance are examined. This was carried out using the equations in the findings displayed in Fig 2.6 for the DOE's target of +50% brake thermal efficiency (BTE); the required losses and gains in efficiency are visible (Splitter et al., 2013a)

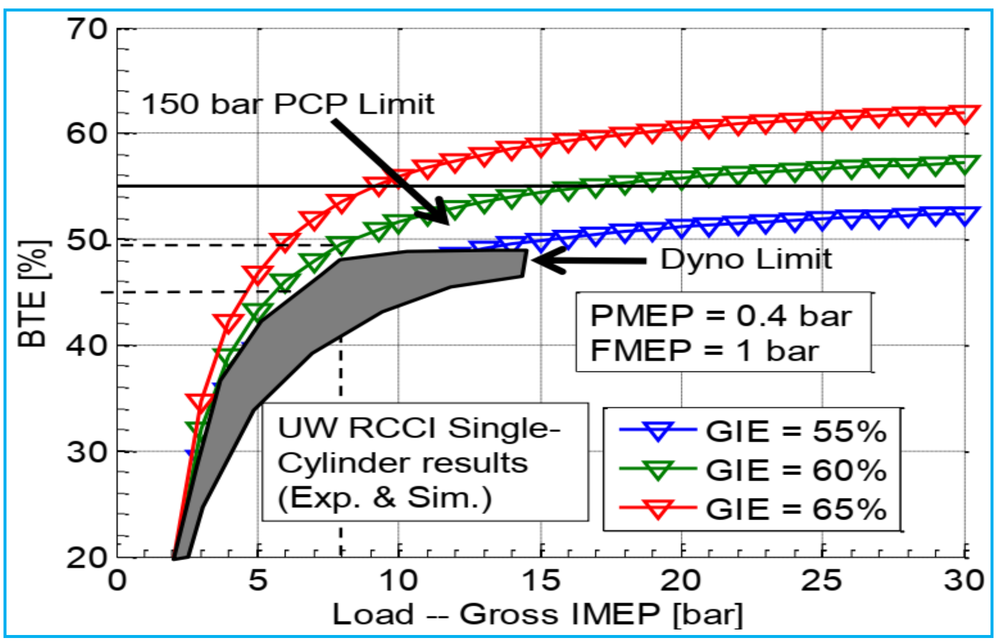

Figure 2.6 Performance and trends required to achieve DOE

Sources: (Splitter et al., 2013a)

In a light-duty diesel engine, the incineration approach known as RCCI with reverse reactivity stratification (R-RCCI) which combines premixed high-reactivity fuel and direct-injection (DI) low-reactivity fuel was investigated at low loads to improve the trade-off between thermal efficiency and peak heat release rate (HRR) of partially premixed combustion (PPC) and the combustion efficiency of reactivity-controlled compression ignition (RCCI). It is discovered that R-RCCI can break the trade-off between nitrogen oxide (NOx) emissions and combustion efficiency by examining its combustion properties. This is because the spray position of the DI fuel, not the 50% burn point (CA50), determines the combustion efficiency of R-RCCI. Indicated thermal efficiency (ITE) and combustion efficiency are significantly enhanced when the timing of the start of injection (SOI) is delayed. This is due to an increase in the amount of fuel injected into the piston bowl. In the meantime, CA50 gradually slows down with delayed SOI timing, hence lowering NOx emissions. Additionally, reverse reactivity control compression ignition(R-RCCI) emits very little soot. Comparing polyoxymethylene dimethyl ethers (PODEn)/P20G80 R-RCCI to PODE n/gasoline R-RCCI, the maximum ITE of the former is noticeably higher. This happens because P20G80's increased reactivity can improve combustion stability and lessen CA50's sensitivity to SOI timing, allowing for an improvement in ITE with a more delayed SOI timing. As seen in Fig 2.7, R-RCCI can, with the same engine configurations, lower the peak pressure rise rate, enhance combustion stability, and increase ITE and combustion efficiency when compared to RCCI at low loads (Duan et al., 2021).

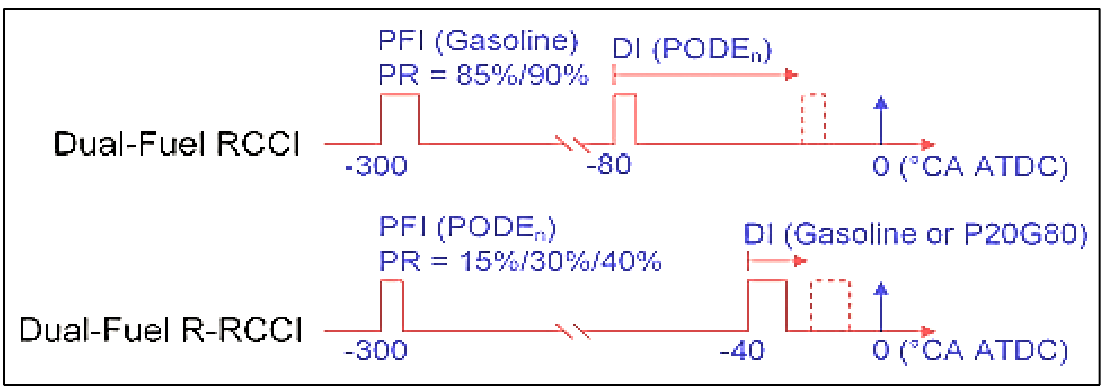

Figure 2.7 Dual-fuel RCCI and R-RCCI operations (PFI, DI)

Sources: (Duan et al., 2021; Saxena et al,.2023)

Because of the higher local fuel concentration in the cylinder, the NOx and soot emissions of RCCI dramatically decline when the premixed ratio is less than 85%. When the premixed ratio of RCCI is greater than 90%, the cylinder's decreased local fuel reactivity causes unstable ignition. Consequently, the two premixed ratios for RCCI in this study 85% and 90% were chosen (Duan et al., 2021). The primary determinants of NOx generation during combustion processes are temperature, reaction time, and oxygen concentration. The graph demonstrates how increased cylinder pressure causes the NOx to grow as the load increases. The reduced

NOx produced by RCCI combustion lowers combustion temperature. RCCI and diesel produce 497 and 857 ppm of NOx, respectively, at peak load. Compared to diesel, the RCCI is 41% lower (Jagankumar et al., 2020). A literature review analysis on published research articles relevant to the research topic involved in identifying, evaluating, and summarizing the current state of knowledge and understanding in a specific field of RCCI has been carried out. A comprehensive literature review conducted as such positioned the study within the existing body of knowledge and demonstrated its significance and originality. The process ensured that the research contributed meaningfully to the field and advanced understanding in the area of study (See Table 2.3). The detailed quantitative validation was presented in Chapter four. Combustion rate control deficiency at higher engine load can be attributed to higher self-ignition features of the direct-injected diesel fuel. There is a need to address issues related to combustion phasing control without using EGR which has a negative impact on increasing emission and reducing power as it is in line with previous observations (Curran et al., 2012). Single-fuel gasoline and methanol port injection fuel have higher HC emissions as it is on par with previous studies (Pan et al., 2020, Ansari et al., 2018). However, expanding the fuel flexibility of reactivity control compression ignition engines and exploring the effects of alternative fuels is an ongoing research priority.

Table 2.3 Single fuel and dual fuel RCCI engine

Author & Year	Parameters (Single Fuel)	CP	HRR	GIE	NOx	Soot	UHC	CO
Mohammadian et al., 2020	As DI ratio % ↑	↑	↑	↑	↓	↓	↓	-
Flavio et al., 2017	↑H_2 fuel Fraction & EGR	-	-	↓	↓↓ & ↓↓	↓↓ & ↓↓	↓ & ↓	-
Jagankumar et al., 2020	As load ↑ for Diesel	-	-		↑	↑	↑	↑
Poorghasemi et al,. [60]	Increasing the PR of NG	-	↓		↓	↓	↑	↑
	Retarding SOI1	-	-	↑	↑	-	↓	↓
	Retarding SOI2	↓	-	↑	↓	↓	↑	↑
Ansari et al., 2018	CDC low load(3-6 bar)	-	-	↑	↑	↑	↓	↓
	RCCI at medium loads	-	-	-	↓	↓↓	↑	↑
	HL RCCI 10 to 12 bar	-	-	↑	↓	↑	↑	↑
Pan et al., 2020	↑Rp Gasoline-Diesel RCCI	↑	↑	↑	↓	↓	↑↑	↓
	↑Rp Iso-butanol-Diesel	↑	↑	↑↑	↓↓	↓↓	↑	↓↓
Curran et al., 2012	Low loads CDC	↓	↓	↓	↑	↑	↓	↓
	Low loads RCCI	↑	↑	↓	↓	↓	↑	↑
	High loads CDC	↓	↓	↑	↑	↑	↓	↓
	High loads RCCI	↑	↑	↑	↓↓	↓	↑	↑
Molina et al., 2015	Med-Max in CP	↑	-	-	↓	↓	↑	↑
	High load- MCP	↑↑	-	-	↓	↓	↑	↑
Wang et al.,2016	Low Load(B-D)	-	-	↑	↓↓	-	↑	↓↓
	Medium load	↑	-	↑	↓	↓	-	-
	High load	↑	-	↑	↓	↓	-	-

In the current study; cetane improvers like (2-EHN, DTBP), blended are used only if the direct injected and port injected fuel is low reactive fuel like (gasoline, ethanol, methanol, NG, and

CNG). But in this study diesel fuel is directly injected and the LRF is used for the PIF. So there is no need for Cetane improvers in the current study since the diesel fuel itself has a higher Cetane number.

2.3.6. RCCI and its appropriate piston bowl design

In RCCI combustion, the design of the piston bowl plays a significant role in achieving efficient and stable combustion. The piston bowl design affects the air-fuel mixture formation, combustion process, and overall performance of the RCCI engine. The shape and geometry of the piston bowl influence the air-fuel mixture formation and distribution within the combustion chamber. The piston bowl design can promote better fuel atomization, air swirl, and turbulence, leading to improved mixing of the fuels and air. This helps in achieving a stratified charge with the desired reactivity gradient for RCCI combustion. The piston bowl design affects the ignition timing control in RCCI combustion. The shape of the bowl and its interaction with the fuel jets influence the ignition and combustion characteristics. Optimizing the piston bowl design can facilitate the desired ignition timing and combustion phasing, ensuring efficient combustion and minimizing the potential for knocking or uncontrolled combustion (Hariharan et al., 2021).

The piston bowl design can have an impact on emissions control in RCCI combustion. By shaping the bowl, it is possible to influence the local air-fuel mixing, combustion duration, and temperature distribution within the combustion chamber. This can help in achieving lower nitrogen oxide (NOx) and particulate matter (PM) emissions, which are critical for meeting stringent emission regulations. The piston bowl design plays a crucial role in achieving stable combustion in RCCI engines. The shape of the bowl affects the in-cylinder flow patterns, turbulence intensity, and fuel-air interaction. A well-designed piston bowl promotes better combustion stability, reducing the likelihood of misfires, combustion variations, and other combustion-related issues. Overall, the piston bowl design in RCCI combustion is an important parameter that can significantly influence the combustion process, efficiency, emissions, and stability. Engine designers and researchers optimize the piston bowl design through computational simulations, experimental studies, and iterative design approaches to achieve the desired performance and emissions targets for RCCI engines (Dempsey et al., 2013).

Global warming, the depletion of nonrenewable energy resources, the enormous cost of petroleum fuel, and serious air pollution have all posed new problems for the widespread use of internal combustion engines. Compression ignition direct injection engines are now more popular in the transportation industry than spark-ignition and gas engines due to their low fuel consumption, higher thermal efficiency, higher compression ratio, leaner air-fuel charge, lower throttling losses; and more durability (Soloiu et al., 2013). Exhaust emission and vehicle fuel efficiency are subject to stringent legislation under present and future legislation. These difficulties necessitate the advancement of advanced engine technologies, and also the implementation of innovative fuels to fossil fuels that are both effective and low in emissions (Mofijur et al., 2019; Reitz, et al., 2010a)**.**

This section provides an in-depth analysis of the equivalence ratio distributions and in-cylinder temperature during the combustion process, to advance our understanding of the best instances' combustion characteristics. The in-cylinder temperature and equivalence ratio distributions at the 50% burning point (CA50) for the ideal scenarios of low, mid, and high loads are shown in Figs 2.8 to 2.10, respectively. It is discovered that the sites of the combustion event and the high fuel vapor concentration are directly associated with the fuel distribution pattern before ignition, which is dictated by the combined impacts of the fuel injection method and piston bowl shape. As depicted in Fig 2.8, both Low-A and Low-B) display a homogeneous equivalence ratio distribution because the direct-injected fuel mass is lower and most of the fuel is premixed at the intake port. For both of the ideal scenarios, this results in the corresponding homogenous combustion characteristics, which is beneficial for the reduction of NOx and soot emissions. This is in line with the earlier findings when operating at low load. As shown in Fig 2.10 (Xu et al., 2021), at mid-load, the local equivalence ratio concentration increases in comparison to low load due to an increase in injected fuel mass.

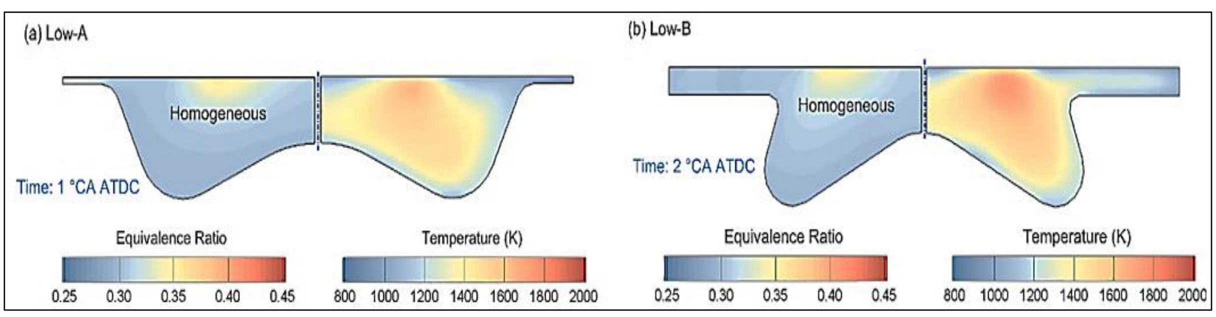

Figure 2.8 T-distributions and the equivalence ratio for Low-A, B at CA50.

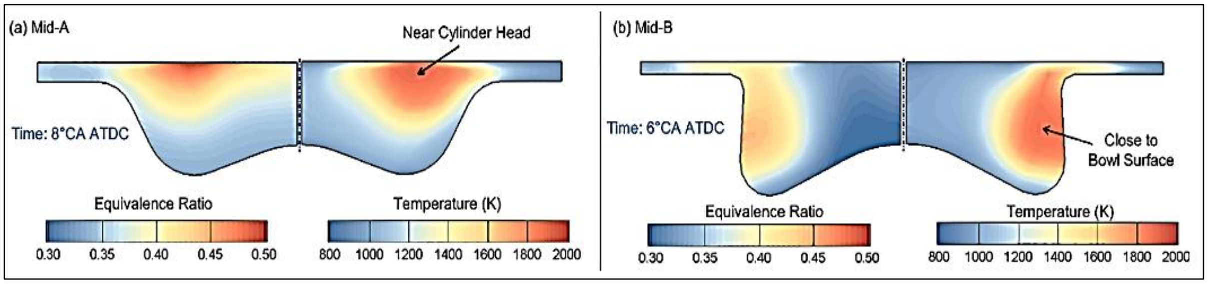

Figure 2.9 Equivalence ratio and T- distributions Mid-A and B.

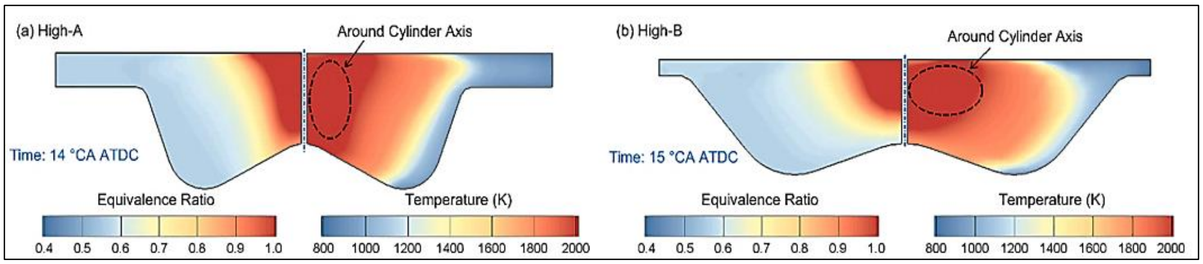

Figure 2.10 Temperature distributions and equivalence ratio

Sources for Fig 2.8, 2.9, 2.10 (Xu et al., 2021)

Several innovative CI combustion methods have been investigated to reduce NOx and soot emissions in a cylinder while retaining HTE (Jacobs et al., 2017; Kokjohn et al., 2011). Various combustion techniques have been investigated to address future demands for cleaner, more efficient engines. The majority of current techniques are classified as low-temperature combustion engines (Micklow, 2016; Ho et al., 2016a; Sharma et al., 2016). A classic diesel-type piston bowl design has been used in several RCCI investigations; however, the mixing requirements for RCCI are projected to differ considerably from those for CDC. Bowl-shaped engine pistons are prevalent in light-duty diesel engines, which benefit from high in-cylinder flows to aid fuel/air mixing. A large and shallow bowl distinguishes the redesigned RCCI piston. As a result, a full understanding of the impact of piston bowl geometry on performance, combustion, and pollution is essential. To provide a clear direction for the current experimental work, a numerical analysis of the influence of combustion chamber shape was conducted first (Dempsey et al., 2013).

In a mixing-regulated combustion mode, conventional diesel engines are intended to burn non-premixed fuel. To aid fuel/air mixing and assure full combustion, this form of combustion needs accurate piston geometry. Due to the early fuel injections, which enable more time for adequate mixing before combustion, further mixing from the piston bowl shape is not required in RCCI. To fully appreciate the benefits of this premixed combustion method, a dedicated

RCCI engine requires a bowl shape that is optimized for RCCI operation. RCCI combustion can benefit from a different piston bowl than traditional diesel combustion, according to previous and continuing research (CDC) (Hanson et al., 2012). CFD engine simulations utilizing the KIVA package were performed to investigate bowl shape parameters to improve thermal efficiency and minimize emissions of RCCI operation in a light-duty engine based on the basic design. The bowl diameter and compression ratio were the two variables in the piston design. The bore radius was adjusted from a narrow, diesel-type bowl to a virtually flat piston because the model may explore the limitations of the design parameters. The radius of the bowl ranged between 49 and 98 percent of the piston radius. The starting engine running circumstances utilized in the model to assess the piston bowl design selected to be reflective of past RCCI incidents. As shown in Fig 2.11, with a piston bowl radius of 2 to 4 cm, the gross indicated thermal efficiency (GIE) rose as the bowl diameter grew. The reduction in heat transfer losses owing to the bigger bowl's smaller surface area generated this gain in GIE (Hanson et al., 2012).

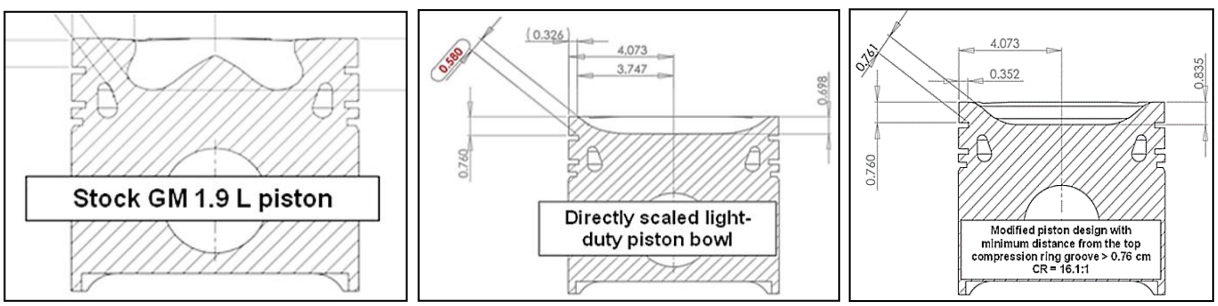

A) OEM PBP B) LDRCCI-HD Bowl C) LD RCCI piston

Figure 2.11 Pistons bowl geometry

Sources: (Hanson et al., 2012)

Using the original diesel injection system and turbo-machinery in a production-type multi-cylinder engine, RCCI operation was successful over a range of engine speeds and loads characteristic of a light-duty vehicle. Both the OEM piston with a high compression ratio and the UW-designed and optimized RCCI piston operated the RCCI well. In comparison to the OEM EURO IV calibration, NOx and PM were reduced by at least one order of magnitude. In addition, HC and CO were elevated by a factor of ten above the OEM calibration. In comparison to RCCI operation using the OEM piston, the double-injection method, and the specially built RCCI piston allowed for a reduction in the maximum pressure rise rate and maximum heat release rate (Hanson et al., 2012). According to (Splitter et al., 2012), the piston-to-liner crevice volume may be a major source of the increased HC emissions from the modified RCCI pistons. There were two pistons utilized, with different bowl shapes and compression ratios. The RCCI findings informed the design of the pistons. The top ring land diameter and squish height of the two pistons varied, as can be seen in the section view. Information about these impacts was discovered in the areas where the research blanks with under-turned pistons were sliced. The top ring land height of the 18.7:1 Cr piston was 6.6 mm, as opposed to 7.6 mm and 10.1 mm for the original CDC piston and the RCCI bathtub, respectively. The 18.7:1 Cr piston's TDC surface area was decreased by 1.2% compared to the 14.88:1 Cr bathtub form and by 5% compared to the CDC piston due to the pancake design's surface area, which would have decreased the possibility of heat transmission. To further reduce surface area for heat transfer, the 18.7:1 piston was surface buffed, in contrast to the 14.88:1 piston.

A comparison study of the wide-shallow and re-entrant engine chambers revealed that the wide-shallow combustion chamber increased the engine operable load range due to the more stable combustion process and decreased likelihood of engine knocking under all operating engine load situations. Under all engine operating conditions, the wide-shallow combustion chamber greatly reduced heat transfer loss. As a result, under light and high load conditions, respectively, the suggested specific fuel consumption was decreased by about 4.8 percent and 6.6 percent for all diesel injection timings. As illustrated in Fig 2.12 (Jafari et al., 2020), diesel injection at 60 CA ATDC dramatically decreased both NOx and soot emissions under low load conditions in both the re-entrant and wide-shallow combustion chambers.

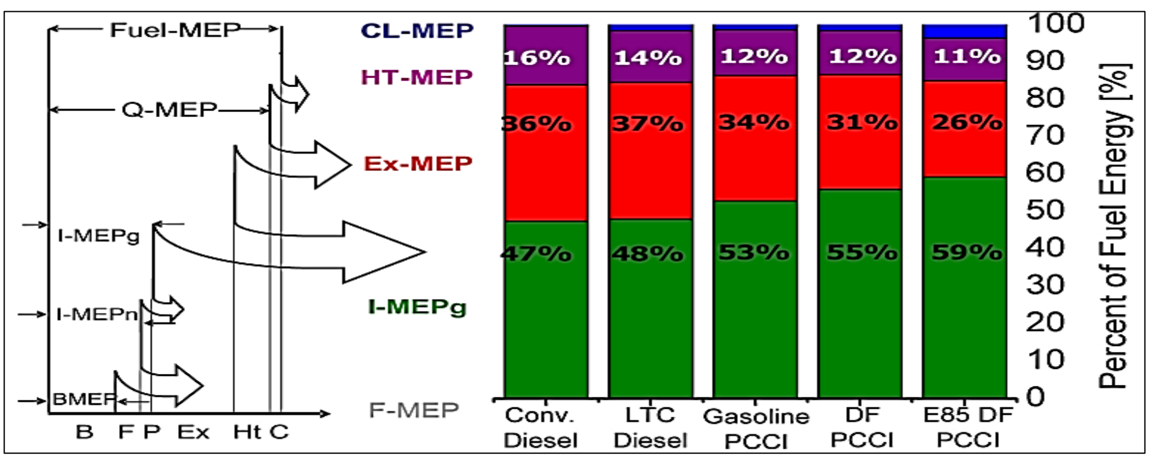

Figure 2.12 Percentage energy content of the base and advanced engine Sources: (Jafari et al., 2020).

As mentioned in the introduction, to reduce well heat transfer while lowering soot and NOx within the squish zone, a range of piston bowl shape designs were developed and tested using computer simulations. More mixing from the piston bowl shape is required for the shorter time DI diesel fuel because of the PBSD, which enables more accurate mixing before combustion (Kuleshov et al., 2014; Zhao et al., 2020).

2.3.7. Injection timing effects on RCCI engine

Injection timing has a significant impact on the performance, combustion characteristics, and emissions of an RCCI engine. By adjusting the timing of fuel injection, the reactivity of the air-fuel blend can be controlled, influencing combustion phasing and overall engine operation. It is important to note that the optimal injection timing for RCCI engines depends on several factors, including engine design, fuel properties, and desired performance characteristics. Engine calibration and control strategies, along with advanced engine management systems, are employed to determine the optimal injection timing and achieve the desired balance between performance, emissions, and fuel efficiency in RCCI engines.

The generation of pollutants and the combustion process in the RCCI engine are studied using mathematical equations and models found in the Converge CFD program (Armin et al., 2021). The computation of the velocity and pressure fields is related to the momentum and continuity equations, while the calculation of the total enthalpy, or static enthalpy, is related to the energy equation. A high reactivity injection plan that advances injection timing (from 30 to 50) causes an increase in cylinder temperature, pressure, and HRR in regions that are nearer the top dead center. Diesel fuel droplets are injected at angles of 55° and 70°, however, they do not entirely mix with the air inside the cylinder. Using a smaller injection angle (55˚) increases the amount of greenhouse gases and CO emissions(Armin et al., 2021). The judgments used two FIPs (500 and 1000 bars) and SOI timings at a constant speed of 2500 rpm had taken place. The lower FIP (500 bars), pressure fluctuations, and ROHR demonstrated enhanced combustion characteristics, however at higher FIP (1000 bars), knocking was seen in some engine operating circumstances. A greater ROHR was seen in the early phases of combustion as a result of the advanced injection timings' fast burning. These findings were also validated by MBF data. Low FIPs improved engine performance, which resulted in lower BSFC and increased BTE at all engine loads. By increasing the SOI, can be enhanced even more. At lower FIP, reduced mass emissions of CO2, HC, and NOx were noted. With increasing engine load, a CI engine's particle number concentration rose. The concentration of particles of all sizes at all loads decreased as the FIP was increased as shown in Fig 2.13 and Fig 2.14. Because improved SOI timings gave fuel-air mixing more time before combustion began, at higher FIP, increasing the injection timings decreased the particle number concentration(Agarwal et al., 2013b).

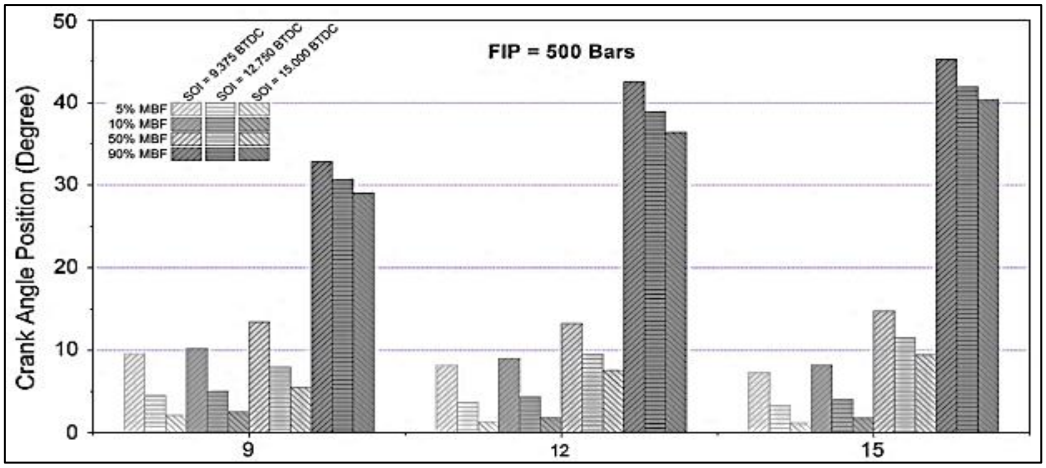

Figure 2.13 Changes in MBF due to different fuel amounts and SOI

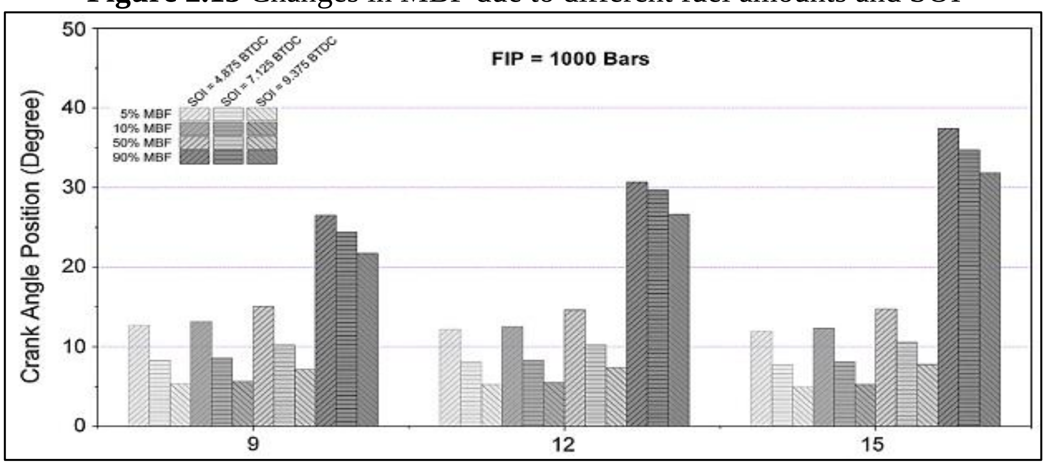

Figure 2.14 Variations in MBF when fuel amounts and SOI are changed

Sources: (Agarwal et al., 2013b).

2.3.8. Ehaust gas recirculation(EGR)

In reactivity-controlled compression ignition (RCCI) engines, exhaust gas recirculation (EGR) is a regularly used technology to manage combustion phasing, minimize NOx emissions, and enhance thermal efficiency. Reintroducing some of the engine's exhaust gases into the intake air charge is known as EGR. The ratio of engine shaft power to fuel input energy is known as the engine's braking thermal efficiency. Peak BTE occurs at the rated power under heavy load conditions since there is less friction and pumping losses (Hanson et al., 2016). Every RCCI case demonstrated lower BTE than CDC at the same total fuel flow rate (Hwang et al., 2018). Depending on the load circumstances, the use of EGR might result in either an increase or decrease in thermal efficiency. Thermal efficiency for dual fuel operation with EGR is often comparable to that of CDC operating (Abdelaal et al., 2012). The average NOx emissions were 8.01 g/kWh without EGR in the study by (Hanson et al., 2016) titled "Comparison of RCCI operation with and without EGR over the full operating map of a heavy-duty diesel engine." Compared to earlier RCCI experiments, the loosened NOx requirements allowed for a peak BTE of 46.8% with lower combustion noise (< 99 dBa) and larger loads (up to 20 bar BMEP). With a cycle average of 4.16 g/kWh, NOx emissions from RCCI operation with EGR were 48% lower. With EGR, the peak BTE dropped to 46.5%. Additionally, compared to non-EGR operation, combustion noise was reduced by 2 dBa. Emissions of CO and HC were comparable to those of earlier RCCI tests, both with and without EGR. Because of the increased intake temperatures and decreased exhaust mass flow, EGR decreased both emissions (Hanson et al., 2016). According to (Dond and Gulhane, 2021), the combination of turbocharger and EGR technology significantly decreased the percentage levels of NOx, HC, and smoke; however, it also increased CO emissions. Reduced NOx and HC levels from engine exhaust were found to be effectively achieved by using delayed SOMI timing.

The study employed a test bench to examine how varied operating conditions and EGR with SCR affect a diesel engine's NO, NO_2, NOx, and fuel consumption rate. When EGR and SCR are utilized in a diesel engine simultaneously, SCR further lowers the NO in exhaust gas based on the reduction of NO emissions by EGR. With an increase in diesel engine load at the same engine speed, the combined effect of EGR and SCR on lowering NO becomes increasingly significant. Under the same operating conditions, the effectiveness of EGR and SCR coupled to reduce NO emission has a threshold that must be crossed before increasing OEV and ANR would no longer significantly reduce NO emission. When the diesel engine was operating at a low load, the NO_2 volume concentration in the engine was low. Little impact is made on the reduction of NO_2 emissions when EGR and SCR are paired. When the engine load increased to 100 or 75%, the NO_2 volume concentration in the engine reached a high point; at the same time, the engine speed was 1885 rpm. When paired with SCR, EGR has a different effect on the reduction of NOx emissions at high engine speeds than when the diesel engine is operating at a low speed. At higher engine speeds than at lower engine speeds, the impact of raising the

OEV on lowering NOx emissions is more noticeable. Conversely, with a low open exhaust valve (OEV), the impact of SCR on lowering NOx emissions is more pronounced. As engine load increases, the diesel engine's fuel consumption rate falls. After being fitted with EGR and SCR, the maximum fuel consumption increased by 3.97% and the minimum fuel consumption increased by 0.60%, indicating that the impact of EGR on the diesel engine's fuel economy is (D. Lou et al., 2022). Ongoing research and development efforts focus on refining the single or dual-fuel RCCI combustion, PBSD, SOIT, and EGR concepts, improving control strategies, and addressing challenges associated with combustion stability and emissions control to make it a viable technology for future internal combustion engines.

2.4. Literature review summary

Conventional diesel engines use compression ignition for superior thermal efficiency and reliability. Diesel engineering is rapidly growing due to modern emissions standards and customer demands. System design is crucial for integrating engineering processes for diesel engine product development, from strategy planning to detailed production designs. Low-temperature combustion is an accepted technology in internal combustion engines due to its nitrogen oxide (NOx) and particulate matter (PM) reduction. Low-temperature combustion approaches normally use injection timing that increases air-fuel emulsion before the start of ignition; hence, rich districts minimize and particulate matter creation is repressed. Low-temperature combustion is, in principle, controlled by knock and based on the self-ignition chemistry of the diesel fuel. Advanced internal combustion diesel engines incorporate various technologies and innovations to improve efficiency, reduce emissions, and enhance performance. Homogeneous charge compression ignition (HCCI) is the first advanced combustion process in internal combustion engines, combining the properties of SI and CI engines. It offers superior brake efficiency, high engine efficiencies, ultra-low NOx emissions, and low particulates compared to gasoline and diesel engines. However, it has drawbacks like low specific output, narrow operating range, lack of ignition control, long start-up time, and high emissions. Premixed charge compression ignition (PCCI) and partially pre-mixed charge ignition (PPCI) are combustion concepts that improve fuel efficiency and reduce emissions in internal combustion engines. PCCI combines diesel and gasoline ignition components, minimizing HCCI limits.

RCCI offers low nitrogen oxide, particulate matter, good thermal efficiency, and fuel flexibility but requires complex engine management systems. Hydrous ethanol can lower NOx emissions, while exhaust gas recirculation (EGR) controls combustion phasing. Dual-fuel RCCI combustion aims to achieve efficient and low-emission combustion in internal combustion engines. It uses diesel fuel as the primary fuel for ignition and combustion control, while LRF is used as a secondary fuel to modulate the mixture's reactivity. However, challenges related to fuel system integration, combustion control, and managing the reactivity gradient need to be addressed for practical implementation. The design of the piston bowl in reactivity-controlled compression ignition combustion is crucial for efficient and stable combustion.

The shape and geometry of the piston bowl influence the air-fuel mixture formation and distribution within the combustion chamber, leading to better fuel atomization, air swirl, and turbulence. Optimizing the piston bowl design can facilitate the desired ignition timing and combustion phasing, ensuring efficient combustion and minimizing the potential for knocking or uncontrolled combustion. The design also impacts emissions control in RCCI combustion, influencing local air-fuel mixing, combustion duration, and temperature distribution within the chamber. The wide-shallow combustion chamber enhanced the engine's operable load range and reduced heat transfer loss, reducing specific fuel consumption under light and heavy load situations, respectively. Injection timing significantly impacts the performance, combustion characteristics, and emissions of a reactivity-controlled compression ignition (RCCI) engine. The optimal injection timing depends on factors like engine design, fuel properties, operating conditions, and desired performance characteristics. Engine calibration and control strategies, along with advanced engine management systems, are used to determine the optimal timing. Advanced injection timings result in greater ROHR in the early combustion phases.

2.5. Research Gaps

Even though RCCI combustion has shown promise in improving fuel efficiency and reducing emissions of NOx, and PM in internal combustion engines, there are still research gaps. Some of the current research areas and challenges in diesel and reactivity control compression ignition engines include:

Developing advanced control strategies is a significant research gap in RCCI engines. RCCI engine combustion involves the simultaneous control of multiple fuel injection parameters, such as quantity and their ratio.

Optimal control strategies need to be developed to achieve stable engine operation. Combustion rate control deficiency at higher engine load due to higher self-ignition features of the direct injected diesel fuel which includes addressing issues related to combustion phasing control without using EGR which has a negative impact on increasing emission and reducing power.

Fuel flexibility and fuel blending of reactivity control compression ignition combustion have been predominantly studied using diesel and gasoline fuels. However, expanding the fuel flexibility of reactivity control compression ignition engines and exploring the effects of alternative fuels is an ongoing research area. The imbalance between efficiency and emissions minimizing peak cylinder temperatures and low NOx emissions due to the combustion phase control problem can be attained by optimizing the piston bowl design.

Investigating the combustion characteristics, emissions, and performance of the RCCI with various alternative fuels, such as biofuels is crucial for understanding the potential of RCCI in future low-carbon and renewable fuel scenarios. Emissions control while RCCI combustion reduces NOx and PM compared to conventional combustion modes, further research is needed to understand and mitigate other emissions, such as hydrocarbons and carbon monoxide.

CHAPTER THREE

3. MATERIALS AND METHODS

3.1. Introduction

In this chapter, all research materials used and the methods that took place at the time of investigations are incorporated. This research typically employs an experimental and numerical approach. There are some common materials and methods used depending on the research objectives. Software for the numerical study on a design of the piston bowl geometry; engine test rig, fuel injection system components, combustion investigative for cylinder-pressure sensor, exhaust gas analyzer (EGA), fuel controlling tools, fuels, and oil are used. The main approach used is the simulation of different piston bowl shape design geometry and the fuel spray model.

3.2. Materials

3.2.1. Diesel engine test rig

The engine model CT100.23 for CT110 configuration of the laboratory engine system test rig is used (See Fig.3.1). The CT 100.15 model pressure transducer for CT 100.23 engine used a quartz pressure transducer. This pressure transducer has a measuring range of 0-100 bar with a maximum allowable pressure of 250 bar. A cylinder pressure transducer is used to monitor operating conditions of the engine combustions for cylinder pressure vs crank angle. An electric motor included in the CT 110 unit starts and slows down the engine. A temperature sensor, flow meter, and circulating pump are all part of the cooling water circulation system. The elastic claw coupling is used to attach the braking unit. It has a connector to detect intake pressure and a sensor to measure the temperature of the exhaust gas.

The engine cooling water circuit capacity of 2.5L and the pump of maximum of 640L/h. The test stand measured the power output of internal combustion engines delivering up to 7.5kW. The main function of the CT 110 was to provide the required braking power. The brake unit is an air-cooled asynchronous motor with an energy recovery unit. The torque and speed are generated using a frequency converter. The energy recovery of the braking energy into the system provided for the highly energy-efficient operation of the test stand. The torque is measured using a suspended brake unit and force sensor. The engine is mounted on a vibrationinsulated base plate and connected to the asynchronous motor. The mass of the base plate in conjunction with the soft bearing support ensures that the test stand runs very smoothly. The asynchronous motor is initially used to start the engine. As soon as the engine is running, the asynchronous motor and energy recovery unit act as a brake unit for applying a load to the engine. The braking power is fed back into the electrical system. In the passive mode of the engine, the asynchronous motor is also used to determine the frictional power of the engine. The switch cabinet contains digital displays for the speed, torque, and temperatures. The measured values are transmitted directly to a PC via USB. The data acquisition software is included (See Fig 3.1).

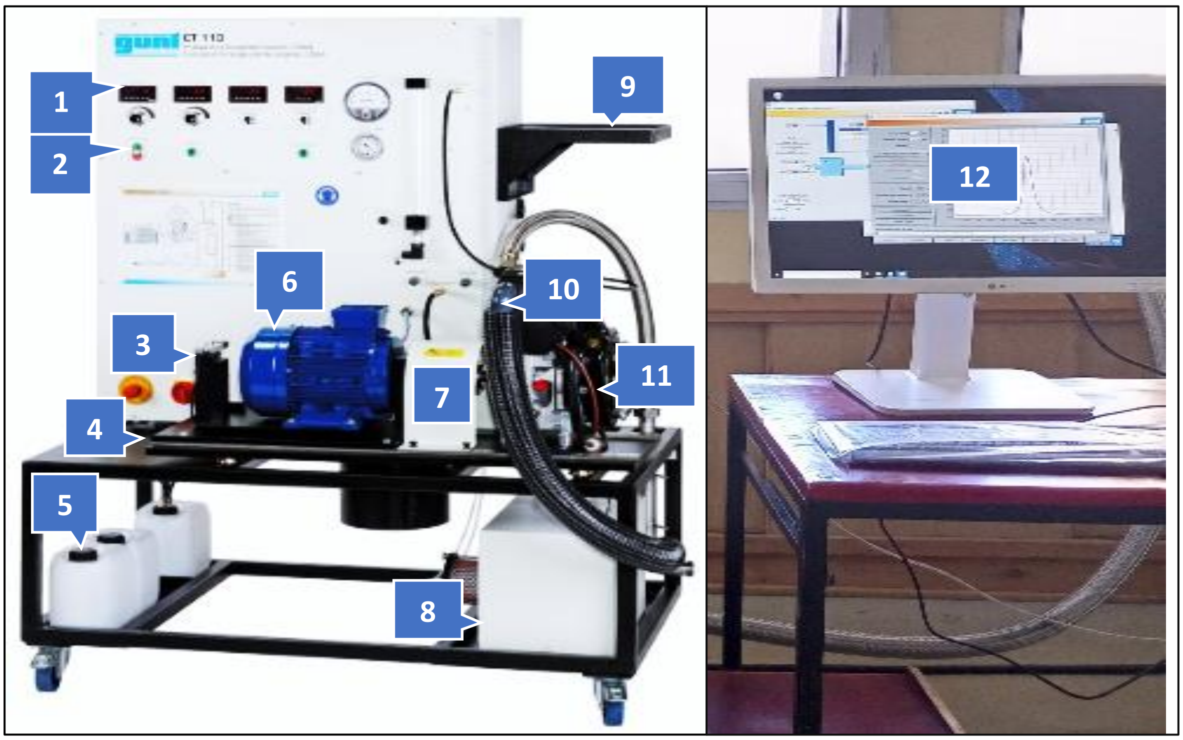

Figure 3.1 Diesel engine test rig

Where:	1	Display	5	Fuel tank with pump	9	Shelf for CT 110
	2	Control board	6	Motor	10	Intake manifold
	3	Force sensor	7	Engine speed	11	Engine
	4	Base plate	8	Stabilization thanks	12	Data acquisition system

The diesel engine shown in Fig.3.1 is modified to a reactivity control compression ignition (RCCI) engine (See Fig 3.2). In the RCCI engine, gasoline-ethanol fuels blend are used for port injection by using a separate fuel reservoir, electronic fuel pump, and electronic fuel port injector for the port injection and diesel fuel for the fuel direct injection. The constant 80% of the diesel and 20% of the gasoline-ethanol blend are used. The 10-15% hydrous ethanol alcohols (C_2H_5OH) and 5-10% of the gasoline fuel are used for advanced RCCI diesel engines

(See Table 3.1). An electronic fuel pump and fuel port injector for LRF are not provided in the engine test rig. Rather, it is separately self-developed for the investigation or study in the advanced engine combustion technology (RCCI). The potentiometer operations in injection volume control mechanism are detailed in the appendix.

Table 3.1 Fuel percentage compositions

Baseline (CDC)			Advanced IC Engine (RCCI)		Combustion simulation
Diesel fuel DI (% Vol)			Diesel(% Vol)	PI blended fuel(in % Vol)	Diesel DI (% Vol)
DI	EPI	GPI	DI	PIBF	DI
100	-	-	-	-	Diesel No-2(100)
100	-	-	80	25/75	Diesel No-2(100)
100	-	-	80	50/50	Diesel No-2(100)

Where: DI- Diesel direct injection, PIBF- port injected blended fuel

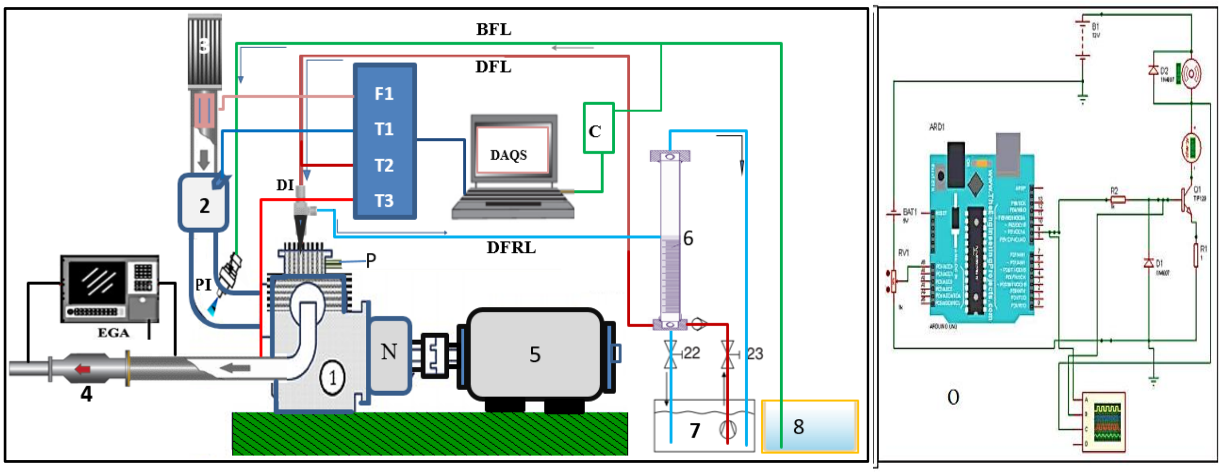

Figure 3.2 Schematic diagram of the RCCI engine

Where:	1	Test Engine	DFRL	Diesel fuel return line	DI	Diesel injector
	2	Quietening vessel	EGA	Exhaust gas analyzer	PI	Port injector
	3	Air filter	C&O	Controlled LRFS	F1	Air flow meter
	4	Exhaust manifold	7	Fuel tank with pump	T1	Intake air temp
	5	Dynamometer	8	Fuel tank with pump (blended)	T2	Fuel temperature
	6	Fuel measuring tube	22	Fuel Drain valve	T3	Exhaust temp
	BFL	Blended fuel line	23	Fuel filling valve	P	Cylinder pressure
	DFL	Diesel fuel line	DAQS	Data acquisition system	N	Crank speed

3.3. Exhaust gas analyzers

An exhaust gas analyzer (model SAXON Junkalor Gmbh) was used to measure and analyze the composition of exhaust gases emitted from the engines. It provides valuable information about the levels of various pollutants present in the exhaust gas, helping to assess the engine's emissions and compliance with emission regulations. The EGA uses infrared absorption to identify the gas components of CO, CO_2, and HC as regular hexane. The separate elements were readily accessible for cleaning and replacement (See Fig. 3.3a). The five gas analyzers (See Fig 3.3b) are genuinely portable and offer easy-to-use features for fault diagnosis, tuning, and pre-MOT testing. The analyzers are also perfect for both static and dynamic testing. It measured CO, HC, CO_2, and O_2, but the EGA shown in Fig. 3.3b is used to measure NOx using electrochemical sensors. A special non-dispersive infrared (NDIR) analyzer that measures any engine exhaust gas and is made to comply with official test standards; HC aids in locating fuel flow and misfire issues; excellent for roadside compliance testing and pre-compliance; rules may apply; take EGA to the vehicle, not vehicle to analyzer; test automobiles under real-world driving situations; lambda and air-fuel ratio aid increase engine efficiency and fuel consumption. Lambda or air-fuel ratio ranges of 0.8-1.2 and NOx 0-5000ppm can be measured. Gasoline, CNG, LPG, and diesel-related emissions can be measured.

a. EGA “INFRALYT” smart b. EGA(KANE-EGA5)

Figure 3.3 Exhaust gas analyzers used to measure emission

Table 3.2 Materials used for the study

Item	Unit	Qty	Remark
Engine dynamometers	Pc	1	-
Gasoline port injector	Pc	1	-
Gasoline fuel	Liter	40	-
Bioethanol fuel	Liter	40	-
Diesel fuel	Liter	40	Number-2
Engine oil	Liter	1	SAE 30
Arduino with the assembly	Pc	1	NUO
Verner caliper	Pc	1	-
Data acquisition system	Ass	1	-
Laze machine	Pc	1	-
Iron bar (35cm diameters)	Meter	1	-
Electric fuel pump	Pc	1	12V
Fuel hose	M	2m	Plastic
Clamps	Pcs	4	-

Materials used for the experiment and analysis of the data are properly shown (See Table 3.2).

3.3.1. Lubricating oil and fuels

3.3.1.1.Lubricating oil for the experiment engine

The diesel engine combustion was filled with the lubricating oil of SAE 30 for the test run lubrication. It is recommended to change the oil after a running-in phase of around five operating hours. The single-grade oil SAE 30 suggested (See Fig 3.4) by the manufacturer is used for the oil change at about every 100 operating hours.

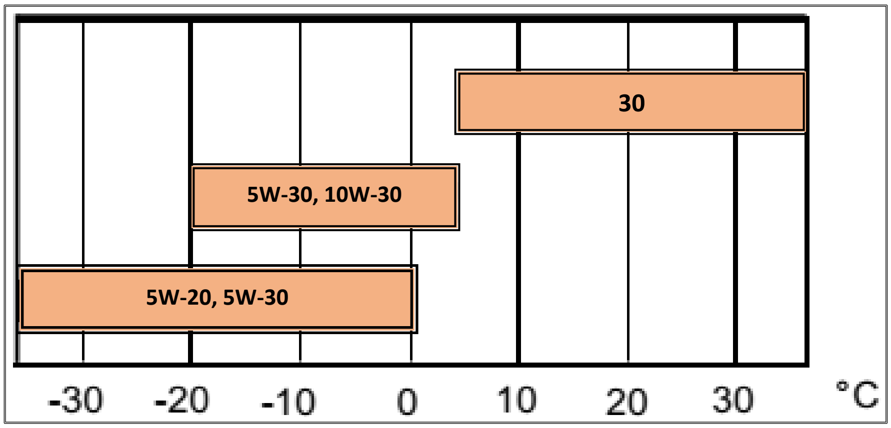

Figure 3.4 Recommended oil types

3.3.1.2.Fuels used for baseline and advanced engine

Internal combustion engines can run on a variety of fuels depending on their design and intended application. The engine fuel for the baseline experiments is diesel fuel. Due to the engine advancement to the RCCI engine, gasoline-ethanol fuels blend are used for port injection and diesel fuel for direct injection. The constant 80% diesel and 20% gasoline-ethanol blend for advanced RCCI engines are used for the experiment.

A. Diesel Fuel

Diesel fuel is a hydrocarbon fuel derived from petroleum and specifically designed for diesel engines, which operate differently from gasoline engines in terms of their combustion process. Diesel fuel has a higher energy density compared to gasoline, meaning it contains more energy per unit volume. Diesel engines rely on compression ignition. In the past, diesel fuel contained higher levels of sulfur, contributing to air pollution. The cetane number is used to measure the ignition quality of diesel fuel. Higher cetane numbers indicate better ignition characteristics, leading to smoother combustion and improved engine performance. Diesel engines are known for their fuel efficiency compared to gasoline engines. They can achieve higher mileage per gallon/liter of fuel due to the higher energy density of diesel fuel and the efficient combustion process.

Diesel fuel is widely used in various applications, including transportation (such as cars, trucks, buses, and trains), industrial machinery, construction equipment, and generators. It's important to note that the specific characteristics of diesel fuel can vary between regions due to differences in refining processes and regulatory requirements. Moreover, advancements in technology and environmental regulations have prompted the development of alternative fuels and more efficient diesel engines in recent years. The diesel fuel properties that are used for the experiment are shown below (See Table 3.3).

Table 3.3 Diesel fuel properties

Parameters	**Test methods**	**Results (max/min)**
Density at 15°C	D4052/1298	0.820-0.860
90% Volume recovered, °C	D86	Max 362
FBP, °C	D86	Max 390
Total Sulfur, % wt	D4294	Max 0.05
Flash point, PMCC, °C	D93	Min.66
Kinematics viscosity @ 40°C	D445	2.0 - 4.5
Cloud point °C	D2500	Max +5
Cetane index	D976	Min 48
Copper strip corrosion 3 hrs @ 100°C	D130	Max No.1
CCR, %Wt	D189	Max 0.2
Ash, Wt	D482	Max 0.01

B. Gasoline fuel

Gasoline fuel or petrol is a widely used fuel in internal combustion engines, particularly in gasoline engines. It is a flammable liquid derived from crude oil refining. It is assigned an octane rating, which measures its resistance to knocking or detonation in an engine. Higher octane numbers indicate better resistance to knocking. The octane rating determines the fuel's performance characteristics and influences engine efficiency. Gasoline engines use spark ignition, where a spark plug ignites the air-fuel mixture in the combustion chamber. Gasoline has a lower energy density compared to diesel fuel; however, gasoline engines can achieve higher RPM and power output due to the faster combustion characteristics of gasoline. Gasoline often includes various additives to enhance performance, protect engine components, and meet environmental regulations. The combustion of gasoline produces CO_2 and other greenhouse gases, contributing to climate change. The physiochemical properties of the gasoline used are shown below (see Table 3.4).

Table 3.4 Specification of gasoline fuel

Parameters	Test methods	Results
Density at 15°C	D4052/1298	0.720-0.740
10% Volume recovered, °C	D86	74
50% Volume recovered, °C	D86	80-127
90% Volume recovered, °C	D86	Max 190
FBP, °C	D86	Max 225
Residue	D86	Max 2
RON	D2699	Min 92
Total Sulfur, % wt	D4294	Max 0.05
Reid Vapor pressure, KPa	D323	41-65
Existence gum, mg/100ml	D381	Max 4
Copper strip corrosion 3 hrs @ 50°C	D130	Max No.1
Doctor test	IP30	Negative
Lead content, g/l	IP 352	Max 0.013

C. Ethanol fuel

Ethanol fuel, also called hydrous bioethanol, is an alcohol-based renewable fuel derived primarily from plant materials. It is commonly used as an additive to gasoline or blended with gasoline to create ethanol-gasoline mixtures. Plant material is processed to extract sugars, which are then converted into ethanol through fermentation by yeast or bacteria. It is considered renewable because the plants used for its production can be grown and harvested repeatedly. Also, producing ethanol from biomass sources has the potential to reduce greenhouse gas emissions compared to fossil fuels, as plants absorb carbon dioxide during growth. Ethanol has a high octane rating, typically around 100 or higher. This rating improves gasoline's anti-knock properties when blended with ethanol, reducing engine knocking and allowing for higher compression ratios. The high octane rating of ethanol can enhance engine performance. Ethanol contains oxygen molecules, which enhance the combustion process and contribute to more complete fuel combustion. This property helps reduce carbon monoxide (CO) and hydrocarbon emissions during combustion.

The use of ethanol blends can help decrease fossil fuel consumption and greenhouse gas emissions. It's important to note that ethanol has a lower energy density than gasoline, meaning it contains less energy per unit volume. Ethanol fuel has become popular as a renewable and potentially more environmentally friendly alternative to fossil fuels. However, when evaluating the overall sustainability of ethanol production and its use as a fuel source, factors like land use, water consumption, and potential impacts on food prices and availability should be taken into account. The hydrous ethanol alcohols (C_2H_5OH) produced from the byproducts of molasses at Methahara Sugar Industry are used as a blend for RCCI diesel engine studies having the following properties (See Table 3.5).

Table 3.5 Ethanol fuel properties

Parameters	Results
Chemical formula	C_2H_5OH
Water content	4 %
Molecular weight	46.07
LHV(MJ/kg)	24.8 - 25.24
Density at 15°C	0.79
Boiling point (°C @ 1atm)	77-78.3
Vapor pressure (kPa at 38 ^{0}C)	15.4
Flash point (°C @ 1atm)	17
Auto ignition temperature(°C)	420–422
Latent heat of vaporization (KJ/kg)	948
Reid Vapor pressure, KPa	17
Solubility in water in 20 ◦C	fully miscible
ON-RON	111.1
ON-MON	91.8-103.3

Source: El-Faroug.,et al 2016, Zakaria.,et al 2022

3.4. Methods

Research methods pertain to the particular tactics, procedures, or approaches utilized to acquire and analyze data, intending to address research objectives. These offered a comprehensive account of how the study was conducted, encompassing outlining the overall plan or strategy devised for the study. Data collection, explaining the process employed to gather data that includes details about the tools, instruments, or measures employed for data collection which is from the experiments, as well as the procedures implemented. The data analyzing mechanism employed for the collected data is described. It may encompass statistical techniques, qualitative analysis methods, or a combination thereof. The section also outlines how the data were coded, categorized, and interpreted to derive meaningful results.

The research methods in these investigations include experimental, combustion simulation, and simulation based on piston bowl shape, and fuel spray model; and design of the experiment is statically analyzed for optimizations, and investigation based on fuel ratio, speeds, and engine load to get optimum operation with the more general conceptual framework or methodology shown (See Fig 3.5).

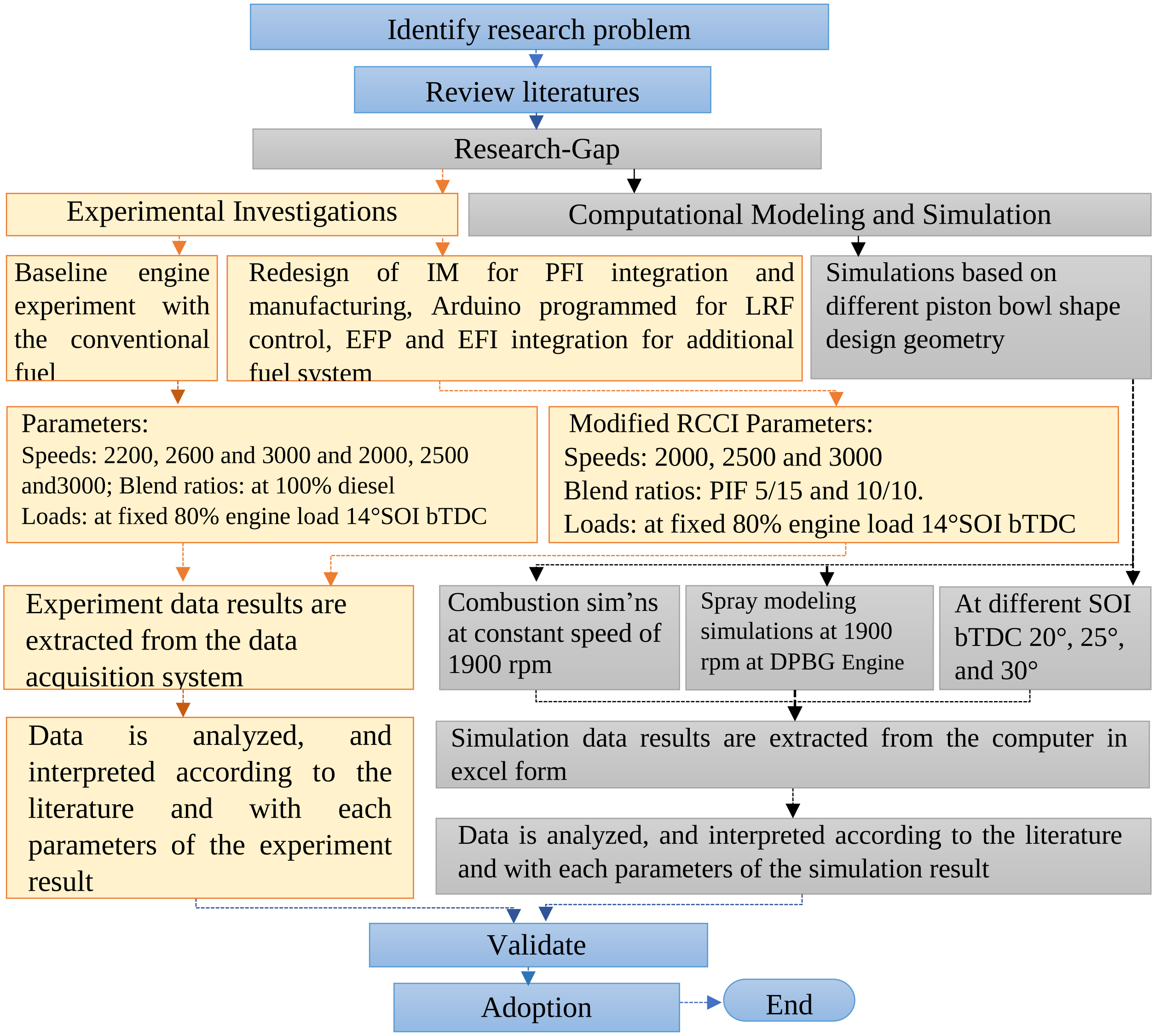

Figure 3.5 Over all conceptual framework of the research

3.4.1. Engine experimental investigation processes

3.4.1.1.Baseline experiments

A 0.309L engine, horizontally mounted, naturally aspired, direct-injected, compression ignition, single-cylinder, water-cooled, constant compression ratio of 23, maximum load (80%), speeds (steady state) with the diesel engine used for the first baseline experiment. The engine configuration's rated power was 5.1kW at the speed of 3000 rpm. The engine was instrumented with a pressure transducer used to monitor the operating conditions of the engine combustions for cylinder pressure versus CA. The experiment was done with the diesel fuel having the physiochemical property (See Table 3.3). The engine experiment took place at the three different speeds of 2200, 2600, and 3000 rpm; and the other three investigations at speeds of 2000, 2500, and 3000 rpm. The comparative analysis was done at a fixed injection timing at 14°SOI bTDC. Engine versus cylinder pressure quantitative information on the combustion process was obtained by analyzing CA data over the compression and expansion strokes of an engine running cycle. The cylinder pressure data was used to calculate the heat release rate (HRR) by using equation (Eq. 3.1), which is the first law of the single zone model (Gad et al., 2021).

$$\mathrm{HRR}(\theta) = \left(\frac{K}{K-1} \times P(\theta) \times dV(\theta)\right) + \left(\frac{1}{K-1} \times V(\theta) \times dP(\theta)\right) \qquad \text{(Eq 3.1)}$$

Where: k is the specific heat ratio (Cp/Cv), θ is the crank position, P is the cylinder pressure, V is the instantaneous chamber volume, and 1.35 is the suitable range for diesel heat-release analysis. Specifically, Heywood (2018) states that the predicted HRR analysis for diesel engines is ≈1.35, which corresponds to air temperatures at the end of the compression stroke. Fig. 3.9 displays the baseline experiment's simple schematic diagram.

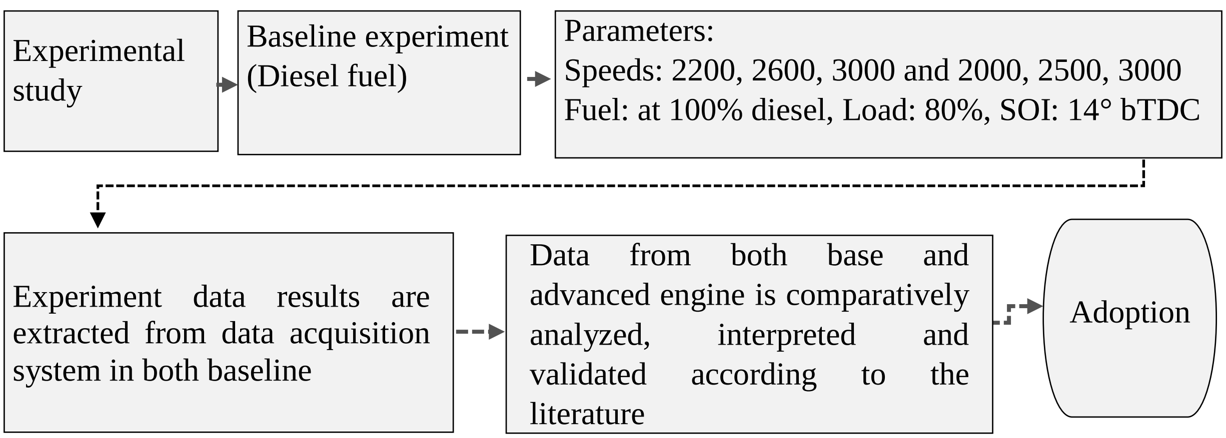

Figure 3.6 Baseline experiment schematic diagram

3.4.1.2.Advanced engine experiments (RCCI)

A. Concepts of RCCI engine

To increase efficiency and lower emissions, the same engine was used in the second experiment, which was upgraded to an advanced low-temperature RCCI combustion engine. While the port gasoline fuel injector is used to inject a bioethanol-gasoline blend into the intake manifold during the intake stroke, the direct injection of diesel fuel supplies fuel to the engine. This is to increase fuel reactivity to prevent a rich region of the fuel in the cylinder not to creating particulate matter and to make cylinder combustion temperature below the NOx formations (See Fig.3.7).

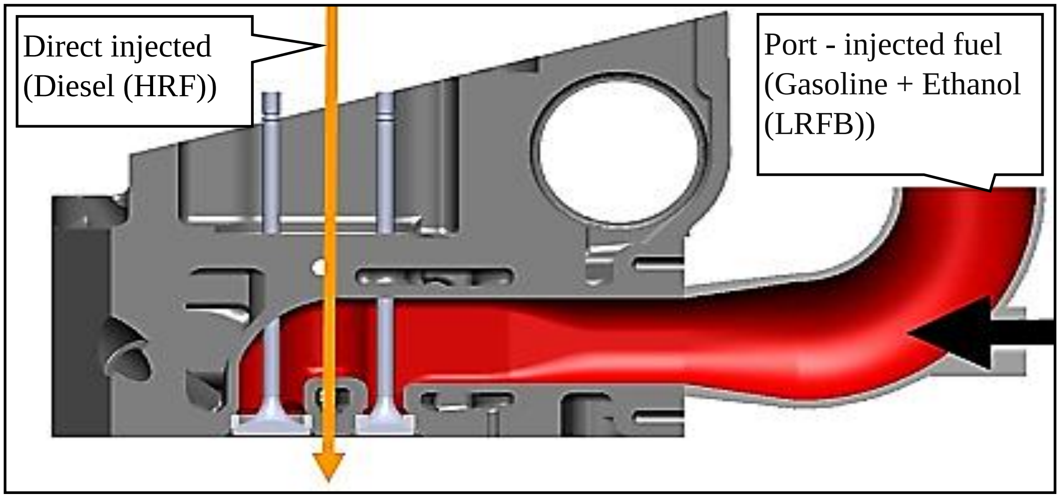

Figure 3.7 Triple fuel RCCI engine strategies applied

The combustion phase, during which efficiency is at its maximum, is determined by analyzing the blends' and diesel fuel's performance and emission characteristics. The total fuel of PFI is 20%, which is controlled by using Arduino, board microcontroller, and 80% of the diesel fuel provided by conventional injection pumps was examined using the one-stage injection technique. The present work used direct injection for the diesel fuel supply, redesigned the intake system with CATIA software, and manufactured using a lathe machine to integrate the additional port fuel injectors. Arduino programming and its full assembly for fuel controlling mechanism is used and, electrically connected to the injector, and the injectors are connected to the fuel pump.

Direct injection of diesel fuel with the properties in (Table 3.3) is into the cylinder at about the ends of compression before the top dead center. In this study, blends having the gasoline properties in (Table 3.4) with ethanol fuel properties in (Table 3.5) were used for investigation. The fuel ratios used for the premixing fuel are to increase the reactivity of the fuel. The fuel is supplied separately by premixing gasoline and bioethanol blend through the port injection into the intake manifold during the intake stroke. Equation (Eq 3.2) illustrates the general definition of the premixed fuel ratio (rp), which is the ratio of port fuel injection (PFI) energy to the total fuel (DI+PFI) energy injected (Pedrozo et al., 2022).

$$r_P = \frac{m.\,LHV_{GE}}{M.\,LHV_D + m.\,LHV_{GE}} \qquad \text{(Eq 3.2)}$$

Where LHV is the lower heating value of each fuel and M and m are the mass flow rates of the primary and secondary fuels, respectively. The primary and secondary fuels (r_p=G25E75 and G50E50) are denoted by the subscripts D for diesel fuel and GE for gasoline-ethanol blended fuel, respectively; however, for baseline compression ignition combustion rp = 0. Fig 3.8 displays the basic schematic diagram for the RCCI engine experiment.

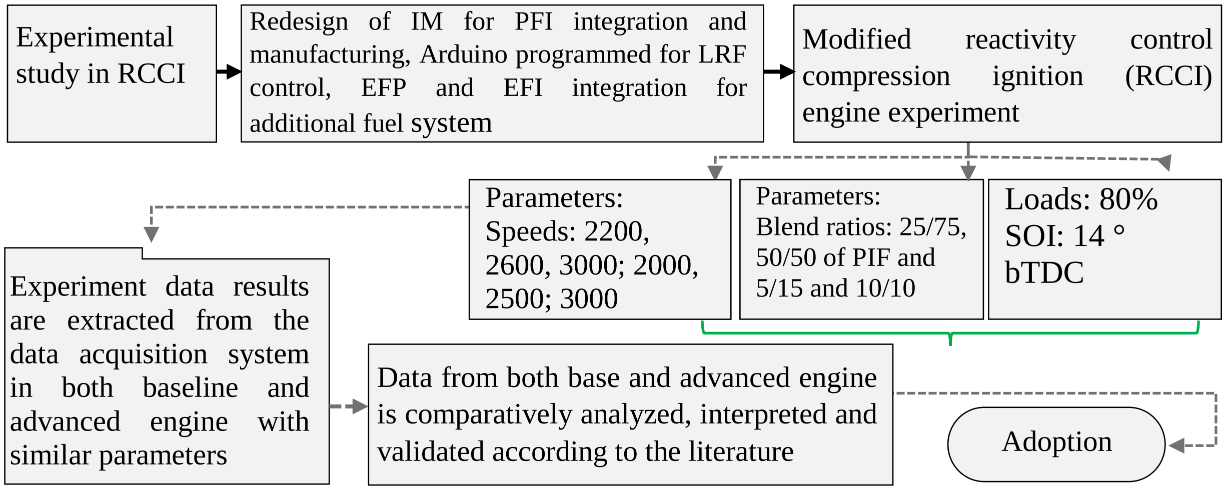

Figure 3.8 Schematic diagram of the RCCI engine experiment

The two general intake and exhaust valve lifts make it feasible to determine valve timings. It is helpful to refer to valve timings relating to one of the three-piston turning points (crank angle 180, 360, and 540) since valve openings and closings usually occur in the vicinity of one of these locations. The valve overlap, or the moment when the intake and exhaust valves are open at the same time, is another crucial factor. Equation (Eq 3.3) states the valve overlap's size. With a total opening angle of 255°CA, the engine for the combustion experiment had the EVO at 65°CA before the bottom dead center and closing at 20°CA after the top dead center. With the valve overlap (VOL) as in Fig. 3.9 and cylinder volume concerning piston position (See Fig. 3.10), the intake valve opens (IVO) 15°CA before the top dead center (bTDC) and closes (IVO) 50°CA after the bottom dead center (aBDC).

$$\text{VOL} = \theta_{\text{EVO}} - \theta_{\text{IVO}} \qquad \text{(Eq 3.3)}$$

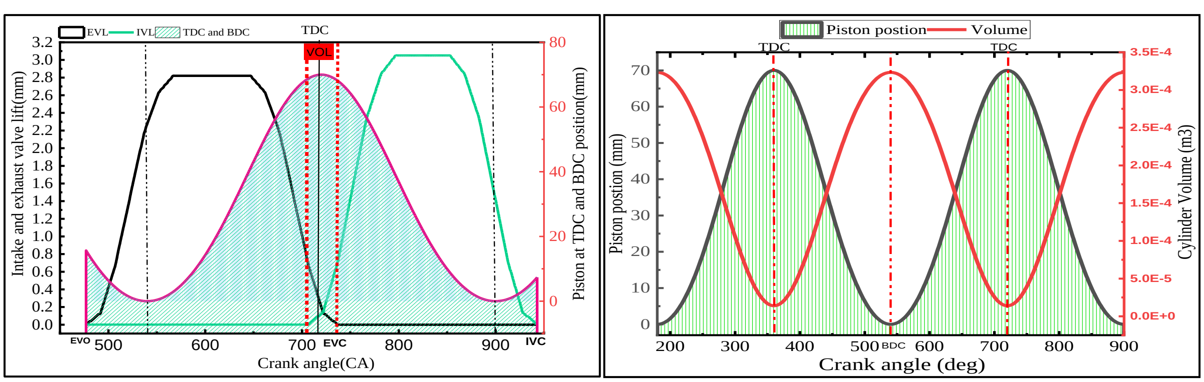

Figure 3.9 Timing and lift of the valves and Piston position and volume.

3.4.2. Designs of experiment

3.4.2.1.Taguchi method design of experiment

The Taguchi method employs DOE to efficiently explore the design space and identify influential factors that affect product quality or performance. By using orthogonal arrays, the method allows for a reduced number of experiments while capturing the main effects and interactions of the factors. L_9 orthogonal arrays are used to systematically design experiments by selecting a subset of factors and levels to be tested. Orthogonal arrays ensure the effects of different factors can be evaluated independently and efficiently with a minimal number of experiments. To understand the effect of the interaction between two factors of engine speeds and port injected fuel blend ratio, the three levels tests were performed and experiment design L9 (3^2) orthogonal array was created to determine the minimum number of experiments and to optimize the emission and performance conditions. This method emphasized the importance of designing products and processes that are less sensitive to variations in input parameters or factors. The SNR is a key element and concept of the Taguchi method.

Signal-to-Noise Ratio (SNR): is used as a measure of performance in the Taguchi method. It quantifies the variation in the output or response variable caused by input factors. The goal is to maximize the SNR, which means minimizing the influence of noise factors and maximizing the effect of controllable factors on the output variable. The control factor settings that minimize the variability brought on by the noise factors are identified by the SNR. Minitab computes the average signal-to-noise ratio for each level of each control factor as well as the SNR for each combination of control factors. When the procedure selected the option when "Larger is better" from the signal-to-noise ratios; the first option's experimental objective is to maximize the response with favorable data features according to the equation (Eq 3.4).

$$\frac{\mathrm{S}}{\mathrm{N}} = -10 \times \mathrm{Log}\left[\sum\left(\frac{y_i}{\mathrm{n}}\right)^2\right] \quad \text{(Eq 3.4)}$$

Table 3.6 L9 Experiment data of emissions and performances

Speed	PFR	NOx	CO	CO_2	HC	Tb	Pb
2200	0	41	0.25	4.04	21	14.2	3.28
2200	25/75	36	0.51	2.62	53	15.2	3.50
2200	50/50	37	0.73	2.34	30	15.2	3.84
2600	0	92	0.68	4.79	23	14.2	3.87
2600	25/75	38	2.7	1.94	313	14.2	3.84
2600	50/50	69	0.92	2.49	34	15.2	4.52
3000	0	152	1.06	6.41	48	14.1	4.52
3000	25/75	33	4.54	3.85	510	14.2	4.52
3000	50/50	115	1.65	3.64	50	14.2	4.43

Where y_i are the measured property values and n is the total number of experiments. In trials, to boost performance and emission, it was found that the two variables' engine speed and premixed gasoline-bioethanol blend ratio were the most effective ones. In linear model analysis, statistical significance refers to the determination of whether the estimated coefficient of the independent variable is different from zero. Taguchi's method approach enables the identification of the most critical factors that have the most significant impact on the performance or quality of a product or process. By focusing on these key factors, resources can be allocated more efficiently to achieve improvements. It employs statistical techniques, such as analysis of variance (ANOVA), to analyze the experimental data and determine the significance of factors. This analysis helps identify the main effects of factors, their interactions, and the optimal levels for achieving the desired performance or quality. By considering the interaction effects and selecting the appropriate two-factor speed blend ratio and the three levels, the method helps identify robust solutions that meet target specifications. The speed, emissions, and performances and their statistical data results of the experiment designs are shown in Table 3.6.

3.4.2.2.Error Analysis

Analysis of uncertainty demonstrates how accurate the experimental test was. The selection of the instrument, the testing environment, calibrations, the testing plans, data collecting, instrumentation, the procedures used, and random errors are the main causes of uncertainty in trial findings. The errors in the result are a direct function of the most significant errors in each parameter that was used to calculate the % uncertainty rate of many instruments that were used to estimate every variable that was taken into consideration. The uncertainty of the various instruments employed in the experimental setup is used to estimate the amount of gasoline used, the specific fuel consumption, the brake power, and the brake thermal efficiency. Errors are often present in experimental testing when measuring various test data. Therefore, to get precision, uncertainty analysis was done to address the errors and deviations that happened throughout the experimental effort. Additionally, the test engine and any other instruments were adjusted before the experiment. For uncertainty analysis, three sample readings of the examined data were first obtained at regular intervals. The maximum mean percentage uncertainty ($\overline{\mathrm{U}}_{\mathrm{max}}$) estimated for the engine out emissions and engine performance of the base equation, uncertainty equation, and maximum percentage uncertainty are indicated or shown in

Table 3.7-3.8, along with the accuracy associated with the measuring instruments, and the detail calculation of the performance is as shown in (Eq 3.5-3.8).

The derived parameter is $Pb = \frac{2\pi NT_b}{60\times10^3} kW, Uncertainty(U) = cT_b\Delta N + cN\Delta T_b$ (Eq 3.5)

Maximum uncertainty (U_{max}) % = $\left(\frac{\Delta N}{N} + \frac{\Delta T_b}{T_b}\right) \times 100\%$ (Eq 3.6)

$BSFC = \frac{TFC}{P_b} = 3.6 \times s.g \times \frac{x}{t} \times \frac{60000}{2\pi NT_b};\ U = \frac{C}{tNT_b}\Delta x + \frac{cx}{t^2NT_b}\Delta t + \frac{cx}{tN^2T_b}\Delta N + \frac{cx}{tNT_b{}^2}\Delta T_b$ (Eq 3.7)

$(U_{max})\% = \left[\frac{\Delta x}{x} + \frac{\Delta t}{t} + \frac{\Delta N}{N} + \frac{\Delta T_b}{T_b}\right] \times 100$ (Eq 3.8)

Table 3.7 Performance accuracy and its maximum uncertainty

Measured value						Accuracy					Max % uncertainty		
N	Tb	Pb	BSFC	X(cm^3)	t(sec)	N ±12rpm	Tb ±0.20	Pb ±0.1	X ± 0.05	T ± 0.01	Tb U_{max})%	Pb, U_{max})%	BSFC U_{max})%
1900	14.16	2.82	0.43	10	51.14	12	0.20	0.1	0.05	0.01	3.56	2.04	2.56
2000	14.67	3.01	0.43	10	42.64	12	0.20	0.1	0.05	0.01	3.33	1.96	2.49
2200	14.84	3.12	0.43	10	31.70	12	0.20	0.1	0.05	0.01	3.21	1.89	2.42
2400	14.86	3.53	0.41	10	29.00	12	0.20	0.1	0.05	0.01	2.84	1.85	2.38
2600	14.50	3.95	0.39	10	24.62	12	0.20	0.1	0.05	0.01	2.54	1.84	2.38
2800	14.14	4.18	0.37	10	20.00	12	0.20	0.1	0.05	0.01	2.40	1.84	2.39
3000	14.14	4.49	0.36	10	17.56	12	0.20	0.1	0.05	0.01	2.23	1.81	2.37

Table 3.8 Measurement uncertainty and instrument accuracy

No	Instrument's name	Magnitude	Range	Accuracy	$\bar{U}_{max}$%	Evaluation method
1	Pressure transducer(bar)	P	0 - 100	± 1 bar	1	Piezoelectric sensor
2	Crank angle encoder	CA	0 -720	± 1 deg	0.1	Magnetic pickup
3	CT 159.02 EG-Analyzer	CO	0-10% vol	± 0.06% vol	10.3	NDRIR
		CO_2	0-20% vol	± 0.1% vol	2.9	
		HC	0-2500ppm	± 3 ppm	7.1	
4	Engine model of CT 100.23	N	0-5000rpm	± 12 ppm	0.51	Partial differentiation using the equation
		Pb	-	± 0.1	2.87	
		Tb	-	± 0.20	1.89	
		TFC	-	± 0.05cm^3	2.43	
5	Temperature sensor	T_1		± 0.01	3.89	Thermocouple
6	Temperature sensor	T_2		± 0.01	3.44	Thermocouple
7	Temperature sensor	T_3	0 - 1000° C	± 0.01	2.05	Calorimeter
8	Kane AUTO gas analyzer	NOx	0 - 5000ppm	± 12 ppm	21.2	Electrochemical sensor
	Overall average maximum uncertainty				**3.2%**	

Where: TFC-total fuel consumption, *and* $\bar{U}_{max}$% - maximum mean percentage uncertainty, NDIR-non-dispersive infrared, T_3- Exhaust gas temperature, T_1-intake air temperature, T_2-fuel temperature

3.4.3. Modeling of combustion simulation

3.4.3.1.Combustion simulation based on piston bowl shape

Because the piston bowl's design significantly influences fuel and air mixing within the combustion chamber, it's recommended to reduce the surface-to-volume ratio. Researchers explored various piston bowl and fuel spray shapes within swirling airflow through computer simulations to decrease heat transfer and minimize soot and nitrogen oxides in the squish zone (Zhao et al., 2020). The unique geometry of the piston bowl allows for precise pre-combustion mixing, particularly crucial for brief direct injection diesel fuel instances. The study aimed to identify the piston bowl geometry that would yield the lowest nitrogen oxides and particulate matter emissions, along with optimal fuel combustion efficiency, using combustion simulations on engines of similar size. The engine in focus was a 0.325L, 4-stroke, water-cooled, single-cylinder diesel engine at AASTU, featuring a fixed compression ratio of 24. Employing software to evaluate bowl-shaped characteristics in light-duty engines through combustion simulations can enhance thermal efficiency and reduce emissions from traditional diesel combustion. The model used for piston bowl design evaluation was based on engine running conditions representative of previous conventional diesel combustion events (Sreedharan and Krishnan, 2018).

The diesel combustion model introduced, called the RK model, along with the (Hiroyasu, 1983) model, incorporates separate emissions sub-models. The core equations of the RK model were originally formulated by Razleytsev between 1990 and 1994. Later, Kuleshov refined and augmented the method. This approach considers the evolving conditions of each fuel spray and the flow dynamics generated by sprays along surfaces, as well as the interactions between sprays and swirl, and between surface flows formed by adjacent sprays. The RK model's capabilities enable the prediction of diesel combustion and emissions. Fig 3.11 illustrates a typical evolution of a spray in the piston bowl, while (Eq 3.9) computes the mass of entrained air for each elementary fuel mass (EFM), factoring in the current distance, velocity, and EFM penetration length until the spray ceases. These parameters are deduced from momentum conservation principles (Kuleshov, 2008):

$$\left(\frac{U}{U_o}\right)^{3/2} = 1 - \frac{l}{l_m} \tag{Eq 3.9}$$

Where U=dl/dt is the current EFM velocity, U_o is the EFM velocity in the injector nozzle, l_m is the EFM penetration length until the spray stops, and l is the current distance from the EFM to the injector. The mass of entrained air (mass ma) for each elementary fuel mass (EFM) can be defined using momentum conservation, as shown by equation (Eq 3.10)

$$U_O \Delta m_f = U_k c_1 \Delta m_f + \Delta m_a \quad \text{(Eq 3.10)}$$

Where: mf is the mass of fuel and ma is the mass of air

The partial solution of the differential equation 1 is shown in (Eq 3.11):

$$3l_m \left[1 - \left(1 - \frac{l}{l_m}\right)^{0.33}\right] - U_0 \tau_k \quad \text{(Eq 3.11)}$$

Where: τ_k is a time of EFM movement from the nozzle up to l.

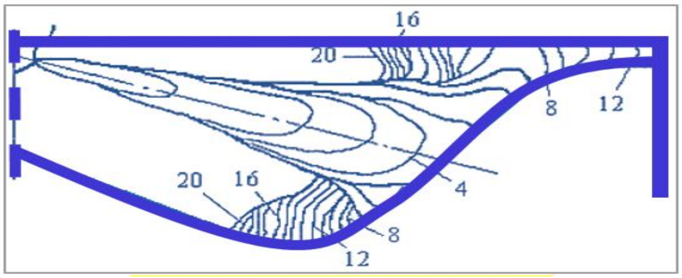

Figure 3.10 Fuel spray pattern

Sources: (Kuleshov, A. S. 2009)

Fuel was injected into the bomb with the piston model. The nozzle size, speed of shooting, and the numbers corresponding to frames of shooting when EFM is stopped in a spray tip is $l = l_m$, $\tau_k = \tau_m$ was seen by (Eq 3.12):

$$l_m = U_o \frac{\tau_m}{3} \quad \text{(Eq 3.12)}$$

From equations (Eqs 3.13, and 3.14) the EFM velocity and the distance from the EFM to the injector are calculated as follows:

$$U = U_O \left(1 - \tau_{k/\tau_m}\right)^2 \quad \text{(Eq 3.13)}$$

$$l = l_m \left[1 - \left(1 - \tau_{k/\tau_m}\right)^3\right] \quad \text{(Eq 3.14)}$$

Parameters of the spray tip are calculated with empirical equations (Lyshevsky, 1971) that were improved by (Razleytsev, 1980). These relations use dimensionless criteria as they are shown in the equations (Eq 3.15 - 3.18):

$$W_e = U_{OM}^2 \, d_n \frac{\rho f}{\sigma f} \quad \text{(Eq 3.15)}$$

$$M = \mu_f^2 / (\rho_f d_n \sigma f) \quad \text{(Eq 3.16)}$$

$$\ni = \tau_s^2 \, \sigma f / (\rho_f d_n^3) \quad \text{(Eq 3.17)}$$

$$\rho = \rho_{air/} \rho f \quad \text{(Eq 3.18)}$$

Where: U_{0m} is an average injection velocity, d_n is a nozzle hole diameter, ρ_f is a fuel density, $\rho_{\mathbf{air}}$ is an air density, σ_f is a fuel surface density, μ_f is a dynamic viscosity coefficient of fuel,τ_s is a current time from the injection beginning. The evolution of a free spray consists of two main phases: a) the initial phase of pulsing evolution; and b) the basic phase of cumulative evolution. The border between these phases is marked as l_g (length) and τ_g (time):

$$l_g = C_s d_n We^{0.25} M^{0.4} \rho^{-0.6} \qquad \text{(Eq 3.19)}$$

$$\tau_g = \frac{l_g^2}{B_s} \qquad \text{(Eq 3.20)}$$

$$B_s = \frac{d_n U_{on} We^{0.21} M^{0.16}}{\left(D_s \sqrt{2}\, \rho\right)} \qquad \text{(Eq 3.21)}$$

Where: *Cs* = 8.25/8.85; Ds = 4.5/5 for diesel cylinder conditions. The spray tip penetration length in the initial (index a) and the base (index b) phases is calculated by the following empirical expressions (Eq 3.22, and 3.23):

$$l_a = A_s \ni^{0.35} \exp\left[-0.2\left(\frac{\tau_s}{\tau_g}\right)\right] \qquad \text{(Eq 3.22)}$$

$$l_b = B_s^{0.5} \tau_s^{0.5} \qquad \text{(Eq 3.23)}$$

The free spray contour angle calculated by the equations (Eq.3.24, Eq.3.25) shown below:

$$\gamma_a = 2\text{Arctg}\left(E_s We^{0.35} M^{-0.07} \ni^{-0.12} \rho^{0.5} e^{0.07\tau_{s/\tau_g}}\right) \qquad \text{(Eq 3.24)}$$

$$\gamma_b = 2\text{Arctg}(F_s We^{0.32} M^{-0.07} \ni^{-0.12} \rho^{0.5}) \text{ in NWF} \qquad \text{(Eq 3.25)}$$

Where: Es = $0.932 F_s We^{-0.03} \ni g^{0.12}$ and $\ni_g = \tau_s^{\ 2} \sigma_f (\rho_f d_n^{\ 3})$; with the assumption $\tau_s = \tau_g$, F_s= 0.0075/0.009 for diesel cylinder conditions. The geometry of the four possible piston bowl geometries below are observed (See Fig 3.12). The Diesel No-2 is used to model combustion, and the thermal Zeldovich mechanism is used to simulate the creation of NOx.

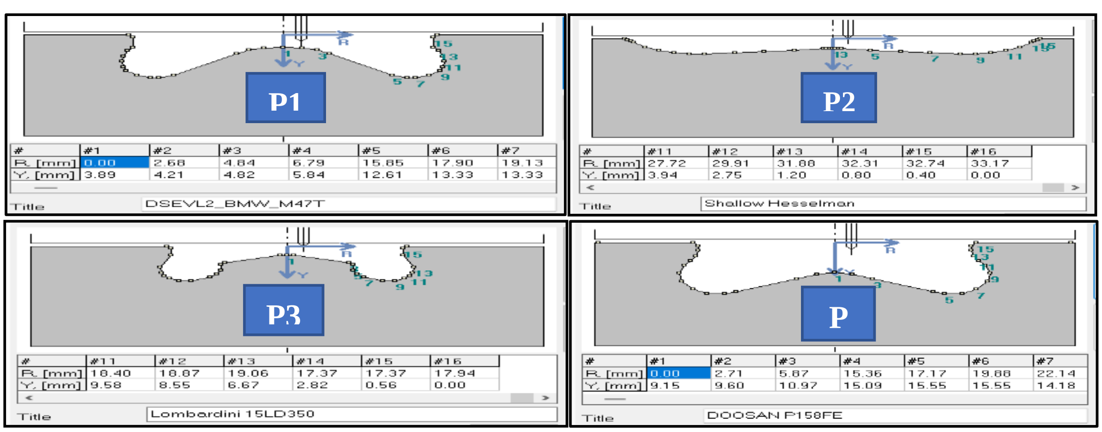

Figure 3.11 Different piston bowl shape geometry configurations

Several diesel fuel spray models have been developed and applied in computational fluid dynamics simulations and engine combustion models. Here are a few commonly used ones:

1. **Lagrangian-Eulerian Spray Atomization Model:** This model combines a Lagrangian approach for individual fuel droplets with an Eulerian approach for the continuous liquid phase. It considers primary atomization, secondary breakup, and collision processes to predict spray characteristics (Subramanian and Science, 2013).
2. **Kelvin-Helmholtz/Rayleigh-Taylor (KH-RT) Model:** Based on the Kelvin-Helmholtz and Rayleigh-Taylor instabilities occurring at the fuel-air interface, this model predicts the breakup of liquid fuel into droplets and their subsequent behavior during combustion (Jia et al., 2022).
3. **Reitz-Diwakar (RD) Model:** Developed by Reitz and Diwakar, this model considers primary atomization, droplet breakup, collision, and coalescence processes. It uses empirical correlations and semi-empirical equations to predict spray characteristics (Sula et al., 2020).
4. **Representative Interactive Flamelet Model:** This model is used for the reason that it combines the spray model with a combustion model to predict spray evolution, turbulent mixing, chemical reactions, flame structure, and heat release rate (Gao et al., 2017). These models rely on various sub-models and correlations to capture the complex physics of diesel fuel spray combustion, including breakup, collision, droplet evaporation, and combustion models. The accuracy of predictions depends on the fidelity of these sub-models. In the current research, fuel sprayed in the cylinder is divided into seven zones based on the modeling of fuel sprays in swirling airflow. Evaporation and burning conditions vary across these zones, with diesel fuel-free spray zones primarily divided into two main sections.

a) **Free spray before impingement:** The three different zones the dense axial core; the dense forward front; and the diluted outside of the sleeve are present in a free spray before impingement (See Fig 3.13 of No 1, 2, and 3).

b) **Free spray after impingement:** Since fuel evaporation calculations are difficult due to the non-homogeneous structure, density, and temperature of the near-wall flow formed after impingement, it is possible to identify typical zones in the NWF with averaged heat and mass transfer coefficients based on similarities to free spray (See Fig 3.13 of No 4, 5, 6 and 7). Following wall impingement, the additional zones are formed as listed below:

$$U_{ma}=l_a[(\frac{0.7}{\tau_s})-(\frac{0.2}{\tau_g})] \quad \text{(Eq 3.26)}$$

$$U_{mb} = 0.5\ l_b\ /\tau_s \quad \text{(Eq 3.27)}$$

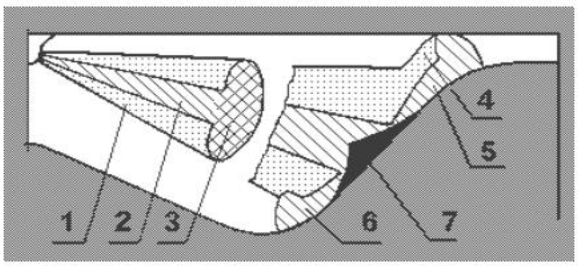

Notations:

1 - Dilute the outer sleeve of a spray
2 - Dense axial core of free spray
3 - Dense forward front
4 - Dilute the outer of a NWF
5 - Dense core of a NWS
6 - Forward front of a NWF
7 - Axial conical core of a NWF

Figure 3.12 Diesel fuel spray zone diagram before and after impregnation
Sources: (A. S. Kuleshov, 2006a)

The following empirical formulas are used to calculate the spray tip velocity at the starting and basic phases indicated (Eq 3.26, and 3.27).

CHAPTER FOUR

4. RESULTS AND DISCUSSIONS

4.1. Speed and fuel blend ratio effect on the diesel and RCCI engine

Exploration for better engine combustion technologies apart from renewable and cleaner energy sources is driven by environmental contamination as well as the current energy crisis (Li et al., 2022). Diesel engines enlarged in popularity due to the advantage of higher fuel conversion efficiency and power output (Sharma et al., 2015). The higher fuel conversion efficiency and power output of diesel engines are a result of their higher compression ratios (Sadabadi, 2015), leaner charges (Benajes et al., 2014), and lower throttle losses (Nguyen et al., 2020; Uherek et al., 2010) as compared to spark ignition engines. However, diesel engines still have difficulty reducing NOx and particulate emissions inside the cylinder to comply with pollution regulation requirements. Therefore, numerous researchers have been straggling evolutionally toward the advancements of internal combustion engines to reduce the aforementioned exhaust emissions.

The reactivity-control compression ignition (RCCI) engine concept was demonstrated as a promising method to achieve high efficiency, clean combustions patented by (Reitz et al., 2016). Engine experiments performed in a heavy-duty test engine over a range of loads compared the RCCI engine to the CDC engine showed that RCCI combustion is capable of operating with near-zero levels of NOx and soot, acceptable pressure rise rate and ringing intensity, and high-indicated thermal efficiency (Kokjohn et al., 2010). To control the combustion process, the RCCI engine controls the ratio of the two fuels with flexible reactivity, one is port injected, and the other directly injected (Zhou, 2017; Rosa et al., 2020). Reactivity control compression ignition engines must abide by strong regulations for both pollution and fuel efficiency under the current and prospective legislation (Splitter et al., 2010). These troubles forced the development of advanced internal combustion engine technology, and substitutes for fossil fuels that can reduce emissions (Hasan, et al., 2019). To reduce emissions while maintaining thermal efficiency, some frontline approaches have been researched (Kokjohn et al., 2010; Li, 2017). The majority of existing methods are categorized as low-temperature combustion engines (Tekgül et al., 2022; Zhao et al., 2003). It was revealed that the RCCI engine combustion has low NOx and PM (Li et al., 2015); however, these emissions still require further investigation for the suggested higher efficiencies. In most of the earlier investigations, different test fuels and engine operating conditions were used to assess the combustion characteristics of baseline compression ignition. Single low reactivity (gasoline, ethanol, natural gas(NG), compressed natural gas(CNG), and methanol) fuel as port-injected fuel, and diesel, biodiesel, and (LRF + small cetane improver) as high reactivity fuel (HRF) for direct injection under a modified RCCI engine was used (Singh et al., 2020). There are no studies reported so far in the open literature on RCCI that investigated combustion, performance, and emission characteristics of the gasoline-ethanol blend used as port-injected fuel at varied ratios. Therefore, the study objective is to use a novel approach that emphasizes comparing the effects of various pre-mixed fuel blend ratios, at different speeds, with baseline diesel combustion, instead of assessing each single fuel for port injection to achieve low emissions and good performance. The comparative performance of each port-injected blend G25E75 of the port injected (5% Gasoline 15% Ethanol by volume of the total fuel), and G50E50 of the port-injected (10% gasoline 10% ethanol, and 80% of the total fuel) with conventional diesel combustion as a baseline case has been investigated under the RCCI combustion mode. Considering higher CO and HC emissions, a known drawback of the RCCI concept, a previous study shows the future direction that it is possible to simultaneously achieve ultra-low engine-out emissions of NOx, PM, and reduced CO, and HC with an innovative fuel mix (Baškovič et al., 2022). The research in this regard arises from studies conducted with port-injected alcohol or gasoline alone having high CO, and HC emissions (Pan et al., 2021). Therefore, it is of great importance to test ethanol-gasoline blends (EGB) in an up-to-date LTC concept of the RCCI. In this regard, combustion, performance, and emissions from diesel engines fueled with port-injected EGB and diesel direct injection were investigated in the study. The aim of this study is also to use sustainable ethanol for fossil energy replacement to reduce emissions and find the operating condition for optimized reduction of CO and HC.

4.1.1. Combustions at the same speed and various blend ratio

The experimental study on the modified RCCI diesel engines used a binary low-reactivity blended fuel gasoline-ethanol, in which the ratios of premixed blends and diesel fuel are varied. The cylinder pressure and HRR at different engine speeds and fuel ratios were studied selecting three speeds 2200, 2600, and 3000rpm. According to the results, the maximum cylinder pressure and HRR at 2200 rpm are from the G50E50 blend, and the minimum cylinder pressure and HRR are for the engine running on conventional diesel fuel. The cylinder pressure and HRR variation at 2200rpm with different fuel blends suggest stable operation of the engine, as shown in Fig.4.1a and Fig.4.1b. As the engine speed is increased to 2600 rpm, the cylinder pressure and HRR of the engine running with three different fuels is seen to be the maximum for G50E50, average for G25E75-RCCI, and minimum for the baseline diesel fuel. At the engine speed of 2600 rpm with G25E75 fuel blend, the oscillation in-cylinder pressure and consequently the HRR tend to indicate somewhat an unstable engine operation. This is in line with the earlier findings (Boronat, 2017). For the baseline, and G50E50 fuel blend, one can notice a smooth pressure and HRR variation. These indicate a stable engine operation and delayed cylinder pressure rise and HRR for the baseline fuel, as shown in Figs 4.2a and Fig 4.2b. The cylinder pressure and HRR of the engine running with port-injected fuel of G50E50 are the highest. The reason is that port injection of blended fuel at the intake manifold tends to increase the time for air-fuel mixture homogeneity in the combustion chamber as compared to the baseline experiment. It is also better than the port-injected blend of G25E75 under its higher energy content of gasoline than ethanol fuel. The observations for the baseline case are in line with the previous results of the pressure and HRR. At the maximum engine speed of 3000 rpm, the maximum cylinder pressure and HRR are for the engine running with the G25E75 blend. The minimum cylinder pressure is obtained at the engine running with diesel fuel, and the intermediate HRR is at the engine running with a fuel blend ratio of G50E50. At 3000-rpm operation with G25E75 fuel blend, oscillations in pressure, and hence HRR were observed.

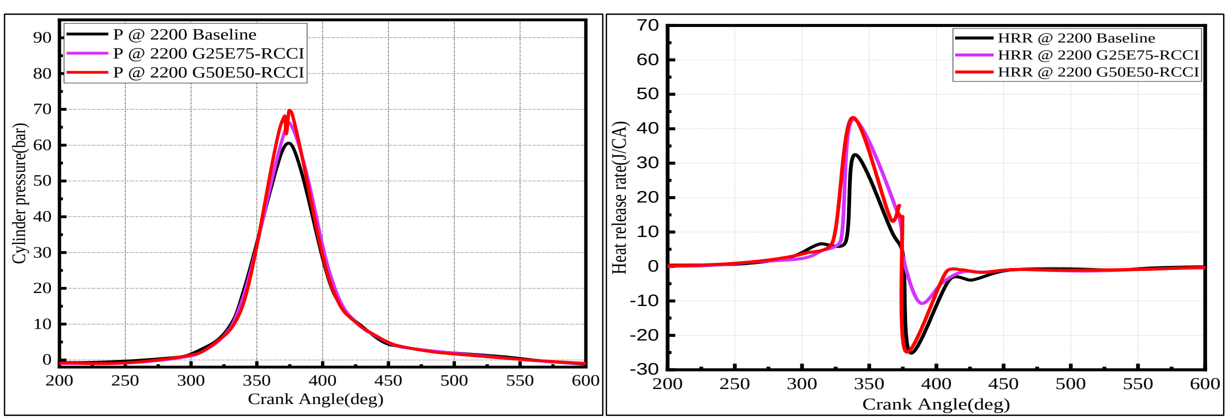

a. Cylinder pressure b. Heat release rate

Figure 4.1 Cylinder pressure and heat release rate

The erratic engine operation took place at higher engine speeds with G25E75, even though for baseline and G50E50 fuel blend exhibited a stable engine operation as can be seen from Fig.4.1a and Fig.4.1b. According to the experimental result, it is possible to infer that the engine running with different fuels at different engine speeds had greater variations in cylinder pressure (see Fig 4.1a, 4.2a, and 4.3a), and the heat release rate (See Fig.4.1b, 4.2b and 4.3b respectively. The observations for the baseline fuel, at all engine speeds, indicate a much more stable engine operation, which is also in line with the previous investigation results (Splitter et al., 2012).

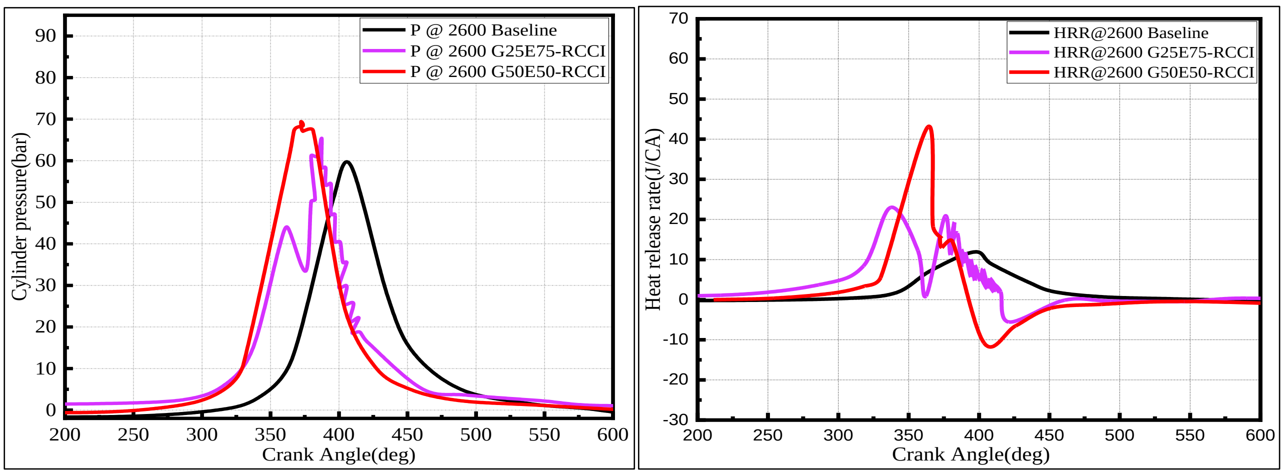

a. Cylinder pressure b. Heat release rate

Figure 4.2 Cylinder pressure and heat release rate

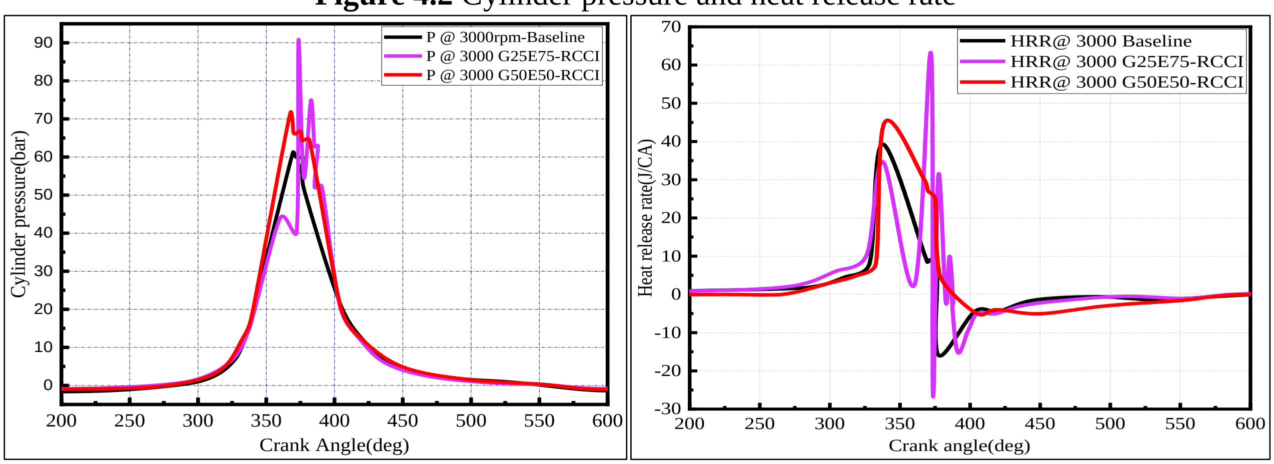

a. Cylinder pressure b. Heat release rate

Figure 4.3 Cylinder pressure and Heat Release Rate

4.1.2. Combustion analysis at the same fuel and different speeds

Each of the fuels, baseline, G25E75-RCCI, and G50E50-RCCI fuel were separately used at various engine speeds. The investigation results showed that the cylinder pressure variation of the baseline case at different speeds is smooth and stable with slightly higher cylinder pressure at the higher speed. A delayed cylinder pressure rise was noted at the lower speed of 2200 rpm, (see Fig.4.4a). Maximum, medium, and lower HRR were found at the speeds of 2200, 3000, and 2600 respectively and late HRR occurrence was observed at the lower speed of 2200 rpm (See Fig. 4.4b). The fuel used for port fuel injection is G25E75 and the diesel direct injected is separately used at various engine speeds. According to the results, the cylinder pressure, and HRR are maximum at the maximum engine speed while being minimum at the speed of 2600, and intermediate at 2200 rpm. The wavy nature of pressure variation and HRR at 2600 and 3000 rpm indicated that there is instability in engine operation, also reported elsewhere (H. Wang et al., 2020). However, better stability in engine operation is observed at the lower engine speed of 2200 rpm, as is shown in Figs.4.4a. The engine running with the premixed fuel ratio of G50E50 RCCI and DI conventional diesel fuel at different engine speeds has slightly greater cylinder pressure at 3000 engine speed. Moreover, the HRR is higher at an engine speed of 3000 and minimum at 2200rpm with average values at an engine speed of 2600rpm. The smooth cylinder pressure and HRR for the engine running with G50E50 fuel indicated stable engine operation (See Fig.4.5a and Fig.4.5b). As per the results, the engine running with the same fuel at different speeds exhibits a slight change in cylinder pressure except when it is running with a higher ethanol content (G25E75). Moreover, at 2600 and 3000 rpm, as can be seen in Fig 4.6a, and was a great change in HRR (see Fig 4.6b).

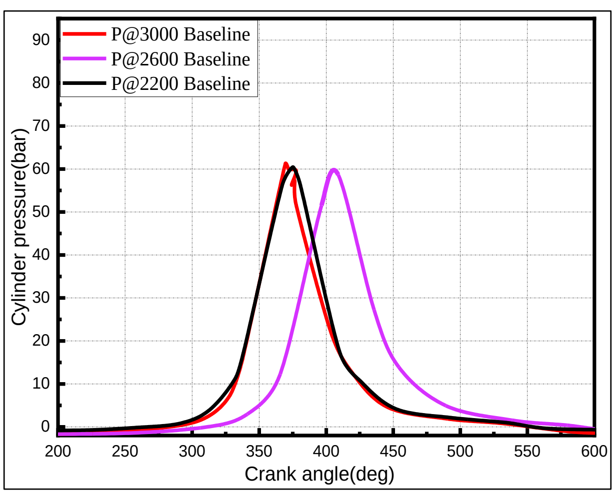

a. Cylinder pressure

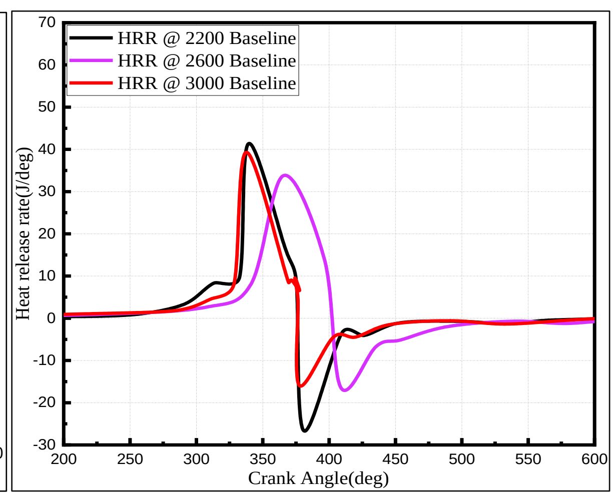

b. Heat release rate

Figure 4.4 Cylinder pressure and heat release rate

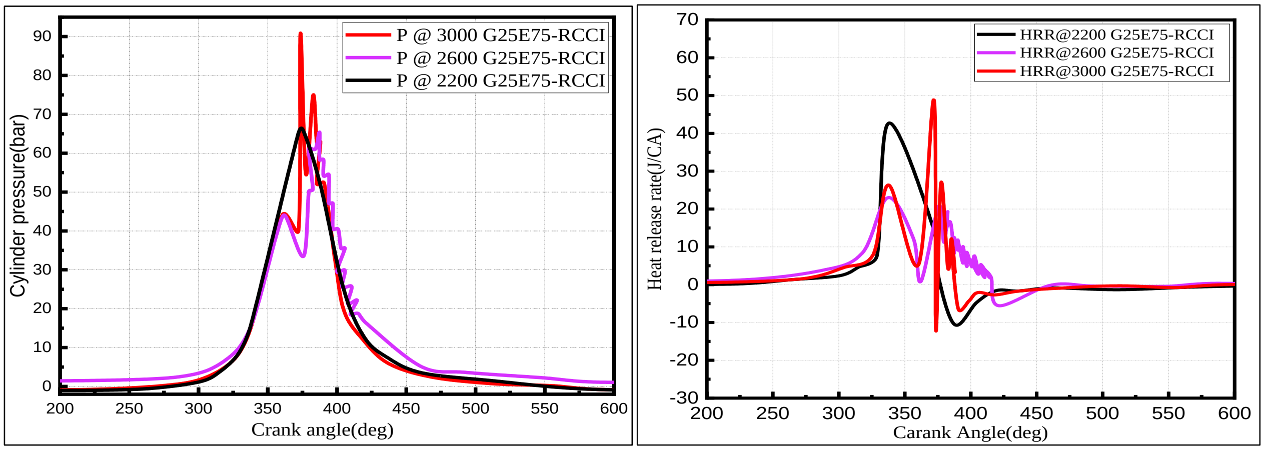

a. Cylinder pressure b. Heat release rate

Figure 4.5 Cylinder pressure and HRR (J/CA)

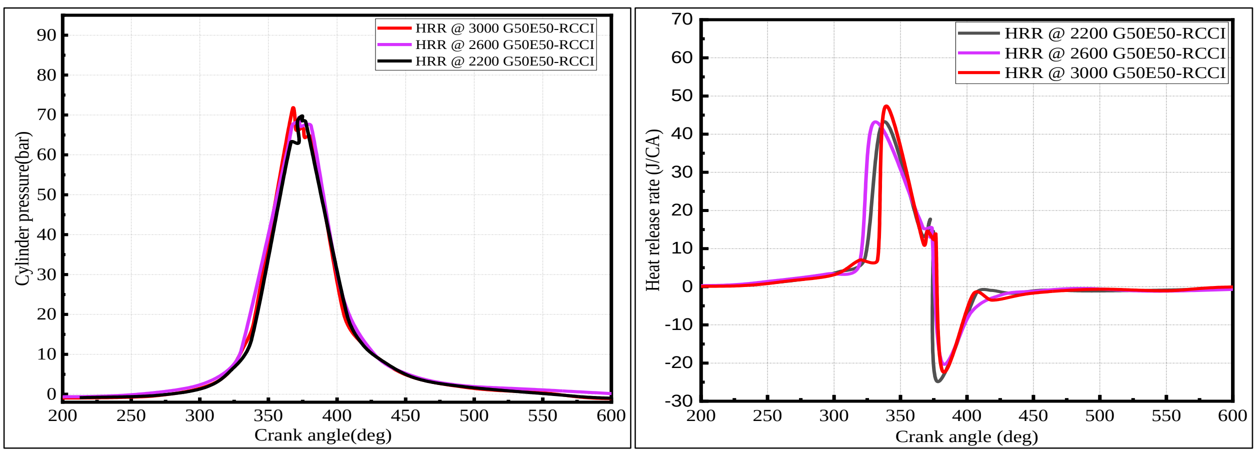

a. Cylinder pressure b. Heat release rate

Figure 4.6 Cylinder pressure and heat release rate

4.1.3. Engine performance characteristics of the experiment

The term engine performance describes an engine's capacity to produce power effectively, including brake power, torque, thermal efficiency, and fuel consumption. All other advanced RCCI engine operating modes were compared to the baseline performance test conducted with a traditional diesel-combustion engine. It includes several factors, including overall operating qualities, emissions, fuel efficiency, power output, and reliability.A balance between power, efficiency, emissions, and the overall user experience is necessary for optimizing engine performance.

4.1.3.1.The brake power of the experiment result

The brake power versus engine from speed ranging from 2000 to 3000 rpm are investigated. The experimental result showed that the brake power of the engine running at the speeds range of 2500-3000rpm with G50E50 and G25E75 port injection fuel is slightly greater than the baseline power (See Fig 4.7). However, the 2200-2400rpm range is the speed at which baseline power is greater. Power from the engine continuously increased as the engine speed increased for all blends which is similar to the performance results reported earlier and in line with (Tibaquirá et al., 2018), and also for pure diesel case.

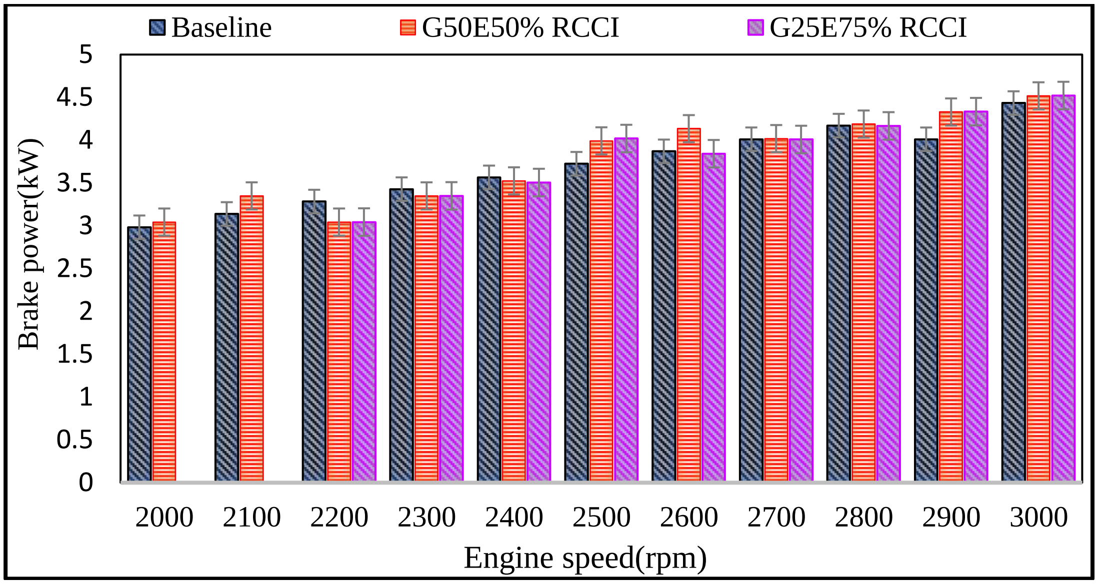

Figure 4.7 Brake power

The engine mechanical limit is constrained and affected as the engine speed is reduced below 2200 rpm for the engine running with the fuel blend of G25E75-RCCI engine operation mode. It is the same for the engine speed below 2000 rpm for the engine running with the fuel of G50E50 blend, but the engine ran smoothly with the baseline fuel until the engine speed declined to idle speed. The power correction factor is the coefficient by which the measured power is multiplied to determine the engine brake power under the reference atmospheric conditions specified. The power data determined must refer to the standard conditions (geodetic height above sea level, air pressure 1.013 bar, and air temperature 20°C) by DIN 70200. The equation (Eq 4.1), (Sodré et al., 2003) below provides the reduced output power. The reduced output power is calculated by using this equation, which may be greater than the output power values determined.

$$P_{red} = \sqrt{\frac{T_{amb} + 273k}{293°C}} \times \frac{1.013bar}{Pamb} \times P \qquad \text{(Eq 4.1)}$$

Where: T_{amb} - is the ambient temperature in °C, and P_{amb} - is the current ambient pressure.

4.1.3.2.The brake torque of the experiment result

The results showed the higher brake torque with the G50E50 and G25E75 in the speed ranges of 2200-2600rpm and consistently lower brake torque values in conventional diesel engines (See Fig.4.8). The constant lower brake torque values for the baseline fuel were recorded at all engine speeds due to the constant load operation for all fuel blends, at speeds greater than 2600rpm. The graph also showed for the blended fuel that the brake torque increased in the speed range of less than 2600. However, the torques peak at about 2400 rpm and then begin to decline with further increasing speeds as it was in line with (Anh, 2020).

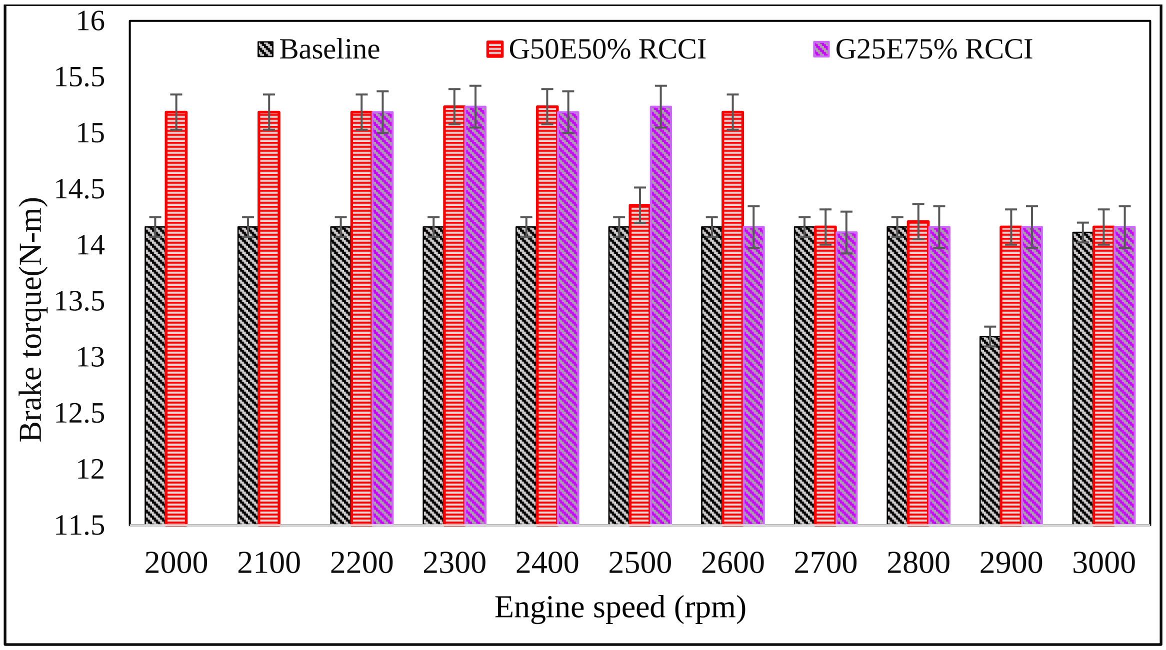

Figure 4.8 Brake torque of the engine

4.1.3.3.Brake thermal efficiency

The brake thermal efficiency is determined by how effectively heat is converted into useful work. The brake thermal efficiency purely depends on the engine design, type of fuel, and engine application. The variation of brake thermal efficiency for different blends and pure diesel fuel is shown (See Fig. 4.9). Among the different blends, the calorific values of ethanol, gasoline, and diesel fuel used are 26800, 42400, and 42500 KJ/kg, respectively. Since the fuels used for this investigation were G25E75 and G50E50 for the port-injected fuel only, it is necessary to find out the calorific value of the blends as follows:

The LHV of the G25E75-RCCI engine combustion mode is shown in equation (Eq 4.2)*:*

$$\mathrm{LHV_{G25E75}} = (15\% \times \mathrm{LHV_E}) + (5\% \times \mathrm{LHV_G}) + (80\% \times \mathrm{LHV_D}) \qquad \text{(Eq. 4.2)}$$

Where: LHV_E= 26800, LHV_G=42,400, and; LHV_D =42,500KJ/kg, then the $LHV_{25/75\text{-}RCCI}$=40, 140KJ/kg

For the engine running with G50E50-RCCI mode operation, the LHV of the blends is found as shown in equation (Eq.4.3).

$$\mathrm{LHV_{G50E50}} = (10\% \times \mathrm{LHV_E}) + (10\% \times \mathrm{LHV_G}) + (80\% \times \mathrm{LHV_D}) \quad \text{(Eq. 4.3)}$$

So that, the $LHV_{50/50\text{-}RCCI}$ = 40,920, and the LHV_{Diesel} = 42,500 KJ/kg respectively

After computing the calorific values of G25E75-RCCI, G50E50-RCCI, and diesel fuel, which are 40,140KJ/kg, 40,920KJ/kg, and 42,500 KJ/kg, respectively. The brake thermal efficiency of the engine running with each fuel computed from equation (Eq.4.4) is illustrated in Fig.4.10.

$$\eta_{\mathrm{b.th}} = \frac{\mathrm{BP}}{\dot{m}_f \times Q_{\mathrm{LHV}}} \times 100 \quad \text{(Eq. 4.4)}$$

Where Q_{LHV} is the lowest heating value of the fuel in KJ/kg and the mass flow rate of fuel flow is in kg/sec.

The thermal efficiency of the engines running at G25E75-RCCI is seen to be slightly greater in the speed range of 2800-3000rpm. The G50E50 blended fuel is good at a speed range of less than 2200 engine speed and diesel engines are seen to be performing better at the speed range of 2200 to 2700rpm respectively. The independent result showed a maximum thermal efficiency of 36% at baseline and speeds of 2600 rpm and a maximum thermal efficiency of 30% at 2500 rpm when operating with G50E50 and G25E75-RCCI. However; the engine running with the G25E75 port-injected ethanol-gasoline blends had a mechanical limit as the engine speed became lower than 2200rpm and the engine running with the G50E50 port-injected fuel at speeds below 2000 due to the different octane values in the port injected fuel (R. Hanson et al., 2013). RCCI mode at higher speeds tends to result in BTE that is on par with pure diesel and this in conjunction with enhanced brake power could be effectively exploited. Since ethanol is a good renewable energy source, sustainable, and can be locally produced (Jagankumar et al., 2020; Jeyakumar et al., 2022; Jeyakumar et al., 2020) the port injection presents an opportunity to replace or substitute fossil-based gasoline with an optimal extent.

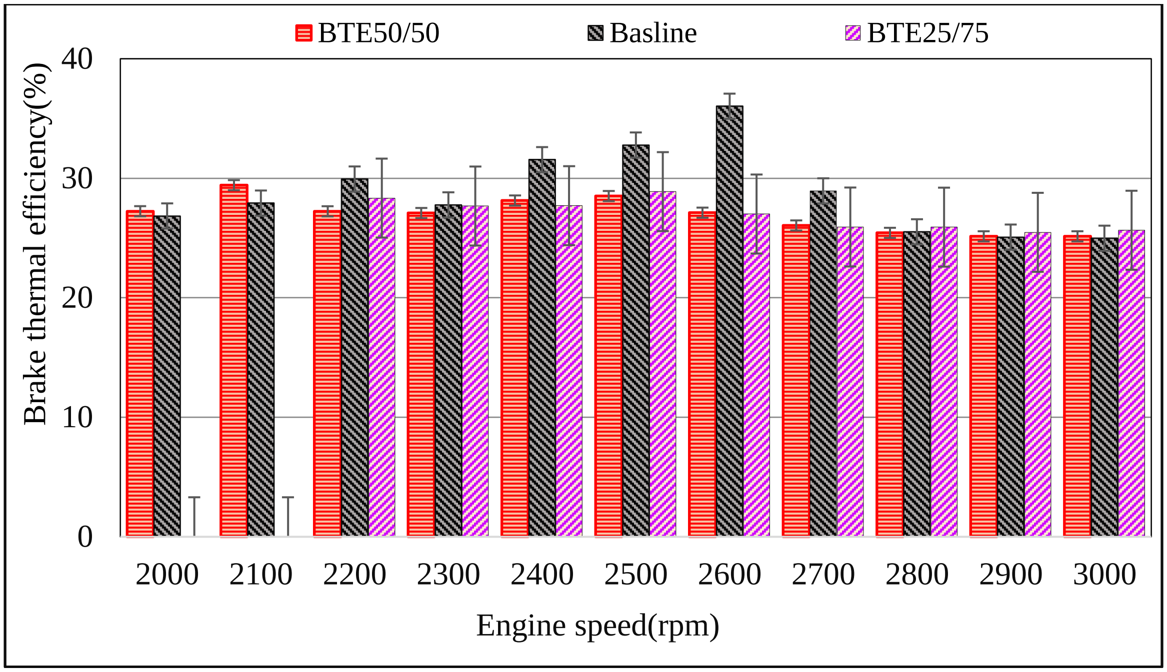

Figure 4.9 Brake thermal efficiency

The error bars for all engine performances and emissions shown in Figs 4.7- Fig 4.9 are a combination of the accuracy and precision of the performances and emission efficiency measurement from the light-duty CDC and RCCI Engines, which approximately indicate that the error bar is small and acceptable as it is explained in (Ansari et al., 2018; Willems et al., 2021). Table 4.1 indicates the data taken from the computer that showed the engine operating condition when experimenting.

Table 4.1 Engine operation data from the data acquisition system

N	T_3	T_1	T_2	F_1	eta	V_s
2000	406.2	33.02	25.93	270	27	0.25
2100	408.7	32.00	25.93	271	27	0.25
2200	534.8	30.00	25.93	290	29	0.25
2300	545.8	29.12	25.92	304	28	0.25
2400	554.2	29.00	25.48	315	26	0.25
2500	566.4	28.02	25.53	325	25	0.25
2600	543.6	28.05	25.52	336	23	0.25
2700	537.2	27.00	25.52	351	22	0.25
2900	443.8	27.00	25.51	368	20.5	0.25
3000	334.7	27.50	25.50	386	20	0.25

Where: N-Engine speed, T_3- Exhaust gas temperature, T_1-intake air temperature, T_2-fuel temperature, F_1-intake air volume (L/min), Vs-swept volume.

4.1.3.4.Brake-specific fuel consumption

Brake-specific fuel consumption is the ratio of the rate of fuel consumption per unit effective power output. Fig.4.10 pinpoints the brake-specific fuel consumption versus engine speed. These results indicate a minimum brake-specific fuel consumption for the baseline and a maximum for G25E75 pre-mixed fuel. Nevertheless, as the speed increases; brake-specific fuel consumption is decreased until the maximum engine speed of 3000 rpm. The BSFC is average for G50E50-RCCI as it is in line with (Tibaquirá et al., 2018).

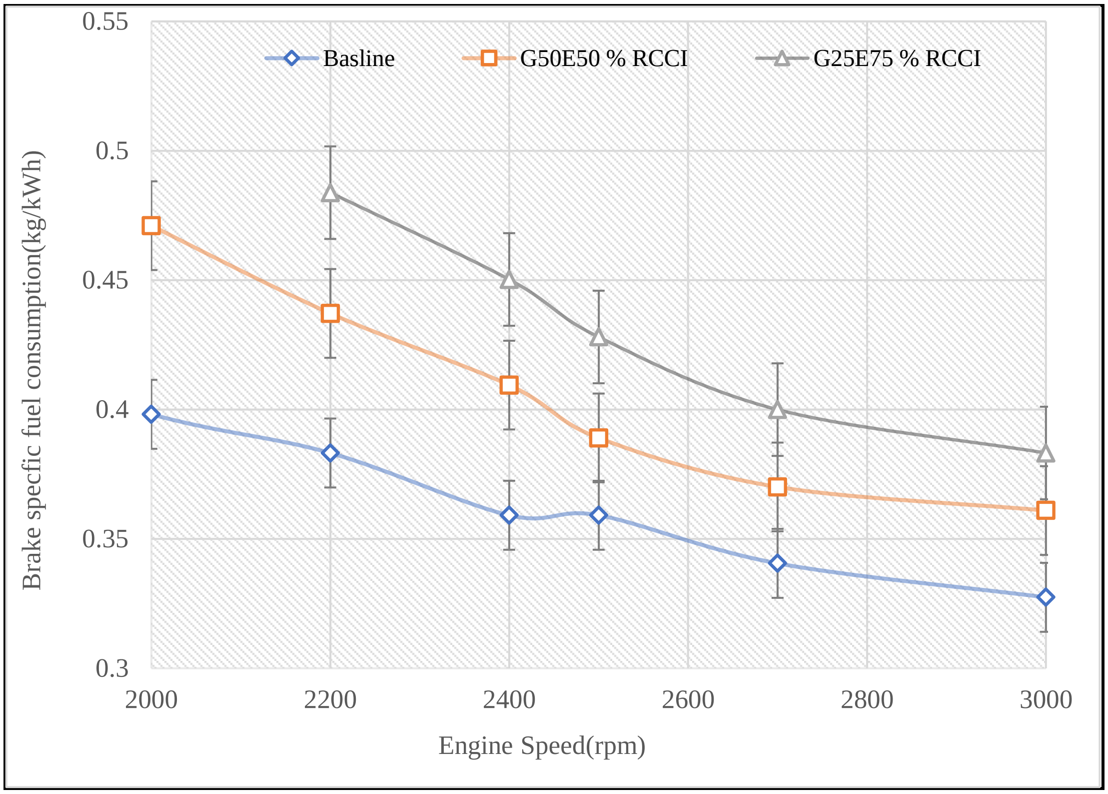

Figure 4.10 Brake-specific fuel consumption

4.1.4. Engine emission

The emissions that need attention from the diesel engine are oxides of nitrogen and particulate matter. Unburned hydrocarbons and carbon monoxide are the central issues for the emissions from the RCCI-diesel operation. Nitrogen oxide emissions, shown in Fig.4.11, from the engine with the highest percentage of ethanol (G25E75-RCCI) are the lowest across the speed range and highest for the engine running with the baseline diesel fuel as it is in line with the previous finding of (Tibaquirá et al., 2018).

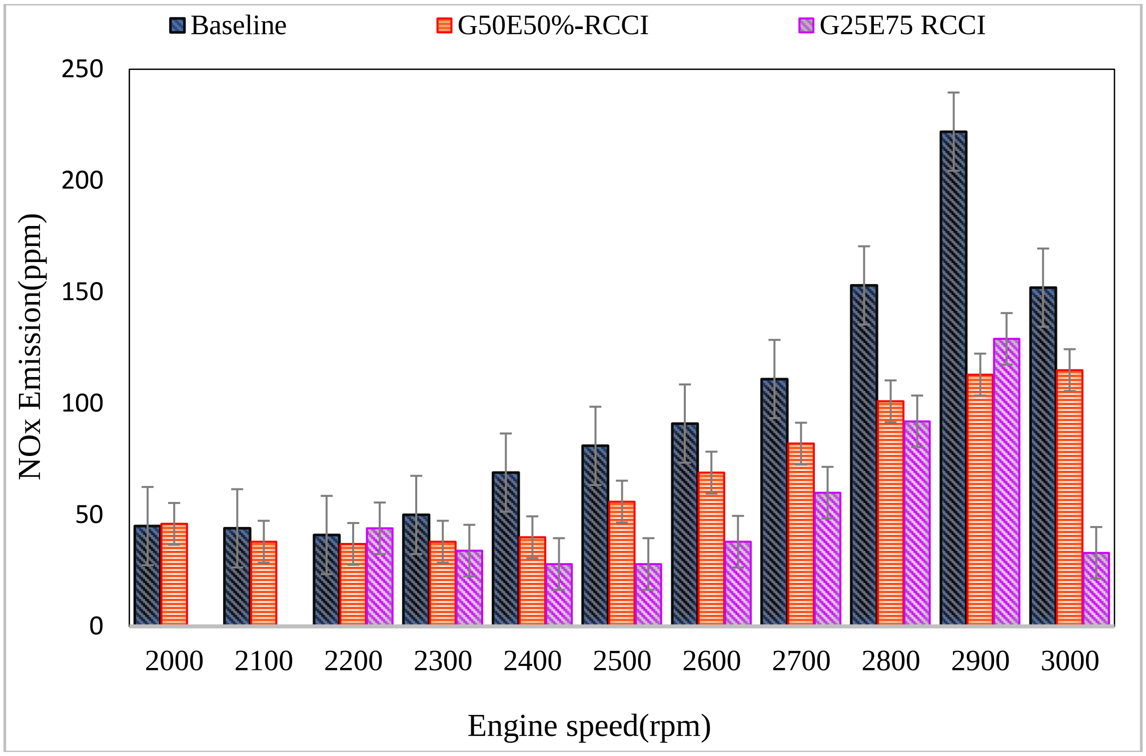

Figure 4.11 NOx emissions

The G50E50 premixed blend has an average value, which is an acceptable targeted result according to this study's objectives. The nitrogen oxide tends to get reduced due to the cooling effect of the ethanol content. Because of the nature of the lean operation of the diesel engine, emissions of carbon monoxide in volume % and unburnt hydrocarbon in ppm were lowest when the engine runs with conventional diesel. The CO and HC emissions of the diesel engines running with the G25E75 are the maximum and average for the engine operating with the G50E50-RCCI. The carbon monoxide and unburned hydrocarbon emission results from the experiment indicate that the RCCI engine operation mode has more CO and HC emissions but low carbon dioxide emissions when compared to the CDC engine across the speed range, as shown in Fig.4.12 and Fig.4.13 below. HC emission with RCCI had seen to approach that of baseline diesel at higher speeds. The higher CO emission from G25E75 at higher speeds could be attributed to the cooling effect associated with higher ethanol content. However, in the lower speed range, both HC and CO emission with this blend seems to be either on par or lower than that of baseline diesel. The carbon dioxide emissions in volume % at all speeds are maximum with conventional diesel combustion. The blend with higher ethanol content yielded substantially lower CO_2 emission except at high speed as shown in Fig 4.14.

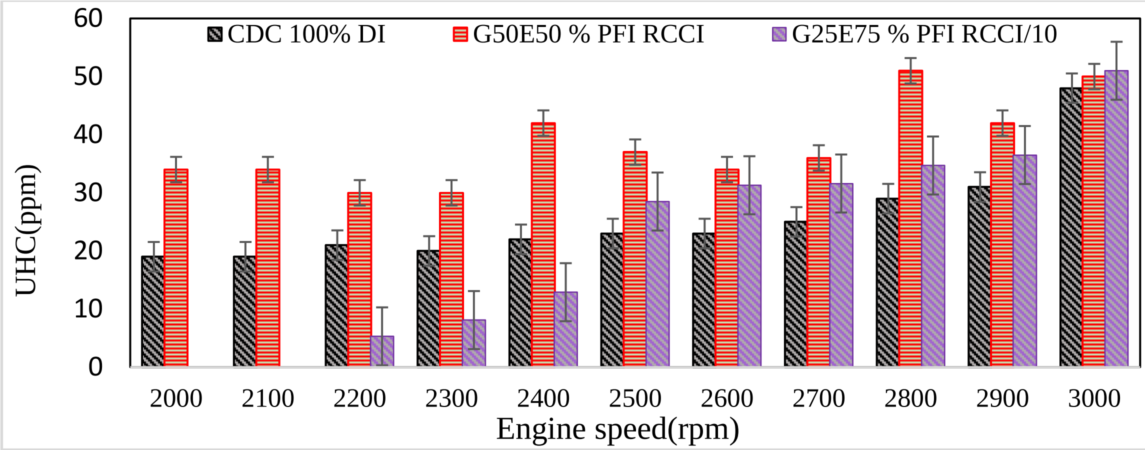

Figure 4.12 HC emission

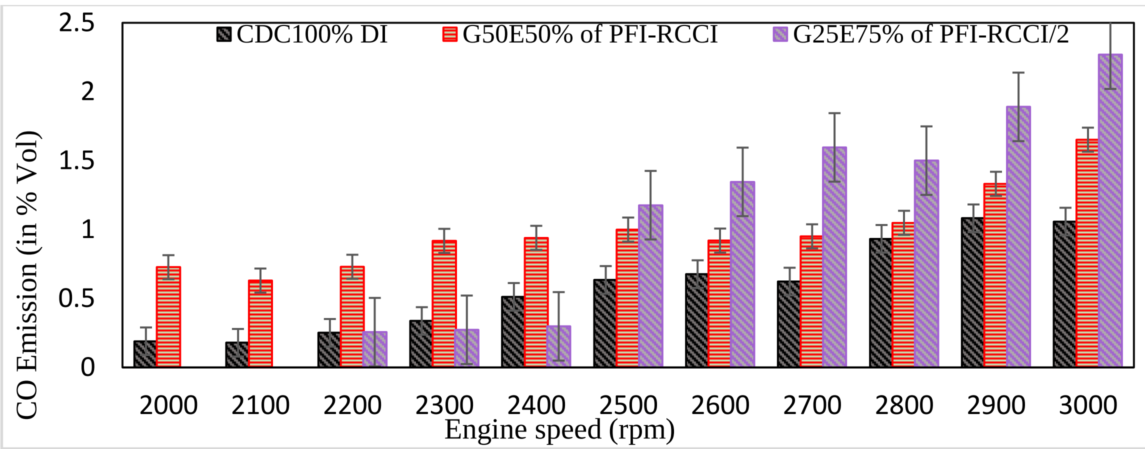

Figure 4.13 CO emissions

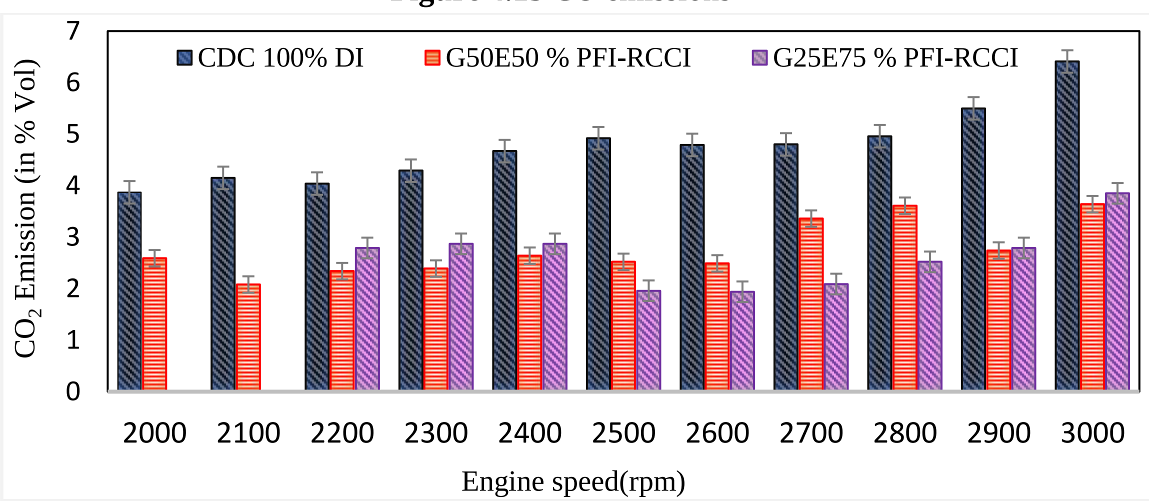

Figure 4.14 CO_2 emission (in % Vol)

4.2. Triple fuel physiognomies on light-duty RCCI engine

Of the two most common types of internal combustion engines, diesel engines are widely used in a variety of economic sectors, including transportation, agriculture, and construction due to their excellent fuel and thermal efficiency, durability, torque, reliability, and lower running cost (Agarwal et al., 2013a). To address future demands for cleaner and more efficient internal combustion engines, the majority of current technologies are classified as LTC. RCCI engines are the most recent promising IC engines that have been proposed to increase combustion, performance, and emission efficiency. The operation principles of RCCI engine combustion is a dual-fuel combustion, that controls the ratio of two fuels with different levels of reactivity injecting the LRF with a port injector into the intake manifold and the HRF directly injected into the cylinder.

In the present study, a gasoline-ethanol blend is used as port-injected fuel at various ratios. Therefore, the objective is to use a novel approach that emphasizes comparing the effects of various fuel blend ratios, at various engine speeds instead of assessing each single fuel for PFI. The comparison of each port-injected (G5E15), and (G10E10) is 20% with different blend ratios as shown in the brackets, and 80% direct injection (D80) RCCI and baseline operation are explored. Higher CO and HC emissions are a drawback of the RCCI concept in which the previous research work shows a future direction that it is possible to simultaneously achieve ultra-low engine-out emissions of NOx, PM, and an innovative fuel mix can also reduce CO, and hydrocarbon which is the issue in RCCI (Baškovič et al., 2022). The research work arises from the investigation conducted with port-injected alcohol or gasoline alone having high carbon monoxide, and unburned hydrocarbon emissions (Pan et al., 2021).

Therefore, it is important to test ethanol-gasoline blends in an up-to-date LTC concept of the RCCI. This investigation aims to use sustainable ethanol energy sources for fossil energy replacement to reduce emissions and find the operating conditions for enhanced reduction of CO and HC. The experimental study on the base engine used diesel fuel alone for the conduction of the experiment; the modified RCCI engine used a different ratio of ethanol-gasoline blended fuel supply into the manifold to enhance fuel reactivity, and diesel fuel directly injected into the cylinder. Under present and upcoming legislation, vehicles must obey strict rules for both pollution and fuel efficiency. The subscripts D(diesel fuel) and GE (gasoline-ethanol) blend represent the primary and secondary fuels (r_p=G5E15, G10E10);

however, for baseline compression ignition combustion (r_p = 0), In all experiments, the SOI timing maintained constant at 14°CA before top dead center (bTDC) at all engine operation conditions. For simplicity, it is practical to define valve timings with the aid where two generic intake and exhaust valve lifts are depicted. Another essential parameter is the valve overlap, the phase when both intake and exhaust valves are open simultaneously. The engine for the experiment study had the EVO/C, and the IVO/C with a total opening as in Table 4.2.

Table 4.2 EV and IV opening and closing point

Valve position	Exhaust valve	Intake valve
Open	65°CA bBDC	15°CA Btdc
Close	20 °CA aTDC	50°CA Abdc
Total open	255°CA	245°CA

Where: bBDC-before bottom dead center, aTDC-after top dead center, IVO: intake valve open; CA: crank angle; IVC: intake valve close; EVO: exhaust valve open; EVC: exhaust valve close. The engine's piston point and the cylinder volume in m^3 for the experiment have the strokes-to-bore dimension.

4.2.1. Cylinder pressure and heat release rate

4.2.1.1.Cylinder pressure results of the experiment

The combustion analysis of the baseline and modified RCCI engines uses the triple fuel strategy, in which the ratios of premixed blends of gasoline-ethanol, and diesel direct injection fuel are used. The cylinder pressure, heat release rate, and cylinder temperature of the engine at different speeds of 2000, 2500, and 3000 rpm with various fuel ratios were studied. According to the result, the maximum cylinder pressure in the engine running with base fuel, G5E15, and G10E10-RCCI are 61.2, 90.76, and 71.3bar at the engine speeds of 3000 rpm respectively, and the minimum cylinder pressure of the base fuel, G5E15, and G10E10 are 58.69, 65.4, and 68.2bar at the engine speeds of 2500-rpm respectively. The average cylinder pressure at the base fuel, G5E15-RCCI, and G10E10-RCCI are 60.4, 66, and 69.8 bar at the engine speeds of 2000 rpm respectively.

As shown in Fig.4.15, the engine running with the base fuel is lower as compared to both G5E15 and G10E10-RCCI engine mode operation. As a whole, the maximum 90.76 bar cylinder pressure is found at 3000 rpm with G5E15 port-injected fuel. In this study, the engine experiment results were validated using baseline, modified RCCI, and the work results of the other.

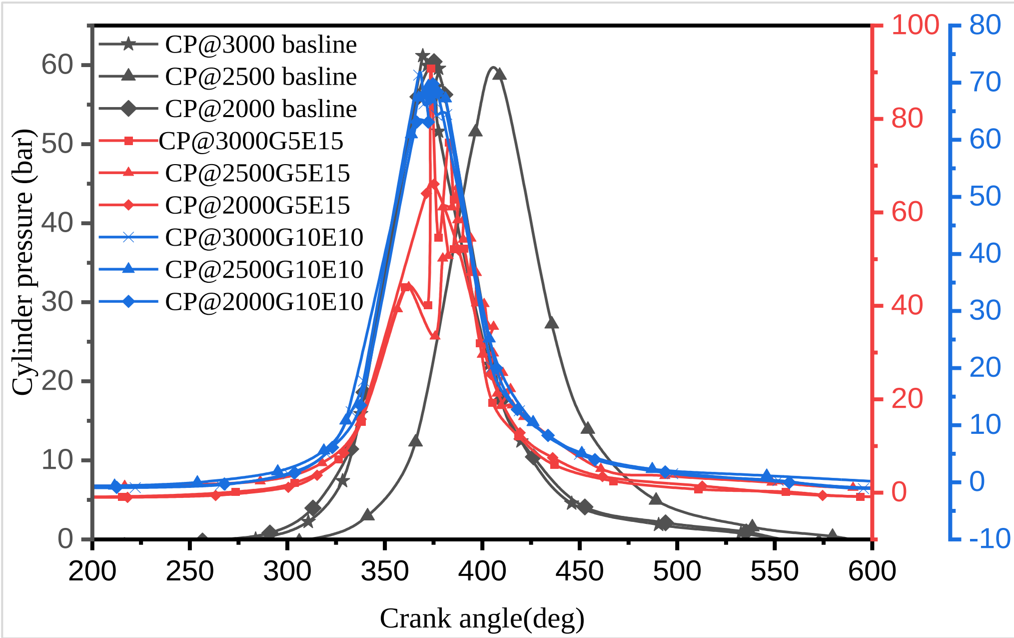

Figure 4.15 Cylinder pressure

4.2.1.2.Heat release rate

The heat release rate during fuel combustion is estimated from the cylinder pressure measurement by applying the first law of the single zone model. The heat release rate of the base and modified RCCI engines are used in the diesel and triple fuel strategy respectively in which the ratios of blended PFI and diesel direct injection are investigated. The heat release rate of the engine at each engine speed of 2000, 2500, and 3000 rpm was studied. According to the experiment results, the maximum heat release rate in the engine running with base fuel, G5E15, and G10E10-RCCI is 39.29, and 63.02 both at 3000rpm and 43.23J/CA at the engine speeds of 2000 rpm respectively. The minimum heat release rate of the base fuel, G5E15, and G10E10 are 11.8, and 22.98 both at the speeds of 2500 rpm and 33.04J/CA at the engine speeds of 3000 rpm respectively. The average heat release rates at the base fuel, G5E15, and G10E10-RCCI are 32.4, and 42.68 at the engine speeds of 2000 and 43.02J/CA at 2500 rpm respectively (See Fig.4.16). The engine running with the base fuel is lower as compared to both G5E15 and G10E10-RCCI engine mode operation. The maximum HRR of 63.02J/CA is at 3000 rpm with G5E15 port-injected fuel. In this investigation, the engine operating conditions were validated using baseline, RCCI engines, and the work reports of the other. Each fuel of the baseline, G5E15, and G10E10 are separately used at varying engine speeds.

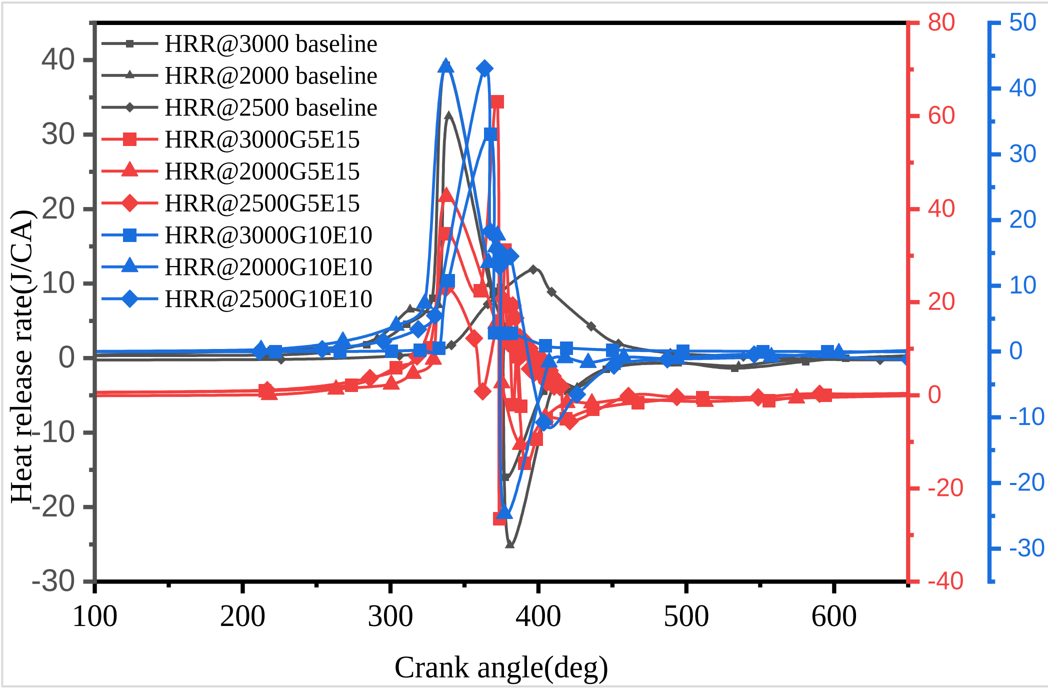

Figure 4.16 Heat release rate

4.2.1.3.The cylinder temperature of the simulation result

In compression ignition engines, the maximum cylinder temperatures (MCT) attained by the fuel depend mainly on the mass of fuel burned during the combustion phase. The cylinder variation of all the test fuels concerning crank angle at different fuel ratios. The maximum cylinder temperature at base fuel is 1780k at 2500 engine speed and for G5E15, and G10E10-RCCI is 1688, and 1775 respectively at the engine speeds of 3000rpm. The minimum cylinder temperature at base fuel, G5E15, and G10E10-RCCI are 1662, 1661, and 1750k respectively at the engine speeds of 2000rpm. The average cylinder temperature with base fuel is 1691.6k at the speeds of 3000rpm and G5E15, and G10E10-RCCI is 1675, and 1760k respectively at the speeds of 2500rpm. The results showed the maximum cylinder temperature of 1780k at the baseline (See Fig 4.17).

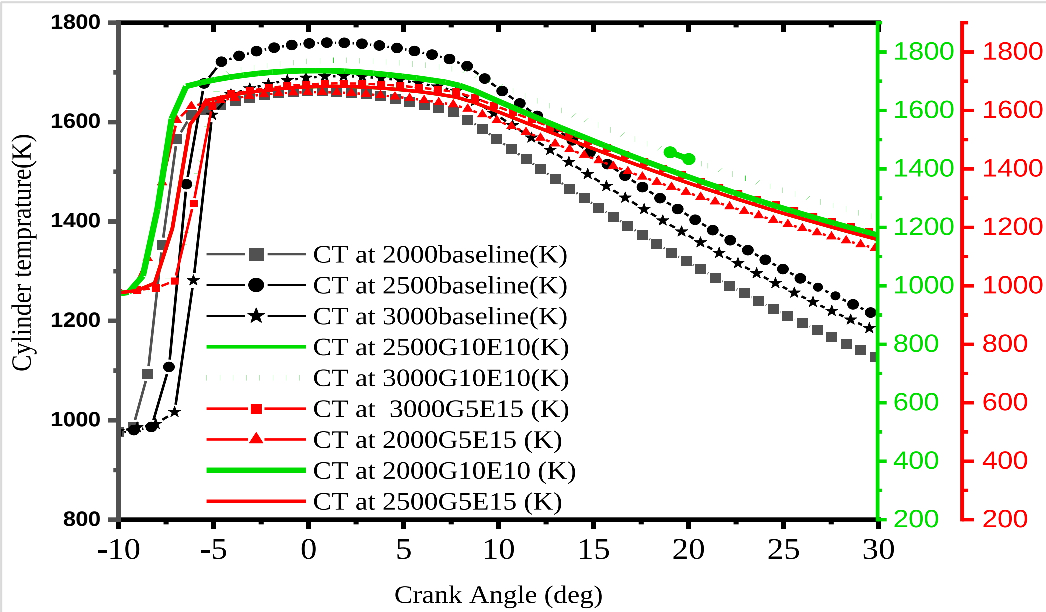

Figure 4.17 Cylinder Temperature

4.2.2. Engine tail pipe exhaust emissions

The discharges from internal combustion diesel engines that need attention are NOx and particulate matter, but HC and CO are not significant issues in diesel engines due to lean engine operation. The oxides of nitrogen from the exhaust emission of the engine running with base fuel, G10E10, G5E15-RCCI are maximum, average, and minimum respectively at the speed ranges of 2400-3000rpm.

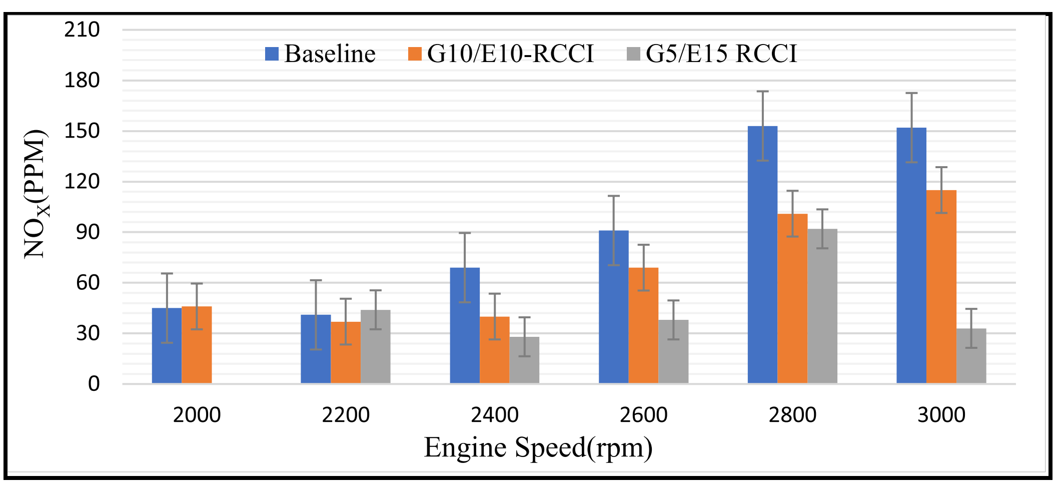

Figure 4.18 Oxides of nitrogen emission

The engine operating with G10E10 premixed fuel has a lower NOx emission at the engine speed of 2200rpm, which is an adequate targeted result according to the objectives of the study. The NOx emission is continuously increasing as the engine speed increases until 2900 rpm and then declines. The NOx is minimized due to the ethanol content having the nature of the cooling effect as shown in Fig.4.18.

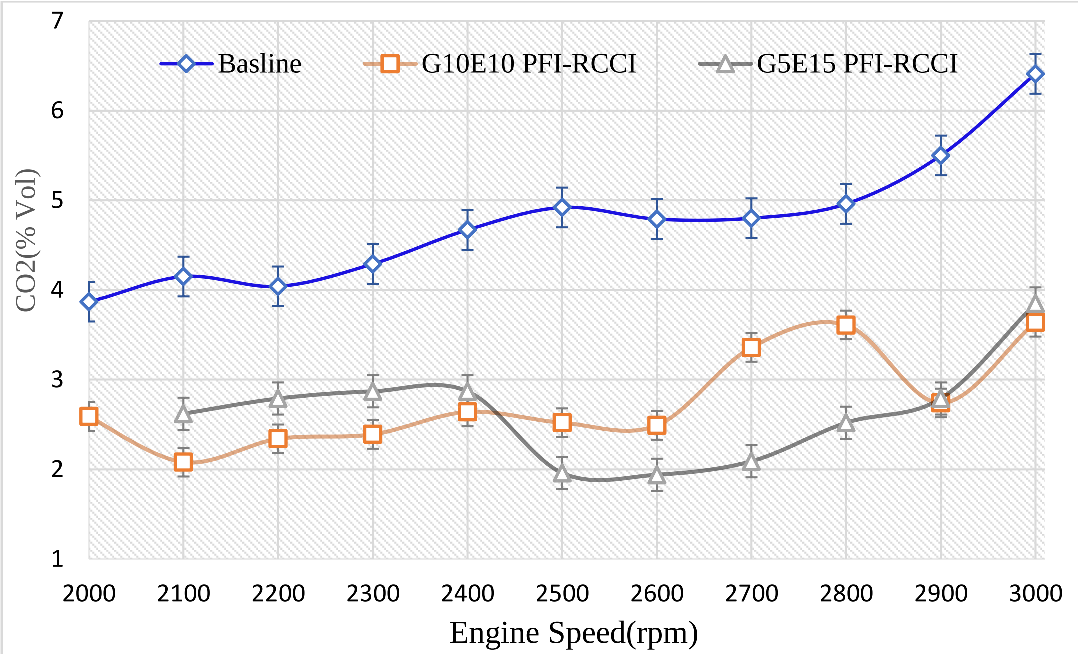

Figure 4.19 Carbon dioxide emissions

Carbon dioxide emissions in percentage volume of a modified diesel engine running with G5E15, G10E10-RCCI, and baseline are minimum, average, and maximum respectively (See Fig.4.19) at a speed greater than 2400rpm. At the speed ranges below 2400rpm, carbon dioxide (CO_2) emission is minimum with the engine running G10E10-RCCI and maximum at the engine running with baseline fuel. Carbons in combusted fuel that are not converted to CO_2 are released as carbon monoxide.

The carbon monoxide emission as a percentage volume versus engine speed and unburned hydrocarbon emissions in particles per million (ppm) experimental results (See Fig 4.20) and 4.21) respectively. For the engine running of G5E15-RCCI; carbon monoxide and unburned hydrocarbon is maximum at speeds greater than 2400rpm, and minimum in both G10E10-RCCI and baseline emission respectively. The CO emission results from the experiment are higher in speeds less than 2400rpm at the engine running of G10E10-RCCI. The CO and HC results from the experiment indicate that the RCCI engine combustion mode has low CO and HC at the fuel G10E10, which can be considered a good finding of the investigation.

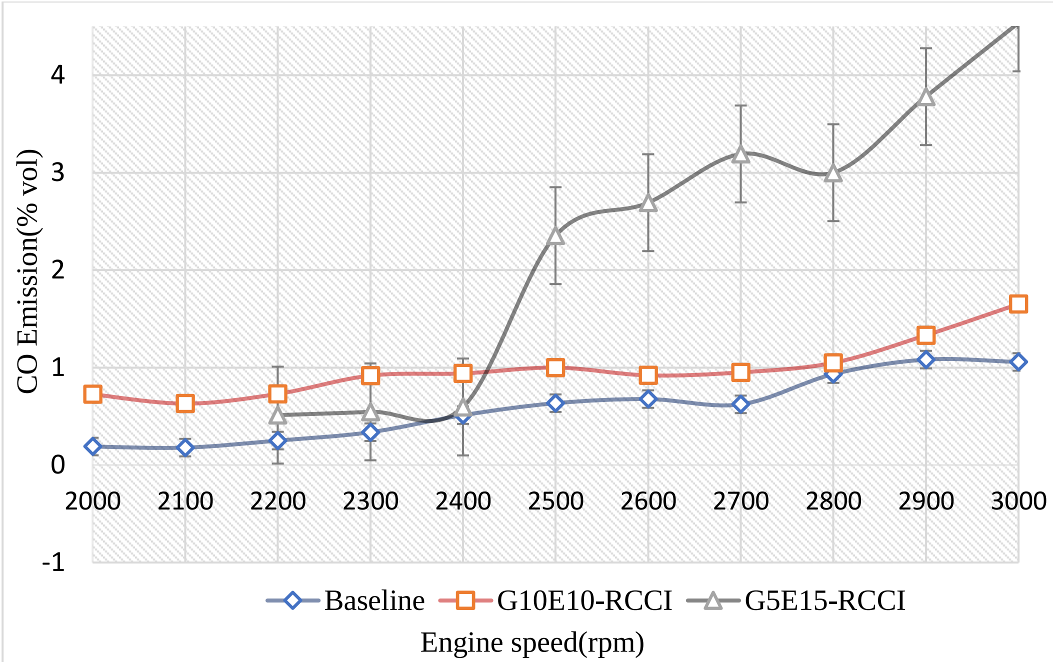

Figure 4.20 Carbon monoxide emissions

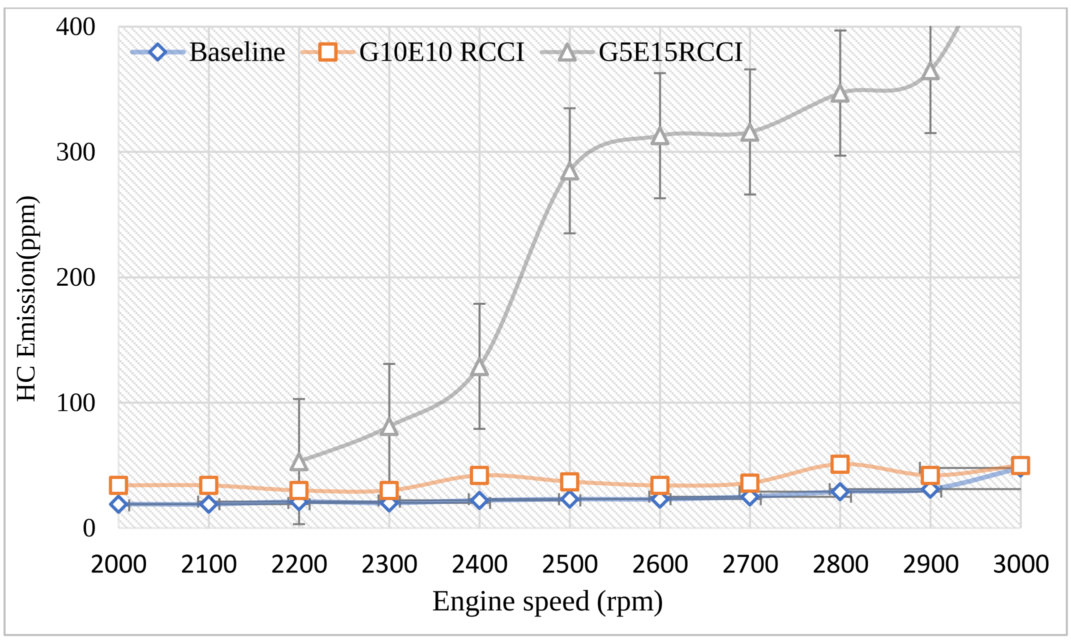

Figure 4.21 Hydrocarbon emissions

4.2.3. Engine performances

The experimental studies were carried out in a base fuel and modified RCCI single-cylinder diesel engine. Engines at different speeds are valued with the performance of brake power, brake torque, brake thermal efficiency, and brake-specific fuel consumption. The baseline experiments took place by using pure diesel fuel in conventional diesel engines to compare with all other modified engine-operating modalities used in the current advanced engine test rig.

4.2.3.1.Engine brake power and torque

Fig 4.22 shows the brake power versus engine speed, ranging from 2000-3000 rpm. The experiment showed that the brake power of the engine running with G10E10, G5E15-RCCI, and baseline fuels are continuously increasing as the speed increased. The brake power of the engine in all experiment cases is the same except with the slight increases of power in G10E10 fuel at engine speeds greater than 2400rpm. At low engine speeds of 2200 and 2400, the brake power is better in an engine running on baseline. These showed that as the amount of ethanol or gasoline in the premixed fuel increases, the brake power is reduced at lower speeds and increased at higher speeds. Fig. 4.23 shows the brake torque versus engine speed with various fuel ratios. Results showed higher engine brake torque at the speed ranges of 2000-2600 rpm with a fuel of G10E10 and 2200-2400rpm with the engine running at the fuel of G5E15 and lower with the conventional diesel engine at all engine speeds cases, which is almost constant. However, the torque peak at 2400 rpm and then begin to decline with more speed. The brake torque is almost constant due to the constant engine load operation during the experiment.

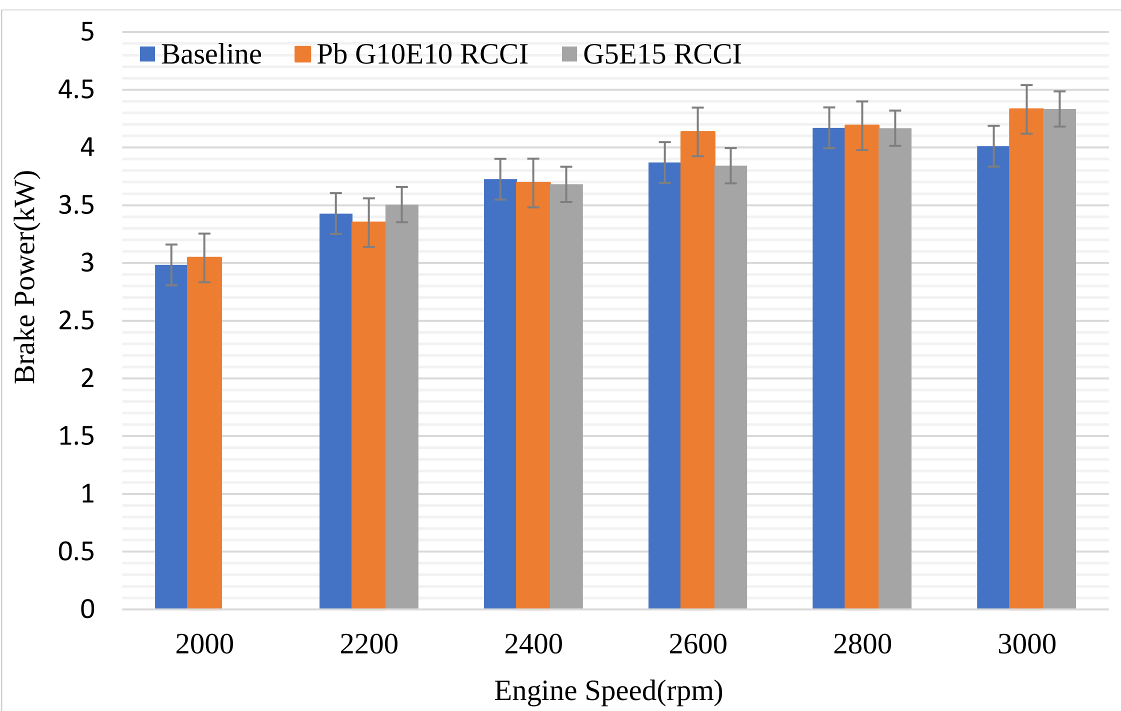

Figure 4.22 Brake power

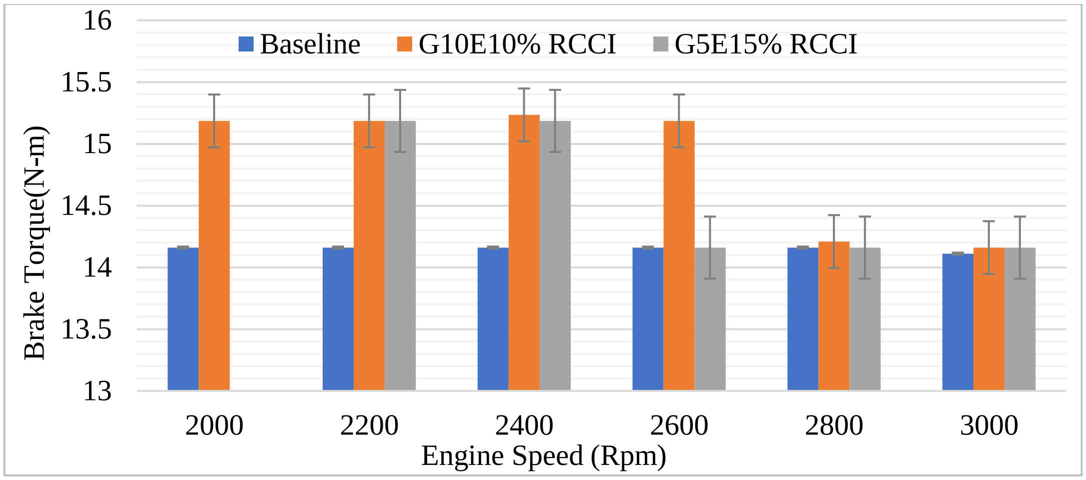

Figure 4.23 Brake torque

4.2.3.2.Brake thermal efficiency

Brake thermal efficiency is the ratio of the brake power obtained from the engine to the fuel energy supplied. The brake thermal efficiency purely depends on the engine design, type of fuel, and engine application. Among the different blends, the calorific values for the current investigations of ethanol, gasoline, and diesel fuel are 26,800, 42,400, and 42,500 kJ/kg respectively. Fig. 4.24 shows the higher brake thermal efficiency at the engine running with the baseline fuel at the speeds ranges of 2200-2600 rpm and higher for the engine running of G5E15 at the higher speeds of 2800 and 3000 rpm. The independent result showed a maximum thermal efficiency of 37% at 2600 rpm and; a minimum of 25.14% at 3000 rpm when both are operating with baseline fuel as it is aligned with (Işık and Aydın, 2016; H. Liu et al., 2018).

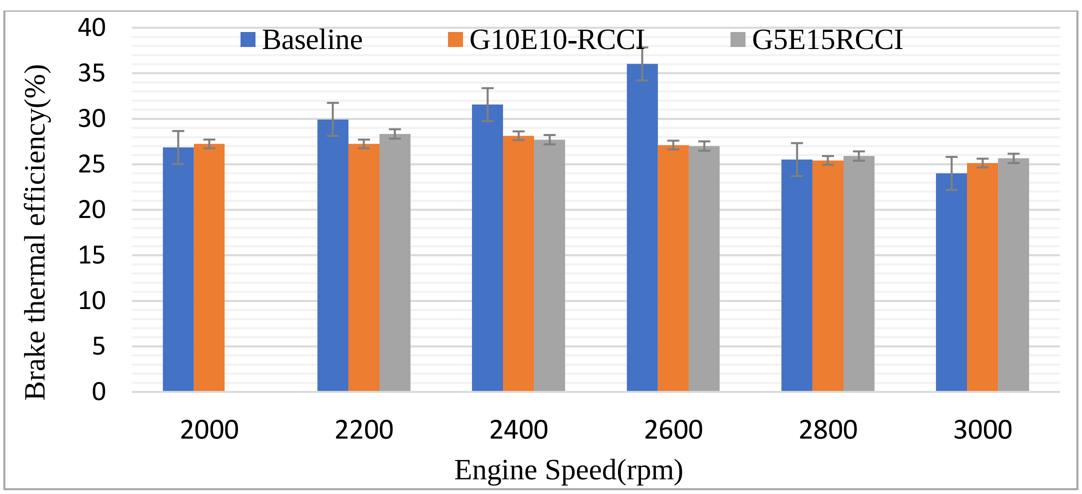

Figure 4.24 Brake thermal efficiency

4.2.3.3.Brake-specific fuel consumption

The engine that burns the fuel-air mixture causes the crankshaft to rotate and measures fuel efficiency using the BSFC. This is to compare the engine's efficiency. The brake-specific fuel consumption is the ratio between the engine's effective power output and the rate of fuel consumption. Fig.4.25 determines the BSFC characteristics versus engine speed. The investigation's result indicates a minimum brake-specific fuel consumption at the baseline experiment at all engine speeds and a maximum at the engine running with G5E15 fuel but an average at the engine running with G10E10.

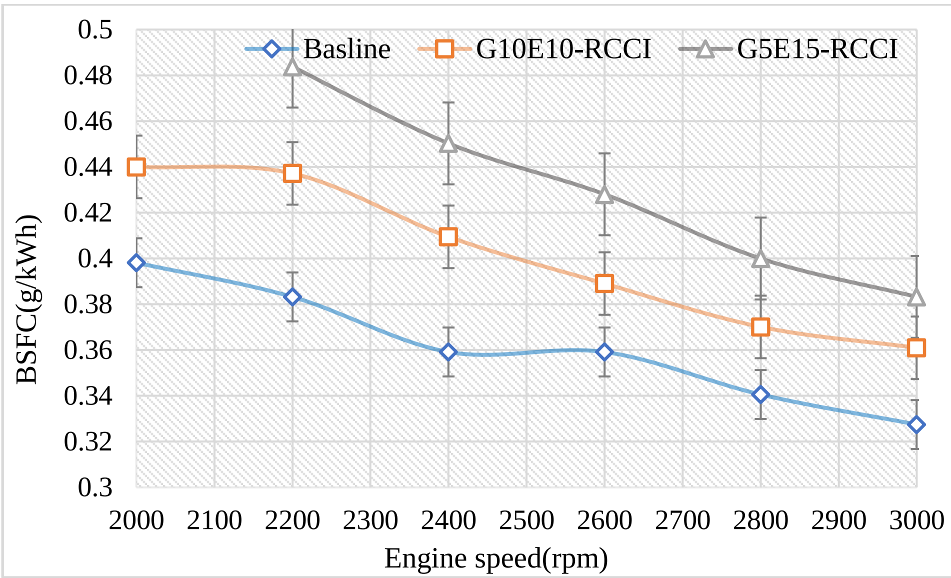

Figure 4.25 Brake-specific fuel consumption

4.2.4. Result validations using other similar work

The present experimental results and those from other similar works are quantitatively shown in the table to validate the investigation as to whether it is in line with other relevant and similar scientific research works or not. As can be seen from (Table 4.3), the maximum cylinder pressure and heat release rate at the higher engine speed in the premixed ratio of G25E75; lower NOx and CO_2 emission, and the higher HC and CO emission in the baseline and advanced RCCI engine are nearly in line with (Agrawal et al., 2021). At the maximum engine load as the premixed ratio of the lower reactive fuel increases; the cylinder pressure and heat release rate are increased along with NOx emission reduction apart from the slight increases of CO and HC are also in line with the result reported earlier (Singh et al., 2021). The improved brake thermal efficiency the reduction of the nitrogen oxide and the increment of HC and CO are also indicated which is directly in line with (Jagankumar et al 2020) at a maximum engine load.

Table 4.3 Single fuel and dual fuel RCCI engine, Single fuel RCCI engine

Author	Parameters	CP	HRR	BTE	NOx	CO2	HC	CO
Present work At 2200	High load base	60	32	29.9	50	4	20	0.3
	High load 25/75	65	42	27.2	38	2.8	50	0.7
	High load 50/50	70	42	28.3	34	2.3	30	0.5
At 2600 rpm	High load base	60	12	36	91	4.8	23	1
	High load 25/75	65	23	27	38	1.9	310	2.7
	High load 50/50	70	42	27.1	69	2.5	34	1.7
At 3000rpm	High load base	61	40	25	152	6.4	40	1
	High load 25/75	91	63	25.6	33	3.9	510	5.6
	High load 50/50	71	46	25.1	115	3.6	58	2.3
Agarwal et al., 2021	1bar at base	45	-	16	16	-	1	15
	1bar at RCCI	45	-	15	2.5	-	18	60
	2bar at base	55	-	22	8	-	0.75	5
	2bar at RCCI	65	-	22.5	4.5	-	9	12
	3bar at base	59	-	29	7.5	-	0.5	3
	3bar at RCCI	75	-	30	3	-	7	10
	4bar at base	60	-	29	6	-	0	2
	4bar at RCCI	76	-	34	3	-	5	8
Singh et al., 2021	1 @ (rp=0)	70	160	18	13	-	25	43
	1 @ (rp=0)	72	20	14	3	-	1	13
	2@(rp=0.25)	72	240	24	6	-	14	33
	2@(rp=0.25)	40	30	22	1	-	3	4
	3@(rp=0.50)	80	170	28	5	-	13	22
	3@(rp=0.50)	40	65	26	1	-	1	3
	4@(rp=0.75)	84	300	34	5	-	11	16
	4@(rp=0.75)	40	22	32	1	-	1	4
Jagankumar et al 2020	75 % load base	-	-	25	600		20	0.15
	75 % load RCCI	-	-	30	300		35	0.25

Where: r_p is a premixed ratio, numbers 1,2,3, and 4 are the engine load in torque (N-m)

4.3. Statistical response analysis of the experiment results

The engine emission problems demanded the development of advanced engine technology as well as an alternative fuel to fossil fuels that is both efficient and emits negligible emissions (Mofijur, Rasul, et al., 2019). Several innovative compression ignition techniques have been investigated to reduce emissions in a cylinder while retaining higher thermal efficiency. To address future demands for cleaner and more efficient power plants, the majority of current techniques are classified as LTC engines. The experimental study on the baseline engine and modified RCCI engine used premixed hydrous bioethanol and gasoline blended fuel supply into the manifold to enhance fuel reactivity and diesel fuel was directly injected into the cylinder. The study aims to use advanced RCCI engines and indigenous hydrous-bioethanol energy substitution to reduce oxides of nitrogen and particulate matter emissions. Even though there are numerous widely used orthogonal arrays, each array is suited for a specific number of independent design variables and levels. The most effective way to experiment to examine the impact of various independent variables, each of which has three set levels and two factors, is to use an L9 orthogonal array. The relationship between speed and the characteristics of the fuel is a typical example of an interaction. To reveal all factors influencing performance and emission characteristics, the common orthogonal arrays define the bare minimum of tests necessary.

4.3.1. Taguchi method approach optimizations

Taguchi's method approach enables the identification of the most critical factors that have the most significant impact on the performance or quality of a product or process. By focusing on these key factors, resources can be allocated more efficiently to achieve improvements. It employs statistical techniques, such as analysis of variance (ANOVA), to analyze the experimental data and determine the significance of factors. This analysis helps identify the main effects of factors, their interactions, and the optimal levels for achieving the desired performance or quality. By considering the interaction effects and selecting appropriate factor levels, the method helps identify robust solutions that meet target specifications. The speed, emissions, and performances and their statistical data results of the experiment designs are shown in Table 4.4.

Table 4.4 L9 Experiment results of emissions and performances

Speed	PFR	NOx	CO	CO_2	HC	Tb	Pb	SNR	LSTD	STD	MEAN	CV
2200	0	41	0.25	4.04	21	14.2	3.28	-25.93	2.73	15.37	13.95	1.10
2200	25/75	36	0.51	2.62	53	15.2	3.50	-28.60	3.06	21.48	18.47	1.16
2200	50/50	37	0.73	2.34	30	15.2	3.84	-26.23	2.73	15.47	14.85	1.04
2600	0	92	0.68	4.79	23	14.2	3.87	-31.87	3.54	34.74	23.08	1.50
2600	25/75	38	2.7	1.94	313	14.2	3.84	-42.20	4.82	123.6	62.27	1.98
2600	50/50	69	0.92	2.49	34	15.2	4.52	-30.12	3.28	26.5	21.01	1.26
3000	0	152	1.06	6.41	48	14.1	4.52	-36.31	4.07	58.56	37.68	1.55
3000	25/75	33	4.54	3.85	510	14.2	4.52	-46.39	5.31	203.6	95.01	2.14
3000	50/50	115	1.65	3.64	50	14.2	4.43	-34.24	3.80	44.75	31.48	1.42

SNR: signal-to-noise ratio LSTD – least square standard deviations STD–Standard deviations CV-Coefficients of variances.

4.3.1.1.Linear model analysis: SNR Vs Speed and PMFB-ratio

Taguchi's research design method is one of the most well-loved optimization strategies. The methodology was created to solve the drawbacks of multifactorial and full factorial designs that are connected to the outcomes attained through extensive experiments of speed, fuel ratio, emissions, and performance. The estimated model coefficient for the signal-to-noise ratio and ANOVA for the signal-to-noise ratio are shown in Table 4.5 and Table 4.8 respectively.

Table 4.5 Estimated model coefficients for SNR.

Term	Coef	SE Coef	T	P
Constant	6.3988	0.7713	8.296	0.001
Speed 2200	-5.7546	1.0908	-5.276	0.006
Speed 2600	0.7647	1.0908	0.701	0.522
PMF-Rati 0	-3.7985	1.0908	-3.482	0.025
PMF-Rati 25/75	2.9879	1.0908	2.739	0.052

Where: S=2.3139, R-Sq=92.05%, R-Sq(adj)= 84.09%

Table 4.6 Analysis of variance for SNR (ANOVA)

Source	DOF	SS	Adj SS	Adj MS	F	P
Speed	2	175.80	175.80	87.901	16.42	0.012
PMF-Ratio	2	72.04	72.04	36.021	6.73	0.053
Residual error	4	21.42	21.42	5.354		
Total	8	269.26				

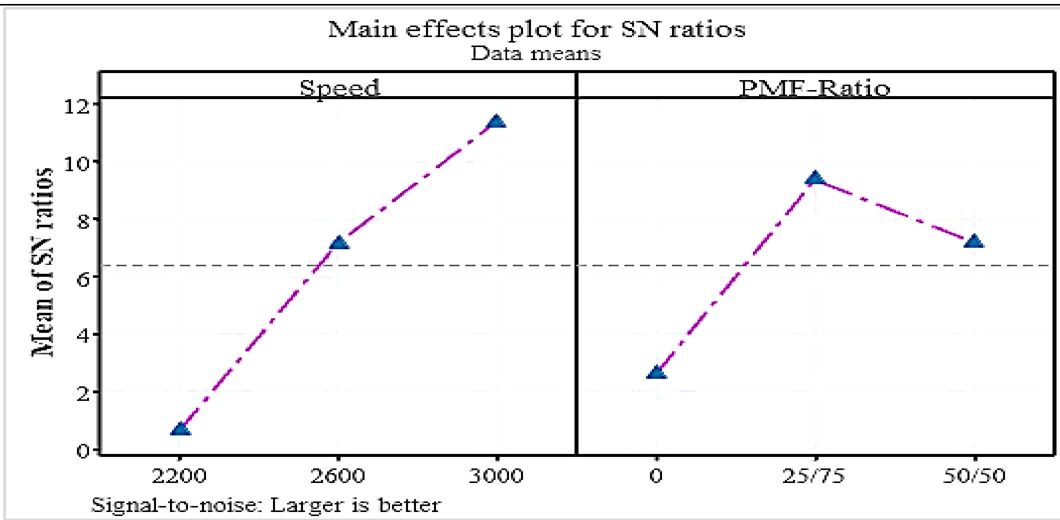

Figure 4.26 Main effect pilots for SN-Ratios

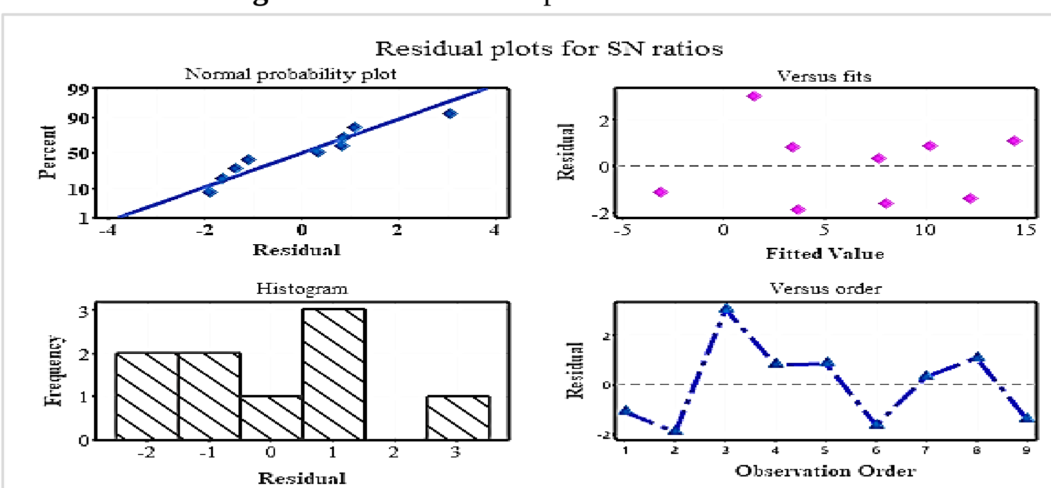

Figure 4.27 Residual pilots for Signal-N-Ratios

4.3.1.2.Linear model analysis: Means vs. speed, PMF-ratios

Table 4.7 Estimated model coefficients for means

Term	Coef	SE Coef	T	P
Constant	35.3149	5.528	6.389	0.003
speed 2200	-19.5536	7.817	-2.501	0.067
speed 2600	0.1433	7.817	0.018	0.986
PMF-Rati 0	-10.4077	7.817	-1.331	0.254
PMF-Ratio 25/75	23.2699	7.817	2.977	0.041

S = 16.5833 R-Sq = 81.11% R-Sq(adj) = 62.22%

Table 4.8 Analysis of variance (ANOVA) for means

Source	DOF	SS	Adj SS	Adj MS	F	P
Speed	2	2277	2277	1138.7	4.14	0.106
PMF-Ratio	2	2446	2446	1222.9	4.45	0.096
Residual-error	4	1100	1100	275.0		
Total	8	5823				

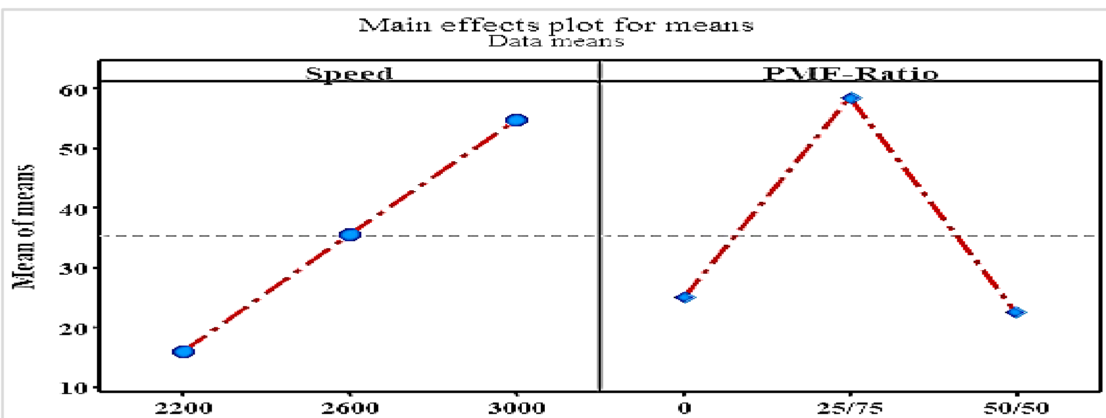

Figure 4.28 Main effect pilot for means

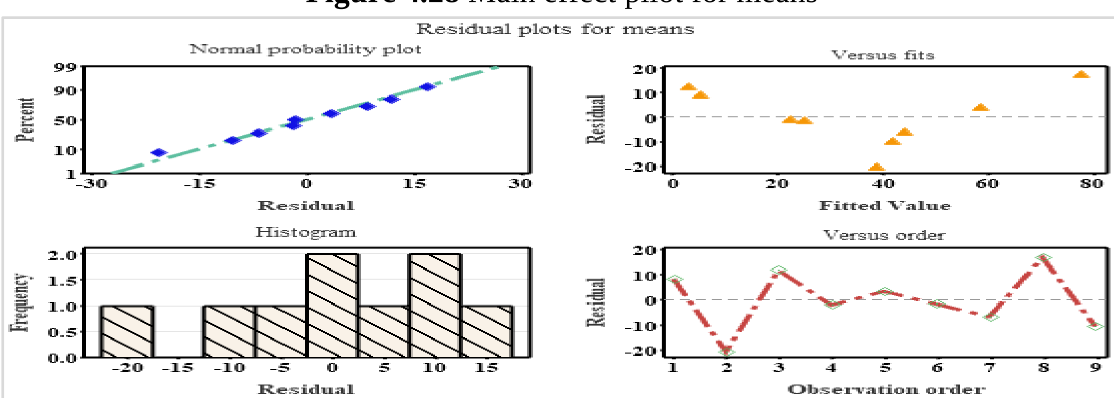

Figure 4.29 Residual pilots for means

4.3.1.3.Linear model analysis: Standard Deviations vs Speed, and PMF-ratio

Table 4.8 Estimated model coefficients for Standard deviations

Term	Coef	SE Coef	T	P
Constant	60.460	14.17	4.266	0.013
speed 2200	-43.017	20.04	-2.146	0.098
speed 2600	1.167	20.04	0.058	0.956
PMF-Rati 0	-24.234	20.04	-1.209	0.293
PMF-Rati 25/75	55.768	20.04	2.783	0.050

S=42.5134 R-Sq = 77.49% R-Sq(adj) = 54.98

Table 4.9 Analysis of variance for standard deviations

Source	DOF	SS	Adj SS	Adj MS	F	P
Speed	2	10810	10810	5405	2.99	0.161
PMF-Ratio	2	14075	14075	7038	3.89	0.115
Residual Error	4	7230	7230	1807		
Total	8	32114				

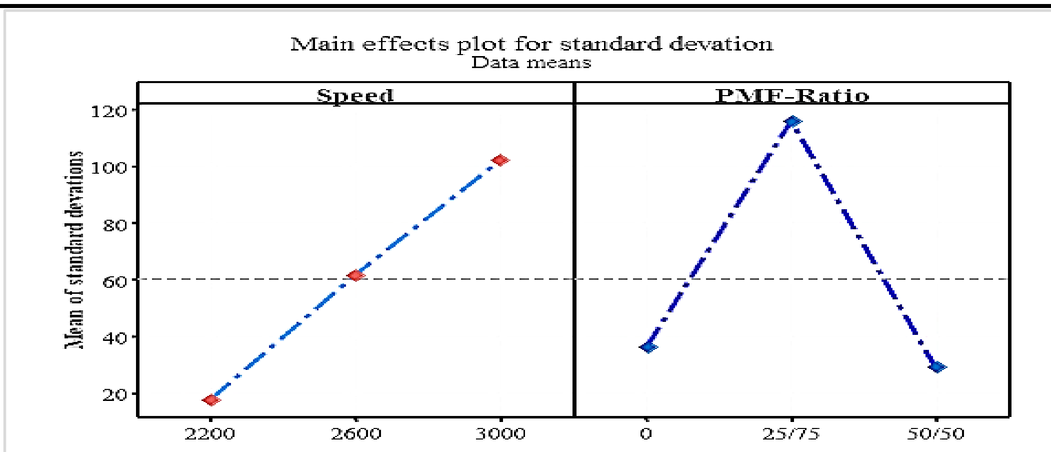

Figure 4.30 Main effect plot for standard deviations

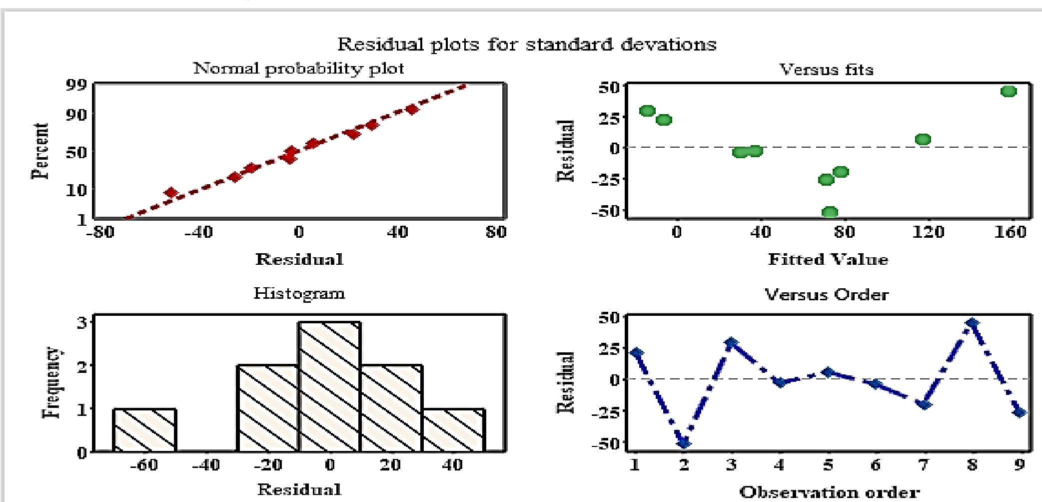

Figure 4.31 Residual pilots for standard deviations

4.3.1.4.Analysis of variance

ANOVA was also used to determine the impact of the effective parameters on the quality characteristic. SNR, means, and STD is subjected to an ANOVA in this section. The degrees of freedom, successive sums of squares, mean square (MS), T-statistic from the MS, and p-values obtained from an ANOVA. ANOVA findings are presented in Tables 4.6, 4.8, and 4.10, with SNR, means, and STD, respectively. The analysis is deemed significant at a level of 5% with a 95% confidence level. The column of p values in this table shows which of the effective parameters is a crucial one and has the most impact.

4.3.1.5.Main effects plots of SNR, Means, and STD

The signal-to-noise ratio means, and standard deviations are just a few examples of the factors that the major effects plots display as they relate to the response characteristic. As a result, the main effect plots of the signal-to-noise ratios, and the speeds had the larger main influence. The premixed blended fuel ratio (PMB-Ratio), as seen in Fig.4.26, 4.28, and 4.30 had the main effect plot, for SNR, means, and standard deviations respectively.

4.3.1.6.Residual plots of SNR, Means, and STD

Fig.4.27, 4.29, and 4.31 exhibits the residual plots for SNR, means, and standard deviations, respectively. A residual plot is a graph where the independent variable is on the horizontal axis and the residuals are displayed on the vertical axis. A linear regression model is adequate for the data if the dots in a residual plot are randomly distributed across the horizontal axis; otherwise, a non-linear model is preferable. A linear model offers a respectable fit to the data, as evidenced by the residual plot's seemingly random pattern. Although there can be a small curve in the middle, the data seems to be mostly linear. Overall, for these data at this level, linear regression is adequate. The design is used to check whether the model adheres to the analyses' underlying assumptions. The graph's residual plots and each residual plot's interpretation are as follows:

- Using a normal probability plot, abnormally found. The residues appear dispersed normally based on an essentially straight line. The data is normally distributed, as demonstrated by the normal probability plot above, and the factors having an impact on the response.
- Outliers, missing higher-order terms, and non-constant variance were found using the residuals vs fitted values display. Around zero, the residuals roughly dispersed randomly.

The residuals vs fitted values plot above shows that the variance is consistent and that there are no outliers in the data.

- The residuals histogram plot aids in the identification of many peaks, outliers, and non-normality. The histogram should roughly be bell-shaped and symmetric. The histogram of the residual points is depicted in the above plot, and it can be seen that it was roughly symmetric and bell-shaped.
- The plot of residuals versus order helps in detecting the time-dependence of residuals. The residuals should exhibit no clear pattern. The above residuals versus order plot indicates the random pattern of the residuals.

Table 4.10 Response for SNR; means, and STD

Response table for SNR			Response table for means			Response table for STD		
Level	Speed	PMF-Ratio	Level	Speed	PMFR	Level	speed	PMF-Ratio
1	0.6441	2.6002	1	15.76	24.91	1	17.44	36.23
2	7.1634	9.3867	2	35.46	58.58	2	61.63	116.23
3	11.3887	7.2094	3	54.73	22.45	3	102.31	28.93
Δ	10.7446	6.7865	Δ	38.96	36.13	Δ	84.87	87.30
Rank	1	2	Rank	1	2	Rank	2	1

Delta value shows the difference between the highest average response values for each factor. According to the investigation; Speed (Delta 10.7446, Rank = 1) has the largest effect on the signal-to-noise ratio and (Delta 38.96, Rank = 1) has the largest effect on the response table of means**.** The premixed fuel ratio (Delta 87.30, Rank = 1) has the largest effect on the standard deviations, but (Delta 84.87, Rank = 2) has the lowest effect on the standard deviations in all options as shown in Table 4.11.

4.3.2. Interaction plot analysis

For data analysis, interaction graphs can be a useful tool. A graph that displays the relationship between two or more variables is an interaction plot. To comprehend how the relationship between two variables changes while a third variable changes, it is frequently used in data analysis. In an interaction plot, the lines on the graph depict the relationship between the two variables, while the x-axis typically displays the values of one variable and the y-axis displays the values of another variable. To illustrate the various levels of the third variable, the lines are generally colored differently.

The Minitab software is used for an interaction plot of two factors' characteristic averages for each combination of factor levels. Therefore, for two factors with three levels each, Minitab plots nine points that represent the nine possible combinations. The levels of one factor indicated on the horizontal axis is a blended fuel ratio, and the vertical axis is the engine speeds, whereas different colored lines and symbols indicate the levels of the emissions and performances. If the lines are parallel to each other, then there is no interaction between the two factors. If the lines are not parallel to each other, then there is an interaction between the two factors. In these results, the lines are not parallel in all emission and performance cases except for Tb and CO_2, which are close to parallel. As shown in Fig. 4.32, NOx, CO, HC, and Pb had the strongest means in engine speed and premixed fuel blend ratio.

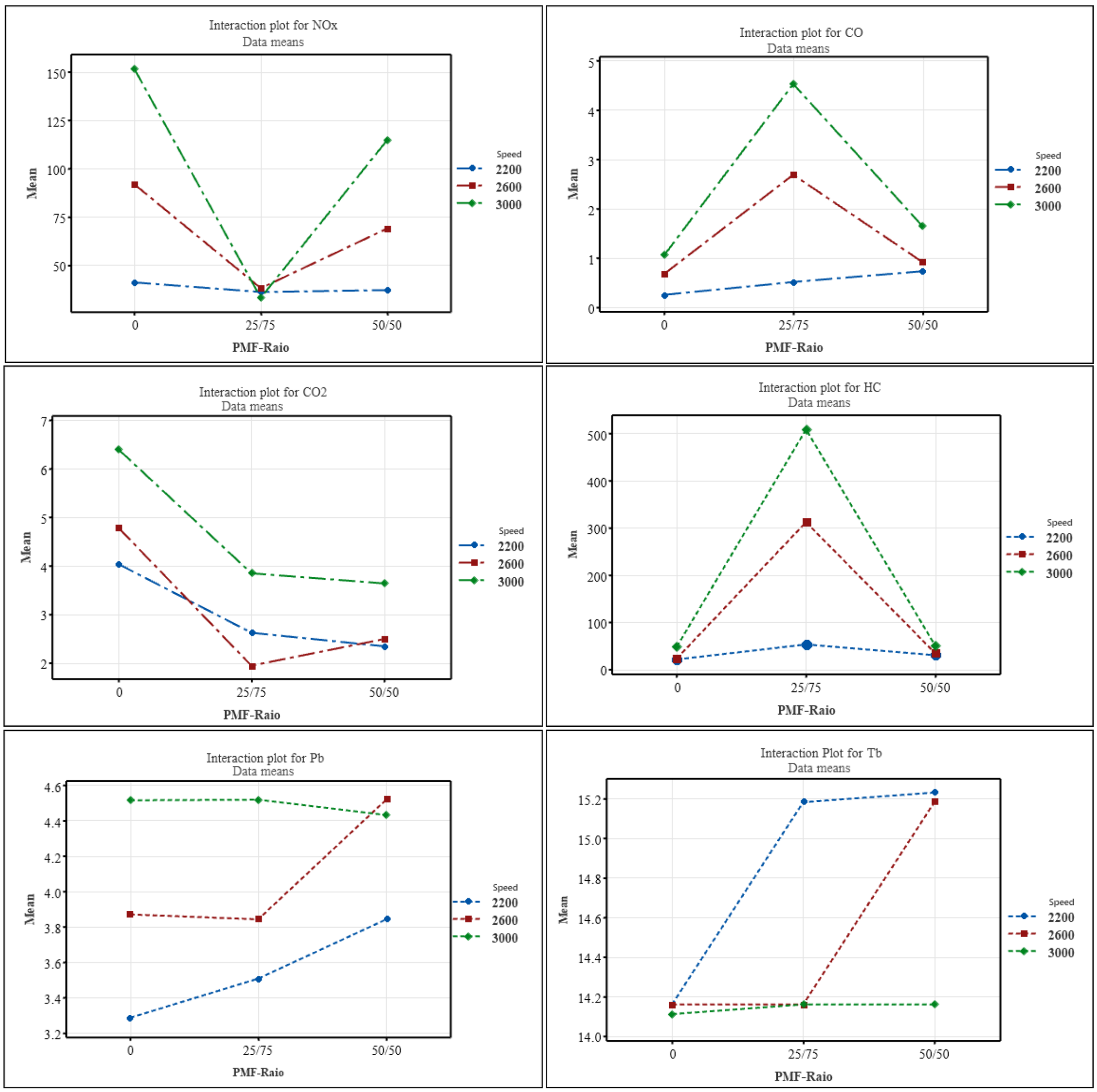

Figure 4.32 Interaction plot for emissions and performances

4.3.3. Contour plots analysis

The attention from the diesel engines is NOx and PM emissions. The contour plots of nitrogen oxides from the exhaust of the engine are minimum at the lower brake power and engine speed, and carbon-dioxide from the engine has the lower at low speed and maximum at lower brake power and maximum at higher speed and brake power (See Figs.4.33, 4.34).

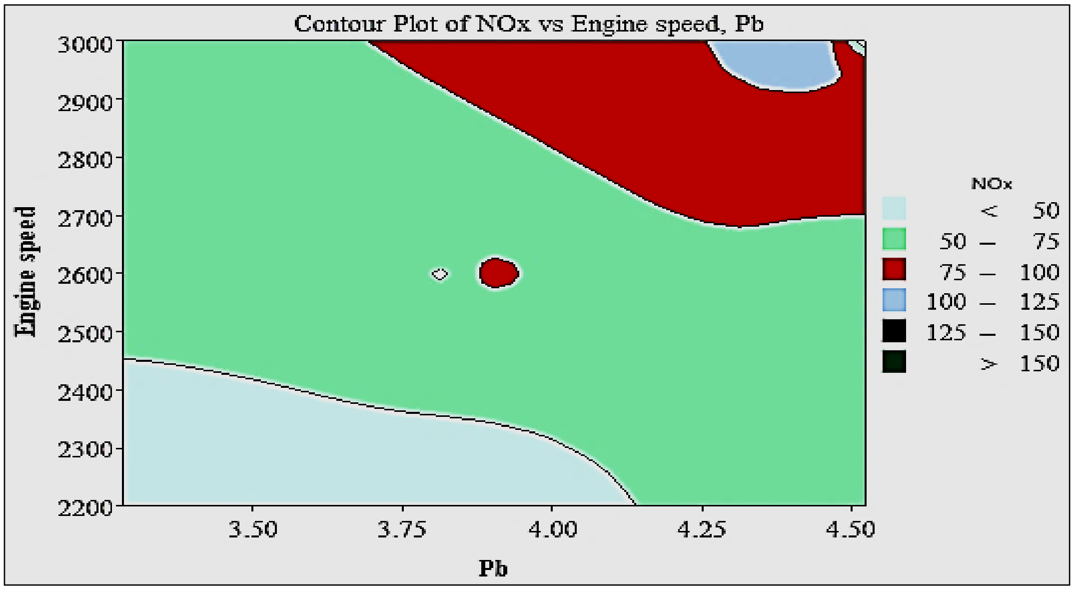

Figure 4.33 NOx emissions of contour pb

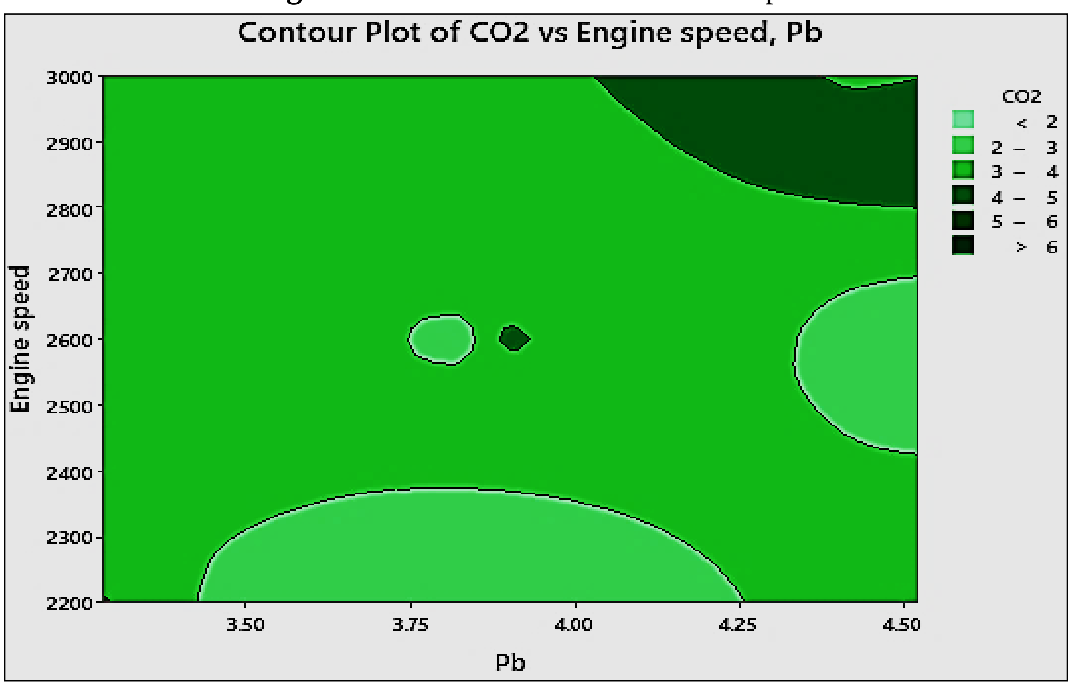

Figure 4.34 CO2 emissions of the contour plot

Fig.4.35 shows the contour plots of carbon-monoxide emission (in % vol), versus engine speed. The unburned hydrocarbon (in ppm) emissions of the diesel engine are shown in Fig

4.36. The CO is maximum (3-4% vol) and lower (at speeds below 2500rpm and brake power below 4.2kW, which is less than 1% vol). Unburned hydrocarbon (in less than 100 ppm) at speeds below 2500rpm in all engine brake power and 100-200ppm in all speeds greater than 2500rpm.

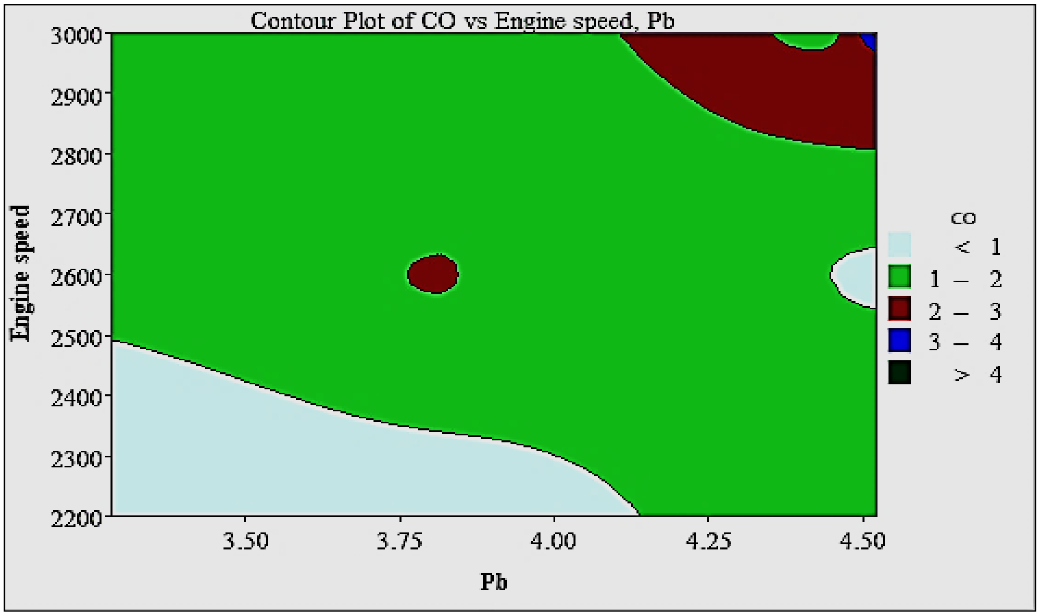

Figure 4.35 Contour pilot of CO of CDC and RCCI Emission

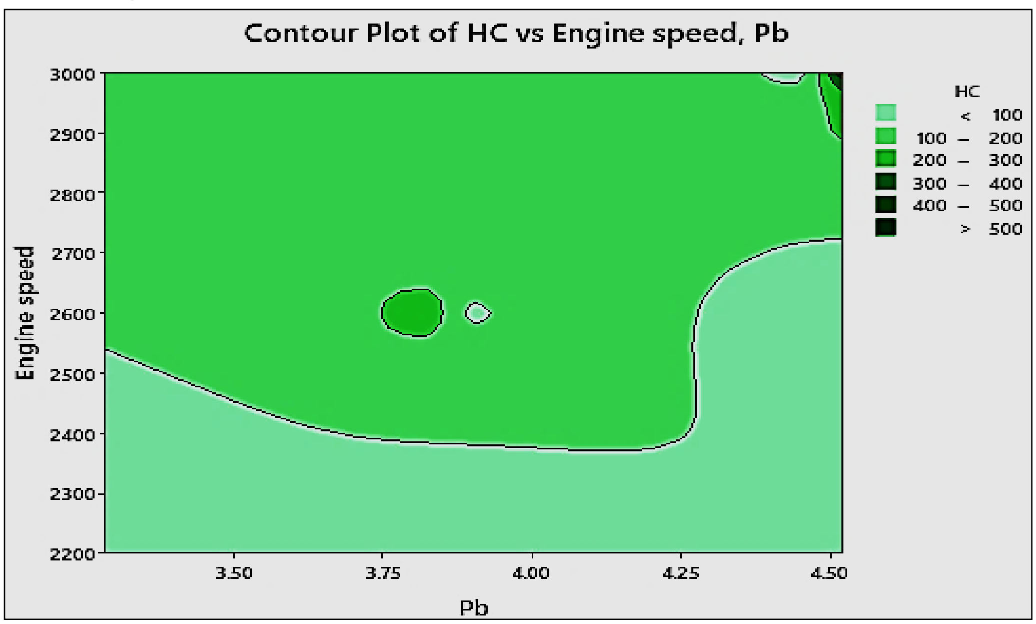

Figure 4.36 Contour pilot of HC of CDC and RCCI Emission

4.3.4. An interval plot analysis

An emissions interval plot graph shows the distribution of data within a specified range. It is often used to visualize the spread of emission data and to identify outliers. In an interval plot, the x-axis typically shows the values of the engine speeds and blend ratio data, the y-axis typically shows the amounts of the emission, and the bars on the graph show the distribution of the data within the specified range. Interval plots can be used to visualize the spread of data, compare the spread of data between two groups, and identify the inter quartile range of data as it is shown in Fig 4.37 to Fig 4.40.

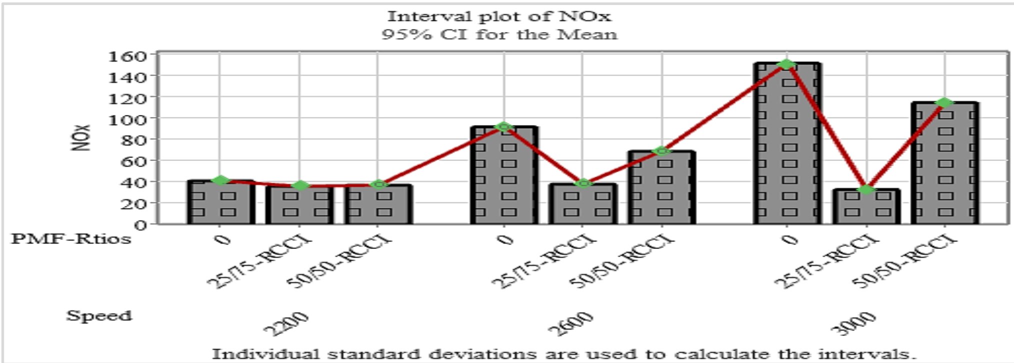

Figure 4.37 Interval plot for NOx

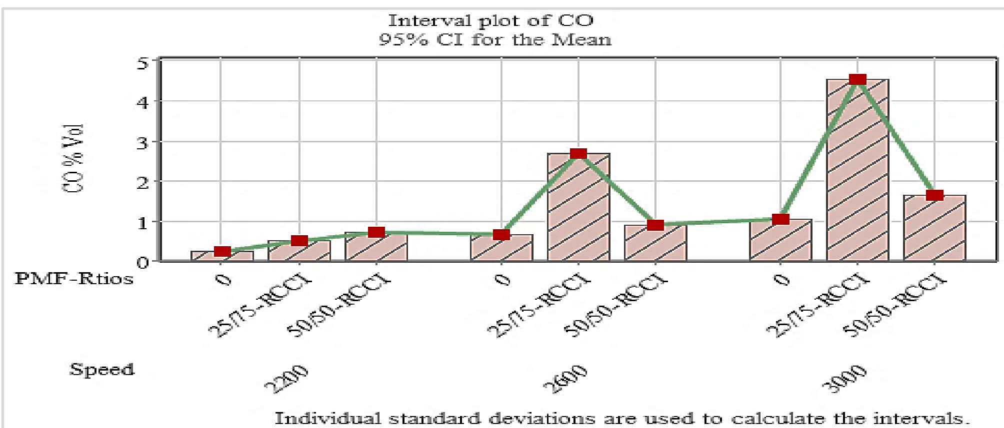

Figure 4.38 Interval plot for CO

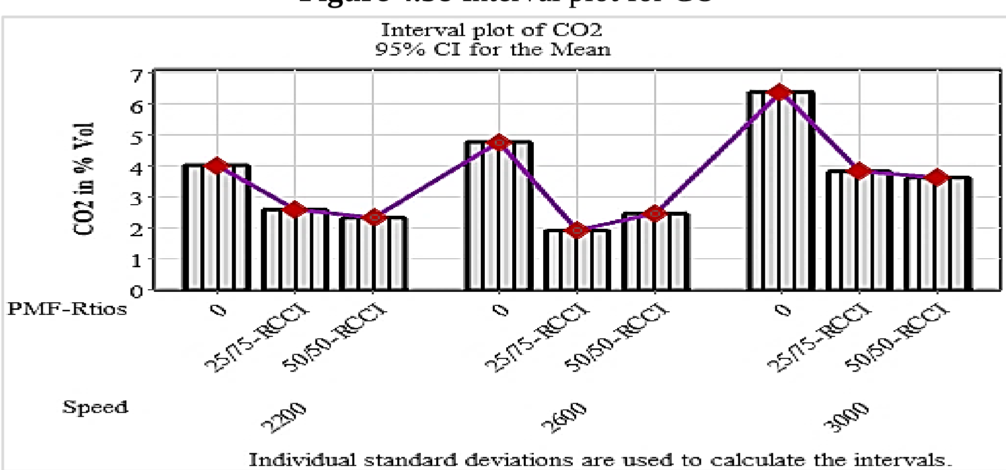

Figure 4.39 Interval plot for CO2

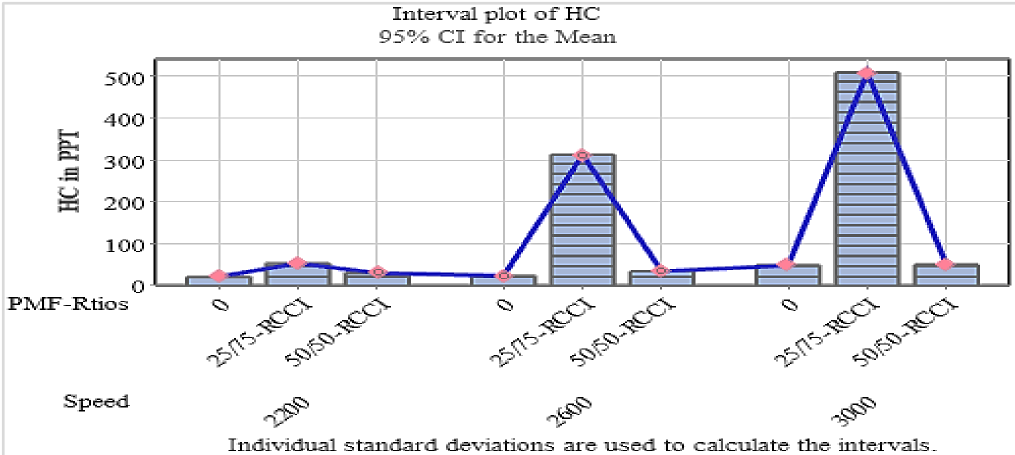

Figure 4.40 Interval plot for HC

4.4. Start of diesel fuel injection timing effects

The test bench engine in the study was a single-cylinder light-duty, water-cooled, 0.325L, 24CR, 4-stroke modified diesel engine to RCCI with detailed engine specifications. A modified diesel engine with reactivity-control compression ignitions was employed to reduce emissions and keep performance. The diesel fuel injector was equipped with a hole diameter of 0.127 mm, and an injection pressure of 137.3 bar was used. The injection of the blended gasoline and ethanol fuel in the port injection has a pressure of 3.5 bar. In the research, a wide range of operating conditions were seen for both diesel-(gasoline-ethanol) blends and RCCI combustion. The detailed operating parameters for each case are listed. The variations in injection timing were achieved by perturbing the in-cylinder temperature and pressure. The logic of the diesel engine shows that the delaying DI fuel injection timing results in poor fuel mixing and incomplete combustion.

4.5. Combustion simulation

Diesel combustion is typically associated with high levels of PM and NOx due to controlled diffusion combustion caused by the fuel-air mixture. One of the biggest challenges facing the engine research community is the stringent regulations that have been implemented globally to lower the emissions of pollutants from ICEs. Unwanted emissions are produced by conventional diesel combustion due to the engine's high temperature and the oxygen that is available outside of the spray plume (Anh, 2020; Şener et al., 2019). More mixing from the piston bowl form is required for the quicker direct injection of diesel fuel because of the piston bowl shape design (Pamminger et al., 2020).

Diesel-RK combustion simulation, which has many of the same capabilities as well-known thermodynamic software, is used for the modeling and simulation research of the diesel engine. Unlike the other programs, the software created by Bauman, Moscow State Technical University of Russia, featured creative applications. The primary focus of the study was on improving the combustion processes of a diesel engine using a modified piston bowl design. There are three different kinds of diesel engine simulation models: multi-zone, quasi-dimensional, and zero (single-zone). For diesel engines to operate at peak efficiency and have the best possible combustion and emission characteristics, the piston bowl geometry is crucial. (Nguyen et al., 2021). Variable combustion chambers caused by different piston bowl shapes are compared, and the results of each combustion simulation are produced and confirmed by the other's work. To verify the predicted numerical results, the pressure fluctuation with the crank angle of the traditional diesel combustion piston bowl geometries was compared under identical load conditions. Trends in the simulation are similar to one another. It is determined how to distinguish between the numerical value and similar analysis of the pressure, temperature, heat release rate, nitrogen oxides, and particulate matter.

4.5.1. Cylinder combustion analysis

4.5.1.1.In-cylinder combustion pressure

The study focused on the combustion simulation of piston bowl shapes, specifically, DSEVL2 BMW M47T, Shallow Hesselman, Lombardini 15LD350, and DOOSANP158FE, as seen in chapter three (3). The four distinct piston bowl designs were selected for additional analysis to maximize performance and lower emissions based on combustion and emissions. The peak cylinder pressure of the DSEVL2 BMW M47T (P1) is 129, the bowl geometry of the Shallow Hesselman (P2) is 131, the Lombardini 15LD350 (P3) is 122, and the DOOSANP158FE (P4) result is 113 bars, according to a comparison of piston bowl based cylinder pressure vs crank angle. Where the maximum in-cylinder pressure surpasses the lower value by 13.8%. As illustrated in Fig 4.41, the maximum cylinder pressure for different piston bowls at a fuel injection pressure of 137 bar are 129, 131, 122, and 113 bar, respectively, for P1, P2, P3, and P4. The longer fuel-air blending time in the Shallow Hesselman configuration leads to a dominant premixed ignition stage, which is preferable.

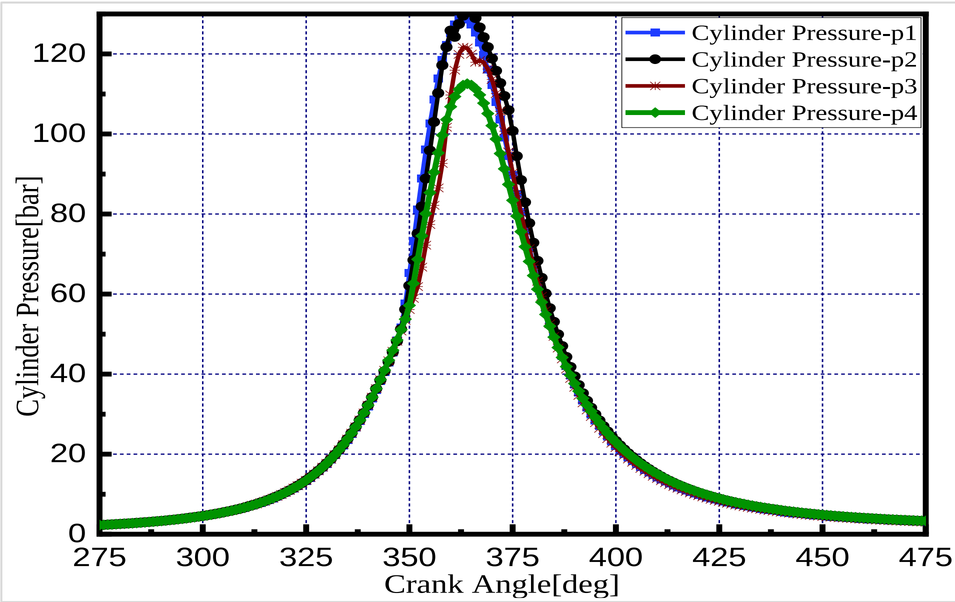

Figure 4.41 In-cylinder pressure at various PBSDG

As a result, the in-cylinder pressure rises as expected (Seelam et al., 2022). For each PBSD geometry, the angles at which the maximum cylinder pressures occur are 3°, 4°, 3°, and 4° degree crank angle a TDC, respectively. The fuel blend has a higher peak combustion pressure due to improved combustion, as it is in line with (Sharma et al., 2015; Sharma, 2015).

4.5.1.2.In-cylinder temperature and heat release rate

It considers and permits the optimization of the geometry of the piston bowl, the design and placement of the injector, and the injection profile, including the use of numerous injections. The model takes into consideration drop sizes, the way free sprays interact with swirl spray and wall impingement, how near-wall flow is created by spray, how fuel hits the cylinder head surface and cylinder liner, and how adjacent sprays cross near-well flow (NWF). The additional cause is the reduced fuel percentage of the near-wall flow dilution, the low fuel percentage in the free spray's core, the low fuel percentage in front of the fuel-free spray, and the lower fuel percentage in the spray's core. These are the causes of the Shallow Hesselman piston's high temperature of 2048k and the DOOSANP158FE result's minimum of 1681k. The form and depth of the piston bowl of the Shallow Hesselman piston dominate the premixed ignition stage, resulting in an 18% greater cylinder temperature than the minimal model values. Since the longer fuel-air blending time in the Shallow Hesselman produces superior results, the in-cylinder temperature rises by Seelam et al., (2021).

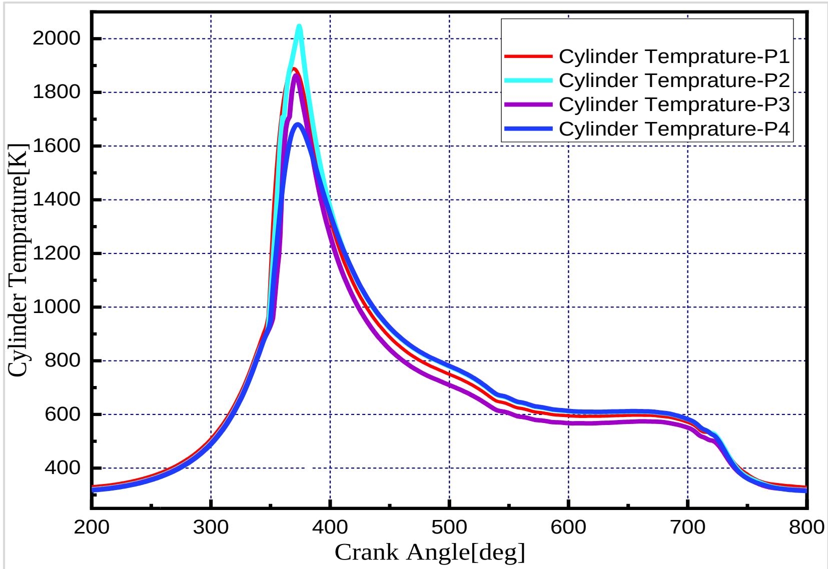

Figure 4.42 In-cylinder temperature for PBSD geometry

The minimum and maximum temperatures should be maintained within a very narrow range of 1400K to 2000K to allow for a complete combustion and clean combustion with low NOx and PM emissions Paykani et al., (2016). Peak local equivalence ratios should also not be significantly higher than stoichiometric Kim et al., (2009). Consequently, the simulation product shows that every cylinder temperature is within allowable bounds, except for the P2's cylinder temperature, which is 2048k (See Fig. 4.42). For use with a basic calculation, equations for the forecasting of a relatively accurate heat release rate for cycle calculations are provided for specific engines operating under normal conditions.

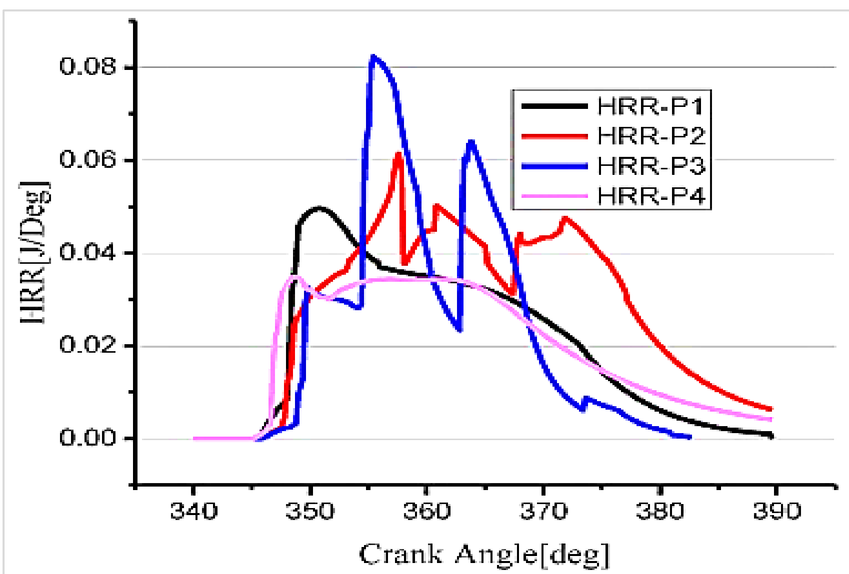

Figure 4.43 The HRR at various piston bowl geometries

Due to pre and post-injection, P2 and P3 have heat release rates of 0.061 and 0.082, respectively; P1 and P4 had heat release rates of 0.05 and 0.035 J/°CA, respectively, from single-stage injections. The P4's PHRR is lower than the P3's HRR by 42.7 %. P2 and P3's PHRRs have a triple injection that is electronically controlled and has a high HRR (See Fig 4.43).

4.5.2. Engine exhaust emissions

Because of the lean engine running, NOx and PM emissions from diesel engines are the main problems; HC and CO emissions are not as serious. The nitrogen oxide levels in the exhaust gas for P1, P2, P3, and P4 are 25.6, 16, 18.2, and 12.74 g/kWh, respectively, as shown in Fig. 4.44. The conversion of the simulation findings from ppm to g/KWh is illustrated in equation (Eq 4.5) by Gopal et al. (2014).

$$NO_x(g/KWh) = \frac{\dot{a}(NO_{x\,mass} * W_f)}{\dot{a}(BP * W_f)} \qquad \text{(Eq 4.5)}$$

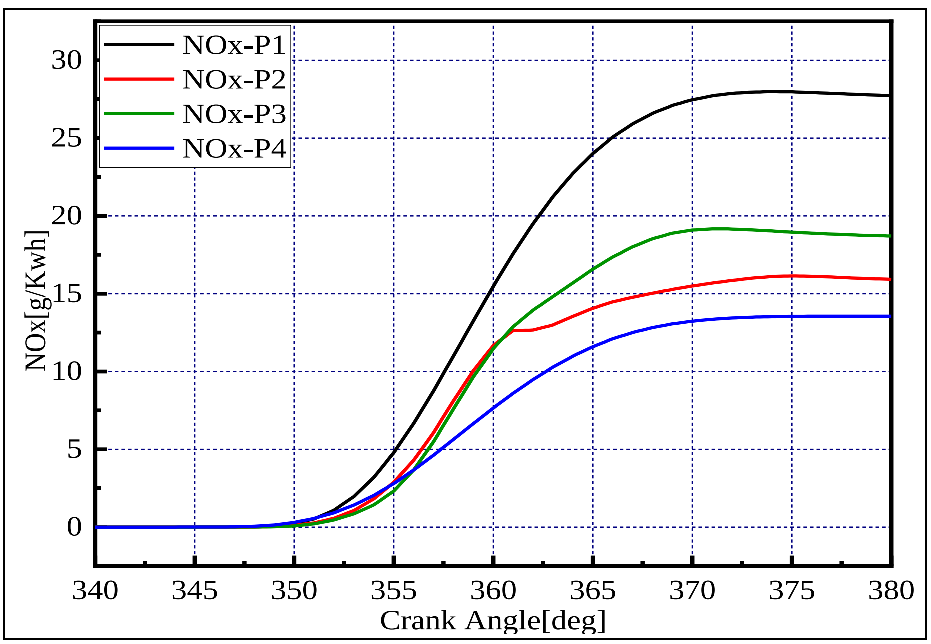

Figure 4.44 NOx emissions concentrations

Although the maximum cylinder temperature of P2 has a low NOx emission, this is because of the PBSD geometry impact in the fuel spray pattern. In-cylinder temperature and NOx emission are directly related to combustion temperature. The reduction of NOx in the P2 in comparison to all others has an impact from the reduced fuel fraction of the near wall flow dilution outside the sleeve, in front of the free spray, and low fuel fraction in the fuel-free spray core (See Fig 4.44). P1 emits 0.35 g/kWh of particulate matter, P2 emits 0.42 g/kWh, P3 emits 0.43 g/kWh, and P4 emits 0.24 g/kWh, as shown in Fig 4.45. Even though PM has significantly decreased, PM in the P1 is associated with a penalty in NOx. Nevertheless, following the peak emission result, the P2's PM is consistently greater than all others. Consequently, additional refinement of the PM of the P1 shape is required to reduce NOx emissions concurrently with maintaining engine performance. The summary emission (SE) of PM and NOx is 4.2, 4.3, 4.9, and 3.6 g/kWh, while the specific NOx emission reductions to NOx in g/kWh are 21, 4, 23.3, and 16. As compared to all the others, a larger PRR is seen in the DSEVL2-BMW-M47T piston bowl due to the increasing air swirl, which is consistent with Seelam et al., (2021). This results in increased NOx emissions.

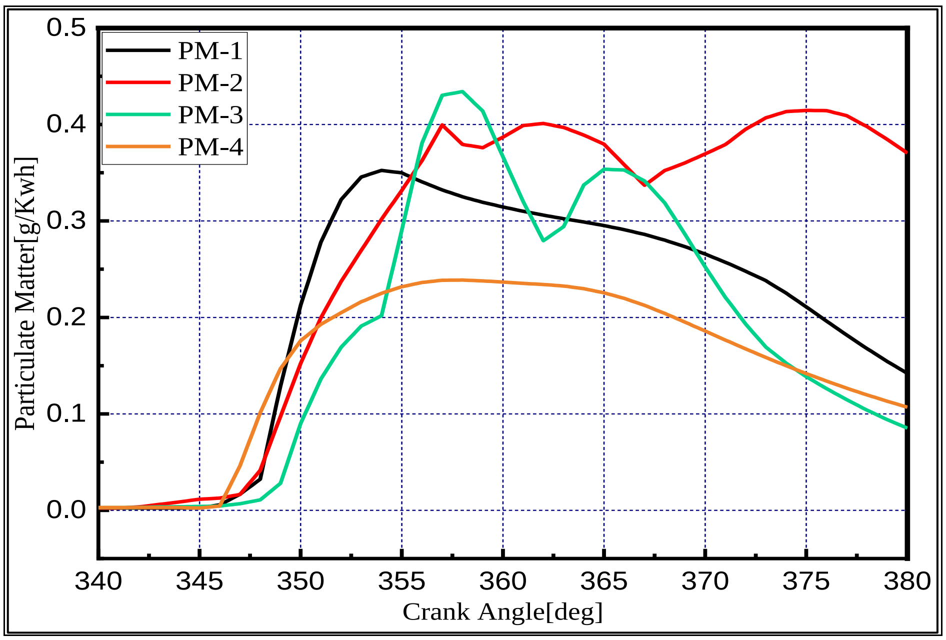

Figure 4.45 Particulate matter concentrations

4.5.3. Simulation of fuel sprays in the swirling airflow

Different kinds of multi-zone phenomenological jet-based combustion models for diesel engines have been created recently. While they share a great deal, they yet represent two fundamental ideologies. The turbulent jet hypothesis serves as the foundation for spray treatment. Cross sections are described by the spray geometry, fuel distribution in the longitudinal and empirical relations, and the spray tip penetration and velocity. According to Chiu et al. (1976), the spray is separated into multiple distinct zones with varying proportions of fuel and air. If not, the spray is thought to be a cone with axial division based on the fuel injection time sequence (Bi et al., 1999). Both in the usual direction and along the axis, the spray is separated into many packages. A tiny amount of fuel was injected at the same time that the fuel spray's axial division occurred. In the model by Hiroyasu et al. (1983), the radial division was designed to equalize a solid angle of a cone, the vertex of which was situated in the nozzle hole. In the model by Rakopoulos and Hountalas (1998), the radial division was constructed as a complex of rectangles. It is possible to account for the interaction of the spray with a swirl using all those model kinds. In the current work, a novel zone generation technique is applied. This results from the need for a more thorough explanation of unique characteristics of fuel spray evolution, such as:

- Conditions of fuel droplet evaporation differ essentially in different spray zones.
- There is fuel redistribution among zones in the process of free spray movement and its interaction with a wall.
- There is the interaction of fuel sprays with the walls of the piston bowl and the possibility of fuel hitting the cylinder liner and the cylinder head surface.
- Account for the wall temperature effect on the fuel evaporation rate in near-wall zones
- Interaction between adjacent sprays in near-wall flows.
- The interaction of spray and their near-wall flow with swirl and walls depicted shown by the equations below as follows:

$$l_{wj} = k_j B_{SW}^{0.5} \tau_W^{0.5} + C_{Wj} P V^{0.5} d_{32}^{-1.5} \int_0^{\tau W} (W_t - U_t) \cos\beta \tau_w \qquad \text{(Eq 4.6)}$$

$$\tau_W = \tau_s - \tau_{SW} \qquad \text{(Eq 4.7)}$$

$$K_j = \sqrt{\sin\gamma_1 \sin\gamma_3} + 1.2\left(1 - \sin\gamma_j\right) - 2\left(\cos\gamma_j\right) \qquad \text{(Eq 4.8)}$$

Where l_{wj} is the length of the NWF spot in each direction (j = 1, 2, 3, 4), γ_j is the shape of the NWF spot that depends on impingement angles (j = 1, 2, 3, 4), and K_j is the effect of impingement angles and Wt is the effect of local swirl velocity. Fig 4.46 illustrates the basic fuel mass motion from injection to spray front zone l_k and spray tip l_m. Eq 3.5 illustrates how the form of the piston bowl greatly influences the equation of motion of an elementary fuel mass (EFM) injected within a tiny time-step and traveling from the injector to the spray tip.

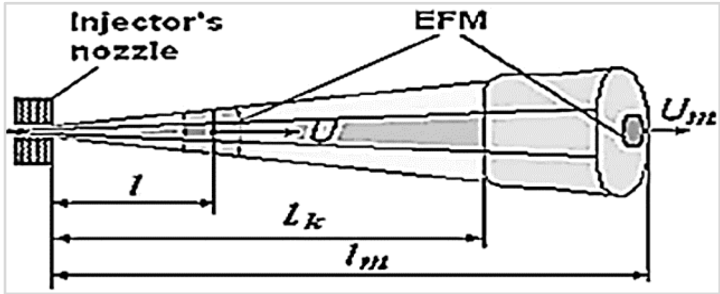

Figure 4.46 The EFM motion from the injection, spray front zone, and spray tip Sources:(Kumar, 2019; Kuleshov, 2006a).

Equations (Eq 4.9) compute the mass of entrained air for each elementary fuel mass (EFM) and account for the current distance, velocity, and EFM penetration length until the spray stops. These values are derived from momentum conservation (Kuleshov, 2008).

$$\left(\frac{U}{U_o}\right)^{3/2} = l - \frac{l}{l_m} \qquad \text{(Eq 4.9)}$$

Where U=dl/dt is the current EFM velocity, Uo= is the EFM velocity in the injector nozzle, and lm is the EFM penetration length until the spray stops. Also, l is the current distance from the EFM to the injector. The mass of entrained air (mass ma) for each elementary fuel mass (EFM) can be defined using momentum conservation, as shown by equation (Eq 4.10):

$$U_O \Delta m_f = U_k(C_1 \Delta m_f + \Delta m_a) \qquad \text{(Eq 4.10)}$$

The fuel sprayed in the cylinder is divided into seven zones by the spray model. The conditions for evaporation and burning vary from zone to zone. Diesel fuel-free spray zones are primarily divided into two sections: free spray before and after impingement. Three different zones the dense axial core, the dense forward front, and the diluted outside of the sleeve are present in a free spray before impingement. Since fuel evaporation calculations are difficult due to the non-homogeneous structure, density, and temperature of the near-wall flow formed after impingement, it is possible to identify typical zones in the NWF with averaged heat and mass transfer coefficients based on similarities to free spray. Following wall impingement, a new set of zones is created, which are the dilute outer sleeve of near-wall flow, the dense forward front of an NWF, the axial conical core of an NWF, and the dense core of an NWF on a piston bowl surface. The corresponding zones are taken into account when fuel knockouts the cylinder liner, and cylinder head surface. Spray forward front depth in equation (Eq 4.7) was computed as follows:

$$b_m = A_m l C F_s We^{0.32} M^{-0.07} \rho^{0.5} \qquad \text{(Eq 4.11)}$$

Where: Am=0.7 is the empirical coefficient distribution of fuel among the spray zone defined for each time step by the following expressions:

In the Core: $\sigma_{Core} = (\sigma_s - \sigma_k)(1 - 0.1 l_k / l)$ (Eq 4.12)

In Front: $\sigma_{front} = 0.8(\sigma_k - \sigma_t)A$ (Eq 4.13)

In dilute: $\sigma_{dilute} = \sigma_t + 0.2(\sigma_k - \sigma_t) + \frac{(\sigma_s - \sigma_k)1l}{l}$ (Eq 4.14)

In NWF: $\sigma_W = 0.8(\sigma_k - \sigma_t)(1 - A)$ (Eq 4.15)

Where: A= 1 before wall impingement and A= 0 after impingement.

The PBD affects the engine efficiency because of that it has different effects on the fuel spray mechanisms like impingement angles, local swirl velocity, length of NWF spot in each direction, and the shape of NWF spot depending on impingement angles. Fuel dilution, free core spray fraction, fuel-free spray front, and near-wall flow structure with the equation (Eq 4.12, Eq 4.13, Eq 4.14, and Eq 4.15) can strongly be affected due to piston head as shown in Fig 4.47 - Fig 4.50 (Seelam et al., 2021, Muralidharan, 2021).

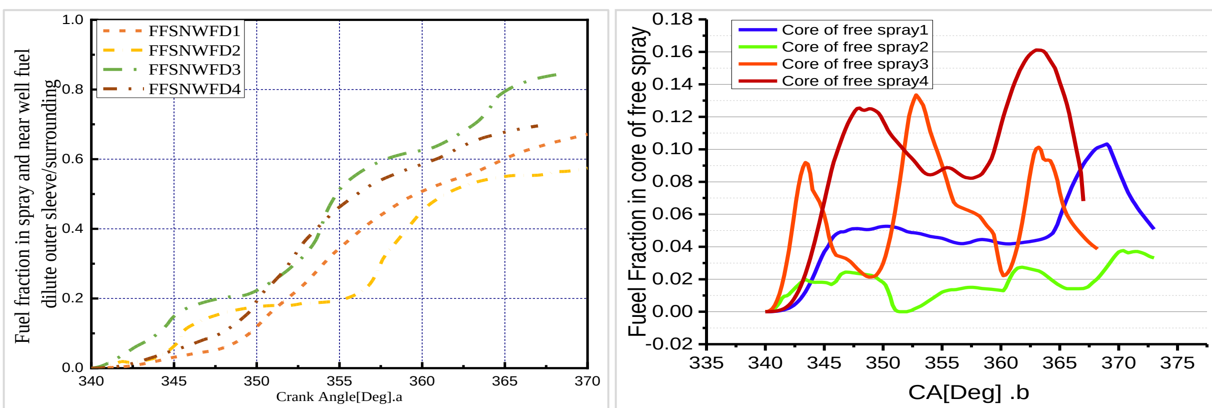

Figure 4.47 Spray and NWF dilution and fuel fraction in the core of free spray

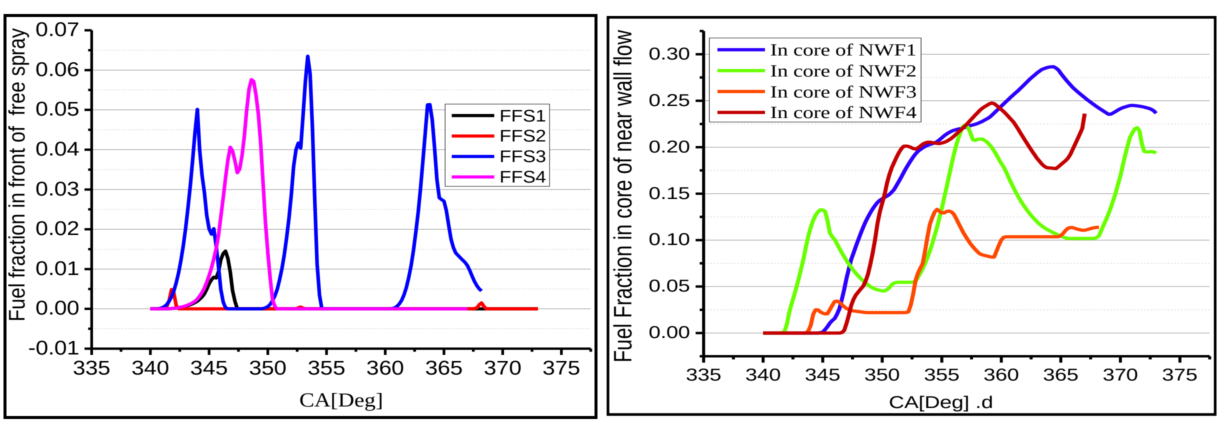

Figure 4.48 Fuel fraction in FOFS and Core of near well flow

4.5.4. Ignition delay period

The ignition delay period of the pilot injection for the second- and third-cylinder chambers are 7.2 and 8.22 and for the main injection are 0.91 and 5.01 and lastly, the post-injection is 0.1 and 2.46 CA respectively. So the ignition delay (ID) period is inversely proportional from pilot-to-post injections as shown in Table 4.12 but the mass fraction and duration of the main injection are more and the combustion duration of the main fuel is greater.

Table 4.11 Pilot, main, and post injections in the piston 2 and 3.

SOI	(BTDC)		Fraction		Mass(g)		Separ (CA)		Duration(CA)		D32 Micron		ID (CA)		Burst (CA)	
Pilot 1	20	17	0.25	0.25	0.0035	0.0031	--	--	6.93	5.037	15	23.2	7.17	8.22	347.2	351.2
Main	8.2	8.1	0.50	0.50	0.0070	0.0062	4.85	3.86.	10.01	7.162	11.2	17.7	0.91	5.01	352.7	356.9
Post 1	-6.7	-2.9	0.25	0.25	0.0035	0.0031	4.85	3.86	7.03	4.880	13.9	20.9	0.10	2.46	366.9	365.4

As it is illustrated in Figs 4.49-Fig 4.52, the diluted outside sleeve before impingement in each combustion chamber is higher. Comparison between calculated spray tip penetration and free spray angle for diesel engine with d_n = 0.12200mm at a fuel pressure of 137.3 bar of different piston bowls are shown in Fig 4.49-Fig 4.52.

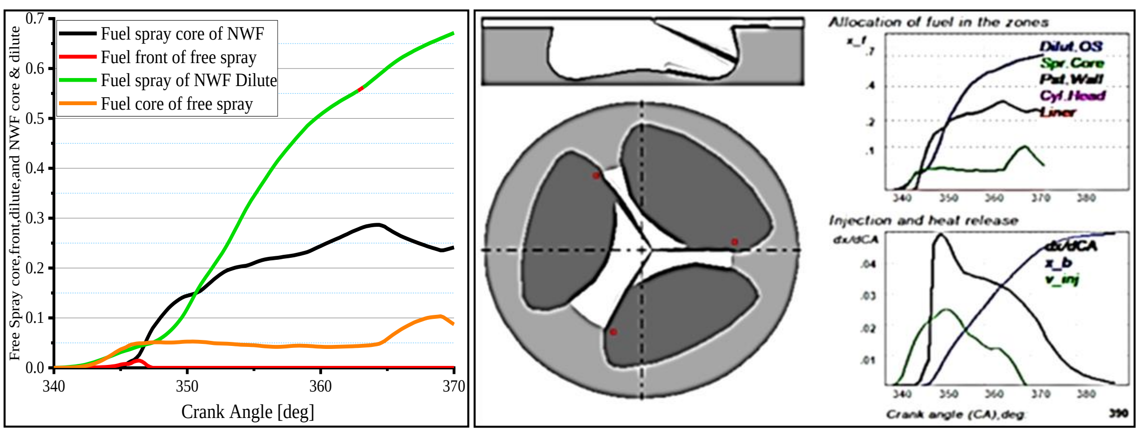

Figure 4.49 DSEVL2 BMW_M472 piston spry core, dilute, front, and NWF.

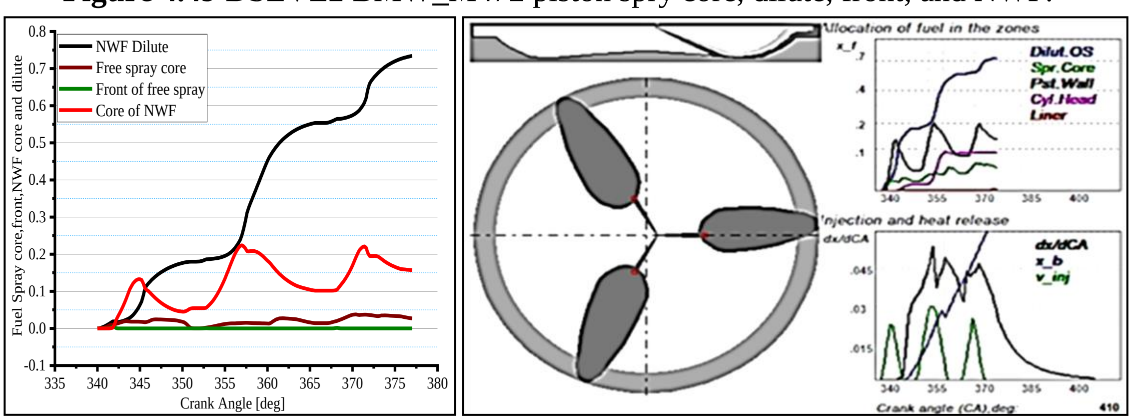

Figure 4.50 Shallow Heselman piston spry core, dilute, front, and NWF.

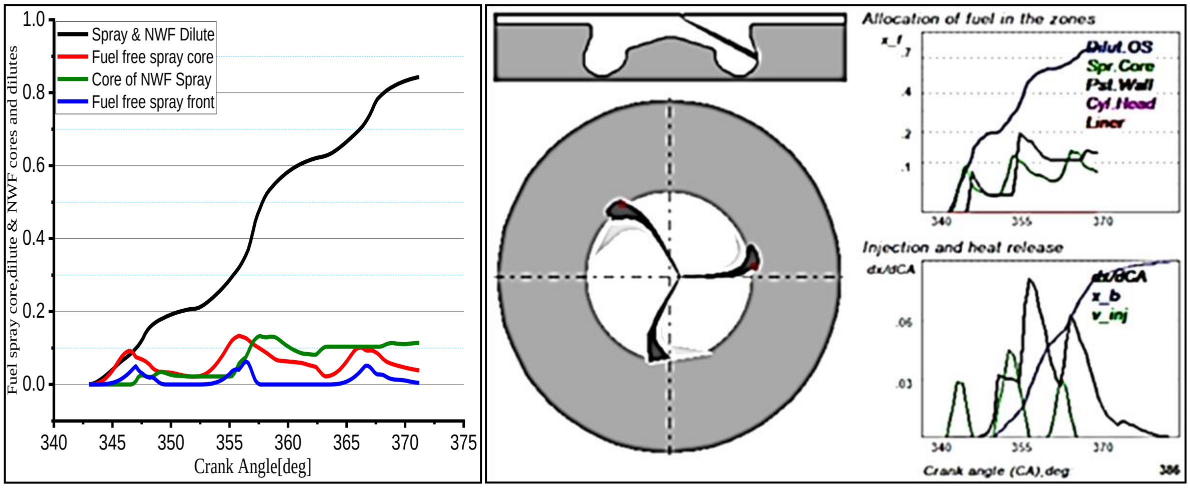

Figure 4.51 Lambardini 15LD350 piston spry core, dilute, front, and NWF

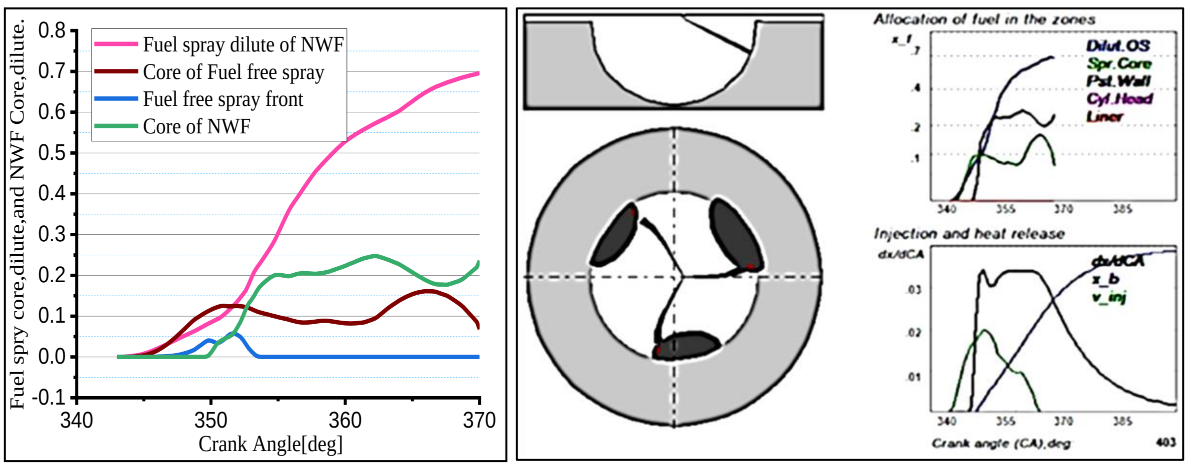

Figure 4.52 The DOSANP158FE piston spry core, dilute, front, and NWF effects

Fig 4.55 shows the results of spray angle evolvements when applying injection strategy under the same injection pressure, and density of the fuel conditions with only different cylinder combustion chamber geometry. The reason for the large spray angle in the initial injection phase is that the fuel had been injected into a relatively stationary air environment. The air at the nozzle outlet was squeezed and pushed into the radial direction however, the spray angle remained nearly stable during the later injection stage (Ergeneman, 2011; Payri et al., 2017; Wu et al., 2019)**.** This is attributed to the increased momentum exchange at higher surrounding gas densities as the fuel droplets are more closely surrounded by environmental gases. It should be noted that the increased ambient density can also reduce the maximum liquid length and better avoid the spray-wall impingement in line with (Zhou et al., 2015)**.**

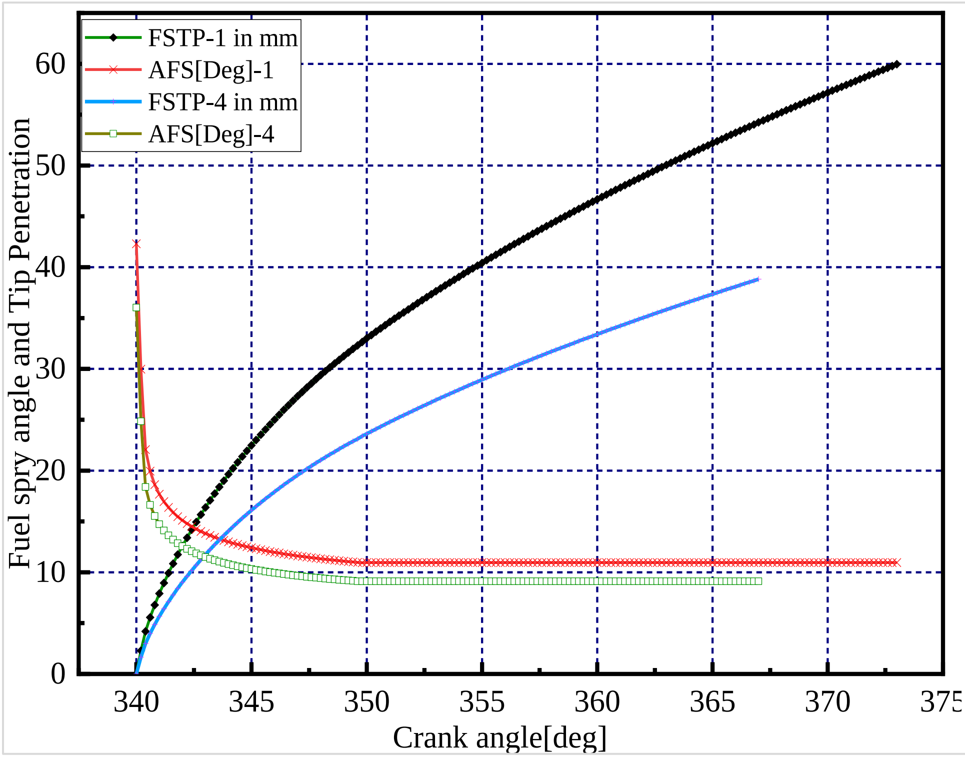

Figure 4.53 Spray angle and tip penetration for the single fuel injection.

The trend of the spray angle is still that it changes drastically during the initial stage of fuel injection. With the increased surrounding gas density, the spray angle tends to rise. The free spray angle and spray tip penetration are for the two single fuel injections and the two triple fuel injections. It is possible to conclude that the spray tip penetration of the single injection as compared to the triple injection is more and the main injection has more spray tip penetration as compared to the post and pilot injected fuel. FSP1 is 60mm and FSP4 is about 39mm.

The main injection spray tip penetration (STP) for the triple injection of FSP2 is 46mm. The pilot is 40, and post-injection is 35mm for the spray penetration; however, the spray penetration for the FSP3 and FSP4 is maximum at about the beginning of injections for the pilot one (See Fig. 4.56). Main and post-injection due to the resistance of the stationary air environment and the squeezed and pushed air into the radial direction at the nozzle outlet as it is in line with (Ergeneman, 2011).

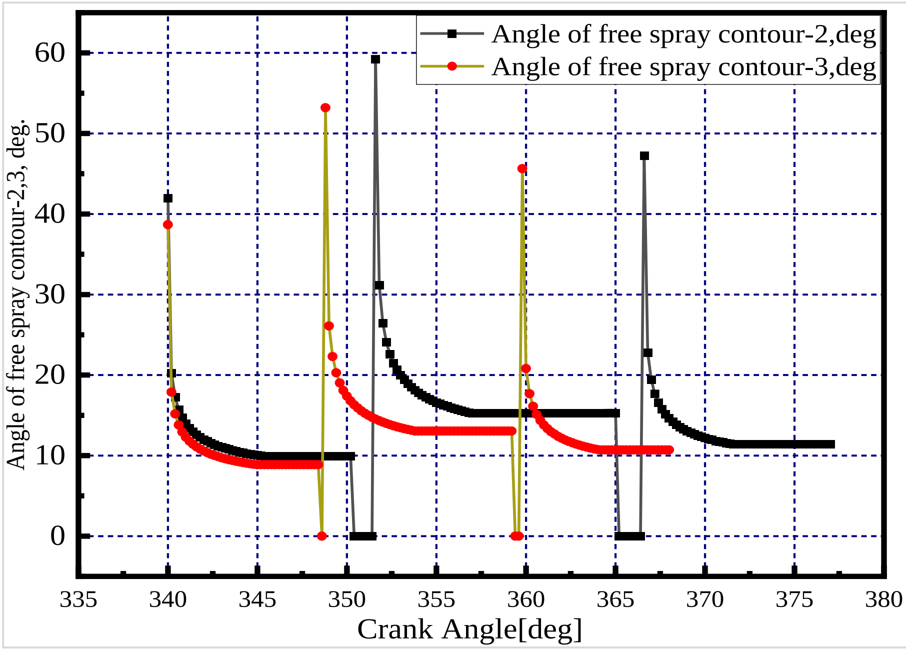

Figure 4.54 Spray angle of the triple fuel injection.

The spray angle for the triple injection of FSA2 is about 20mm spray tip penetration for the main injection, 15mm spray tip penetration for the pilot, and 15mm spray tip penetration for the post-injection. However, the maximum spray angle in STP3 for the pilot, main, and post-injection is at the spray tip of 10, 15, and 12mm spray tip penetration, respectively. As compared to the single and multiple injections, the single injection fuel supply has greater spray tip penetration (See Fig 4.57).

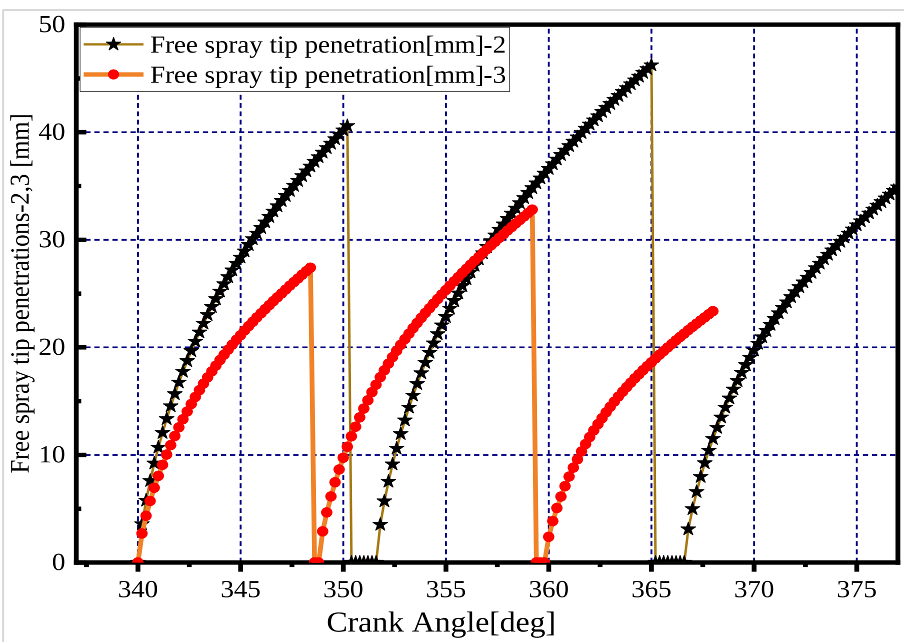

Figure 4.55 STP for the triple (pilot, main, and Post) fuel injection.

4.5.5. Present work validation

The simulation results and the experiment results with other similar works are shown in the table to confirm the investigation with the other similar scientific research works. As it is seen from (Table 4.12), the maximum cylinder pressure at the Shallow Hesselman piston bowl is similar to the shallow bowl; and the lower NOx emission is in line with (Pham et al., 2022). Emission, CP, and CT simulation and experiment results can be seen to be validated with a similar piston geometry as it is in line with previous results (Venkateswaran et al., 2010). The DSEVL2 BMW M47T (P1) has the same CP with the toroidal bowl, TCC, RCCI-OEM, and Omega, which have similar piston designs (Ganji., 2018).

Table 4.12 Emission, CP, and CT simulation and experiment results and their comparison

Authors	Toroidal bowl & similar piston design								Hemispherical bowl & similar piston design						
	№	CP	CT	HRR	NOx	PM	CO		№	CP	CT	HRR	NOx	PM	CO
Present work	P1	↑↑	↑	↓	↑↑	↓	↑	Present work	P2	↑↑	↑↑	↑	↓	↑	
Ganji., 2018.	TRB	↓	↓	-	↓	-	↓	Pham et al., 2022.	HSB	↑↑	-	↑	↑↑	-	↓↓
	TCC	↑↑	-	-	↑↑	↓	-		HCC	↓	-	-	↓↓	↓↓	
	OEM	↑↑	-	↑	↓	↓	↑		MRCCI	↑	-	↑	↓	↓	↑
	Omega	↑↑	↑↑	↑↑	↑↑	↓	-		HM	↑	↑	↑	↑	↑↑	-
Authors	Re-entrant bowl & Similar piston design							Authors	DOOSANP158FE & similar piston design						
	№	CP	CT	HRR	NOx	PM	CO		№	CP	CT	HRR	NOx	PM	CO
Present work	P3	↓	↑	↑↑	↑	↑↑	↓↓	Present work	P4	↓↓	↓	↓↓	↓↓	↓↓	-
Venkateswaran et al., 2010	REB	↓↓	-	↑↑	↑	-	↑↑	Xu et al., 2021	-	-	-	-	-	-	-
	SCC	↓	-	-	↓	↑↑	-		-	-	-	-	-	-	-
	CDC	↓	-	↓	↑↑	↑	↓		-	-	-	-	-	-	-
	SC	↓	↓	↓	↓	↓	-		DC	↓↓	↓↓	↑	↓↓	↑	

Where: ↑↑ maximum value, ↑ -second value, ↓-Third value, ↓↓- minimum value, HSB-Hemispherical bowl, TRB-Toroidal bowl, and REB-Re-entrant bowl, HCC- Hemispherical combustion chamber, SCC- shallow depth combustion chamber, TCC–toroidal Combustion chamber, OEM-omega bowl, HM-hemispherical bowl, SC-single curved, DC-double curved, P1-DSEVL2 BMW M47T, P2-Shallow Hesselman, P3-Lombardini 15LD350, P4 - DOOSANP158FE.

4.5.6. Effects of injection timing (SOI)

Effects of injection timing (SOIT), reactivity control compression ignition (RCCI) is the advanced low-temperature combustion engine using gasoline-ethanol blends of low reactivity fuels as a port fuel injections and diesel as high reactivity fuel of direct injection, respectively to reduce NOx and PM. The majority of the reactivity control compression ignition studies used conventional fossil fuels for low and high-reactivity fuels. The next generation of internal combustion engines, however, definitely requires fuel diversity due to future oil shortages. The effects of injection timing on performance and emission were investigated at 20°, 25°, and 30°

start of injection timing before the top dead center with a step of 5° crank angle in all simulations results are studied and compared. Accordingly, advancing the start of injection timing (ASOI) has the optimum pressure and temperature (OCPT); maximum cylinder pressure and temperature (MCPT) takes place at the OSOI timing and lower cylinder pressure and temperature (LCPT) is found at retarded start of injection (RSOI) before top dead center. So, according to this study; cylinder temperature and pressure are directly proportional in which pressure and temperature are maximum at the optimum start of injection timing (OSOI); minimum at 20°or RSOI, and optimum at 30°(ASOI) (See Fig.4.58a and 4.58b respectively.

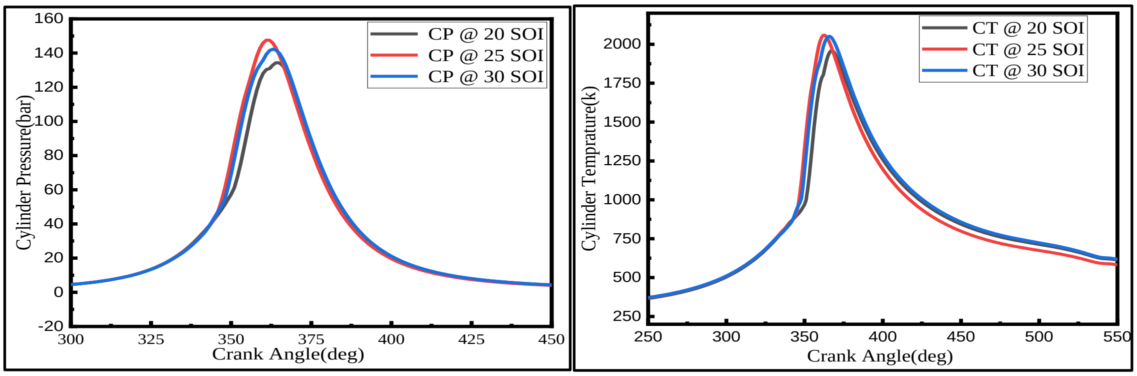

a. Cylinder pressures b. Cylinder temperatures

Figure 4.56 In-cylinder pressure and temperatures

The apparent heat release rate is affected as the start of injection timing is varying in 5° intervals or steps from retarded, optimum, and advanced (30 CA before top dead center). Start of injection as shown in Fig.4.59, the maximum quantity of heat release rate at retarded start of injection (RSOI) before the top dead center, as well as the heat release rate, is minimum at the advanced and optimum start of injection bTDC. Generally, the retard injection timing has more heat release rate and in the advanced and optimum start of injection, timing is minimum in heat releasing rate (See Fig.4.59).

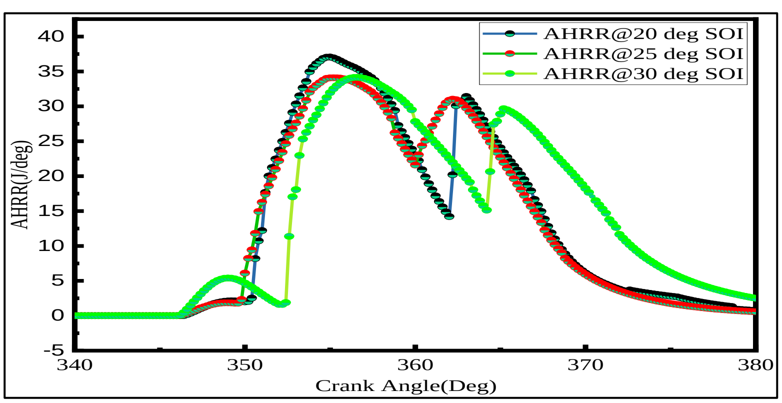

Figure 4.57 The heat release rate

Oxides of nitrogen emission are maximum at the optimum and advanced start of injection and minimum at the retarded starts of injection bTDC as shown in Fig.4.60a. The maximum soot is at 20 and 30° SOI bTDC and has a minimum value at 25° SOI bTDC as shown in Fig 4.60b. The inspiring outcome of this combustion method is that it can be directly controlled using the start of injection timing, which is impossible with most other LTCs. The oxides of nitrogen and particulate matter emission result are minimum at retarded SOI timing and maximum at the advanced start of injection.

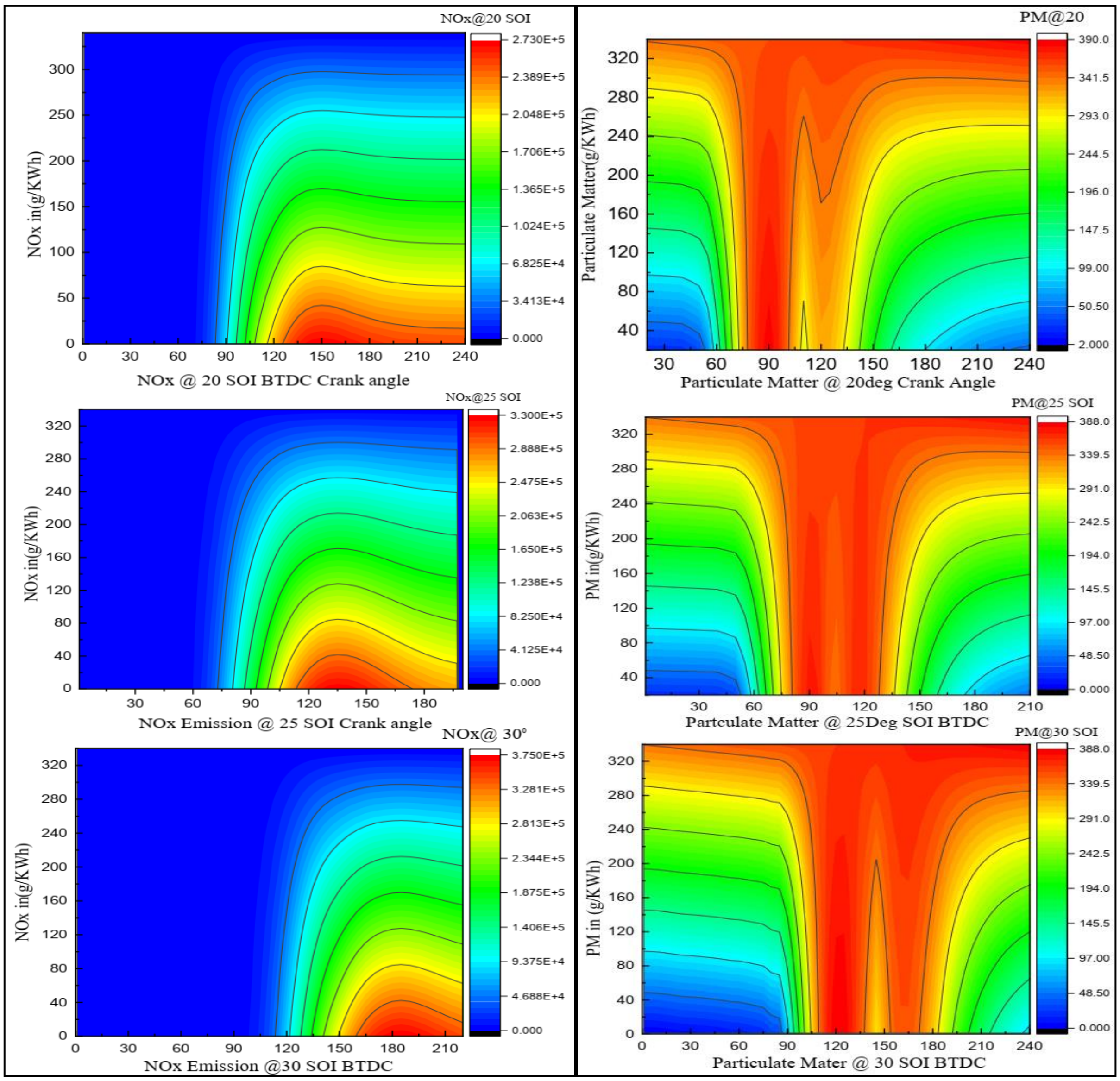

a. NOx b. Particulate matter

Figure 4.58 NOx and PM emission contour plot

The start of injection has a maximum mechanical and indicated efficiency at the retarded stage of injection respectively, and a maximum indicated mean effective pressure; minimum specific fuel consumption; maximum brake power at a retarded start of injection, and maximum brake torque at advanced start of injection. In-cylinder combustion shows the maximum cylinder pressure at the optimum start of injection and minimum cylinder temperature at the retarded SOI, ringing intensity is low, and maximum injection pressure 1385.4 bar (See Table.4.13). The ringing intensity, Ignition delay, and degree bTDC of the investigation are shown in Fig.4.61.

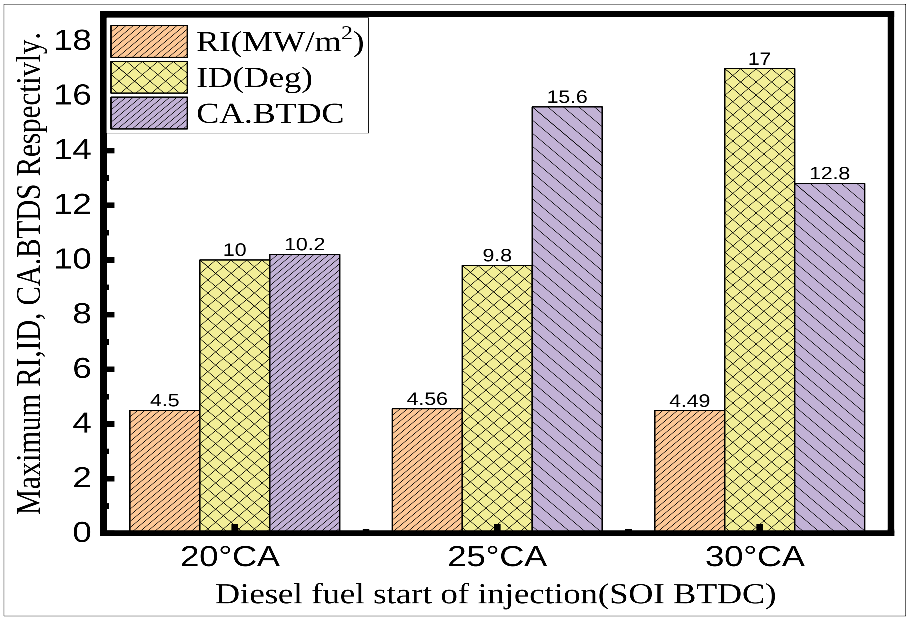

Figure 4.59 Ringing intensity and ignition delay

Table 4.13 Maximum performance, efficiency, and power

SOI	N	P_b	T_b	η_m	η_i	IMEP	SFC
20°CA	1900	2.43	12.2	0.78	0.40	6.3	0.28
25°CA	1900	1.88	9.4	0.73	0.34	5.3	0.36
30°CA	1900	2.36	11.9	0.77	0.35	6.2	0.33
Units	rpm	kW	N-m	-	-	Bar	kg/kWh
Combustions in the cylinder							
SOI	P_m	T_m	RI	In-P	ID	SOC	CD
20°CA	134	1959	4.5	639	10	10.2	48.4°CA
25°CA	148	2058	4.56	624	9.8	15.6	40.9°CA
30°CA	142	2052	4.49	1385	17	12.8	57.3°CA
Units	bar	K	MW/m^2	Bar	Deg	B.TD	Deg

CHAPTER FIFE

5. CONCLUSION AND RECOMMENDATION

5.1. Conclusions

The experimental investigation based on the speeds, fuel blend ratio, and advanced low-temperature RCCI engines combining highly reactive direct injection and low reactive port-injected fuel were revealed in the study. The numerical investigation based on DPBG, and main fuel injection timing effects also took place. The engine's combustion, performance, and emission characteristics were compared to the baseline diesel engine operation. Based on the results, the following conclusions are drawn as shown below:

The G25E75 port-injected fuel operation has a maximum cylinder pressure and HRR of 91 bar and 64 J/CA at 3000 rpm and minimum of 60 bars at 2200 rpm and 12 J/CA for baseline fuel occurring at 2600 rpm. The engine operating is smoother in the baseline, G50E50 fuel, and slightly unstable for the G25E75 blend. At higher engine load and higher and medium speed, the engine has properly functioned which indicates that there is good combustion phase control.

The NOx and CO_2 with G25E75 PFI RCCI are substantially reduced compared to the CDC Engine. HC and CO which are the critical issues in RCCI combustion, seem to be lower compared to diesel at the lower speed. By far the best overall emission is observed in the RCCI engine at the intermediate speed range tested. However, the lower CO and HC from the G50E50-RCCI engine is a target result that can be taken as a novel discovery of the study.

The brake power with RCCI is higher for both the blends (75/25 or 50/50) at higher speeds; the brake torque is consistently higher compared to the baseline across the entire speed range. The RCCI at lower speeds is almost on par with CDC at a higher speed range, with the high ethanol content blend showing somewhat higher efficiency.

The delta value shows the highest average response values for each factor. Speed (delta 10.7446, rank = 1) has the main effect on the SNR, and delta 38.96, rank = 1, has the largest effect on the response of Means at engine speeds of 3000rpm. The premixed fuel ratio of maximum ethanol (Delta 87.30, Rank = 1) has the main effect on the STD. The lines are not parallel to each other, and then there is an interaction between the two factors. The lines are not parallel in all emission and performance cases except for brake torque and CO_2, which are close to parallel. NOx, CO, HC, and brake power had the strongest means in engine speed and PMFB ratio.

The speeds had the higher main effect plots of SNR at the speeds of 3000rpm. The PBF ratios of maximum ethanol had the strongest main effect plots for Means and STDs. The residues appear dispersed normally based on a straight line using a normal probability plot. The data was normally distributed, as demonstrated by the normal probability plot, and the factors had an impact on the response.

The simulation with the variation of different shape design of the piston bowl exhibited the peak cylinder pressure and cylinder temperature of the Shallow Hesselman are 131bar and 2048.2k respectively and the lower is in the DOOSANP158FE which are 112bar and 1680k respectively. The temperature is within the acceptable limit of 1400-2000 except for the temperature of 2048.2k.

The NOx emissions of the P4 is 12.74 which is lower than all the other pistons while the NOx of the P1 (25.6g/KWh) is higher than all because of the cylinder pressure, which causes an increase in temperature. Although the cylinder temperature and NOx emission are proportional, NOx of P2 is lower due to the lower fuel fraction of NWF dilution outer the sleeve, low fuel fraction in the core of the free spray, low fuel fraction in fronts of the free spray, and low fuel fraction in the core of the fuel-free spray reduce NOx.

The exciting outcome from this combustion is that it is directly controlled using SOI timing which is impossible with most other LTC concepts and the NOx and PM emission result is minimum at retarded SOI timing and maximum at ASOI. The diesel engine RCCI declined cylinder pressure and cylinder temperature, and MHRR at the RSOI but maximum at OSOI in both cylinder pressure and cylinder temperature.

5.2. Recommendations

There is a mechanical limit to the port-injected fuel of G25E75 and G50E50-RCCI engine functioning modes at lower engine speeds of less than 2000 and 1900 rpm, respectively. It recommended the next scholar and engine researchers identify a different fuel that can raise the mechanical limit at lower engine speeds. The simulation results for the baseline are only viewed at different shape designs of piston geometry; so it recommended the academician and IC engine researchers consider how fuel injection pattern affects engine performance, combustion, and emission characteristics.

5.3. Future Direction

Up until now, nearly all of the work on the RCCI concept including the work we have done is on the steady-state settings. On the other hand, most thermal propulsion systems utilized in transportation applications have irregular operating conditions. To meet the new real-driving emissions rules and minimize engine-out emissions, it is imperative to study transient behavior in the RCCI concept across the whole load spectrum. This would bridge the gap between steady state and transient operation, making the adoption of the RCCI idea in mass manufacturing easier. To find the overall optimal operating point, more work in this area might be done by adjusting the blend ratio of the port-injected fuel.

REFERENCES

Abdelaal, MM, Hegab, AH J Energy conversion, and management. (2012). Combustion and emission characteristics of a natural gas-fueled diesel engine with EGR. *64*, 301-312.

Aceves, Salvador M, Smith, J Ray, Westbrook, Charles K, and Pitz, WJ. (1999). Compression ratio effect on methane HCCI combustion.

Agarwal, Avinash Kumar, Srivastava, Dhananjay Kumar, Dhar, Atul, Maurya, Rakesh Kumar, Shukla, Pravesh Chandra, and Singh, Akhilendra Pratap. (2013a). Effect of fuel injection timing and pressure on combustion, emissions and performance characteristics of a single cylinder diesel engine. *Fuel*, *111*, 374-383. doi:10.1016/j.fuel.2013.03.016

Agarwal, Avinash Kumar, Srivastava, Dhananjay Kumar, Dhar, Atul, Maurya, Rakesh Kumar, Shukla, Pravesh Chandra, and Singh, Akhilendra Pratap %J Fuel. (2013b). Effect of fuel injection timing and pressure on combustion, emissions and performance characteristics of a single cylinder diesel engine. *111*, 374-383.

Akalin, Guray, Erdogan, Sinan, and Sarkodie, Samuel Asumadu %J Environmental Impact Assessment Review. (2021). Do dependence on fossil fuels and corruption spur ecological footprint? , *90*, 106641.

Al-Yasiria, Ahmed Jassim Alib, Maan Abood Alic, Raed Saiad Bekheetd, and Nima, Heider. (2020). Renewable energy sources in international energy markets: reality and prospects. *11*(3).

Alam, Md Ashfaque, and Prasad, Anil Kumar %J Proceedings of the Institution of Mechanical Engineers, Part E: Journal of Process Mechanical Engineering. (2023). Performance and exhaust emission characteristics of a CI engine fuelled with diesel-biodiesel-methane-nitromethane. 09544089231190767.

Albayrak, Arda, Gezer, Onur, Özener, Orkun, Büyük, Cihan, and Özkan, Muammer %J Fuel. (2023). The effect of multiple injection on CI engine pollutant emissions and green house gases. *349*, 128667.

Allen, Cody M, Joshi, Mrunal C, Gosala, Dheeraj B, Shaver, Gregory M, Farrell, Lisa, and McCarthy, James %J International Journal of Engine Research. (2021). Experimental assessment of diesel engine cylinder deactivation performance during low-load transient operations. *22*(2), 606-615.

Andrey Kuleshov, Khamid Mahkamov, Andrey Kozlov, Yury Fadeev, (2014), "Simulation of dual-fuel diesel combustion with multi-zone fuel spray combustion model," ASME 2014 Internal Combustion Engine Division Fall Technical Conference ICEF2014-5700, October 19-22, 2014, Columbus, IN, USA, 14 p.

A.S. Kuleshov : "Model for predicting air-fuel mixing, combustion and emissions in DI diesel engines over whole operating range", SAE Paper No. 2005-01-2119, 2005.

Ansari, Ehsan, Shahbakhti, Mahdi, and Naber, Jeffrey %J Applied Energy. (2018). Optimization of performance and operational cost for a dual mode diesel-natural gas RCCI and diesel combustion engine. *231*, 549-561.

Armin, Gholinia, Mahbod, Pourfallah, Mosayeb, Ranjbar, Mohsen, and Akbar, Ali. (2021). Investigation of the fuel injection angle/time on combustion, energy, and emissions of a heavy-duty dual-fuel diesel engine with reactivity control compression ignition mode. *Energy Reports, 7*, 5239-5247. doi:10.1016/j.egyr.2021.08.115

Aydın, Hüseyin %J Energy. (2021). An innovative research on variable compression ratio in RCCI strategy on a power generator diesel engine using CNG-safflower biodiesel. *231*, 121002.

Baškovič, Urban Žvar, Oprešnik, Samuel Rodman, Seljak, Tine, and Katrašnik, Tomaž %J Fuel. (2022). RCCI combustion with renewable fuel mix–Tailoring operating parameters to minimize exhaust emissions. *311*, 122590.

Belgiorno, Giacomo, Di Blasio, Gabriele, Beatrice, Carlo %J Natural Gas Engines: For Transportation, and Generation, Power. (2019). Advances of the natural gas/diesel RCCI concept application for light-duty engines: comprehensive analysis of the influence of the design and calibration parameters on performance and emissions. 251-266.

Benajes, Jesús, García, Antonio, Monsalve-Serrano, Javier, and Boronat, Vicente. (2017). Achieving clean and efficient engine operation up to full load by combining optimized RCCI and dual-fuel diesel-gasoline combustion strategies. *Energy Conversion and Management, 136*, 142-151. doi:10.1016/j.enconman.2017.01.010

Benajes, Jesús, García, Antonio, Monsalve-Serrano, Javier, Boronat, Vicente %J Energy Conversion, and Management. (2017). Achieving clean and efficient engine operation up to full load by combining optimized RCCI and dual-fuel diesel-gasoline combustion strategies. *136*, 142-151.

Benajes, Jesús, Molina, Santiago, García, Antonio, Belarte, Eduardo, and Vanvolsem, Michel %J Applied Thermal Engineering. (2014). An investigation on RCCI combustion in a heavy duty diesel engine using in-cylinder blending of diesel and gasoline fuels. *63*(1), 66-76.

Chiu, WS, Shahed, SM, and Lyn, WT %J SAE Transactions. (1976). A transient spray mixing model for diesel combustion. 502-512.

Corcione, FE. (2009). Study of advanced combustion mechanisms for clean engines at Istituto Motori.

Corcione, Felice, Valentino, Gerardo, Tornatore, Cinzia, Merola, Simona, and Marchitto, Luca. (2011). *Optical investigation of premixed low-temperature combustion of lighter fuel blends in compression ignition engines* (0148-7191). Retrieved from

Dahodwala, Mufaddel, Joshi, Satyum, Koehler, Erik, Franke, Michael, Tomazic, Dean, and Naber, Jeffrey. (2020). *Investigation of Diesel-CNG RCCI combustion at multiple engine operating conditions* (0148-7191). Retrieved from

Dec, John E., Yang, Yi, and Dronniou, Nicolas. (2011). Boosted HCCI - Controlling Pressure-Rise Rates for Performance Improvements using Partial Fuel Stratification with Conventional Gasoline. *SAE International Journal of Engines, 4*(1), 1169-1189. doi:10.4271/2011-01-0897

Dempsey, Adam B, Curran, Scott, and Reitz, Rolf D %J SAE International Journal of Engines. (2015). Characterization of reactivity controlled compression ignition (RCCI) using premixed gasoline and direct-injected gasoline with a cetane improver on a multi-cylinder engine. *8*(2), 859-877.

Dempsey, Adam B, Walker, N Ryan, and Reitz, Rolf %J SAE International Journal of Engines. (2013). Effect of piston bowl geometry on dual fuel reactivity controlled compression ignition (RCCI) in a light-duty engine operated with gasoline/diesel and methanol/diesel. *6*(1), 78-100.

Deshwar, Pranay, Kumar, Gaurav, Subramanian, Balaji, Panchal, Shreyash Hemant, Thangavel, Venugopal, Ismail, Saleel, et al. (2023). Simultaneous reduction of NOx and smoke emissions in gasoline-ethanol blended RCCI Engine with biogas as a ternary fuel. *24*(2).

Dhahad, Hayder A, Fayad, Mohammed A, Chaichan, Miqdam T, Jaber, Alaa Abdulhady, and Megaritis, T %J Fuel. (2021). Influence of fuel injection timing strategies on performance, combustion, emissions and particulate matter characteristics fueled with rapeseed methyl ester in modern diesel engine. *306*, 121589.

D.H. Qi and C.F. Lee (2016) Combustion and emissions behavior for ethanol–gasoline-blended fuels in a multipoint electronic fuel injection engine, International Journal of Sustainable Energy, 35:4, 323-338, DOI: 10.1080/14786451.2014.895004

Dond, Dipak K., and Gulhane, Nitin P. (2021). Effect of a turbocharger and EGR on the performance and emission characteristics of a CRDI small diesel engine. *Heat Transfer*, *51*(1), 1237-1252. doi:10.1002/htj.22350

Duan, Xu, Xiongbo, Sun, Zhengxin, Deng, Xingyu, Liu, Banglin, Jingping, et al. (2021). Effects of injection timing and EGR on combustion and emissions characteristics of the diesel engine fuelled with acetone–butanol–ethanol/diesel blend fuels. *231*, 121069.

Dwarshala, Siva Krishna Reddy, Rajakumar, Siva Subramaniam, Kummitha, Obula Reddy, Venkatesan, Elumalai Perumal, Veza, Ibham, and Samuel, Olusegun David %J Energies. (2023). A Review on Recent Developments of RCCI Engines Operated with Alternative Fuels. *16*(7), 3192.

Elkelawy, Medhat, El Shenawy, EA, Mohamed, Sherif A, Elarabi, Mostafa M, Bastawissi, Hagar Alm-Eldin %J Energy Conversion, and X, Management:. (2022). Impacts of using EGR and different DI-fuels on RCCI engine emissions, performance, and combustion characteristics. *15*, 100236.

Elkelawy, Medhat, Shenawy, E.A. El, Mohamed, Sherif A., Elarabi, Mostafa M., and a, Hagar Alm-Eldin Bastawissi. (2022). Impacts of EGR on RCCI engines management: A comprehensive review. *Energy Conversion and Management: X, 13 (2022) 100133*. doi:10.1016/j.ecmx.2022.100216

Eng, JA. (2002). *Characterization of pressure waves in HCCI combustion* (0148-7191). Retrieved from

Fernandes, Suneeta D, Trautmann, Nina M, Streets, David G, Roden, Christoph A, and Bond, Tami C %J Global Biogeochemical Cycles. (2007). Global biofuel use, 1850–2000. *21*(2).

Firmansyah, Aziz, Abdul Rashid Abdul, Heikal, Morgan Raymond, Abidin, Ezrann Zharif Zainal, and Panchatcharam, Naveenchandran. (2018). Reactivity Controlled Compression Ignition (RCCI) of Gasoline-CNG Mixture. *ItecOpen*. doi:10.5772/intechopen.72880

Gad, MS, He, Zhixia, El-Shafay, AS, and EL-Seesy, Ahmed I %J Case Studies in Thermal Engineering. (2021). Combustion characteristics of a diesel engine running with Mandarin essential oil-diesel mixtures and propanol additive under different exhaust gas recirculation: Experimental investigation and numerical simulation. *26*, 101100.

Ganesan, V. R. (2006). Internal combustion engines. *Semantic scholar, 2006*, 1-99.

Gao, Zhenxun, Jiang, Chongwen, and Lee, Chun-Hian %J Proceedings of the Combustion Institute. (2017). Representative interactive flamelet model and flamelet/progress variable model for supersonic combustion flows. *36*(2), 2937-2946.

García, Antonio, Carlucci, Paolo, Monsalve-Serrano, Javier, Valletta, Andrea, and Martínez-Boggio, Santiago %J Applied Energy. (2021). Energy management optimization for a power-split hybrid in a dual-mode RCCI-CDC engine. *302*, 117525.

Giampietro, Mario, Ulgiati, Sergio, and Pimentel, David %J BioScience. (1997). Feasibility of large-scale biofuel production. *47*(9), 587-600.

Golzari, Reza. (2018). Experimental study of the impact of port and direct fuel injection strategies on the efficiency, performance and emissions of a downsized gdi engine. (PhD), Brunel University London,

Gopal, Rajendiran, Kavandappa-Goundar, Mayilsamy, Ramasamy, Subramanian, Natarajan, Nedunchezhian, and Ramasamy, Venkatachalam. (2014). Experimental and regression analysis for multi cylinder diesel engine operated with hybrid fuel blends. *Thermal Science*, *18*(1), 193-203. doi:10.2298/tsci130130127g

Gu¨rbu¨z, Hu¨seyin, and Sandalcı, Tarkan. (2022). Numerical analysis of diesel injection strategies on emissions and performance in CH4/diesel powered RCCI diesel engine with high ratio EGR. *Alexandria Engineering Journal (2023) 64, 517–526*. doi:10.1016/j.aej.2022.09.012

Gurusamy, Manikandaraja, and Subramanian, Balaji %J Fuel. (2023). Study of PCCI engine operating on pine oil diesel blend (P50) with benzyl alcohol and diethyl ether. *335*, 127121.

Habtamu, Deresso, Ramayya, Ancha Venkata, Babu, Nallamothu Ramesh, Balkeshwar, Singh, and Bisrat, Yoseph. (2022). Investigation of Partially Pre-mixed Charge Ignitions (PPCI) Engine Mode. *Journal of Harbin Institute of Technology (New Series)*. doi: 10.11916/j.issn.1005-9113.2022001

Hanson, Reed, Curran, Scott, Wagner, Robert, and Reitz, Rolf %J SAE International Journal of Engines. (2013). Effects of biofuel blends on RCCI combustion in a light-duty, multi-cylinder diesel engine. *6*(1), 488-503.

Hanson, Reed, Ickes, Andrew, and Wallner, Thomas. (2016). *Comparison of RCCI operation with and without EGR over the full operating map of a heavy-duty diesel engine* (0148-7191). Retrieved from

Hanson, Robert M, Prilusky, Jaime, Renjian, Zhou, Nakane, Takanori, and Sussman, Joel L %J Israel Journal of Chemistry. (2013). JSmol and the next-generation web-based representation of 3D molecular structure as applied to proteopedia. *53*(3-4), 207-216.

Hariharan, Deivanayagam, Rahimi Boldaji, Mozhgan, Yan, Ziming, Gainey, Brian, Lawler, Benjamin %J Journal of Engineering for Gas Turbines, and Power. (2021). Exploring the effects of piston bowl geometry and injector included angle on dual-fuel and single-fuel RCCI. *143*(11), 111013.

Heubaum, Harald, and Biermann, Frank %J Energy Policy. (2015). Integrating global energy and climate governance: The changing role of the International Energy Agency. *87*, 229-239.

Heywood, John B. (2018). *Internal combustion engine fundamentals*: McGraw-Hill Education.

Hiroyasu, Hiroyuki, Kadota, Toshikazu, and Arai, Masataka %J Bulletin of JSME. (1983). Development and use of a spray combustion modeling to predict diesel engine efficiency and pollutant emissions: Part 1 combustion modeling. *26*(214), 569-575.

Hoang, Anh Tuan, Murugesan, Parthasarathy, Elumalai, PV, Balasubramanian, Dhinesh, Parida, Satyajeet, Jayabal, Chandra Priya, et al. (2023). Strategic combination of waste plastic/tire pyrolysis oil with biodiesel for natural gas-enriched HCCI engine: Experimental analysis and machine learning model. *280*, 128233.

Hussain, Ilyas, and Immanuel, RJ. (2021). Composite materials and its advancements for a cleaner engine of future. In *Advances in Engine Tribology* (pp. 169-191): Springer.

Hwang, Jeffrey T, Kane, Seamus P, and Northrop, William F. (2018). *Demonstration of single-fuel reactivity controlled compression ignition using reformed exhaust Gas recirculation* (0148-7191). Retrieved from

Isermann, Rolf %J Berlin: Springers Berlin Heidelberg. (2014). Engine modeling and control. *1017*.

Işık, Mehmet Zerrakki, and Aydın, Hüseyin %J Fuel. (2016). Analysis of ethanol RCCI application with safflower biodiesel blends in a high load diesel power generator. *184*, 248-260.

Jagankumar, KR, Prakash, N, Prasad, C, Shridhar, VA, Singh, M Dinesh, and Sathyamurthy, Ravishankar. (2020). *An experimental investigation on single cylinder RCCI engine fuelled with diesel/petrol*. Paper presented at the Journal of Physics: Conference Series.

Jagankumara, K R, Prakasha, N, Prasada, C, Shridhara, V A, Singha, M Dinesh, and Sathyamurthyb, Ravishankar. (2020). An experimental investigation on single cylinder RCCI engine fuelled with diesel/petrol. *Journal of Physics: Conference Series*. doi:10.1088/1742-6596/1706/1/012200

Jeyakumar, Huang, Nagarajan, Balasubramanian, Zuohua, Le, Dhinesh, Nguyen, Anh Tuan, Pandian, Xuan Phuong, et al. (2022). Experimental evaluation over the effects of natural antioxidants on oxidation stability of binary biodiesel blend. *International Journal of Energy Research, 46*(14), 20437-20461. doi:10.1002/er.7956

Jeyakumar, Nagarajan, Narayanasamy, Bose, Balasubramanian, Dhinesh, and Viswanathan, Karthickeyan. (2020). Characterization and effect of Moringa Oleifera Lam. antioxidant additive on the storage stability of Jatropha biodiesel. *Fuel*, *281*. doi:10.1016/j.fuel.2020.118614

Jia, Ming, Pan, Haiyang, Bian, Ye, Zhang, Zonghan, Chang, Yachao, Liu, Hong %J Atomization, et al. (2022). Calibration of the constants in the Kelvin-Helmholtz Rayleigh-Taylor (KH-RT) breakup model for diesel spray under wide conditions based on advanced data analysis techniques. *32*(6).

Jia, Ming, Xie, Maozhao, and Wang, Tianyou %J International Journal of Engine Research. (2013). Numerical investigation of the influence of intake valve lift profile on a diesel premixed charge compression ignition engine with a variable valve actuation system at moderate loads and speeds. *14*(2), 151-179.

Joshi, Girdhar, Pandey, Jitendra K, Rana, Sravendra, Rawat, Devendra S %J Renewable, and Reviews, Sustainable Energy. (2017). Challenges and opportunities for the application of biofuel. *79*, 850-866.

Juneja, Harpreet Singh, and Sandhu, Sarbjot Singh. (2019). *Experimental Investigation of PPCI Engine fuelled with Ethanol.* Paper presented at the IOP Conference Series: Materials Science and Engineering.

Kakoee, Alireza, Bakhshan, Younes, Aval, Sattar Motadayen, Gharehghani, Ayat %J Energy conversion, and management. (2018). An improvement of a lean burning condition of natural gas/diesel RCCI engine with a pre-chamber by using hydrogen. *166*, 489-499.

Karthikeya Sharma, T, Amba Prasad Rao, G, Madhu Murthy, K %J Journal of the Brazilian Society of Mechanical Sciences, and Engineering. (2015). Effect of swirl on performance and emissions of CI engine in HCCI mode. *37*, 1405-1416.

Kesicki, Fabian, and Yanagisawa, Akira %J Energy Efficiency. (2015). Modelling the potential for industrial energy efficiency in IEA's World Energy Outlook. *8*, 155-169.

Kim, Hyungtae, Kim, Seungdo, Dale, Bruce E %J Environmental science, and technology. (2009). Biofuels, land use change, and greenhouse gas emissions: some unexplored variables. *43*(3), 961-967.

Kimura, Shuji, Aoki, Osamu, Kitahara, Yasuhisa, and Aiyoshizawa, Eiji %J Sae Transactions. (2001). Ultra-clean combustion technology combining a low-temperature and premixed combustion concept for meeting future emission standards. 239-246.

Kokjohn, S L, Hanson, R M, Splitter, D A, and Reitz, R D. (2010). Fuel reactivity controlled compression ignition (RCCI): a pathway to controlled high-efficiency clean combustion. *International Journal of Engine Research*. doi:10.1177/1468087411401548

Kokjohn, S. L., Hanson, R. M., Splitter, D. A., and Reitz, R. D. (2011). Fuel reactivity controlled compression ignition (RCCI): a pathway to controlled high-efficiency clean combustion. *International Journal of Engine Research, 12*(3), 209-226. doi:10.1177/1468087411401548

Kokjohn, Sage L, Hanson, Reed M, Splitter, Derek A, and Reitz, Rolf D %J SAE International Journal of Engines. (2010). Experiments and modeling of dual-fuel HCCI and PCCI combustion using in-cylinder fuel blending. *2*(2), 24-39.

Kokjohn, Sage Lucas. (2012). *Reactivity controlled compression ignition (RCCI) combustion.* The University of Wisconsin-Madison,

Kuleshov, A. S. (2006). Use of Multi-Zone DI Diesel Spray Combustion Model for Simulation and Optimization of Performance and Emissions of Engines with Multiple Injection. *SAE TECHNICAL PAPER SERIES*.

Kuzuoka, Kohei, Kamio, Junichi, and Hashimoto, Kohtaro. (2016). *Effect of Mixture Stratification and Fuel Reactivity on Dual-Fuel Compression Ignition Combustion Process for SI-Based Engine* (0148-7191). Retrieved from

Li, J., Yang, W. M., An, H., Zhou, D. Z., Yu, W. B., Wang, J. X., et al. (2015). Numerical investigation on the effect of reactivity gradient in an RCCI engine fueled with gasoline and diesel. *Energy Conversion and Management, 92*, 342-352. doi:10.1016/j.enconman.2014.12.071

Li, Jing, Wang, Dajian, Zhuang, Cong, Gong, Shiqi, and Li, Songhong %J Processes. (2022). Numerical Investigation of the Knocking Combustion Characteristics of the N-Butanol/N-Octanol RCCI Engine. *10*(10), 2142.

Li, Jing, Yang, Wenming, and Zhou, Dezhi. (2017). Review on the management of RCCI engines. *Renewable and Sustainable Energy Reviews, 69*, 65-79. doi:10.1016/j.rser.2016.11.159

Li, Jing, Yang, Wenming, Zhou, Dezhi %J Renewable, and Reviews, Sustainable Energy. (2017). Review on the management of RCCI engines. *69*, 65-79.

Tingting, Li. (2017). *A High Efficiency and Clean Combustion Strategy for Compression Ignition Engines: Integration of Low Heat Rejection Concepts with Low Temperature Combustion.*

Liu, Chang, Qian, Jin, Ye, Yifan, Zhou, Hua, Sun, Cheng-Jun, Sheehan, Colton, et al. (2021). Oxygen evolution reaction over catalytic single-site Co in a well-defined brookite TiO2 nanorod surface. *4*(1), 36-45.

Liu, Haifeng, Ma, Guixiang, Hu, Bin, Zheng, Zunqing, and Yao, Mingfa %J Energy. (2018). Effects of port injection of hydrous ethanol on combustion and emission characteristics in dual-fuel reactivity controlled compression ignition (RCCI) mode. *145*, 592-602.

Lou, D., Kang, L., Zhang, Y., Fang, L., and Luo, C. (2022). Effect of Exhaust Gas Recirculation Combined with Selective Catalytic Reduction on NO (x) Emission Characteristics and Their Matching Optimization of a Heavy-Duty Diesel Engine. *ACS Omega, 7*(26), 22291-22302. doi:10.1021/acsomega.2c01123

Lou, Diming, Lou, Guokang, Wang, Bo, Fang, Liang, and Zhang, Yunhua. (2021). Effect of LP-EGR on the Emission Characteristics of GDI Engine. *Machines, 10*(1). doi:10.3390/machines10010007

Manente, Vittorio, Zander, Claes-Goeran, Johansson, Bengt, Tunestal, Per, and Cannella, William. (2010). *An advanced internal combustion engine concept for low emissions and high efficiency from idle to max load using gasoline partially premixed combustion* (0148-7191). Retrieved from

Marriott, Craig D, and Reitz, Rolf D %J SAE Transactions. (2002). Experimental investigation of direct injection-gasoline for premixed compression ignited combustion phasing control. 863-874.

Mikulski, Maciej, Balakrishnan, Praveen Ramanujam, Doosje, Erik, and Bekdemir, Cemil. (2018). *Variable valve actuation strategies for better efficiency load range and thermal management in an RCCI engine* (0148-7191). Retrieved from

Mofijur, M, Hasan, Mohammad Mehedi, Mahlia, TMI, Rahman, SM Ashrafur, Silitonga, AS, and Ong, Hwai Chyuan %J Energies. (2019). Performance and emission parameters of homogeneous charge compression ignition (HCCI) engine: a review. *12*(18), 3557.

Mofijur, M, Rasul, Mohammad, Hassan, NMS, and Uddin, MN %J Energy Procedia. (2019). Investigation of exhaust emissions from a stationary diesel engine fuelled with biodiesel. *160*, 791-797.

Mohammadian, Amir, Chehrmonavari, Kakaee, Hamed, Paykani, Amirhasan, and Amin. (2020). Effect of injection strategies on a single-fuel RCCI combustion fueled with isobutanol/isobutanol+ DTBP blends. *278*, 118219.

Mohammadnejad, S, Amani, E, Hosseini, R, Chitsaz, I, Kamali, A %J Journal of the Brazilian Society of Mechanical Sciences, and Engineering. (2019). Effects of the swirl ratio and spray angle on the mixture stratification in a diesel–NG RCCI engine. *41*(5), 233.

Nageswaran, Bharath Anand, Yangdongfang, Yang, D, Reitz Rolf, and Christopher, Rutland. (2015). *Comparison of variable valve actuation, cylinder deactivation and injection strategies for low-load RCCI operation of a light duty engine* (0148-7191). Retrieved from

Nguyen, Lam Duc, Lewis, Amari N, Leyva-Mayorga, Israel, Regan, Amelia, and Popovski, Petar %J arXiv preprint arXiv:.13477. (2021). B-ETS: A trusted blockchain-based emissions trading system for vehicle-to-vehicle networks.

Nguyen, Tien Duy, Anh, Trung Tran, Quang, Vinh Tran, Nhat, Huy Bui, and Duy, Vinh Nguyen %J AIMS Energy. (2020). An experimental evaluation of engine performance and emissions characteristics of a modified direct injection diesel engine operated in RCCI mode. *8*(6).

Nguyen, Tuannghia, Pham, MinhHieu, and Anh, Tuan Le. (2020). Spray, combustion, performance and emission characteristics of a common rail diesel engine fueled by fish-oil biodiesel blends. *Fuel, 269*. doi:10.1016/j.fuel.2020.117108

Nguyen, Tuannghia, Pham, MinhHieu, and Le Anh, Tuan %J Fuel. (2020). Spray, combustion, performance and emission characteristics of a common rail diesel engine fueled by fish-oil biodiesel blends. *269*, 117108.

Olmeda, Pablo, Garcia, Antonio, Monsalve-Serrano, Javier, and Sari, Rafael Lago %J Applied Thermal Engineering. (2018). Experimental investigation on RCCI heat transfer in a light-duty diesel engine with different fuels: Comparison versus conventional diesel combustion. *144*, 424-436.

Pamminger, Michael, Hall, Carrie M., Wang, Buyu, and Wallner, Thomas. (2020). A control-oriented combustion model framework for compression ignition engines operating on low-reactivity fuel. *International Journal of Engine Research, 22*(6), 1924-1938. doi:10.1177/1468087420918038

Pan, Suozhu, Cai, Kai, Cai, Min, Du, Chenbo, Li, Xin, Han, Weiqiang, et al. (2021). Experimental study on the cyclic variations of ethanol/diesel reactivity controlled compression ignition (RCCI) combustion in a heavy-duty diesel engine. *237*, 121614.

Paykani, Kakaee, Amin, Reitz, Amir-Hasan Rahnama Pourya, and D, Rolf. (2015). Progress and recent trends in reactivity-controlled compression ignition engines. *International Journal of Engine Research, 17*(5), 481-524. doi:10.1177/1468087415593013

Paykani, Amin, Kakaee, Amir-Hasan, Rahnama, Pourya, and Reitz, Rolf D %J International Journal of Engine Research. (2016). Progress and recent trends in reactivity-controlled compression ignition engines. *17*(5), 481-524.

Pedrozo, Hector Alejandro, Reartes, SB Rodriguez, Vecchietti, Aldo R, Díaz, María Soledad, Grossmann, Ignacio E %J Computers, and Engineering, Chemical. (2021). Optimal design of ethylene and propylene coproduction plants with generalized disjunctive programming and state equipment network models. *149*, 107295.

Pedrozo, Vinícius B, Wang, Xinyan, Guan, Wei, and Zhao, Hua %J International Journal of Engine Research. (2022). The effects of natural gas composition on conventional dual-fuel and reactivity-controlled compression ignition combustion in a heavy-duty diesel engine. *23*(3), 397-415.

Pfleger, Brian F, and Takors, Ralf %J Current Opinion in Biotechnology. (2023). Recent progress in the synthesis of advanced biofuel and bioproducts. *80*, 102913.

Poorghasemi, Kamran, Saray, Rahim Khoshbakhti, Ansari, Ehsan, Irdmousa, Behrouz Khoshbakht, Shahbakhti, Mehdi, and Naber, Jeffery D %J Applied energy. (2017). Effect of diesel injection strategies on natural gas/diesel RCCI combustion characteristics in a light duty diesel engine. *199*, 430-446.

Rakopoulos, Constantine D, and Hountalas, DT %J SAE transactions. (1998). Development and validation of a 3-D multi-zone combustion model for the prediction of DI diesel engines performance and pollutants emissions. 1413-1429.

Ram, SONU RAM Sonu, Yadav, Raj Kumar, and Singh, Indraj %J U. Porto Journal of Engineering. (2023). Combustion and Exhaust Emission Improvement in a 3-Cylinder Mpfi Engine Through Downsizing. *9*(3), 194-208.

Raut, Akshat, Bidarvatan, Mehran, Borhan, Hoseinali, and Shahbakhti, Mahdi. (2018). *Model predictive control of an RCCI engine.* Paper presented at the 2018 Annual American Control Conference (ACC).

Reitz, Rolf Deneys, Hanson, Reed M, Splitter, Derek A, and Kokjohn, Sage L. (2016). *Engine combustion control via fuel reactivity stratification*. Retrieved from

Rosa, Josimar Souza, Martins, Mario Eduardo Santos, Telli, Giovani Dambros, Altafini, Carlos Roberto, Wander, Paulo Roberto, and Rocha, Luiz Alberto Oliveira %J Fuel. (2020). Exploring the effects of diesel start of injection and water-in-ethanol concentration on a reactivity controlled compression ignition engine. *281*, 118751.

Ryskamp, Daniel A, Frye, Amber M, Phuong, Tam TT, Yarishkin, Oleg, Jo, Andrew O, Xu, Yong, et al. (2016). TRPV4 regulates calcium homeostasis, cytoskeletal remodeling, conventional outflow and intraocular pressure in the mammalian eye. *6*(1), 30583.

Sadabadi, Kaveh Khodadadi. (2015). *Modelling and control of combustion phasing of an rcci engine*: Michigan Technological University.

Seelam, Navyasree, Gugulothu, Santhosh Kumar, Bhasker, Burra, Mulugundum, SivaSurya, Sastry, Gadepalli Ravikiran %J Environmental Science, and Research, Pollution. (2022). Investigating the role of fuel injection pressure and piston bowl geometries to enhance performance and emission characteristics of hydrogen-enriched diesel/1-pentanol fueled in CRDI diesel engine. 1-15.

Selvan, P Karthik, Dhinesh, PK, Vaanan, R Tamil %J International Journal of Engineering Research, and Technology. (2018). Performance Analysis on PCCI Engine with Duel Fuel Mode Condition. *7*(3), 346-350.

Şener, Ramazan, Özdemir, Mehmed R., and Yangaz, Murat U. (2019). Influence of piston bowl geometry on combustion and emission characteristics. *Proceedings of the Institution of Mechanical Engineers, Part A: Journal of Power and Energy, 233*(5), 576-587. doi:10.1177/0957650919854637

Sharma, T Karthikeya %J Journal of advanced research. (2015). Performance and emission characteristics of the thermal barrier coated SI engine by adding argon inert gas to intake mixture. *6*(6), 819-826.

Sharma, T. Karthikeya, Rao, G. Amba Prasad, and Murthy, K. Madhu. (2015). Homogeneous Charge Compression Ignition (HCCI) Engines: A Review. *Archives of Computational Methods in Engineering, 23*(4), 623-657. doi:10.1007/s11831-015-9153-0

Shen, Mengqin, Tuner, Martin, Johansson, Bengt, and Cannella, William. (2013). *Effects of EGR and Intake Pressure on PPC of Conventional Diesel, Gasoline and Ethanol in a Heavy Duty Diesel Engine*. Paper presented at the SAE TECHNICAL PAPER SERIES.

Shinde, Abhishek Balasaheb, Umadi, Omkar Anil, Gawali, Shivaji V, Kamble, Arun %J International Research Journal of Engineering, and Technology. (2020). Common Rail Direct Injection. *7*(4), 3095-3102.

Silva, LS, Silva, JA, Henríquez, JR, de Lira Junior, JC %J Arabian Journal for Science, and Engineering. (2023). Numerical Analysis of Effects of Engine Downsizing and Turbocharging on the Parameters of Performance and Emissions of an Internal Combustion Engine. *48*(3), 2795-2805.

Singh, Akhilendra Pratap, Kumar, Vikram, and Agarwal, Avinash Kumar. (2020). Evaluation of comparative engine combustion, performance and emission characteristics of low temperature combustion (PCCI and RCCI) modes. *Applied Energy, 278*. doi:10.1016/j.apenergy.2020.115644

Sodré, J R, Soares, SMC %J Journal of the Brazilian Society of Mechanical Sciences, and Engineering. (2003). Comparison of engine power correction factors for varying atmospheric conditions. *25*, 279-284.

Soloiu, Valentin, Duggan, Marvin, Harp, Spencer, Vlcek, Brian, and Williams, David %J Energy. (2013). PFI (port fuel injection) of n-butanol and direct injection of biodiesel to attain LTC (low-temperature combustion) for low-emissions idling in a compression engine. *52*, 143-154.

Solouk, Ali, and Shahbakhti, Mahdi %J Energies. (2016). Energy optimization and fuel economy investigation of a series hybrid electric vehicle integrated with diesel/RCCI engines. *9*(12), 1020.

Soo-Young. (2019). Application of bioethanol to advanced CI engines; dual fuel and RCCI combustion modes – a review. *International Journal of Green Energy, 16*(14), 1105-1130. doi:10.1080/15435075.2019.1653878

Splitter, Derek, Reitz, Rolf, Hanson, Reed %J SAE International Journal of Fuels, and Lubricants. (2010). High efficiency, low emissions RCCI combustion by use of a fuel additive. *3*(2), 742-756.

Splitter, Derek, Wissink, Martin, DelVescovo, Dan, and Reitz, Rolf D. (2013). *RCCI engine operation towards 60% thermal efficiency* (0148-7191). Retrieved from

Splitter, Derek, Wissink, Martin, Kokjohn, Sage, and Reitz, Rolf D. (2012). *Effect of Compression Ratio and Piston Geometry on RCCI Load Limits and Efficiency*. Paper presented at the SAE Technical Paper Series.

Srihari, S, Thirumalini, S, and Prashanth, K %J Renewable Energy. (2017). An experimental study on the performance and emission characteristics of PCCI-DI engine fuelled with diethyl ether-biodiesel-diesel blends. *107*, 440-447.

Subramaniam, Shankar %J Progress in Energy, and Science, Combustion. (2013). Lagrangian–Eulerian methods for multiphase flows. *39*(2-3), 215-245.

Sula, Constantin, Grosshans, Holger, Papalexandris, MV %J Flow, Turbulence, and Combustion. (2020). Assessment of droplet breakup models for spray flow simulations. *105*, 889-914.

Tekgül, Bulut, Karimkashi, Shervin, Kaario, Ossi, Kahila, Heikki, Lendormy, Éric, Hyvönen, Jari, et al. (2022). Large-eddy simulation of split injection strategies in RCCI conditions. *26*(3), 590-611.

Thomas, Jeffrey. (2018). *Investigation of Novel hydrous ethanol dual fuel strategies for reduction emission for fixed calibration diesel engine.* (Ph.D), University of Minnesota,

Tibaquirá, Juan E., Huertas, José I., Ospina, Sebastián, Quirama, Luis F., and 2, José E. Niño. (2018). The Effect of Using Ethanol-Gasoline Blends on the Mechanical, Energy and Environmental Performance of In-Use Vehicles. *Energies*. doi:10.3390/en11010221

Uherek, Elmar, Halenka, Tomas, Borken-Kleefeld, Jens, Balkanski, Yves, Berntsen, Terje, Borrego, Carlos, et al. (2010). Transport impacts on atmosphere and climate: Land transport. *44*(37), 4772-4816.

Wang, Hu, Zhong, Xin, Mi, Shan, and Yao, Mingfa. (2020). Numerical investigation on the combustion characteristics of PODE3/gasoline RCCI and high load extension. *Fuel, 263*. doi:10.1016/j.fuel.2019.116366

Wang, Yifeng, Yao, Mingfa, Li, Tie, Zhang, Weijing, and Zheng, Zunqing %J Applied Energy. (2016). A parametric study for enabling reactivity controlled compression ignition (RCCI) operation in diesel engines at various engine loads. *175*, 389-402.

Wategavea, S.P., Banapurmathb, N.R., Sawantb, M.S., Elahi, Manzoore, Soudagard, M., Mujtabae, M.A., et al. (2021). Clean combustion and emissions strategy using reactivity controlled compression ignition (RCCI) mode engine powered with CNG-Karanja biodiesel. *Journal of the Taiwan Institute of Chemical Engineers 000 (2021) 1□16*. doi:10.1016/j.jtice.2021.04.055

Willems, Robbert, Willems, Frank, Deen, Niels, and Somers, Bart %J Fuel. (2021). Heat release rate shaping for optimal gross indicated efficiency in a heavy-duty RCCI engine fueled with E85 and diesel. *288*, 119656.

Wong, Victor W, and Tung, Simon C %J Friction. (2016). Overview of automotive engine friction and reduction trends–Effects of surface, material, and lubricant-additive technologies. *4*, 1-28.

Xin, Qianfan Harry. (2011). *Overview of diesel engine applications for engine system design-part 3: operating and design characteristics of different applications* (0148-7191). Retrieved from

Xu, Guangfu, García, Antonio, Jia, Ming, and Monsalve-Serrano, Javier. (2021). Computational optimization of the piston bowl geometry for the different combustion regimes of the dual-mode dual-fuel (DMDF) concept through an improved genetic algorithm.*Energy Conversion and Management, 246*. doi:10.1016/j.enconman.2021.114658

Xu, Guangfu, Jia, Ming, Li, Yaopeng, Chang, Yachao, Liu, Hong, and Wang, Tianyou %J Fuel. (2019). Evaluation of variable compression ratio (VCR) and variable valve timing (VVT) strategies in a heavy-duty diesel engine with reactivity controlled compression ignition (RCCI) combustion under a wide load range. *253*, 114-128.

Yang, Liuhanzi, Zhang, Shaojun, Wu, Ye, Chen, Qizheng, Niu, Tianlin, Huang, Xu, et al. (2016). Evaluating real-world CO2 and NOX emissions for public transit buses using a remote wireless on-board diagnostic (OBD) approach. *218*, 453-462.

Yi, Sun Abbasi, Kashif Raza Hussain, Albaker, Khadim, Abdullah Alvarado, and Research, Gondwana. (2023). Environmental concerns in the United States: Can renewable energy, fossil fuel energy, and natural resources depletion help? *, 117*, 41-55.

Zhang, Felix. (2023). *Biofuels for transportation.* Paper presented at the Journal of Physics: Conference Series.

Zhao, Fuquan, Asmus, Thomas N, Assanis, Dennis N, Dec, John E, Eng, James A, and Najt, Paul M. (2003). Homogeneous charge compression ignition (HCCI) engines.

Zhou, D. Z., Yang, W. M., An, H., Li, J., and Shu, C. (2015). A numerical study on RCCI engine fueled by biodiesel/methanol. *Energy Conversion and Management, 89*, 798-807. doi:10.1016/j.enconman.2014.10.054

VISBLE OUTPUTS

I. Original research papers published

1. Habtamu Deresso, Ramesh Babu, Venkata Ramaya, and Bisrat Yoseph (2022). “Numerical study of different shape design of piston bowl for diesel engine combustion in a light duty single-cylinder engine.” *Heliyon, 8*(6), e09602. https://doi.org/10.1016/j.heliyon.2022.e09602 https://www.cell.com/heliyon/pdf/S2405-8440(22)00890-8

2. Habtamu Deresso, Venkata Ramaya, Ramesh Babu, Balewgize Amare Zeru.(2023). “Experimental study on the effect of speed and port-injected fuel blend ratio on a reactivity-control compression ignition (RCCI) engine performance.” *Energy Conversion Management*:https://doi.org/10.1016/j.ecmx.2023.100448 https://www.sciencedirect.com/science/article/pii/S2590174523001046

3. Habtamu Deresso, Venkata Ramaya, Ramesh Babu (2023). “Experimental study of triple fuel physiognomies on LDRCCI diesel engine combustion”. *Result in Engineering*. https://doi.org/10.1016/j.rineng.2023.101451 https://www.sciencedirect.com/science/article/pii/S2590123023005789

4. Habtamu Deresso, Venkata Ramaya, Ramesh Babu, Bisrat Yoseph (2023). “Response analysis of an experimental study on the effect of speed and premixed fuel ratio on performance and emissions in RCCI engine” *International Journal of Chemical Engineering (Hindawi)* ID-8707726, 2024. https://doi.org/10.1155/2024/8707726

II. Related research papers published

5. Getachew Alemayehu1, Ramesh Babu Nallamothu1, Habtamu Deresso, Rajendiran Gopal (2022) “Dieseline Ratio Impacts on Emissions in Optimized PCCI-DI Combustion in Diesel Engine” International Journal of Innovative Research in Engineering. ISSN No: 2582-8746

6. Helen Tadesse, Balkeshwar Singh, Habtamu Deresso, Shimelis Lemma, Gyanendra Kumar Singh, Ashish Kumar Srivastava, Namrata Dogra & Ajay Kumar “Investigation of production bottlenecks and productivity analysis in soft drink industry: a case study of East Africa Bottling Share Company” https://doi.org/10.1007/s12008-023-01715-9

III. Published in monograph and proceedings

7. Habtamu Deresso,Venkata Ramayya Ancha, Ramesh Babu Nallamothu, Experimental investigation of Bio-ethanol blend ratios effect on RCCI Diesel Engine Combustion , Contemporary Problems of Power Engineering and Environmental Protection, 2022, (Eds.) Krzysztof Pikoń and Magdalena Bogacka, PP 106-118, ISBN: 978-83-964116-2-4 http://www.epae.polsl.pl/\ https://omega.polsl.pl/info/book/PSL060d2530f9394b4d8c0b11d44b45b09f/

8. Habtamu Deresso, Venkata Ramaya, Ramesh Babu (2022) Numerical investigation on a hydrous bioethanol effect on the light-duty RCCI engine combustion, International Conference on Green Fuels for Bio-based Circular Economy, 11th-12th May 2023, Jimma University Institute of Technology (IC-GFBCE-2023) ISBN 978-99990-995-3-0, PP143-150

VI. International and national conference certificates (Total Quts 8):

1. EPAE (2022) *Environmental protection and Energy conference,* Silesian University of technology, Poland (Quts. 2).
2. *International Conference on Recent Advance in Civil and Mechanical Engineering (2023),* Kings College of Engineering, India (Qut.1).
3. *International Conference on Innovations and Challenges in Engineering and Technology for Sustainable Development (ICET-2023 or 2024),* Arba Minch University, Ethiopia (Quts 2).
4. *International Conference on Green Fuels for Bio-based Circular Economy (IC-GFBCE-2023)* held during 11th -12th May 2023, Jimma University institute of technology and ASTU respectively, Ethiopia (Quts.2).

APPENDIX A. ENGINE WHEN CONDUCTING EXPERIMENT

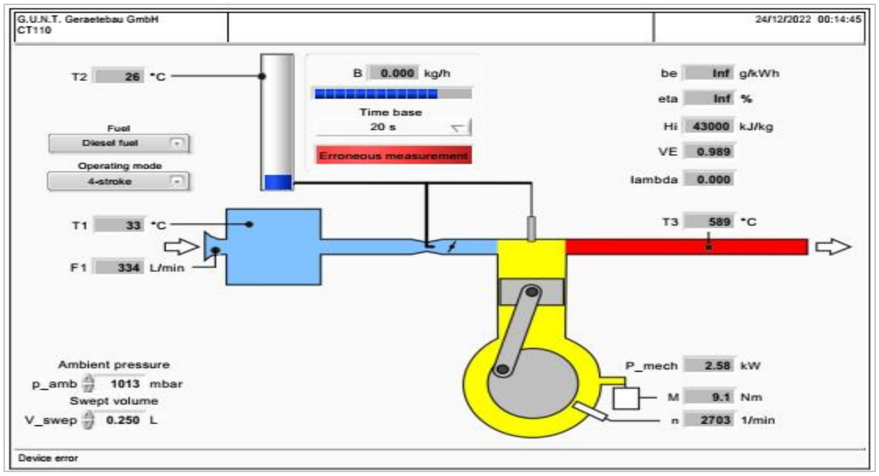

APPENDIX B. EMISSION INTERVAL PLOTS

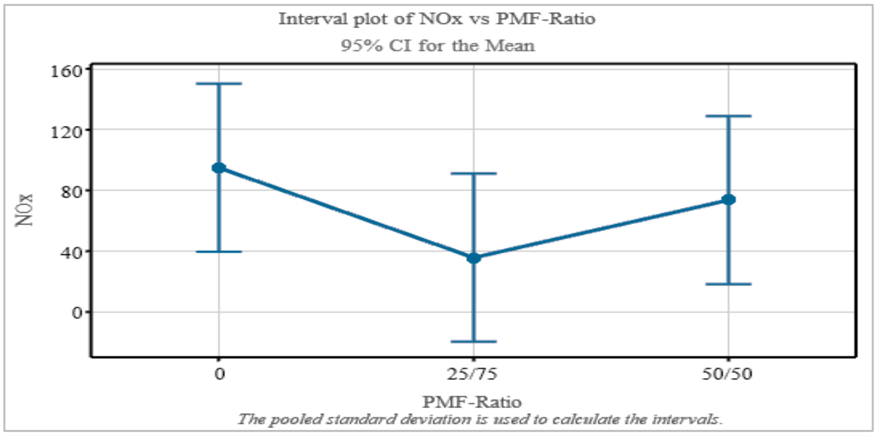

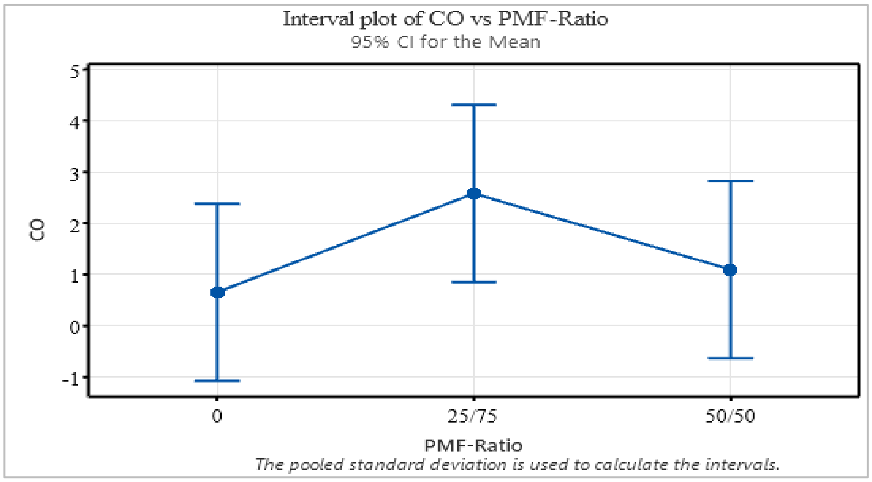

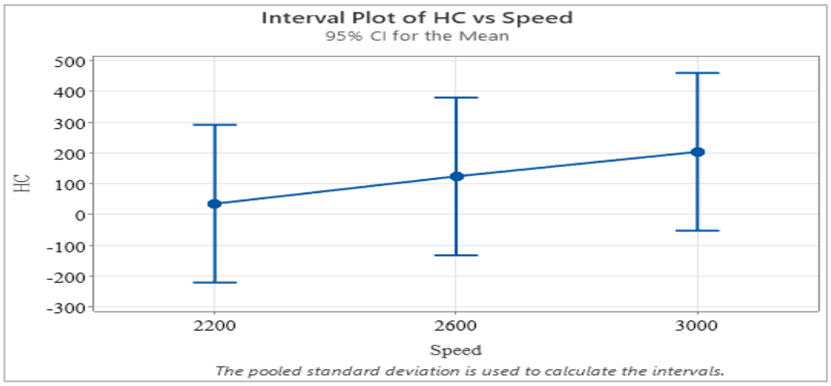

APPENDIX C. BOXPLOT OF EMISSION

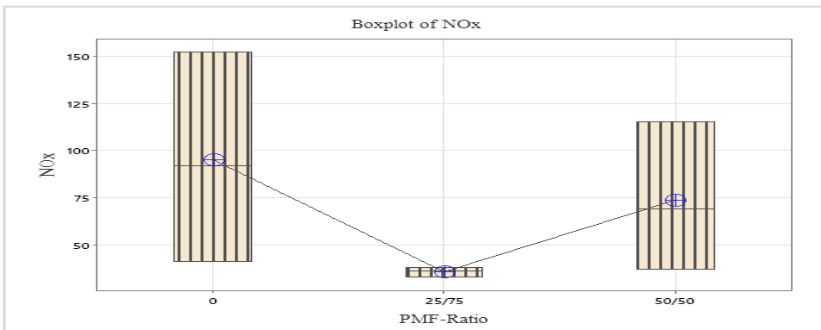

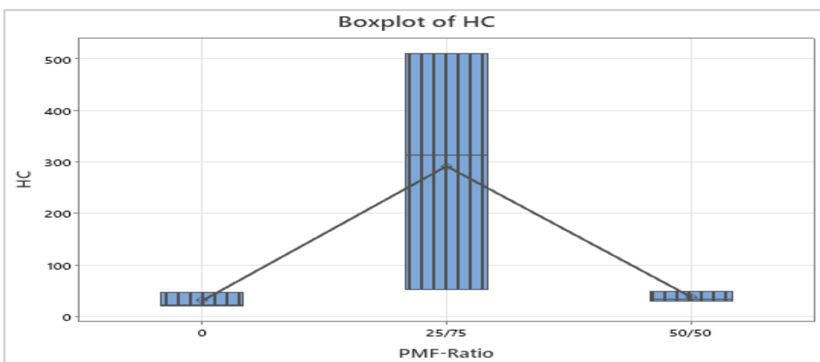

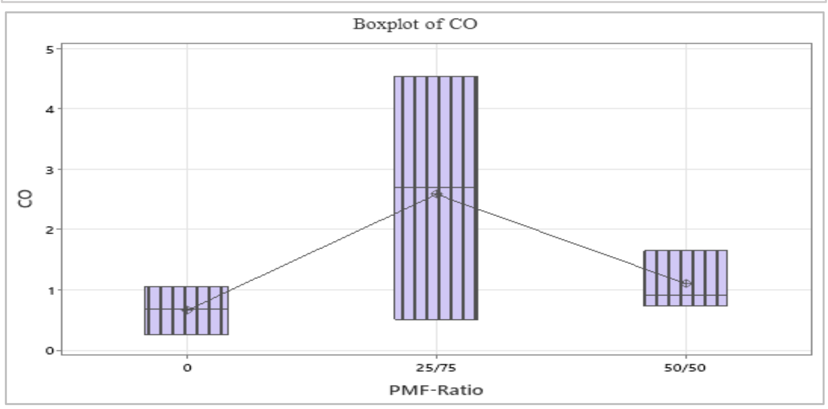

APPENDIX D. BOXPLOT OF PERFORMANCE

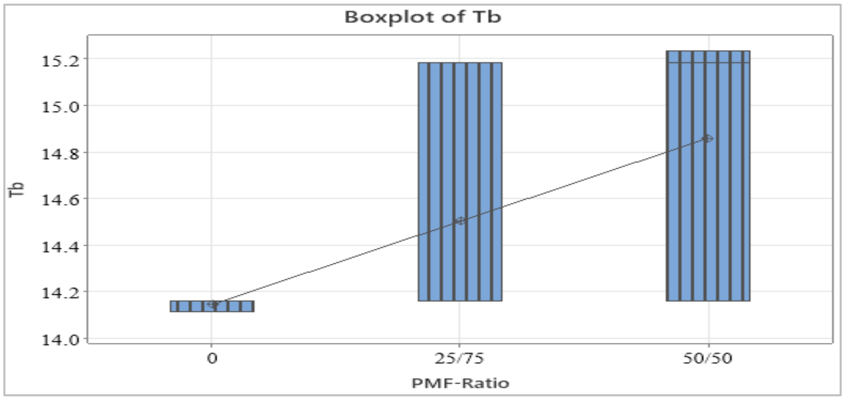

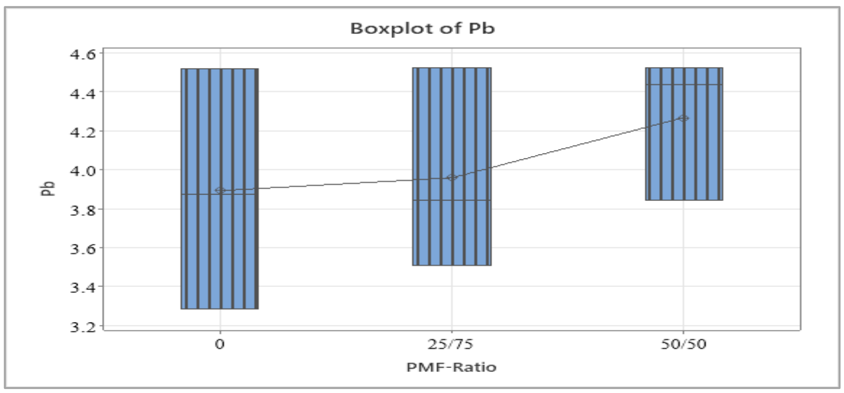

APPENDIX E. POTENTIOMETER ANGLE AND INJECTIONS VOLUME

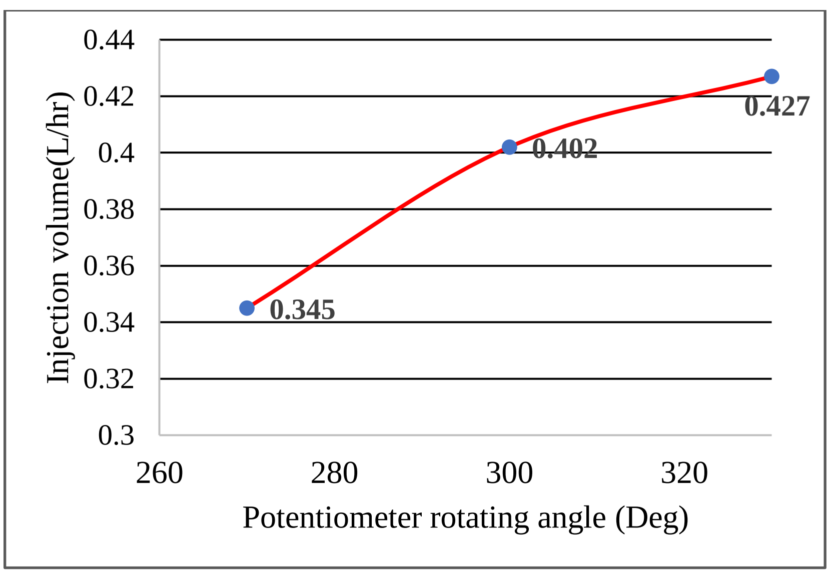

PPENDEX F. FUEL PROPERIES FROM EPE

Telefax 251-(0)11-551 29 38
251-(0)11-551 79 56
251-(0)11-554 19 05
Email - eth-petroleum@ethionet.et

Telephones:
P.B.X. (251) - 011-551 32 88
Direct: (251) - 011-551 00 45,
(251) - 011-552 60 30,
(251) - 011-554 19 04,
P.O.Box 3375
Addis Ababa - Ethiopia

የኢትዮጵያ ነዳጅ አቅራቢ ድርጅት
ETHIOPIAN PETROLEUM SUPPLY ENTERPRISE

Ref. No 3625/14/2014

ሕዳር 2 2 2014

ለኢትጰያ ፌደራላዊ ዴሞክራሲያዊ

አዳማ ሳይንስና ቴክኖሎጂ ዩኒቨርስቲ

<u>አዲስ አበባ</u>

ህዳር 10 2014 ዓ.ም በቁጥር 7/2.1.3/7.80/1337/14 በተፃፈ ደብዳቤ የተጠየቀውን መረጃ በዚህ ደብዳቤ ሸኚነት የላክን መሆኑን እንገልጻለን፡፡

ከሠላምታ ጋር

ኢሳያስ ፍስሃ
የዕቅድና ድርጅት ልማት
አገልግሎት ኃላፊ

/አአ

አባሪ፡-6ገጽ

ወደ ኢትዮጵያ የገባ ነዳጅ መጠን በሜ.ቶን

ዓ/ም(G/C)	ቤንዚን	የአውሮፕላን ነዳጅ / ላምባ	ነጭ ናፍጣ	ቀላል ጥቁር ናፍጣ	ከባድ ጥቁር ናፍጣ	ድምር
1990/1	9,622	85,282	185,920	-	-	280,824
1991/2	53,524	72,612	226,267	14,458	-	366,861
1992/3	28,713	116,247	249,963	-	-	394,923
1993/4	29,457	119,300	224,150	-	-	372,907
1994/5	43,213	150,062	304,358	-	-	497,633
1995/6	75,381	192,063	336,448	-	-	603,892
1996/7	67,351	207,868	413,117	-	-	688,336
1997/8	111,520	222,435	454,024	99,489	-	887,468
1998/9	134,763	238,545	541,364	96,021	-	1,010,693
1999/2000	142,019	223,077	548,013	109,268	-	1,022,377
2000/1	129,588	224,536	620,186	51,852	69,410	1,095,572
2001/2	132,808	248,711	622,094	38,412	80,087	1,122,112
2002/3	148,354	269,210	679,747	41,698	93,370	1,232,379
2003/4	130,370	292,766	687,991	47,121	89,844	1,248,092
2004/5	147,149	333,079	771,807	45,109	109,755	1,406,899
2005/6	137,232	368,670	811,013	41,385	116,822	1,475,122
2006/7	148,368	411,357	925,389	42,406	116,435	1,643,955
2007/8	138,973	482,219	1,072,793	49,608	137,679	1,881,272
2008/9	149,953	505,700	1,202,994	36,373	116,331	2,011,351
2009/10	155,760	529,786	1,237,077	10,700	100,870	2,034,193
2010/11	143,879	548,765	1,182,725	34,281	97,102	2,006,752
2011/12	161,470	553,780	1,402,848	36,496	107,984	2,262,578
2012/13	193,032	613,735	1,322,548	37,423	122,875	2,289,613
2013/14	211,598	700,744	1,558,342	37,128	114,995	2,622,807
2014/15	237,773	712,748	1,703,263	40,638	127,669	2,822,091
2015/16	307,817	735,920	1,929,581	35,953	70,986	3,080,258
2016/17	366,659	820,605	2,235,303	41,609	37,583	3,501,759
2017/18	441,542	738,106	2,507,672	35,785	47,483	3,770,589
2018/19	506,739	819,999	2,496,722	31,081	35,068	3,889,608
2019/20	558,552	621,455	2,529,148	37,397	42,409	3,788,961
2020/2021	652,573	444,022	2,535,455	30,160	57,413	3,719,623
ድምር	5,895,753	12,603,404	33,518,322	1,121,852	1,892,170	55,031,501

HZB
22/03/14

SPECIFICATION OF GASOIL

S/N	PARAMETER	TEST METHOD	LIMITS (MAX/MIN)
1.	Density @15 ^{O}C	D 4052/1298	0.820-0.860
2.	90% volume recovered, ^{O}C	D 86	Max. 362
3.	FBP, ^{O}C	D 86	Max 390
4.	Color	D 1500	Max 2
5.	Total sulfur, %wt	D 4294	Max 0.05
6.	Flash point, PMCC, ^{O}C	D 93	Min. 66
7.	Kinematic viscosity @ 40 ^{O}c	D 445	2.0-4.5
8.	Cloud point, ^{O}C	D 2500	Max +5
9.	Cetane index	D 976	Min 48
10.	Copper strip corrosion 3 hrs @100 ^{O}C	D 130	Max No. 1
11.	CCR ,%Wt	D 189	Max 0.2
12.	Ash , %Wt	D 482	Max 0.01
13.	Water and sediment, V/V %	D 2709	Max 0.05

SPECIFICATION OF GASOLINE

S/N	Parameter	Test method	LIMITS (MAX/MIN)
1.	Density @15^{O}C	D 4052/1298	0.720-0.740
2.	10% volume recovered, ^{O}C	D 86	Max. 74
3.	50% volume recovered, ^{O}C	D 86	80-127
4.	90% volume recovered, ^{O}C	D 86	Max 190
5.	FBP, ^{O}C	D 86	Max 225
6.	Residue	D 86	Max 2
7.	Research octane number(RON)	D 2699	Min 92
8.	Total sulfur, %wt	D 4294	Max 0.05
9.	Reid vapor pressure, kPa	D 323	41-65
10.	Existence gum, mg/100ml	D 381	Max 4
11.	Copper strip corrosion 3 hrs @50 ^{O}C	D 130	Max no 1
12.	Doctor test	IP 30	Negative
13.	Lead content, g/l	IP 352	Max 0.013

SPECIFICATION OF Jet A-1

S/N	Parameter	Test method	Limit
1.	Color, saybolt	D 156	report
2.	Appearance	Visual	C&B
3.	Total acidity, mgKOH/g	D 3242	Max 0.015
4.	Aromatics, vol%	D 1319	Max 25
5.	Sulfur, mercaptan, wt %	D 3227	Max 0.003
6.	Total sulfur, %wt	D 4294	Max 0.3
7.	Doctor test	IP 30	Negative
8.	10% volume recovered, ^{O}C	D 86	Max 205
	FBP, ^{O}C	D 86	Max 300
	Distillation residue, vol %	D 86	Max 1.5
	Distillation loss, vol %	AD 86	Max 1.5
9.	Flash point. ^{O}c	D 56/ IP 170	Min 38
10.	Density @15^{O}C	D 4052/1298	0.775-0.840
11.	Freezing point,	D 2386	Max. -47
12.	Kinematic Viscosity @-20 ^{O}c	D 445	Max. 8
13.	Net heat of combustion, Mj/kg	D 3338	Min 42.8
14.	Smoke point, mm	D 1322	Min. 25
15.	Naphthalene content, Vol%	D 1840	Max. 3.0
16.	Copper strip corrosion 2 hrs @100 ^{O}C	D 130	Max no. 1
17.	JFTOT control temp.	D 3241	260
	Filter pressure drop, mm Hg	D 3241	Max 25
	Heater tube deposit	D 3241	Max no. 3 peacock
	Heater tub color, visual	D 3241	report
	Test volume, ml	D 3241	report
18.	Existence gum, mg/100ml	D 381	Max. 7
19.	MSEP with static dissipater additive	D3948	Min 70
	MSEP without static dissipater additive	D3948	Min 86
20.	Particulate matter	D 5452	Max 1.0
21.	Electrical conductivity, pS/m	D 2624	50-600
22.	FAME, ppm	IP 583	Max 50
23.	BOCLE wear diameter, mm	D 5001	0.85

SPECIFICATION OF LIGHT FUEL OIL

S/N	Parameter	Test method	Limit
1.	Specific gravity @15^{O}C	D 4052/1298	Max 0.975
2.	Flash point, PMCC, ^{O}C	D 93	Min 55
3.	Total sulfur, %wt	D 4294	Max 3.0
4.	Calorific value, calc, BTU/LB	Calculated	Min 18500
5.	Kinematic viscosity @ 40 ^{O}c	D 445	45-80
6.	Pour point, ^{O}c	D 97	Max 10
7.	Ash, %Wt	D 482	Max 0.05
8.	CCR, %Wt	D 189	Max 16
9.	Water and sediment, V/V %	D 1796	Max 0.5

SPECIFICATION OF HEAVY FUEL OIL

S/N	Parameter	Test method	Limit
1.	Specific gravity @15^{O}C	D 4052/1298	Max 0.975
2.	Flash point, PMCC, ^{O}C	D 93	Min 66
3.	Total sulfur, %wt	D 4294	Max 3.5
4.	Calorific value, calc, BTU/LB	Calculated	Min 18500
5.	Kinematic viscosity @ 40 ^{O}c	D 445	Max 180
6.	Pour point, ^{O}c	D 97	Max 10
7.	Ash, %Wt	D 482	Max 0.1
8.	CCR, %Wt	D 189	Max 16
9.	Water and sediment, V/V %	D 1796	Max 0.5